KU LEUVEN

ARENBERG DOCTORAL SCHOOL
FACULTY OF SCIENCE

Von Willebrand factor and ADAMTS13 in stroke, thrombotic thrombocytopenic purpura, and malaria

Sebastien Verhenne

Supervisor:
Prof. Dr. K. Vanhoorelbeke

Co-Supervisors:
Prof. Dr. S.F. De Meyer
Prof. Dr. Z. Debyser

Dissertation presented in partial fulfilment of the requirements for the degree of Doctor in Science – Biochemistry and Biotechnology

December 2016

VON WILLEBRAND FACTOR AND ADAMTS13 IN STROKE, THROMBOTIC THROMBOCYTOPENIC PURPURA, AND MALARIA

Sebastien VERHENNE

Supervisor:
Prof. Dr. K. Vanhoorelbeke

Co-supervisors:
Prof. Dr. S.F. De Meyer
Prof. Dr. Z. Debyser

Members of the
Examination Committee:
Prof. Dr. E. Decaestecker
Prof. Dr. H. Deckmyn
Prof. Dr. A. Gils
Prof. Dr. P. Lenting
Prof. Dr. J. Thevelein
Prof. Dr. P. Van den Steen

Dissertation presented in partial fulfilment of the requirements for the degree of Doctor of Science: Biochemistry and Biotechnology

December 2016

PREFACE – DANKWOORD

We did it! Ik heb er jarenlang naartoe gewerkt en eindelijk is het zover: ik heb mijn doctoraatstitel behaald. Niet alleen, maar dankzij de hulp en onvoorwaardelijke steun van collega's, vrienden en familie. Het is dan ook hoog tijd om een aantal mensen te bedanken.

Karen en Simon, begeleiders van mijn doctoraatsthesis, uiteraard! Eerst en vooral omdat jullie mij de kans gaven om een doctoraat binnen een internationaal gerenommeerd onderzoekslabo aan te vatten. Maar ook omdat jullie wetenschappelijke kennis en jullie enthousiasme me elke dag stimuleerden om het beste van mezelf te geven. Jullie gaven me de vrijheid om bepaalde projecten uit te werken en hielden me in toom wanneer ik mijn eigen werk vanuit een te kritisch standpunt bekeek.
Karen, ik wil je ook bedanken om er mij (vaak) op te wijzen dat het behalen van een doctoraat meer is dan alleen maar 'output genereren'. Naast het wetenschappelijke aspect van een doctoraat is er namelijk ook het persoonlijke aspect. Dankzij jouw tips en de manier waarop je mij hebt begeleid, heb ik mij door lastige periodes geworsteld en heb ik geleerd wat teamwork is. Het mooiste bewijs van jouw impact is de metamorfose die ik heb ondergaan sinds de aanvang van mijn doctoraat.
Simon, bedankt om mij af en toe op mijn werkpunten te wijzen en om mij het volle vertrouwen te schenken in mijn functie als assistent. Jouw professionele aanpak in combinatie met een flinke dosis humor (en sarcasme) hebben me meermaals de zaken doen relativeren. Het doctoraat hoefde dan ook niet altijd centraal te staan. Op elk moment kon ik bij jullie terecht met problemen of bedenkingen van minder wetenschappelijke aard. Bovendien zijn jullie erin geslaagd een uitstekende groepssfeer te creëren. Het spreekt dan ook voor zich dat de vele congressen en labo-activiteiten me lang zullen bijblijven!
Een speciaal woordje van dank ook voor Hans. Mede dankzij jou kon ik mijn doctoraat binnen LATRON aanvatten, want wie anders had destijds de moed om een onderzoeksgroep rond trombose en hemostase aan de Kulak op te starten? Al was je niet rechtstreeks betrokken bij mijn onderzoek, ik heb op heel wat vlakken veel van jou geleerd. Je bent niet alleen een uitstekend onderzoeker, maar ook een fantastisch persoon. Mocht er op het Kulak-kerstbal een *lifetime achievement award* in de categorie 'Leukste Prof' uitgereikt worden, dan stemde ik voor jou!

Ik wil graag de leden van de examencommissie bedanken voor het kritisch nalezen van mijn thesis. Jullie suggesties betekenden een wetenschappelijke meerwaarde voor deze scriptie.

In het kader van mijn assistentschap richt ik graag een woord van dank aan Jan Beirlant en Hans Pottel. Een assistent van de faculteit Geneeskunde die doctoreert aan de faculteit Wetenschappen… Geen evidentie, maar jullie inspanningen hebben ertoe bijgedragen dat ik deze functie kon opnemen. Eenmaal aangesteld, kwam ik onder de vleugels van Prof. M. De Cuyper. Marcel, jij leerde me de kneepjes van het assistentschap en deed me dankzij jouw enthousiasme en kennis inzien dat organische chemie best wel cool in elkaar zit. Een ideaal uitgangspunt om tijdens de werkzittingen en practica het enthousiasme van de studenten aan te wakkeren! Ook al geniet je ondertussen van je welverdiende emeritaat, ik denk nog vaak terug aan onze goede samenwerking. Ook een welgemeende dankjewel aan Prof. W. Thielemans, die altijd bereid was om uitleg te geven en zijn licht te laten schijnen op problemen van organische aard.

Mijn LATRON-collega's verdienen uiteraard ook hun plaats in dit dankwoord.
Frederik, het spreekt voor zich dat ik jou als eerste vermeld. Op de werkvloer een fantastische collega, naast de werkvloer een heel goede vriend. Ik bewonder je passie voor wetenschappelijk onderzoek en ik sta vaak versteld van je uitgebreide kennis. Mede dankzij jouw expertise heb ik mijn eerste *first author*-artikel in *Blood* kunnen publiceren, waardoor ik vandaag mijn doctoraatstitel kan behalen. Het FACS-experiment dat tot in de vroege uurtjes duurde (Simon, we wachten nog altijd op die traktatie…), is misschien wel het mooiste voorbeeld van onze goede samenwerking. Ook op niet-wetenschappelijk vlak zaten we op dezelfde golflengte. Met een grote glimlach denk ik vaak terug aan onze belevenissen tijdens de congressen in Amsterdam, Bari (*la la la la la la la laaaa*), Toronto en Stowe, onze korte *road trip* in het noordoosten van de VS, onze 'Band of Brothers'-tripjes naar Normandië en Bastogne, en onze bewondering voor Carmen Electra (misschien is dit wel het moment om die poster terug te geven…). Dikke merci *brother from another mother* en veel succes in je verdere carrière!

Een speciale vermelding voor Inge ('Erotische Eend'), Nele ('Zingende Zwaan'), Aline ('Vatbaar Veulen') en Linda. Als groentje tussen dit vrouwengeweld terechtkomen, was niet niks. Vaak schuchter en verlegen kwam ik jullie om uitleg vragen. Maar telkens opnieuw waren jullie bereid om mij te helpen. Hoewel van het schuchter en verlegen zijn ondertussen

geen sprake meer is, blijft jullie bereidwilligheid grenzeloos. Ik denk dat het wel duidelijk is geworden hoezeer ik jullie bewonder. Enorm bedankt voor jullie kwaliteitsvolle bijdrage aan de verschillende projecten. Meer nog wil ik jullie bedanken voor de aangename werksfeer (al blijf ik erbij dat Studio Brussel voor een nog betere werksfeer zou zorgen). Ik vond het fantastisch om mijn verhalen (al dan niet serieus van aard) met jullie te delen en om naar jullie verhalen te luisteren. Ik zal jullie missen!

Who runs the lab? Girls, girls… meerbepaald Irina, An-Sofie, Elien R., Elien V., Elodie, Shannen en Sirima. Irina, mijn TranspoSMART-*buddy in crime*! Het was leuk om samen met jou de wereld van de niet-virale gentherapie te verkennen en de kracht van Sleeping Beauty te ontdekken. Bedankt ook voor je luisterend oor wanneer er mij iets van het hart moest. An-Sofie, de manier waarop jij jouw onderzoek aanpakt, getuigt van grote klasse. Hoewel jouw onderzoek vooral in het teken van 'anti-' staat, ben ik 'pro' An-Sofie. Elien V. en Elien R., de eindmeet komt ook voor jullie stilletjesaan in zicht! Ik wens jullie beiden dan ook veel goeie moed en succes bij het schrijven en verdedigen van de finale scriptie. Elodie, ik heb er alle vertrouwen in dat je jouw onderzoek 'NET'jes zal afronden. Blijven kleuren, die klonters! Shannen, je loopt (al is 'snelwandelen' een betere woordkeuze) nog maar een jaar rond in het labo, en toch ben je er al niet meer weg te denken. Doe verder zoals je bezig bent, en je zal gauw 'je schaapjes op het droge hebben'. Sirima, although I gave you hard times in the beginning (my apologies!), you adapted quickly. Within several months, you helped me to generate many of the results that are discussed in this manuscript. Every time I struggled with an experiment, your enthusiasm and optimism kept me going. I am grateful that I could guide you through your first year as a PhD student.

De drijvende krachten achter de PI's kunnen hier uiteraard ook niet ontbreken!
Wim Maes, bedankt voor je tips bij immunologische en flow cytometrische kwesties, en bij vraagstukken met betrekking tot mijn verdere beroepskeuze. Jouw gevoel voor humor, doorspekt met ironie en sarcasme, bracht me vaak aan het lachen en liet me de eentonigheid van het schrijven eventjes vergeten.
Claudia, in de voorbije 2 jaar heb je een diepe indruk op mij gemaakt. Vooral de manier waarop jij je engageert voor andere mensen in het lab, vind ik bewonderenswaardig! Dank voor je wetenschappelijke input bij verschillende projecten en een grote dankjewel om vele congresavonden om te toveren tot onvergetelijke momenten.

Kim, my favourite American lab member! Although I will not have the privilege to work with you, I have a feeling that your passage will be a success. I also want to thank you once more for letting us stay at your place in Boston and for giving me the ultimate rooftop-experience!
Enkele collega's hebben ondertussen het LATRON-schip verlaten en koers gezet richting andere oorden. Hendrik, bedankt voor de opvolging tijdens het eerste jaar van mijn doctoraat. Met de nodige portie humor leerde je me de kneepjes van het vak in afwezigheid van Karen en Simon. Karen D.C., mijn eerste Gordon Conference was er één met jou en was er dan ook eentje om niet snel te vergeten – net als de daaropvolgende trip naar Boston en New York. Ik wens je heel veel succes met je verdere carrière in de VS. Louis ('Luigi'), wat was ik blij dat jij je in de zomer van 2011 aanbood. Eindelijk wat mannelijk tegengewicht in het vrouwenbastion dat LATRON heet. Mede dankzij jouw spontaniteit en enthousiasme evolueerde ik gaandeweg van 'schuchter en verlegen' naar – laten we het houden op – 'minder schuchter en verlegen'. Bedankt voor je hulp bij het oplossen van mijn computerissues en bij het maken van figuren. En uiteraard ook voor je (weliswaar minder wetenschappelijke) bijdrage aan heel wat memorabele congresavonden. Verder wil ik ook Tim, Bauke, Katleen Broos, Benedicte, Elien D.C. en Vicky bedanken voor hun hulp bij kloneringen en opzuiveringen, en voor de leuke babbels tijdens de middagpauze.

Mijn welgemeende dank gaat ook uit naar Prof. Dr. Philippe Van den Steen, Thy en Leen voor hun hulp bij de opzet van het malaria-project, naar Dr. A. Lambrecht en de stralingsfysici van de dienst Radiotherapie van het AZ Groeninge voor hun hulp bij de transplantatie-experimenten, en naar zowel thesis- (Sarah, Hanne, en Tim) als kijkstage- (Pieternel en Lukas) studenten voor hun inzet en bijdrage aan diverse projecten.

Graag had ik ook de andere medewerkers binnen het IRF (onder meer de mensen van Biologie, Fysiologie en Chemie) en de faculteit Geneeskunde (onder andere Christèle, Griet, Petra, Faes, Liesbeth en Elise) bedankt. In het bijzonder wens ik een woord van dank te richten aan Wim Noppe, Katleen D en Sigrid.
Wim, de nestor van het IRF… De studenten hebben het volledig mis: onder die strenge blik zit een fantastische persoonlijkheid. Ik bedank je dan ook graag voor je hulp bij eiwitopzuiveringen en VGM-aangelegenheden, en voor de vele amusante gesprekken tijdens middag- en koffiepauzes. Dat ik nu zelf Star Wars- en Star Trek-personages van elkaar kan

onderscheiden, zegt veel over je invloed op me. *May the force be with you*, Wim (dat is toch van Star Wars, niet?)!
Katleen D., *the queen of mice*… Ten eerste wil ik je bedanken voor al jouw proefdier-gerelateerde zorgen! Ten tweede ben ik je een woord van dank verschuldigd omdat jouw positieve instelling me vaak heeft opgebeurd. Jouw kijk op de zaken stemde me tot nadenken en tot zelfreflectie.
Sigrid, bedankt voor al je administratieve hulp!

Naast inspanning was er natuurlijk ook nood aan ontspanning! Gelukkig kon ik daarvoor op de 'boys' rekenen. Jacob, Reindert, Tom en Xander…Waar te beginnen? De minste reden was genoeg om af te spreken. Ik kon altijd bij jullie terecht als ik met een probleem zat. Jullie hebben me geleerd om te relativeren en me op tijd te ontspannen. Onze (*legen…wait for it…dary*) reizen behoren dan ook tot dé hoogtepunten van de afgelopen jaren!
Een groot deel van mijn ontspanning vond ik ook in het voetbal. Ik kan me niet voorstellen wat er zonder voetbal van mij zou geworden zijn. Hoewel het al meer dan 23 jaar deel uitmaakt van mijn leven, zullen vooral de eerste ploeg van KVC Zwevegem Sport en KVK Avelgem me altijd bijblijven. Het groepsgevoel dat ik bij beide clubs zowel op als naast het veld mocht ervaren, was fantastisch. Ik wil dan ook alle spelers en trainers die hiertoe hebben bijgedragen van harte bedanken! In deze context is een dankwoordje voor mijn kinesist Xavier op zijn plaats. Jouw enthousiasme en humor maakten mijn revalidatie draaglijk. Elke kinebeurt was een moment van ontspanning tijdens het schrijven van deze thesis.
Daphné, jou wil ik graag bedanken om mij te doen inzien dat er belangrijkere zaken zijn dan werk en voetbal. Jouw kijk op de wereld heeft me geleerd om open te staan voor nieuwe ervaringen.

Uiteraard wil ik ook mijn familie bedanken. In het bijzonder gaat mijn dank uit naar mijn ouders. Mama en papa, voor jullie was het niet altijd even makkelijk, aangezien ik weinig vertelde over het reilen en zeilen aan de Kulak – ondanks jullie nieuwsgierigheid. Dat weerhield jullie er echter niet van om mij onvoorwaardelijk te steunen. Dit is dan ook het ideale moment om te zeggen dat mijn liefde en respect voor jullie heel groot zijn. Zonder jullie stond ik hier niet. Bedankt!
Charlotte en Koen, ook jullie verdienen een woordje van dank. Als (schoon)broer was ik er niet altijd op de momenten dat jullie mij nodig hadden, terwijl ik wel altijd bij jullie

terechtkon. Jullie 2 kleine bengeltjes, Manon en Noah, geven mijn leven kleur en toveren telkens weer een glimlach op mijn gezicht. Een dikke knuffel voor elk van jullie!

Mémé en pépé, oma en opa… Jullie hebben mij belangrijke waarden in het leven meegegeven en jullie hebben me gevormd tot wie ik vandaag de dag ben. Dat ik elke keer weer probeer het beste van mezelf te geven, is jullie verdienste. Ik hoop dan ook dat jullie – hier of daarboven – trots op me zijn.

TABLE of CONTENTS

SUMMARY

Von Willebrand factor (VWF) is a multimeric plasma glycoprotein that plays a dual role in hemostasis: (I) VWF promotes the adhesion of platelets to exposed subendothelium at sites of vascular injury, and (II) acts as a carrier molecule for clotting factor VIII, thereby protecting it from premature clearance. Upon endothelial injury, VWF binds to collagen and adopts a conformation that allows binding of glycoprotein (GP) Ib on platelets. The VWF-GPIb interaction slows down platelets and enables them to roll over the surface and to engage other platelet receptors. In turn, rolling platelets become activated, firmly attach, and aggregate in order to seal off the injured vessel wall. The platelet-tethering capacity of VWF mainly depends on its multimeric size, with ultra-large (UL-) VWF multimers being hyperreactive. In circulation, VWF multimer size, and hence its thrombogenic potential, is regulated by the proteolytic enzyme ADAMTS13 (a disintegrin and metalloprotease with thrombospondin-1 motifs, member 13). Under normal conditions, ADAMTS13 cleaves large, highly reactive VWF multimers anchored to endothelial membrane or in circulation specifically into smaller, less reactive VWF multimers.

Biosynthesis of VWF is restricted to endothelial cells and megakaryocytes, the precursor cells of platelets. Endothelial cell-derived VWF is either constitutively secreted into plasma and subendothelium, or stored in Weibel-Palade bodies. VWF that is produced in megakaryocytes ends up in α-granules of platelets. VWF present in storage granules is enriched in UL-VWF multimers that are secreted in a regulated process in response to a range of stimuli. Although endothelial cell- and platelet-derived VWF are products from the same gene, various biochemical differences between both VWF sources have been described. Whereas it is generally believed that endothelial cell-derived VWF, and in particular plasma VWF, is the major contributor in hemostasis and thrombosis, little is known on the contribution of platelet-derived VWF in these processes.

To gain more insight into the *in vivo* biological activity of platelet-derived VWF, we performed crossed bone marrow transplantations between wild-type C57BL/6J and VWF knock-out (*Vwf*$^{-/-}$) mice to generate chimeric mice with VWF only in platelets (VWF PLT chimeric mice) and chimeric mice specifically lacking platelet VWF (VWF EC chimeric mice). Tail clip bleeding times and arterial occlusion times following $FeCl_3$-induced arterial thrombosis in VWF EC chimeric mice were normal compared to wild-type mice, whereas bleeding times were prolonged and no occlusive thrombi were formed in VWF PLT chimeric

mice. These data indicate that platelet-derived VWF alone is not able to support normal hemostasis and arterial thrombus formation and that platelet-derived VWF is not essential in these processes. However, using a mouse model of ischemic stroke, we have demonstrated that the local release of platelet-derived VWF alone can promote intracerebral thrombosis following ischemic brain injury. Indeed, transient occlusion of the middle cerebral artery of VWF PLT chimeric mice resulted in stroke lesions and intracerebral deposition of fibrin(ogen) that were similar to those observed in both wild-type mice and VWF EC chimeric mice. In addition, we found that platelet-derived VWF fosters ischemic stroke injury via GPIb-dependent mechanism. This study sheds an unexpected new light on the biological activity of platelet-derived VWF and further supports the idea that blocking the VWF-GPIb axis would be an interesting novel treatment strategy in ischemic stroke.

Cleavage of VWF by ADAMTS13 is crucial to maintain normal hemostasis. Severe ADAMTS13 deficiency (<5-10% of normal activity) caused by mutations in the *ADAMTS13* gene can result in congenital thrombotic thrombocytopenic purpura (TTP). TTP is a rare thrombotic disorder that is characterized by the accumulation of UL-VWF multimers and spontaneous deposition of VWF- and platelet-rich thrombi in the microcirculation. Patients suffering from acute TTP episodes most often present with thrombocytopenia, hemolytic anemia, and organ damage, ultimately leading to death if left untreated. Treatment of congenital TTP is infusion of fresh frozen plasma in order to increase plasma ADAMTS13 activity levels (>5-10% of normal values). Patients at high risk for disease recurrence often receive prophylactic plasma infusions of which the number depends on the patient's phenotype. However, plasma infusion can result in complications and carries the risk for viral/prion transmission. Moreover, lifelong plasma therapy is stressful and has a negative impact on the patient's quality of life. Given the severity of the disease and the limitations of plasma prophylaxis, gene therapy for congenital TTP would offer an interesting alternative, as correction of the underlying defect would result in lifelong expression of ADAMTS13 avoiding the need for plasma infusion.

In this study, we used the non-viral Sleeping Beauty (SB100X) transposon system to deliver a functional copy of the *Adamts13* gene to ADAMTS13 knock-out (*Adamts13*$^{-/-}$) mice. Liver-directed hydrodynamic co-delivery of a transposon plasmid encoding ADAMTS13, along with a hyperactive transposase source resulted in expression of high levels of transgene ADAMTS13 up to 25 weeks after delivery. Evaluation of the VWF multimer distribution revealed a decrease in the relative amount of high molecular weight VWF multimers in

Adamts13$^{-/-}$ mice expressing high levels of transgene ADAMTS13 compared to non-treated *Adamts13*$^{-/-}$ mice, indicating that the therapeutic gene was biologically active in vivo. Moreover, using a mouse model of TTP, we demonstrated that *Adamts13*$^{-/-}$ mice that received therapeutic gene transfer were protected against TTP after challenge with recombinant VWF. Up to 20 weeks after gene transfer, no profound thrombocytopenia, hemolytic anemia, and organ damage were observed when mice expressing high levels of transgene ADAMTS13 were challenged. In conclusion, these data demonstrate that SB transposon-mediated gene therapy is a potent strategy to prevent acute TTP episodes in mice. Therefore, we believe that the present study may pave the way to a SB transposon-mediated gene therapy that will cure congenital TTP in humans.

An increasing body of evidence has suggested that a dysregulated balance between VWF and ADAMTS13, i.e. high VWF and/or low ADAMTS13 activity levels, may play a causal role in a variety of diseases. During the last decade, clinical studies have demonstrated that human malaria is associated with endothelial cell activation, the accumulation of UL-VWF multimers, and a reduction in ADAMTS13 activity. Whether these alterations constitute epiphenomena or play an active role in malaria-associated acute respiratory distress syndrome (MA-ARDS), a common complication of malaria with a high mortality rate, is currently unknown.

To address this issue, we used an established murine model of MA-ARDS, in which wild-type C57BL/6J mice were infected with *Plasmodium* (*P.*) *berghei* NK65 parasites. During the course of infection, VWF antigen levels were increased whereas VWF multimer distribution and ADAMTS13 activity levels were normal. At end-stage disease, however, a marked decrease in high molecular weight VWF multimers and a significant reduction in ADAMTS13 activity were observed. This was accompanied by a profound thrombocytopenia. Lack of VWF did not prevent thrombocytopenia from occurring, indicating that VWF does not contribute to malaria-related thrombocytopenia. Absence of VWF slightly but significantly altered disease course as evidenced by shortened survival times in *Vwf*$^{-/-}$ mice. Interestingly, we observed elevated peripheral blood parasitemia levels but reduced pulmonary pathology in *Vwf*$^{-/-}$ mice compared to wild-type mice. The biological mechanism by which VWF might influence peripheral blood parasitemia levels and pulmonary pathology in MA-ARDS is still unclear. Further studies will be of great importance to clarify the mechanisms that link VWF/ADAMTS13 alterations and malaria disease progression, and to explore new therapeutic avenues.

SAMENVATTING

Von Willebrand factor (VWF) is een geglycosyleerd multimeer eiwit dat een dubbele rol in de hemostase vervult: (I) VWF bevordert de adhesie van bloedplaatjes aan blootgesteld subendotheliaal weefsel ter hoogte van de beschadigde bloedvatwand, en (II) bindt en beschermt stollingsfactor VIII tegen vroegtijdige proteolyse in de circulatie. Bij beschadiging van het endotheel bindt VWF aan collageen en ondergaat het een conformatieverandering die een interactie met glycoproteïne (GP) Ib op bloedplaatjes toelaat. De interactie tussen VWF en GPIb remt de bloedplaatjes af en stelt hen in staat om over het endotheel te rollen en andere bloedplaatjesreceptoren aan te wenden. Rollende bloedplaatjes worden op hun beurt geactiveerd, hechten zich vervolgens stevig vast, en vormen finaal een aggregaat zodat de beschadigde bloedvatwand gedicht wordt. De capaciteit van VWF om bloedplaatjes te binden hangt van de multimeergrootte af, waarbij de 'ultralange' (UL-) VWF multimeren hyperreactief zijn. In de circulatie wordt de grootte van de VWF multimeren, en bijgevolg de trombogene activiteit van VWF, gereguleerd door het enzym ADAMTS13 ('A Disintegrin and Metalloprotease with ThromboSpondin-1 motifs, member 13'). Onder normale omstandigheden knipt ADAMTS13 de grote, meest reactieve VWF multimeren, die aan het endotheel verankerd zijn of vrij in circulatie voorkomen, in kleinere, minder reactieve multimeren.

De synthese van VWF is beperkt tot endotheelcellen en megakaryocyten, de voorlopercellen van bloedplaatjes. VWF van endotheliale oorsprong (VWF EC) wordt ofwel consitutief in het plasma en de subendotheliale ruimte gesecreteerd, ofwel als UL-VWF multimeren opgeslagen in Weibel-Palade lichaampjes. VWF dat in megakaryocyten aangemaakt wordt, komt in de granules van bloedplaatjes terecht (VWF PLT). Het opgeslagen VWF is rijk aan UL-VWF multimeren die op een gereguleerde manier worden vrijgezet na stimulatie van het endotheel of bloedplaatjes. Hoewel VWF EC en VWF PLT door hetzelfde gen gecodeerd worden, werden reeds verscheidene biochemische verschillen tussen beide beschreven. Hoewel er in het algemeen van uitgegaan wordt dat VWF EC, en in het bijzonder plasma VWF, de belangrijkste bijdrage in het proces van hemostase en trombose levert, is er weinig gekend over de rol van VWF PLT in deze processen.

Om meer inzicht te verwerven in de *in vivo* biologische activiteit van VWF PLT werden beenmergtransplantaties tussen wild type C57BL/6J muizen en VWF-deficiënte muizen (*Vwf* $^{/-}$) uitgevoerd. Op deze manier werden enerzijds chimere muizen met enkel VWF in

bloedplaatjes (VWF PLT chimere muizen) en anderzijds chimere muizen met enkel VWF in endotheelcellen (VWF EC chimere muizen) ontwikkeld. In vergelijking met wild type muizen was de bloedingstijd en arteriële trombusvorming in VWF EC chimere muizen normaal, terwijl in VWF PLT chimere muizen de bloedingstijd verlengd was, alsook geen occlusieve trombus gevormd werd, Deze data tonen aan dat VWF PLT niet essentieel is in het proces van hemostase en arteriële trombusvorming, en dat VWF PLT alleen niet in staat is om deze processen te ondersteunen. In een muismodel voor ischemische beroerte werd echter aangetoond dat de lokale vrijzetting van VWF PLT kan bijdragen tot intracerebrale trombose na het optreden van ischemische hersenschade. Tijdelijke occlusie van de middelste cerebrale arterie resulteerde immers in een herseninfarct en een intracerebrale afzetting van fibrine/fibrinogeen in VWF PLT chimere muizen, waarvan de omvang vergelijkbaar was met deze in wild type muizen en VWF EC chimere muizen. De bijdrage van VWF PLT in de ontwikkeling van het infarct verliep bovendien via een GPIb-afhankelijk mechanisme.
Deze studie werpt een nieuw licht op de biologische activiteit van VWF PLT en steunt het idee dat het blokkeren van de VWF-GPIb as een interessante nieuwe strategie is voor de behandeling van ischemische beroerte.

Het knippen van VWF door ADAMTS13 is van cruciaal belang voor het behoud van de hemostase. Een ernstig tekort van ADAMTS13 (<5-10% van de normale activiteit) als gevolg van mutaties in het ADAMTS13 gen kan aanleiding geven tot congenitale trombotische trombocytopenische purpura (TTP). TTP is een zeldzame trombotische aandoening die gekenmerkt wordt door een opstapeling van UL-VWF multimeren in plasma en de afzetting van VWF- en bloedplaatjes-rijke klonters ter hoogte van de microcirculatie. Tijdens een acute fase presenteren patiënten zich met trombocytopenie, hemolytische anemie, en orgaanschade, hetgeen tot de dood kan leiden indien geen adequate behandeling voorhanden is. De standaardbehandeling voor congenitale TTP is de infusie van vers ingevroren plasma, teneinde de ADAMTS13 activiteit in plasma te verhogen (>5-10% van de normale waarde). Patiënten met een hoog risico op herval komen in aanmerking voor een profylactische behandeling, waarbij het aantal infusies afhankelijk is van het fenotype van de patiënt. De infusie van plasma kan echter leiden tot complicaties en de overdracht van ziekteverwekkende virussen en prionen. Bovendien gaat een levenslange plasmatherapie gepaard met stress en heeft het een negatieve impact op de levenskwaliteit van de patiënt. Gezien de ernst van de aandoening en de beperkingen van de huidige behandeling zou gentherapie als een belangrijke alternatieve behandelingsoptie beschouwd kunnen worden.

Herstel van het onderliggend genetisch defect zou immers resulteren in een levenslange expressie van ADAMTS13 waardoor infusie van plasma niet langer noodzakelijk is.
In deze studie maakten we gebruik van het niet-viraal *Sleeping Beauty* (SB) transposon systeem om een functioneel kopij van het ADAMTS13 gen in ADAMTS13-deficiënte (*Adamts13*$^{-/-}$) muizen te introduceren. Hydrodynamische injectie van transposon DNA, dat codeert voor ADAMTS13, in combinatie met plasmide DNA dat codeert voor hyperactief transposase resulteerde in de lever-gemedieerde expressie van hoge hoeveelheden transgeen plasma ADAMTS13, en dit tot 25 weken na toediening. Analyse van het multimeerpatroon toonde aan dat de relatieve hoeveelheid hoog moleculair gewicht multimeren in deze muizen verlaagd was ten opzichte van niet-behandelde *Adamts13*$^{-/-}$ muizen, wat aangeeft dat het transgeen ADAMTS13 biologisch actief was. Sterker nog, gentherapeutisch-behandelde *Adamts13*$^{-/-}$ muizen waren beschermd tegen TTP. In *Adamts13*$^{-/-}$ muizen die hoge hoeveelheden transgeen ADAMTS13 tot expressie brengen werd immers geen uitgesproken trombocytopenie, hemolytische anemie, en orgaanschade waargenomen na het toedienen van een hoge dosis exogeen recombinant VWF, en dit tot en met 20 weken na gentransfer. Alles samen tonen deze data aan dat deze niet-virale gentransferstrategie een veelbelovende therapie is om acute TTP in muizen te voorkomen. We zijn er dan ook van overtuigd dat de huidige onderzoeksresultaten zullen bijdragen tot de ontwikkeling van een klinisch relevante SB transposon-gemedieerde strategie voor de behandeling van congenitale TTP.

Een toenemend aantal publicaties doet vermoeden dat er mogelijk een oorzakelijk verband bestaat tussen tal van aandoeningen en een verstoord evenwicht tussen VWF en ADAMTS13, d.i. een verhoogde VWF en/of een verlaagde ADAMTS13 activiteit. Gedurende de afgelopen 10 jaren hebben klinische studies aangetoond dat de humane malaria vorm gepaard gaat met de activatie van endotheelcellen, een opstapeling van UL-VWF multimeren in plasma, en een afname van de activiteit van ADAMTS13. Of deze veranderingen al dan niet een oorzakelijke rol spelen in malaria-geassocieerde ‘acute respiratory distress syndrome’ (MA-ARDS), een frequent voorkomende, vaak lethale complicatie van malaria, is tot op heden niet gekend.

Om dit te onderzoeken maakten we gebruik van een muismodel voor MA-ARDS, waarbij wild type C57BL/6J muizen met *Plasmodium (P.) berghei* NK65 parasieten geïnfecteerd werden. Tijdens het verloop van de infectie was de hoeveelheid VWF in plasma verhoogd, terwijl zowel het multimeerpatroon van VWF als de activiteit van ADAMTS13 normaal was. In het eindstadium van de ziekte werd echter een opmerkelijke daling in hoog moleculair gewicht multimeren en ADAMTS13 activiteit waargenomen. Dit ging eveneens gepaard met een uitgesproken trombocytopenie. Afwezigheid van VWF kon dit laatste niet voorkomen, wat erop wijst dat VWF niet in het proces van malaria-geassocieerde trombocytopenie betrokken is. Na infectie overleefden VWF-deficiënte muizen significant minder lang dan wild type muizen, al was het verschil beperkt. Opmerkelijk was dat de parasitemiewaarden in perifeer bloed en de longpathologie in geïnfecteerde VWF-deficiënte muizen respectievelijk verhoogd en verlaagd waren ten opzichte van geïnfecteerde wild type muizen. Het mechanisme waarmee VWF de parasitemie en longpathologie in MA-ARDS mogelijks beïnvloedt, blijft momenteel onduidelijk. Verdere studies zijn dan ook noodzakelijk om de link tussen de progressie van MA-ARDS en de veranderingen in VWF en ADAMTS13 verder uit te klaren, en om nieuwe behandelingsopties te verkennen.

LIST of ABBREVIATIONS

AA	amino acid
AAV	adeno-associated virus
ADAMTS13	a disintegrin and metalloprotease with thrombospondin-1 motifs, member 13
aVWS	acquired von Willebrand syndrome
BAL	broncho-alveolar lavage
BMT	bone marrow transplantation
BSA	bovine serum albumin
CM	cerebral malaria
CRISPR/Cas	clustered regularly interspaced palindromic repeats and CRISPR-associated
C-terminal	carboxyl-terminal
CUB	complement component C1r/C1s, urinary epidermal growth factor and bone morphogenetic protein-1
DAB	3,3'-diaminobenzidine
DTCS	non-catalytic ADAMTS13 domains including disintegrin domain (D), thrombospondin-1 motif (T), cysteine domain (C), and spacer domain (S)
DDAVP	1-desamino-8-D-arginine vasopressin
DNA	deoxyribonucleic acid
EC	endothelial cell
ECM	extracellular matrix
ELISA	enzyme-linked immunosorbent assay
F	clotting factor
FRETS-VWF73	fluorescent resonance energy transfer using a short fluorogenic 73 amino acid VWF peptide
FVIII:C	clotting factor VIII activity
GP	glycoprotein
HMW	high molecular weight
HRP	horseradish peroxidase
HT	hepes tyrode

iRBC	infected red blood cell
Kb	kilobase
KO	knockout
LDH	lactate dehydrogenase
LMW	low molecular weight
LRP1	lipoprotein receptor-related protein-1
M	metalloprotease domain
MA-ARDS	malaria-associated acute respiratory distress syndrome
MCA	middle cerebral artery
MDTCS	ADAMTS13 truncated after spacer domain
MMW	medium molecular weight
MNC	mononuclear cell
NAC	N-acetylcysteine
N-terminal	amino-terminal
P	*Plasmodium*
PBS	phosphate buffered saline
pDNA	plasmid DNA
PEI	polyethylenimine
PEX	plasma exchange
PPP	platelet-poor plasma
PRP	platelet-rich plasma
rADAMTS13	recombinant ADAMTS13
RBC	red blood cell
RT	room temperature
rVWF	recombinant von Willebrand factor
SB	Sleeping Beauty
SDS	sodium dodecyl sulphate
T	thrombospondin motif
TBS	tris buffered saline
TBST	tris buffered saline containing 0.05% Tween20
TF	tissue factor
TIR	terminal inverted repeat
TMA	thrombotic microangiopathy

tMCAO	transient middle cerebral artery occlusion
t-PA	tissue-plasminogen activator
TTC	2,3,5-triphenyltetrazolium chloride
TTP	thrombotic thrombocytopenic purpura
UL	ultra large
u-PA	urokinase-plasminogen activator
VWD	von Willebrand disease
VWF	von Willebrand factor
VWF EC	chimeric mice expressing VWF only in endothelial cells
VWF PLT	chimeric mice expressing VWF only in platelets
VWFpp	VWF propeptide
WPB	Weibel-Palade body
WT	wild-type

CHAPTER 1

GENERAL INTRODUCTION: VWF AND ADAMTS13 IN HEALTH AND DISEASE

1.1. HEMOSTASIS

Blood is a liquid tissue that plays a crucial role in the human body: it provides organs with necessary nutrients and removes metabolites. To accomplish this task, blood relies on different cell types that are suspended in a protein-rich aqueous solution (plasma). Blood cells are derived from immature progenitor cells, called hematopoietic stem cells, residing in the bone marrow (Figure 1). In the presence of specific growth factors progenitor cells mature, differentiate, and finally give rise to 3 types of blood cells that are released into the blood stream. Erythrocytes (or red blood cells, RBCs) are the most abundant cells (4-6 million cells per µl), accounting for 40-45% of the total blood volume. These anucleated, biconcave cells contain hemoglobin enabling them to transport oxygen and carbon dioxide. Thrombocytes (or platelets), like erythrocytes, lack a nucleus as these small discoid-shaped cells are derived from the cytoplasm of megakaryocytes. Platelets constitute the second largest number of blood cells in circulation (200-500 thousand cells per µl) and primarily maintain the integrity of the blood vessel wall through their ability to promote repair of injured blood vessels and stop bleeding. Leukocytes (or white blood cells) are less numerous (4-11 thousand cells per µl) and account for only 1% of the total blood volume. Depending on their structural and functional characteristics, these nucleated cells contribute to the innate or adaptive immune response thereby protecting the human body against foreign microorganisms such as viruses and bacteria.

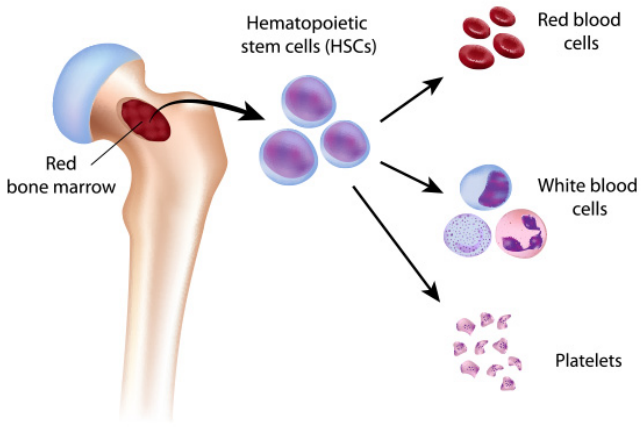

Figure 1: Blood cell components. Circulating blood cells are derived from immature progenitor cells (hematopoietic stem cells) residing in the bone marrow. During maturation and differentiation, progenitor cells give rise to different blood cell lineages (red blood cells, white blood cells, and platelets) that are released into the blood stream. Figure adapted from lyceum.algonquincollege.com

Erythrocytes represent the largest cell mass, occupying the greatest part of the lumen and pushing the leukocytes and platelets to the vessel wall in flowing blood. Whereas the velocity of blood flow is relatively low near the vessel wall, it progressively increases near the center of the vessel. The sliding motion of adjacent layers of fluid moving at different velocities creates a 'shearing' effect, an effect that is associated with the application of tangential forces in the direction of flow. The tangential force of the flowing blood exerted on the endothelial surface of the blood vessel is called shear stress. This hemodynamic mechanical force is directly proportional to the shear rate, which is characterised as the difference in flow velocity as a function of the distance to the vessel wall (expressed in cm/s per cm, or inverse seconds s^{-1}). In turn, the shear rate is directly proportional to the blood flow and viscosity, and indirectly proportional to the vessel diameter. Consequently, cells within blood vessels with a small diameter and high flow (such as arterioles and capillaries) experience high shear stress, whereas cells circulating in vessels with a large diameter and low flow (such as veins and large arteries) experience low shear stress.

Preservation of a normal blood flow is the result of a dynamic physiological process called hemostasis that is crucial to supply organs with essential nutrients. Hemostasis enables an organism to seal off an injured vessel wall, to keep blood in its fluid state, and to remove a blood clot after restoration of the vessel wall. Historically, the hemostatic process was divided into primary hemostasis, where platelet-vessel wall interactions lead to the formation of an initial platelet plug, and secondary hemostasis or coagulation, where clotting factors interact to generate insoluble fibrin that strengthens and stabilizes the initial platelet thrombus. However, current insights indicate that both processes happen simultaneously and are mechanistically intertwined (Figure 2).[1] Finally, fibrinolysis also plays an important role in hemostasis. The fibrinolytic pathway ensures blood flow by limiting thrombus growth and removing the clot after tissue repair.

1.1.1. Primary hemostasis

Under normal conditions platelets flow over the intact endothelial surface with no adhesion or aggregation. Upon vessel injury, however, blood is exposed to the procoagulant subendothelial extracellular matrix (ECM) and platelet adhesion, activation, and aggregation occurs. These platelet-vessel wall interactions depend on local rheological conditions, i.e. the hemodynamic mechanical forces that differ throughout the circulation.[2] At low shear rates ($<800\ s^{-1}$, such as veins and large arteries) platelets interact directly with ECM proteins such

as collagen, fibronectin, and laminin, whereas at high shear rates (>800 s^{-1}, such as small arteries and capillaries) platelets bind via intermediary proteins (e.g. von Willebrand factor, VWF) to the ECM. Multiple platelet receptors are involved in this process and cooperate to form a stable adhesive platelet plug.[3] The platelet glycoprotein (GP) Ib-IX-V receptor complex is crucial for the initial recruitment of platelets, in particular at sites of high shear rates.[4,5] GPIb-IX-V interacts with VWF, a multimeric plasma glycoprotein that is bound to collagen present in the ECM and acts as an adhesive surface for circulating platelets. Through fast association-dissociation kinetics, the VWF-GPIb-IX-V interaction decelerates platelets enabling them to roll over the surface and allowing them to engage other platelet receptors like GPVI and integrin $\alpha_2\beta_1$.[6] Direct binding of GPVI and $\alpha_2\beta_1$ to collagen allows the rolling platelets to firmly attach to collagen.[4,7]

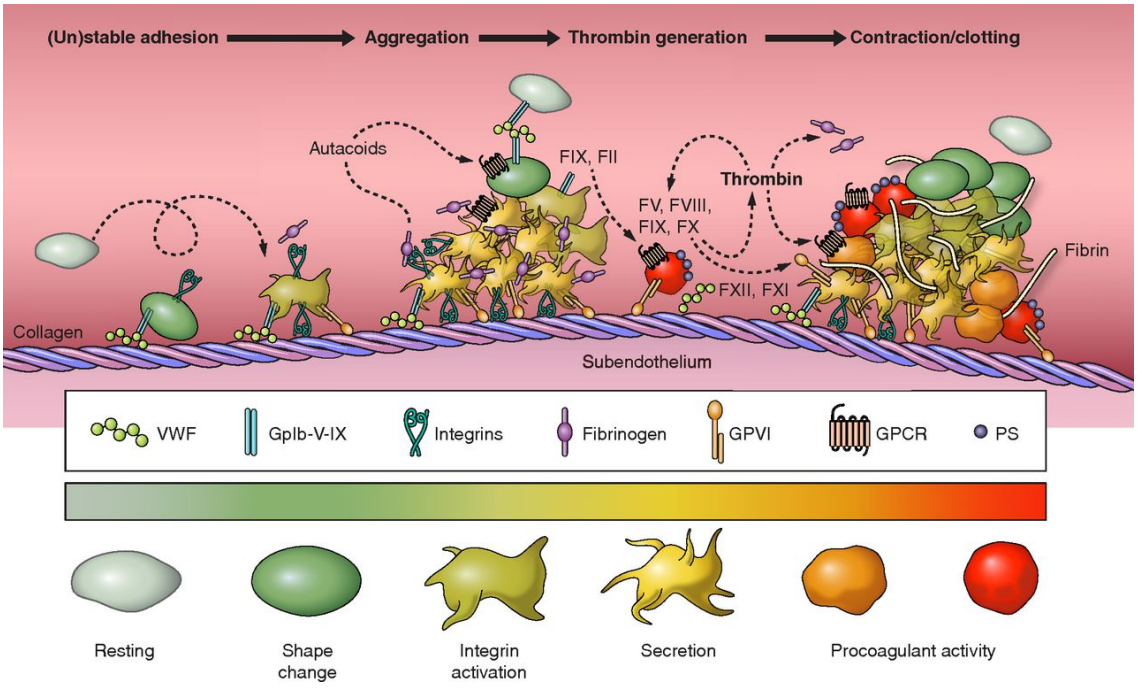

Figure 2: Schematic representation of the hemostasis process. Discoid, non-activated rolling platelets interact with subendothelial collagen and von Willebrand factor (VWF) at sites of vascular injury. Initial reversible adhesion activates rolling platelets, a process that is associated with an increased intracellular Ca^{2+} concentration, as depicted by the heat map (green: low Ca^{2+} signal; red: high Ca^{2+}signal). Activated platelets spread, secrete agonists from storage granules, and bind VWF and fibrinogen through integrin activation resulting in irreversible adhesion and aggregation. In concert with these events, thrombin is generated which in turn has multiple effects including platelet activation and amplification of the coagulation cascade via active coagulation factors bound to the phosphatidylserine (PS)-rich platelet surface. Increased amounts of thrombin propagate clot formation

and ultimately convert soluble fibrinogen into insoluble fibrin strands that stabilize the initial platelet thrombus. Adapted from Versteeg *et al.*[1]

VWF/GPIb-IX-V and GPVI/collagen binding induce cell-signalling pathways that are associated with an intracellular increase in Ca^{2+} concentration and subsequent platelet activation (Figure 2).[8,9] Morphological alterations (from discoid to irregular shape), secretion of agonists from storage granules (such as platelet-activating molecules ADP and thromboxane) or cross-linking agents (VWF and fibrinogen)), and conformational transitions of integrins ($\alpha_{IIb}\beta_3$ or GPIIb/IIIa) from a low-affinity to a high-affinity state, are the main processes that characterize platelet activation. Following irreversible platelet adhesion, binding of the activated integrin receptor GPIIb/IIIa to both VWF and fibrinogen results in cross-linking of platelets and the formation of a platelet aggregate.[5,10] Local feedback activation, by means of agonist secretion from storage granules, is crucial for further aggregation and subsequent growth of the primary platelet plug.

1.1.2. Secondary hemostasis

Following endothelial injury, coagulation factors respond through a complex cascade of reactions, called the coagulation cascade (Figure 3). Herein, each clotting factor exists as an inactive serine protease that is converted by an upstream activated enzyme. Tissue factor (TF), a membrane protein that is abundantly expressed on the surface of subendothelial cells, is considered the key initiator of coagulation.[11] Following vascular damage, TF acts as an enzyme cofactor and forms a complex with circulating activated clotting factor VII (FVIIa). The TF:FVIIa complex leads to subsequent activation of clotting factor X and prothrombin after which small amounts of thrombin are produced. Thrombin in turn plays a central role in coagulation as it exerts multiple effects.[12] Thrombin activates platelets and additional circulating coagulation factors that are involved in the amplification of the coagulation process. These additional clotting factors (FV, FVIII, FIX, and FX) are bound to the phosphatidylserine-rich surface membrane of a.o. activated platelets and contribute to a positive feedback loop that enhances thrombin generation (Figure 3). In addition to its crucial role in clot propagation, thrombin also cleaves fibrinogen to generate insoluble fibrin strands that upon cross-linking by FXIII form a solid fibrin meshwork that stabilizes the primary hemostatic plug.

Natural inactivation of the coagulation system via inhibitory pathways is essential to prevent uncontrolled, widespread clot formation. Coagulation is predominantly downregulated by the

protease inhibitors tissue-factor pathway inhibitor and antithrombin, and by the enzyme-based protein C/protein S pathway (Figure 3). Both protease inhibitors eliminate coagulation factors by targeting the active sites: tissue-factor pathway inhibitor directly binds and inhibits FXa or the TF:FVIIa complex, whereas antithrombin, one of the most important inhibitors, displays high affinity for thrombin, as well as FIXa and FXa. In contrast, protein C in complex with protein S does not attack the active site but proteolytically inactivates FVIIIa and FVa.

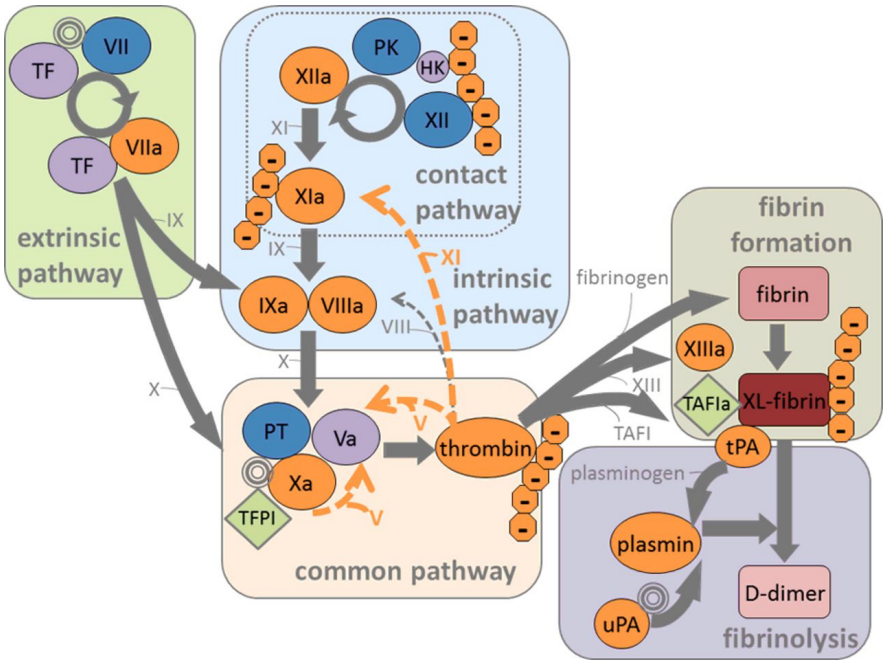

Figure 3: Schematic overview of the secondary hemostasis. The coagulation cascade is mainly initiated by the interaction between exposed tissue factor (TF) and circulating activated clotting factor VII (FVIIa) (extrinsic pathway). The TF:FVIIa complex activates FX (FXa) which results in the formation of the prothrombinase complex and the subsequent generation of small amounts of thrombin. In turn, thrombin performs multiple reactions including the conversion of fibrinogen into fibrin and the activation of the transglutaminase FXIII (FXIIIa) generating cross-linked fibrin strands (XL-fibrin). Thrombin generation is propagated by means of positive feedback loops and another pathway in which negatively charged surfaces from activated platelets and additional coagulation factors (FXII, FXI, FIX, and FVIII) are involved (intrinsic pathway). Endogenous thrombolytic agents, such as tissue-type and urokinase-type plasminogen activators (tPA and uPA, respectively), drive plasmin-mediated fibrinolysis which results in the degradation of cross-linked fibrin and the prevention of excessive thrombus formation. Both coagulation and fibrinolysis are under control of several inhibitory pathways. For example, the protease-inhibitor tissue-factor pathway inhibitor (TFPI) reduces coagulation by targeting the active site of FXa whereas activated thrombin-activatable

fibrinolysis inhibitor (TAFIa) tempers fibrinolysis by diminishing the efficiency of plasminogen activation by tPA. Figure adapted from Mutch.[13]

1.1.3. Fibrinolysis

After the damage in the vessel wall is repaired, another cascade of proteases, called the fibrinolytic system, dissolves the clot and counteracts pathological thrombus formation (Figure 3).[14,15] Plasmin is the primary 'fibrinolysin' and is activated from plasminogen by either urokinase-type plasminogen activator (u-PA) or tissue-type plasminogen activator (t-PA). Plasmin degrades the thrombus by cleaving the fibrin polymers that stabilize the thrombus. Like the coagulation process, the fibrinolytic system is highly regulated to assure balanced hemostasis.[16] The most potent regulator, α_2-antiplasmin, directly inhibits plasmin activity. Other important antifibrinolytic proteins attenuate fibrinolysis by limiting *de novo* plasmin generation either through inhibition of plasminogen activation (e.g. plasminogen-activator inhibitor (PAI)-1 and PAI-2) or through modification of the fibrin surface (e.g. thrombin-activatable fibrinolysis inhibitor) (Figure 3).

The balance between procoagulant and anticoagulant mechanisms ensure proper hemostasis. Genetic or acquired defects in one of the abovementioned phases may result in either excessive hemorrhage or pathological thrombus formation (thrombosis). In this introduction we will focus on VWF and its regulating enzyme, the VWF-cleaving protease ADAMTS13. We will discuss how genetic or acquired defects may affect their activity and contribute to bleeding- and thrombosis-related events.

1.2. VON WILLEBRAND FACTOR

VWF is a multimeric plasma glycoprotein that fulfils a dual role in hemostasis. On the one hand, VWF acts as a molecular bridge between platelets and the subendothelial ECM at sites of vascular injury under high shear conditions (Figure 2). On the other hand, VWF acts a carrier for FVIII in circulation, thereby protecting FVIII against premature proteolytic degradation. Reduced levels or malfunctioning of VWF may result in bleeding episodes, whereas elevated levels or hyperreactivity is associated with thrombotic events.[17,18] This demonstrates that both levels and activity of circulating VWF need to be tightly regulated.

1.2.1. Biosynthesis and secretion of VWF

The *VWF* gene is located on the short arm of chromosome 12 and contains 52 exons that span approximately 180 kilobase (kb). VWF is made exclusively in endothelial cells (ECs) and megakaryocytes as a 9 kb pre-pro-VWF monomer transcript that consists of a signal peptide (22 amino acids (AAs)), a propeptide (741 AAs), and a mature VWF subunit (2050 AAs). This VWF precursor protein is subjected to a series of intracellular processes including removal of the signal peptide and propeptide, glycosylation, and multimerization (Figure 4).[19] After translocation to the endoplasmatic reticulum, the signal peptide is removed to give a precursor, pro-VWF. Following glycosylation, pro-VWF dimers are formed by interprotein disulfide bridge formation through cysteine residues located in the carboxyl (C)-termini of pro-VWF subunits (‘tail-to-tail’ dimerization). In turn, these pro-VWF dimers are transported to the Golgi apparatus where they are further glycosylated and aligned in a side-by-side manner. Subsequently, amino (N)-terminal domains of pro-VWF subunits are covalently linked via interchain disulfide bridge formation. In this way, a pool of multimers with variable size, ranging from 2 to >60 subunits, is generated (‘head-to-head’ multimerization). In addition, the VWF propeptide (VWFpp) is cleaved but remains non-covalently associated with the mature VWF subunit.

Following synthesis, the differentially sized multimers are packaged into secretory granules. In ECs, VWF multimers are stored in specific, rod-shaped secretory organelles called Weibel-Palade bodies (WPBs; Figure 5A-B).[20,21] Newly formed immature WPBs are trafficked to the cell periphery where they will either undergo exocytosis basally or become anchored to F-actin allowing maturation of the WBPs for regulated release.[19,22] During maturation, multimerization is continued within the organelle and VWF multimers are

assembled into helicoidal structures or tubules (Figure 5C).[23,24] Whereas random fusion of immature WPBs with the plasma membrane accounts for basal VWF release, helical assembly of VWF in mature WPBs enables rapid, orderly secretion of massive amounts of large VWF multimers upon agonist-induced stimulation of the endothelium.

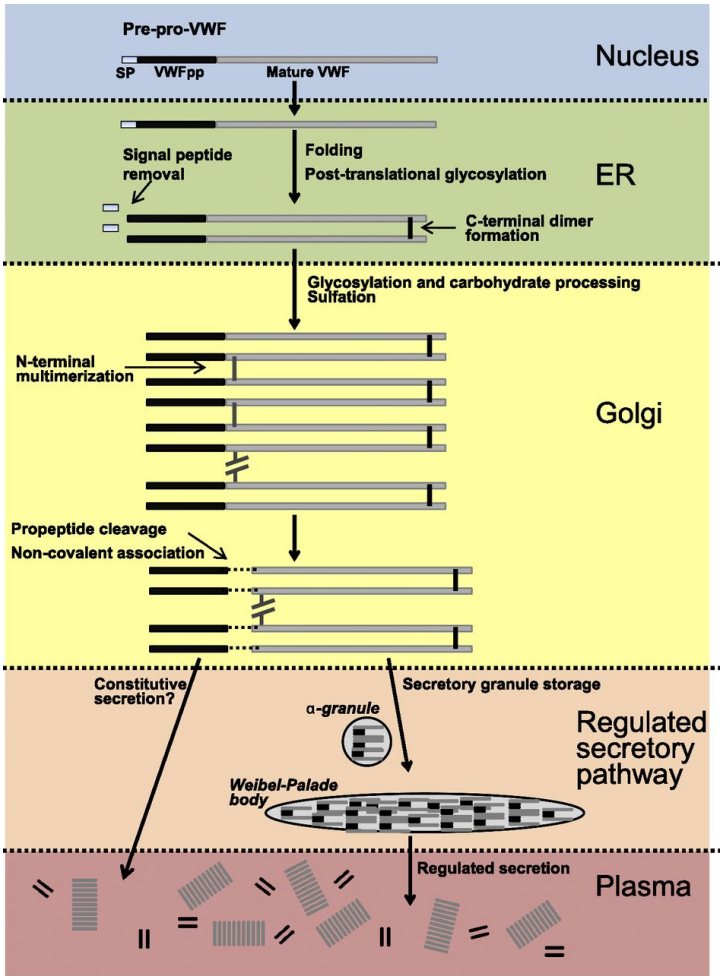

Figure 4: Intracellular processing of VWF. The *VWF* gene is transcribed as pre-pro-VWF mRNA and directed to the endoplasmatic reticulum (ER). After removal of the signal peptide, pro-VWF monomers are glycosylated and covalently linked via their carboxyl (C)-termini to form pro-VWF dimers. In the Golgi, glycosylation continues, multimers are formed via amino (N)-terminal linkage of pro-VWF dimers, and the VWF propeptide is cleaved from the mature VWF subunit. Following synthesis, VWF multimers are transported and packaged into secretory organelles. Whereas VWF in α-granules and WBPs is secreted via regulatory pathways, VWF from endothelial cells is also released in a constitutive manner. Figure adapted from Haberichter.[25]

In megakaryocytes and platelets, the VWF multimers are stored within the α-granules and also organized in tubular structures.[26] In contrast with ECs, platelets only release their VWF cargo upon agonist stimulation.

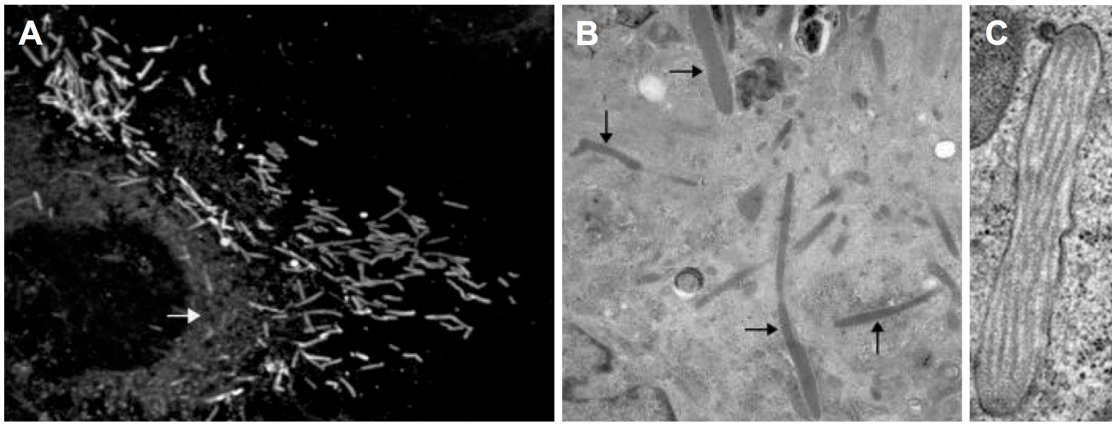

Figure 5: Morphology of Weibel-Palade bodies (WPBs) in endothelial cells. (A) Immunofluorescent image showing numerous WPBs after staining with an antibody against VWF. (B-C) Electron microscopic images demonstrating the rod-shaped size of WPBs (B, arrows) and the tubular structure of VWF within these secretory granules (C). Figures adapted from (A,B) Valentijn *et al.*[27] and (C) Metcalf *et al.*[23]

The newly synthesized VWF multimers exists in various sizes, and are referred to as low (L), medium (M), high (H), and ultra-large (UL) molecular weight (MW) VWF multimers. Under normal conditions, the LMW, MMW, and HMW VWF multimers circulate in the blood (i.e. plasma VWF), whereas the UL-VWF multimers remain in their storage organelles awaiting agonist-induced release.

1.2.2. Structure-function relationship

As mentioned above, VWF is best known for its contribution to the hemostatic process: it mediates the attachment of platelets at sites of vascular injury and act as a carrier for FVIII. The biological activity of circulating VWF depends on the ability to interact with its physiological ligands. Each VWF monomer is composed of homologous domains arranged in the following order: D1-D2-D'-D3-A1-A2-A3-D4-C1-C2-C3-C4-C5-C6-CK in which D1-D2 represents VWFpp and D'-D3-A1-A2-A3-D4-C1-C2-C3-C4-C5-C6-CK the mature VWF subunit.[28] Whereas VWFpp plays an important role in the *de novo* multimerization process and packaging of VWF[25,29,30], the mature VWF subunit contributes to platelet adhesion and aggregation. Indeed, many of the domains within the mature VWF subunit contain functional binding or cleavage sites that contribute to specific procoagulant functions (Figure 6). The D'/D3 domains interact with FVIII. The A1 domain is important for binding with GPIbα on platelets. The A1 domain is also involved in collagen binding, although the major collagen-

binding site is located within the A3 domain. The A2 domain contains the cleavage site for the VWF-cleaving protease, A Disintegrin And Metalloprotease with ThromboSpondin-1 motifs, member 13 (ADAMTS13). The C4 domain interacts with the platelet receptor GPIIb/IIIa.

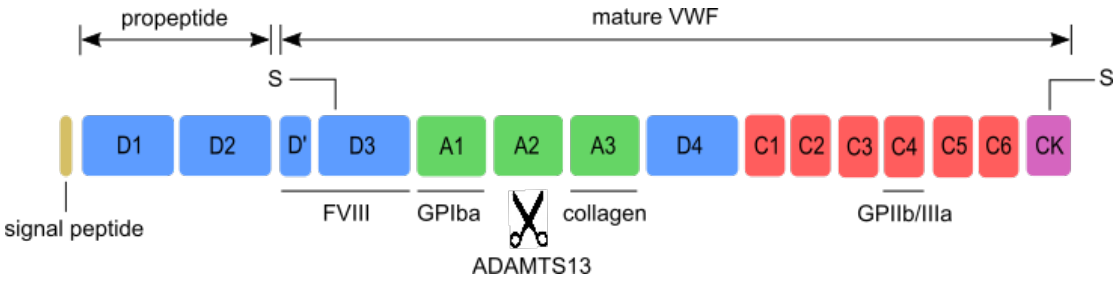

Figure 6: Domain structure of VWF. VWF is synthesized as pre-pro-VWF monomer subunit consisting of a signal peptide, a propeptide, and a mature VWF subunit. Pro-VWF monomers, consisting of the VWF propeptide and the mature VWF subunit, undergo 'tail-to-tail' dimerization and 'head-to-head' multimerization through the formation of disulfide bonds between the cysteine-rich regions in the carboxyl-terminal CK domains and amino-terminal D3 domains, respectively. The main physiological ligands of VWF as well as the ADAMTS13 cleavage site are indicated below the domains with which they interact.

The platelet-tethering function of VWF is determined by its multimeric composition and its ability to undergo structural transitions. As each monomer contains the essential elements for platelet binding, the process of multimerization markedly enhances the activity of VWF.[31,32] Experimental evidence showed that both the binding capacity for GPIb and GPIIb/IIIa, and the platelet aggregating activity under high shear conditions increases with the degree of multimerization of VWF.[33,34] These effects may be due to a higher number of binding sites in larger multimers and a higher binding affinity between HMW multimers and platelets, increasing platelet adhesion and aggregation.[35] The circulating HMW VWF multimers are therefore the most functionally efficient, whereas MMW and LMW VWF multimers are less functionally efficient.[36] Interestingly, no VWF-platelet interactions are observed in circulation under normal conditions.

In a normal situation, the majority of plasma VWF circulates in a globular, latent conformation.[37] In globular VWF, the collagen-binding site within the A3 domain is exposed, whereas the A1 domain is inaccessible for platelet binding enabling VWF to examine the blood vessel wall without unnecessary binding to platelets. In response to vascular injury,

however, the conformation of VWF rapidly alters. Via the exposed collagen-binding sites in the A3 domain, globular VWF is immobilized onto the collagen-rich subendothelial matrix. Shear forces in the blood then unfold the immobilized VWF into an elongated conformation thereby exposing the previously hidden platelet-binding sites within the A1 domains (Figure 7A). The subsequent interactions between VWF and different platelet receptors facilitate stable adhesion of platelets and the formation of a primary hemostatic plug at the site of injury, as described in section 1.1.1.

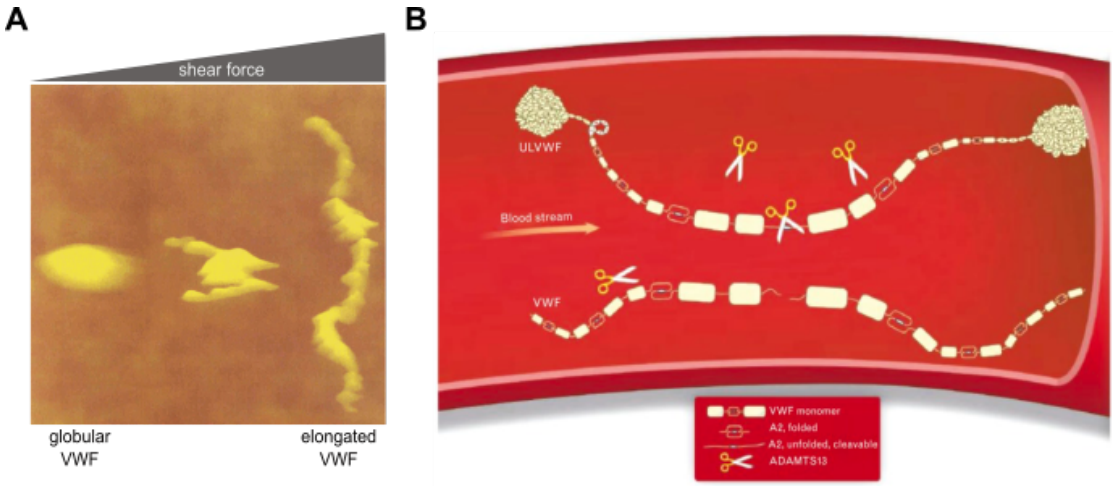

Figure 7: Shear-induced unfolding of VWF and cleavage by ADAMTS13. (A) Effect of shear forces on the conformation of VWF. In the absence of shear stress, atomic force microscopy images VWF as a globular protein. When shear forces are applied, VWF extends in the direction of the shear field and adopts an elongated conformation. (B) Size regulation of VWF by ADAMTS13. Ultra-large VWF multimers may spontaneously unfold in circulation due to their increased responsiveness to shear forces. Shear-force induced elongation of VWF exposes the ADAMTS13-cleavage site within the A2 domain of VWF enabling ADAMTS13 to cleave VWF multimers in smaller fragments. Figures adapted from (A) Siedlecki *et al.*[38] and (B) Stockschlaeder *et al.*[36]

Shear-induced unfolding of VWF does not only expose cryptic platelet-binding sites but also reveals the cryptic cleavage site for the VWF-cleaving protease, ADAMTS13. ADAMTS13 cleaves the Tyr^{1605}-Met^{1606} scissile bond within the A2 domain of VWF thereby reducing the multimer size, and hence its hemostatic activity (Figure 7B). Although this metalloprotease is constitutively active, it only cleaves VWF in response to shear since the ADAMTS13-cleavage site is shielded and resistant to proteolysis in the globular conformation. Regulation of the VWF multimer size is necessary to prevent the accumulation of highly adhesive and

hyperresponsive UL-VWF multimers in circulation. More details on how ADAMTS13 and VWF interact will be discussed in section 1.3.2.

In circulation, 1-2% of the available VWF monomers circulate as a tight non-covalent complex with 95-98% of FVIII in plasma (a ratio of 1 FVIII molecule to 50 VWF monomers).[39,40] At the site of vascular injury, FVIII is locally activated by thrombin and released from the VWF D'/D3 domains making it available as an effective procoagulant cofactor in the coagulation cascade (as described in section 1.1.2.). The VWF-FVIII interaction protects FVIII against proteolytic inactivation by plasma proteases thereby prolonging its plasma half-life from 1-2 to 12 hours. The extremely low FVIII levels and hemophilia A-like bleeding phenotype associated with the complete lack of plasma VWF illustrate the clinical importance of the VWF-FVIII interaction.[41] Additionally, the VWF-FVIII complex formation also plays a role in FVIII function, immunogenicity, and clearance.[42]

Abnormalities in either the quantity or quality of VWF multimers, especially the HMW VWF multimers, may cause a bleeding diathesis called von Willebrand disease, which will be described in section 1.2.4.

1.2.3. Clearance of VWF

In addition to its biosynthesis, clearance of VWF contributes to the steady-state levels of VWF in plasma. In the last decade, some factors and mechanisms affecting clearance kinetics and VWF survival have been identified.[19,43] Studies in humans revealed that the glycosylation pattern of VWF[44,45] and specific mutations within the *VWF* gene[46,47] affect plasma VWF levels by influencing its clearance rate. For instance, normal subjects with the O blood group or subjects with the heterozygous AA substitution R1205H within the *VWF* gene have a reduced VWF survival and lower plasma VWF levels compared to normal subjects with the non-O blood group or without mutations.[44,46]

The mechanism, by which VWF is cleared, has been partly elucidated. Recent studies have demonstrated that the basal clearance of VWF predominantly occurs in the liver, more specifically by macrophages that bind VWF through the low-density lipoprotein receptor-related protein-1 (LRP1).[48-50] The importance of macrophage LRP1 in VWF clearance is illustrated by the increased survival of VWF and the increased VWF antigen levels in

macrophage-specific LRP1-deficient mice.[50] In addition to LRP1, several other carbohydrate receptors such as the asialoglycoprotein receptor[51], Siglec-5[52], and CLEC4M[53] are identified as clearance receptors that are able to bind and internalize VWF.

In search for other determinants involved in the catabolic pathway of VWF, ADAMTS13 has also been proposed as a potential candidate.[54] However, several studies have demonstrated that removal of VWF from the circulation occurs independent of ADAMTS13.[55-57] Whether other proteases contribute to VWF clearance kinetics requires further investigation.

1.2.4. Von Willebrand disease

The average plasma concentration of VWF is 10 μg/ml[58], although variability within the population is broad[59]. Deficient or dysfunctional VWF results in von Willebrand disease (VWD), an inherited autosomal bleeding disorder first described by Erik von Willebrand in 1926. VWD is the most common bleeding disorder with prevalence up to 1% based on low VWF levels.[60,61] The incidence of bleeding requiring treatment, however, varies from 0.01% to 0.002%.[62-64] Characteristic bleeding symptoms associated with VWD include easy bruising, mucosal hemorrhages (especially epistaxis and menorrhagia), excessive bleeding from superficial wounds, bleeding from the oral cavity or gastrointestinal tract, prolonged bleeding during or after surgery, and less commonly, hemarthroses and soft tissue hematomas. The bleeding tendency is usually directly related to the extent of the deficiency or defect, although most VWD patients appear to have a mild phenotype.[65]

1.2.4.1. Congenital VWD

Congenital VWD is caused by mutations within the *VWF* gene and classified into three main categories based on quantitative (type 1 and type 3 VWD) or qualitative (type 2) abnormalities in VWF (Table 1).[66,67] Type 1 VWD accounts for 65 to 80% of all cases of VWD and is characterized by a mild to moderate reduction in plasma VWF levels and parallel decreases in FVIII levels. Epidemiological studies have indicated that 2/3 of type 1 VWD patients have identifiable *VWF* mutations, of which 70% appear to be missense mutations spread throughout the entire *VWF* gene.[67] The majority of the mutations lead to reduced expression or reduced intracellular transport of dimeric pro-VWF[68], or faster clearance of the protein from the circulation[47]. Patients present with a wide spectrum of symptoms, from asymptomatic to severe bleeding episodes, depending on the severity of the VWF and FVIII deficiency.

Table 1: Classification of VWD

VWD type	Inheritance pattern	Location mutation	Pathophysiologic mechanism	Phenotype
1	autosomal-dominant	Throughout *VWF* gene	Partial deficiency in VWF:Ag and/or FVIII	mild to moderately severe
2A	autosomal-dominant	VWF A2 domain; VWF D1, D2, D' and D3 domains; VWF CK domains	↓ platelet-dependent VWF function, ↓ HMW multimers	moderately severe
2B	autosomal-dominant	VWF A1 domain	↑ platelet-dependent VWF function, ↓ HMW multimers	moderately severe
2M	autosomal-dominant	VWF A1 and A3 domains	↓ platelet-dependent VWF function, normal multimer pattern	moderately severe
2N	autosomal-recessive	VWF D' and D3 domains	↓ binding to FVIII, normal multimer pattern	moderately severe
3	autosomal-recessive	Throughout *VWF* gene	Severe/complete deficiency in VWF:Ag and severe decrease in FVIII	severe

Type 3 VWD is characterized by very low to undetectable levels of VWF and associated low levels of FVIII due to mutations that disrupt normal VWF expression from both alleles. Despite its low prevalence (ranging from 0.5 to 5 cases per million), more than 110 mutations, primarily point mutations (missense or null) and deletions scattered over the entire *VWF* gene, have already been identified. Type 3 is the most severe form of VWD and is often associated with the occurrence of hemophilia A-like symptoms, such as soft tissue hematomas and joint bleeding, given the low levels of FVIII.

Type 2 VWD affects 20-35% of the patients and is associated with normal VWF levels but abnormal structure or function of VWF. Bleeding symptoms in patients with type 2 VWD are generally more severe than for type 1 VWD.[69] Based on the underlying defect, i.e. a mutation in one of the functional domains of VWF, type 2 VWD is divided in 4 different subtypes: A, B, M and N. (I) Subtype 2A VWD is the most common qualitative variant that is characterized by a decreased platelet-dependent function of VWF caused by the loss of HMW (and MMW) VWF multimers. Genetic defects include mutations in either VWFpp or CK domain that lead to defective multimer assembly, and mutations in the A2 domain that

increase the susceptibility to proteolysis by ADAMTS13. In addition, some genetic VWF variants are intracellular retained or degraded, or show loss of regulated storage.[70] (II) Subtype 2B VWD, is associated with increased and often spontaneous binding of VWF to platelet GPIb. This gain-of-function phenotype is caused by molecular defects residing within the A1 domain of VWF. HMW VWF multimers are lost from plasma as spontaneous binding of platelets to VWF facilitates proteolysis by ADAMTS13[71,72] and also results in faster clearance of the VWF-platelet complexes[73]. (III) In subtype 2M VWD, VWF has a decreased function despite (near-) normal multimeric distribution. The majority of mutations cause impaired binding of the A1 domain to GPIb. Defective binding to collagen (due to mutations in the VWF A3 domain) has also been reported. (IV) Finally, subtype 2N VWD is characterized by a decrease in the affinity of VWF for FVIII, caused by homozygous or compound heterozygous mutations in the VWF D' or D3 FVIII binding domain. FVIII levels are disproportional compared to VWF and vary between 5% and 40%.[74] Due to this severe reduction in plasma FVIII, the clinical phenotype is comparable to mild hemophilia A, characterized by joint and muscle hematomas.[75]

1.2.4.2. Acquired von Willebrand syndrome

Acquired von Willebrand syndrome (aVWS) is a rare clinical bleeding disorder that mimics inherited VWD. Although aVWS patients present without a personal or familial history of bleeding diathesis and mostly synthesize normal amounts of VWF, they characteristically exhibit prolonged bleeding and low VWF and FVIII levels. This hemorrhagic condition is associated with a number of underlying disorders such as cardiovascular diseases, autoimmune diseases, and lympho- and myeloproliferative disorders.[76] The pathogenic mechanism depends on the underlying disorder: (I) binding of VWF to (non-) specific autoantibodies forming immune complexes that are removed by specific immunological cells[77]; (II) adsorption of VWF onto malignant cells leading to increased clearance[78,79]; and (III) increased susceptibility for proteolysis by ADAMTS13 under conditions of high shear stress.[80,81] Although the underlying conditions may be heterogeneous, the main feature causing bleeding is the accelerated removal of the hemostatically active VWF multimers from the circulation.

1.2.4.3. Current and future treatment options

Current treatment

Current management of VWD focuses on increasing the concentration of circulating VWF in VWD patients.[82] The therapeutic approaches that are used to control and prevent bleeding depend on the type of VWD and involve the release of endogenous VWF from endothelial WPBs or the administration of exogenous VWF, whether or not in combination with adjuvant therapy.

Desmopressin (1-desamino-8-D-arginine vasopressin; DDAVP), a synthetic derivative of vasopressin, induces the secretion of endogenous VWF from WPBs resulting in a 2- to 5-fold increase in VWF levels within one hour in patients that adequately respond.[83,84] DDAVP is the treatment of choice in VWD patients expressing low levels of functionally intact VWF, i.e. the majority of type 1 VWD patients and some patients with type 2A and 2M, whereas it is ineffective in type 3 patients, and even contraindicated in type 2B patients. Treatment with DDAVP is recommended as first-line therapy for minor surgery and bleeding.

When DDAVP is ineffective, inadequate, or contraindicated, VWD patients require the administration of exogenous VWF/FVIII concentrates. This includes all patients with type 3 VWD, and most with type 2 and severe type 1 VWD. Replacement therapy is recommended for on-demand treatment of clinically significant bleeding events or for prevention of excessive bleeding in VWD patients undergoing major surgery. In addition, prophylactic use of VWF/FVIII concentrates prevents severe bleeding among the most affected VWD patients and improves quality of life.[85,86]

The use of DDAVP or VWF/FVIII concentrates is often combined with the administration of antifibrinolytic or topical agents. Whereas antifibrinolytic agents (such as aminocaproic acid) inhibit the natural process of thrombus dissolution by decreasing plasmin activity, topical agents (such as recombinant human thrombin) enhance thrombus formation at sites of application. However, both agents are considered adjunctive therapies that have been most effective with increased VWF levels.[87]

Future treatment

To overcome the hurdles associated with the use of blood as source of VWF, researchers have developed a highly pure (>99% purity) recombinant VWF (rVWF) protein by *in vitro* cell culture.[88] The major characteristic of rVWF is its homogenous and intact VWF multimer distribution, including a portion of UL-VWF multimers, which may predict a greater

hemostatic efficacy than plasma-derived VWF (Figure 8).[88,89] In a recent phase 3 clinical trial, it was demonstrated that only a single infusion of rVWF together with recombinant FVIII resolved most bleeding events in severe VWD patients without eliciting thrombotic or serious adverse events.[90] These clinical data demonstrate that use of rVWF is safe, well tolerated, and hemostatically effective in severe VWD, making it at present the most appealing alternative for current treatment.

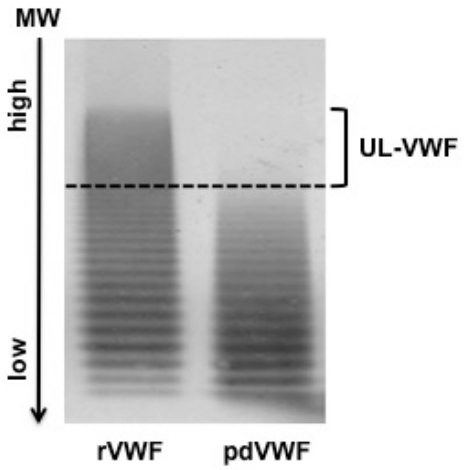

Figure 8: Electrophoretic analysis of recombinant von Willebrand factor versus plasma-derived von Willebrand factor. Multimers in recombinant von Willebrand factor (rVWF) and plasma-derived von Willebrand factor (pdVWF) were separated using a low resolution SDS-agarose gel electrophoresis and stained with a polyclonal anti-VWF antibody. Preparations of rVWF contain a high portion of ultra large (UL-) VWF multimers, whereas this portion is absent in pdVWF. Figure adapted from Turecek et al.[89]

Recently, the option of gene therapy for treatment of VWD has gained interest. Rather than relying on repetitive on-demand therapy, correction of the genetic defect would ideally cure the disease and therefore offer a long-term, possible lifelong, treatment improving the patient's quality of life. VWD is a good candidate for gene therapy: it is a monogenetic disease and as VWF is secreted into the circulation, the need for tissue- and organ-specific targeting is obviated. In 2006, our group first described the feasibility of gene therapy for type 3 VWD.[91,92] Since then, we and others have tested various gene therapeutic approaches targeting the liver using both viral[93] and non-viral gene transfer techniques[94-96] in VWD mice, albeit with limited success. Future studies that will focus on EC-targeting and long-term expression using non-viral integrating approaches will provide more insight into the therapeutic value of VWD gene therapy.

1.2.5. Differences in plasma VWF and platelet-derived VWF

Biosynthesis of VWF is restricted to ECs and megakaryocytes after which it is present in plasma, the subendothelial space, and platelets. Although EC-derived VWF, and in particular plasma VWF, and platelet-derived VWF are products from the same gene, a number of structural and functional differences have been described.[97] First, Williams *et al.* described differences in the capacity to support platelet-vessel wall interactions as platelet VWF binds more efficiently to GPIIb/IIIa and heparin, whereas it is less capable of binding to GPIb in comparison with plasma VWF.[98] Second, analysis of the carbohydrate composition revealed substantial posttranslational differences. Platelet-derived VWF exists as a distinct glycoform, with different N- and O-linked glycosylation patterns, reduced sialic acid and galactose content, and absent expression of AB blood group determinants compared to plasma VWF.[98,99] This divergent glycosylation profile renders platelet-derived VWF more resistant to proteolysis by ADAMTS13[100,101] and may also mediate the differences in functional properties[98]. A third important difference between platelet-derived VWF and plasma VWF is the difference in multimeric organization. Whereas VWF in plasma is distributed as a range of multimers, VWF in platelets is enriched in hemostatically active multimers.[102-104] Altogether, these differences support the idea that VWF function is determined in part by its compartimentalization. Therefore, it is of interest to unravel the relative contribution of EC-derived VWF, in particular plasma VWF, and platelet-derived VWF to hemostasis. To date, research groups have already used various animal models for VWD to gain better insights into the compartimental role of VWF. These animal models include pigs[105], dogs[106], and genetically modified mice[107]. Similar to human type 3 VWD, no VWF is detectable in plasma, platelets, and ECs of these VWD animals. In addition, VWD animals have low levels of circulating FVIII and exhibit prolonged bleeding times upon experimental injury.

Since 10-20% of the total VWF content is present in platelets and very little is thought to be released in a constitutive manner, it is generally believed that EC-derived, and in particular plasma VWF, plays a major role in hemostasis. Evidence for this role stems from experiments of crossed bone marrow transplantations (BMT) carried out in normal and VWD pigs. In normal animals transplanted with VWD bone marrow that produced EC-derived VWF but lack platelet VWF, the bleeding time was partially corrected.[108] In line with these observations, VWD pigs or VWD dogs in which plasma VWF was reconstituted by means of infusion of VWF concentrate also showed, respectively, partial or full correction of the

bleeding phenotype.[109,110] In addition, more recent data obtained in mice also point towards a crucial role of EC-derived VWF, and in particular plasma VWF, in hemostasis. Transplantation of VWD bone marrow in normal mice or restoration of plasma VWF via hydrodynamic injection of VWF-expressing plasmid DNA in VWF deficient mice resulted in normal bleeding times upon experimental injury.[96,111] All together, these data suggest that plasma VWF is necessary although not always sufficient to completely correct the bleeding phenotype.

Indeed, there is a vast body of evidence suggesting a role of platelet-derived VWF in primary hemostasis. For example, by performing *in vitro* perfusion studies, it has been shown that when normal platelets are resuspended in VWD plasma, platelet deposition on collagen was significantly higher than when VWD platelets are resuspended in VWD plasma.[111,112] Additional evidence is derived from crossed BMT carried out in normal and VWD pigs or VWD mice demonstrating that the bleeding time in some, but not all, chimeric animals that have platelet VWF but lack EC-derived VWF was partially corrected.[110,111,113] These data are consistent with the slightly increased bleeding time that was observed in chimeric pigs expressing only EC-derived VWF upon experimental injury.[108] Interestingly, clinical observations from type 1 VWD patients further contribute to the idea that platelet VWF is necessary for normal hemostasis. Whereas type 1 VWD patients with normal platelet VWF levels have almost normal bleeding times, prolonged bleeding times are found in patients with low platelet VWF.[114] In addition, not only in VWD patients, but also in healthy individuals an inverse relationship between platelet VWF and bleeding time has been demonstrated indicating that platelet VWF is major determinant of primary hemostasis.

1.3. ADAMTS13

In normal circulation, the size, and hence hemostatic activity, of newly secreted VWF or VWF free in circulation is modulated by the VWF-cleaving protease called ADAMTS13.

1.3.1. Biosynthesis and secretion

The *ADAMTS13* gene is located on chromosome 9 and spans 29 exons encompassing approximately 37 kb.[115] The transcript of full-length ADAMTS13 is approximately 5 kb and encodes a 1427 AA protein. ADAMTS13 is primarily synthesized and released from hepatic stellate cells that reside in the interstitial area of the liver.[116,117] Synthesis of ADAMTS13 has also been observed in vascular ECs.[118,119] Although ECs only produce trace amounts of ADAMTS13 *in vitro*, the constitutive release from these cells may be an important source of circulating plasma ADAMTS13 considering their vast number throughout the vasculature. In addition, variable expression of ADAMTS13 has been found in megakaryocytes and platelets[120,121], glomerular podocytes[122], and glial cells[123]. It is secreted into the circulation as an active, glycosylated multidomain protease that is divided into an N- and a C-terminal part (Figure 9).[124]

1.3.2. Structure-function relationship

Similar to other proteases belonging to the ADAMTS family, the N-terminal part consists of a metalloprotease (M) domain, a disintegrin-like (D) domain, the first thrombospondin type 1 repeat (T), a cysteine-rich (C) domain, and a spacer (S) domain (MDTCS part). The C-terminal regions are more variable within the ADAMTS family. In case of ADAMTS13, the C-terminal part comprises 7 additional thrombospondin type 1 repeats (T2-T8) and 2 Complement component C1r/C1s, Urinary epidermal growth factor and Bone morphogenetic protein-1 (CUB) domains (T2-C2 part) (Figure 9).

Plasma ADAMTS13 circulates as a constitutive active enzyme that binds and cleaves the Tyr^{1605}-Met^{1606} bond within the A2 domain of VWF thereby regulating the size of VWF multimers in circulation. This cleavage, however, is the result of a multistep process in which both N- and C-terminal portions are involved: Whereas the N-terminus contributes to the recognition and productive cleavage of VWF, the C-terminus is involved in initial docking to VWF and the regulation of ADAMTS13 activity.

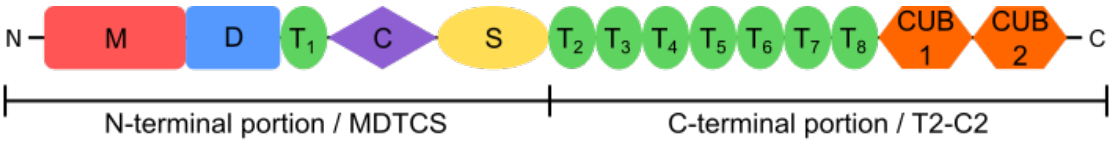

Figure 9: Domain structure of ADAMTS13. Full-length human ADAMTS13 consists of a metalloprotease (M) domain, a disintegrin-like (D) domain, the first thrombospondin type-1 repeat (T_1), a cysteine-rich (C) domain, a spacer (S) domain, 7 additional thrombospondin type-1 repeats (T_2-T_8), and 2 Complement component C1r/C1s, Urinary epidermal growth factor and Bone morphogenetic protein-1 (CUB) domains. The M, D, T, C, and S domains are part of the amino (N)-terminal portion of ADAMTS13, whereas T2-T8 and the 2 CUB domains belong to the carboxyl (C)-terminal portion.

1.3.2.1. The amino-terminal portion of ADAMTS13

The M domain contains the proteolytic site that cleaves the Tyr^{1605}-Met^{1606} bond in the VWF A2 domain. The M domain is characterised by the presence of zinc- and calcium-binding sequences that ensure the enzymatic activity and structural integrity of the catalytic site.[125] The M domain alone, however, has little or no specific catalytic activity towards VWF substrates.[126,127] Kinetic studies using recombinant ADAMTS13 proteins revealed that the addition of other non-catalytic domains within the N-terminal portion of ADAMTS13 increases the cleavage specificity and efficiency.[126,127] It is currently known that VWF-binding exosites within the DTCS-region of ADAMTS13 work in concert and extensively interact with exosites in the A2 domain of VWF thereby positioning the Tyr^{1605}-Met^{1606} bond into the cleavage cleft (Figure 10).[128] Despite the coherent actions of the proximal domains, ADAMTS13-mediated cleavage only occurs when the VWF A2 domain is unfolded. In contrast with globular VWF in which the ADAMTS13-cleavage site is shielded and highly resistant to proteolysis, shear stress-induced unfolding of the A2 domain exposes the Tyr^{1605}-Met^{1606} bond. Subsequently, further unravelling exposes new regions within the C-terminal region of the VWF A2 domain that are engaged by complementary exosites present in the DTCS-region of ADAMTS13.[129-131] Finally, the scissile bond is docked into subsites of the M domain of ADAMTS13 and positioned for cleavage.[132]

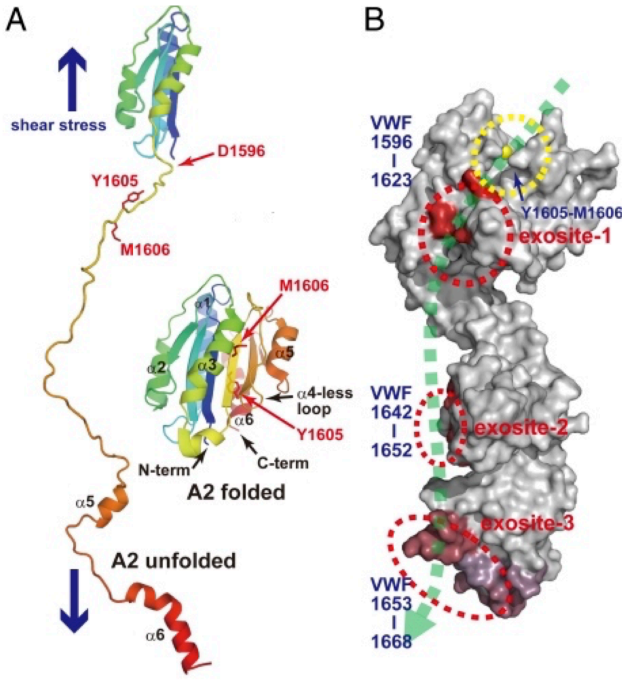

Figure 10: VWF-ADAMTS13 exosite interactions. (A) The secondary structure of the folded and unfolded VWF A2 domain. In absence of shear, the ADAMTS13-cleavage site (Y1605-M1606) is buried and resistant to proteolysis. When shear stress is applied, the A2 domain unfolds and subsequently exposes both the scissile bond and exosite-binding regions. (B) VWF-MDTCS binding model. The surface of the amino-terminal portion, MDTCS, is shown in grey. Zinc ions, shown in yellow, are bound in the catalytic cleft that is indicated by a yellow dotted ellipsoid. The red dotted ellipsoids represent the exosites within MDTCS that engage complementary binding sites in the VWF A2 domain that is indicated as a green dotted line. Figure is adapted from Akiyama *et al.*[129]

1.3.2.2. The carboxyl-terminal portion of ADAMTS13

To date, much less is known about the role of T2-T8 and the 2 CUB domains. Whereas some studies have shown that T2-C2 is dispensable for protease function under both static[126] and flow[133] conditions, other studies have demonstrated that distinct functions may be attributed to these domains. In 2009, our group and others found that the C-terminal ADAMTS13 domains T5-C2 are able to interact with the surface-exposed D4CK domain in soluble (globular) VWF.[134,135] Because the nature of this interaction was different to the binding that is required for proteolysis, the authors suggested that these distal domains probably serve as a docking site for VWF and participate as the initial step in a multistep reaction finally leading to proteolysis. This idea is in line with the *in vitro* observations that both the thrombospondin type 1 repeats (T2-T8) and 2 CUB domains cooperate to recognize VWF under flow.[133,136] The physiological relevance was supported by observations made in murine studies. Banno *et*

al. demonstrated that thrombus growth in mice lacking the 2 C-terminal thrombospondin type 1 repeats (T7-T8) and 2 CUB domains was accelerated compared to mice encoding full-length ADAMTS13.[137] In addition, our group showed that removal of the CUB domains in murine ADAMTS13 abolished the processing of VWF strings on stimulated endothelium.[138] These data suggest that the C-terminal portion of ADAMTS13 positively regulates VWF processing and subsequent thrombus formation under flow.

In addition, recent evidence has demonstrated that the C-terminal domains of ADAMTS13, and in particular the CUB domains, may negatively regulate the function of ADAMTS13. Data from our and other groups revealed that the addition of specific monoclonal antibodies targeting the CUB domains to human ADAMTS13 enhanced its proteolytic activity and revealed cryptic epitopes within the S domain under static conditions.[139-141] Based on these initial data, it is now proposed that ADAMTS13, similar to VWF, undergoes conformational changes regulating its activity. In a normal situation, the CUB domains interact with the central S domain, an interaction that results in the folding of ADAMTS13. In this globular, folded conformation, critical VWF A2 domain-binding exosites within the S domain are shielded and unable to support efficient binding to VWF. Interestingly, ADAMTS13 unfolds upon docking of the CUB domains to VWF D4CK. In this unfolded conformation, the exosites within the S domain are able to directly engage the complementary binding sites within VWF A2 thereby enhancing the cleavage process.

In conclusion, these data demonstrate that ADAMTS13-mediated cleavage of VWF is a multi-step process (Figure 11A). This process is initiated by the docking of the C-terminal domains within ADAMTS13 to VWF D4CK. Whereas binding of the distal ADAMTS13 domains to VWF D4CK in globular VWF is unproductive, binding to D4CK in elongated VWF triggers new interactions as the unfolded VWF A2 domain exposes high affinity binding sites for the proximal ADAMTS13 domains. High affinity binding of the ADAMTS13 S domain is followed by additional interactions between the remaining DTCS domains and exosites within VWF A2. Altogether, these interactions position the catalytic site of the M domain towards the scissile bond, Tyr^{1605}-Met^{1606}, which results in VWF proteolysis.

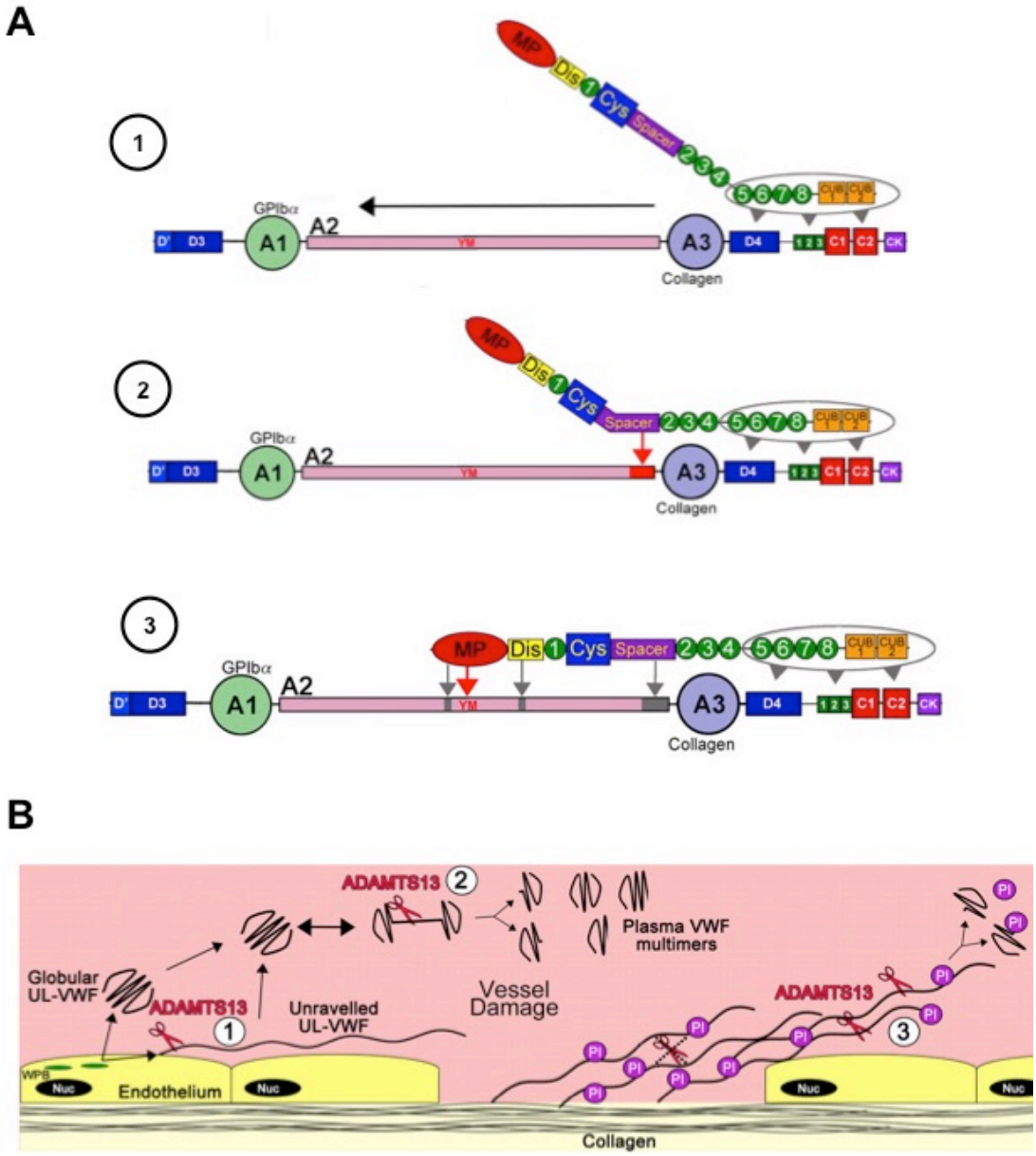

Figure 11: ADAMTS13-mediated cleavage of VWF. (A) Schematic representation of the interaction between full-length ADAMTS13 and VWF leading to VWF proteolysis. 1) Docking of the distal ADAMTS13 domains to VWF D4CK enables binding of ADAMTS13 to VWF. 2) Unfolding of the VWF A2 domain facilitates binding of the ADAMTS13 spacer domain to the VWF A2 domain. 3) High affinity binding of the spacer domain unfolds ADAMTS13 enabling the proximal ADAMTS13 domains within the DTCS region to interact with additional exosites within VWF A2. Following these interactions, the catalytic site of ADAMTS13 within the metalloprotease domain is positioned to engage and cleave the Tyr^{1605}-Met^{1606} scissile bond. (B) Schematic representation of the location of ADAMTS13-mediated cleavage of VWF. 1) Upon exocytosis from Weibel-Palade bodies (WPBs), UL-VWF can be directly secreted in the circulation, whereas a portion can remain attached to the endothelium. Endothelial-bound VWF becomes stretched in response to shear forces in the circulation that facilitates cleavage by ADAMTS13. The resulting smaller multimers are released in

circulation and adopt a globular, latent conformation. 2) Shear-induced unfolding of globular VWF may occur during passage through microvessels. Spontaneous unravelling of UL-VWF exposes the scissile bond that is cleaved by ADAMTS13 under normal conditions. Smaller multimers are less responsive to shear forces and maintain the globular conformation. 3) At sites of vascular injury, plasma VWF binds to exposed collagen, unfolds, and recruits platelets. Whereas ADAMTS13 is locally inactivated, it may process bound VWF multimers downstream of injury site thereby regulating platelet aggregation. Figures adapted from Crawley *et al.*[142]

ADAMTS13 is constitutively active with no specific inhibitor found in plasma. The importance of conformational changes within the VWF A2 domain implies that the activity of ADAMTS13 is regulated at the substrate level. Indeed, ADAMTS13 becomes functionally relevant when shear stress induces VWF stretching, a situation that seems to occur at 3 distinct locations in the circulation (Figure 11B): (I) when VWF is tethered to the endothelial surface upon secretion[143], (II) when VWF circulates free in plasma[144], or when VWF binds downstream of the site of injury[142]. Regardless of the location, the scissile bond and exosites are more easily exposed in the highly adhesive UL-VWF multimers due their increased responsiveness to shear stress. By cleaving UL-VWF when it is partially unfolded by shear stress, ADAMTS13 helps to maintain VWF in smaller, less reactive forms that experience less shear and adopt a quiescent, globular conformation.

Regulating the VWF multimer size by ADAMTS13 is crucial for normal hemostasis. Increased susceptibility for ADAMTS13 cleavage results in the loss of circulating HMW VWF multimers and bleeding episodes (type 2A VWD; see section 1.2.4.1.), whereas lack of ADAMTS13 activity results in the persistence of circulating UL-VWF multimers and increases the risk for thrombotic events (see section 1.4).

1.4. THROMBOTIC THROMBOCYTOPENIC PURPURA

Modulation of the VWF multimer size by ADAMTS13 is crucial in maintaining hemostasis. If left unchecked, thrombosis instead of hemostasis may occur. Thrombotic thrombocytopenic purpura (TTP) is a life-threatening disease caused by a deficiency in ADAMTS13 that is either the result of mutations in the *ADAMTS13* gene (congenital or hereditary TTP) or the presence of anti-ADAMTS13 antibodies (acquired TTP). Severely deficient ADAMTS13 function results in the presence and persistence of highly adhesive UL-VWF multimers in circulation (Figure 12) which can unfold and expose cryptic platelet-binding sites in the absence of vascular injury.[145] The spontaneous tethering of platelets to unfolded circulating VWF leads to the formation of circulating platelet aggregates which in turn can occlude microvessels (Figure 13). Consequently, widespread microvascular thrombosis in various organs may lead to ischemic organ failure and ultimately death if left untreated.

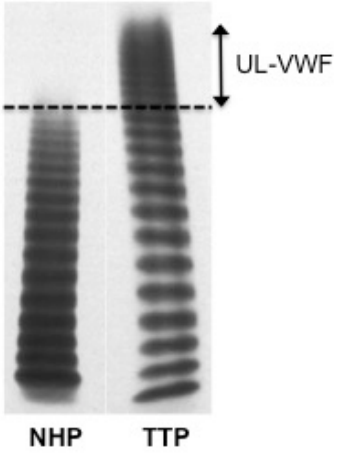

Figure 12: Presence of UL-VWF multimers in patients with a severe deficiency of ADAMTS13 activity. The distribution of VWF multimers in plasma of normal individuals (NHP) and a patient with no ADAMTS13 activity (TTP) was analyzed by SDS-agarose gel electrophoresis. Whereas no UL-VWF multimers are found in NHP, UL-VWF multimers do appear in plasma when ADAMTS13 activity is absent (TTP). The dotted line indicates the area of UL-VWF multimers. Adapted from Veyradier *et al.*[146]

TTP is a rare thrombotic disorder with an estimated annual incidence of 6 cases per million per year in the UK.[147] Based on the primary mechanism causing a deficiency in ADAMTS13 activity, TTP can be clinically classified into 2 major forms, congenital or acquired TTP.

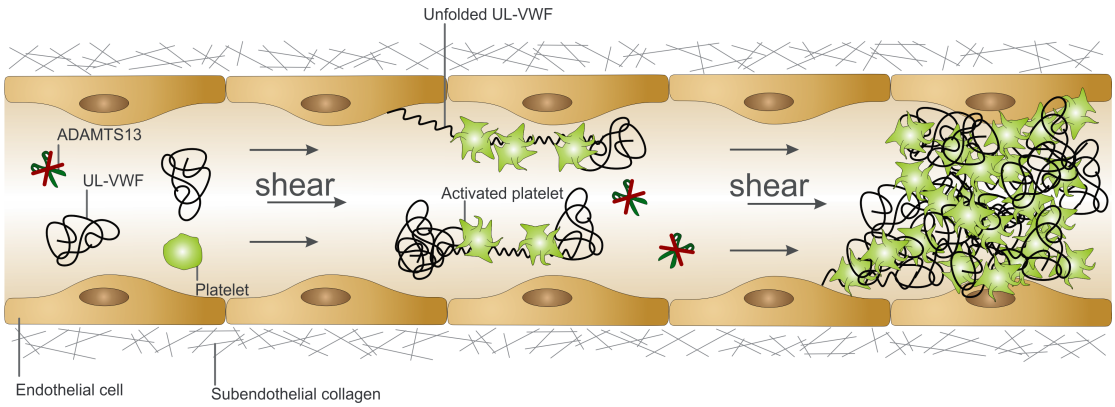

Figure 13: Pathophysiology of TTP. Severe ADAMTS13 deficiency, either the result of mutations in the *ADAMTS13* gene or of autoantibodies directed against the circulating protease, leads to the persistence of ultra large (UL-) VWF multimers at the endothelial surface or in circulation. In areas of high shear stress (such as in arterioles or capillaries) these highly adhesive molecules may unfold and spontaneously recruit platelets. In turn, the resulting circulating VWF-rich platelet aggregates may obstruct the microvasculature causing tissue ischemia and organ failure.

1.4.1. Congenital TTP

Congenital (or hereditary) TTP, also known as Upshaw-Schulman syndrome, is a rare recessively inherited disease that accounts for ≤5% of all TTP cases.[115,148] To date, more than 140 mutations distributed throughout the *ADAMTS13* gene have been identified. The majority of these mutations are single amino acid missense substitutions while the remaining part include deletions, insertions, nonsense mutations, and intronic splice site mutations.[149] Whereas heterozygous carriers have half-normal ADAMTS13 activity in plasma (40-70% of normal values) and are generally asymptomatic, individuals with homozygous or compound heterozygous mutations have a severe ADAMTS13 deficiency (<10% of normal value) and most certainly develop TTP.[150] Via site-directed mutagenesis and expression studies *in vitro* it has been demonstrated that *ADAMTS13* mutations are associated with impaired synthesis, catalytic activity, or secretion.[151,152] The genetic heterogeneity is reflected in the variable clinical presentation of congenital TTP patients in terms of disease onset and severity. This variability could at least be partly explained by the residual ADAMTS13 activity found in the patient's plasma which is influenced by the *ADAMTS13* genotype.[153] However, it is generally accepted that additional factors besides *ADAMTS13* mutations also contribute to the unpredictable nature of congenital TTP. Other genetic defects, such as mutations in complement factor H gene, have been suggested.[154] On the other hand, environmental/external triggers are known to influence the phenotype as patients often

encounter a first bout of TTP in situations that are associated with VWF release and elevated VWF levels, such as pregnancy or infection.[155-157]

1.4.2. Acquired TTP

In acquired TTP, which accounts for the majority of the TTP cases (95%), a severe deficiency in ADAMTS13 function is caused by autoantibodies directed against the circulating protease.[149] In most acquired TTP patients the antibody-mediated ADAMTS13 deficiency is not associated with an underlying clinical condition ('idiopathic' TTP). Epitope analysis revealed that most TTP patients harbour type G immunoglobulins that target multiple domains of ADAMTS13.[158] Antibodies against the N-terminal part of the protease are found in more than 90% of the acquired TTP patients, while antibodies directed against the C-terminal domains are present in 30-50% of the patients.[149] Pathogenic autoantibodies can contribute to severe ADAMTS13 deficiency (<10% of normal activity) through direct inhibition of ADAMTS13. It has been shown that the majority of these inhibitory autoantibodies primarily target antigenic sites within the spacer domain, which plays a critical role in substrate recognition.[131,159,160] Direct inhibition of ADAMTS13, however, is not the only pathogenic mechanism responsible for ADAMTS13 deficiency. Scheiflinger *et al.* reported a patient with confirmed TTP who presented with high titer anti-ADAMTS13 antibodies that did not neutralize the protease activity.[161] In a more recent cohort study Thomas *et al.* demonstrated that acquired TTP patients lacking detectable inhibitory antibodies often have very low ADAMTS13 antigen levels.[160] These data suggest that antibody-mediated clearance of ADAMTS13 antigen is a major cause of loss of ADAMTS13 activity in acquired TTP patients.

1.4.3. Clinical presentation and diagnosis

The onset of disease is usually acute, although flu-like symptoms may manifest during the preceding days. The clinical presentation is characterized by thrombocytopenia, microangiopathic hemolytic anemia, and widespread microvascular thrombosis with consequent clinical manifestations. Thrombocytopenia can be explained by the consumption and incorporation of platelets in VWF-rich microthrombi, while hemolytic anemia, characterized by the presence of schistocytes (fragmented red blood cells) in peripheral blood smears, is due to the mechanical rupture of RBCs in the obstructed microvasculature (Figure 14). The widespread presence of thrombi in terminal arterioles and capillaries is associated

with tissue ischemia and organ injury.[162,163] In most cases, this results in cerebral (e.g. confusion, seizures, and coma), renal (e.g. hematuria and proteinuria), and cardiac manifestations (e.g. congestive heart failure, infarction, and arrhythmias).[164] After onset, the disease rapidly progresses and runs a fatal course as the majority of patients die when not properly treated.

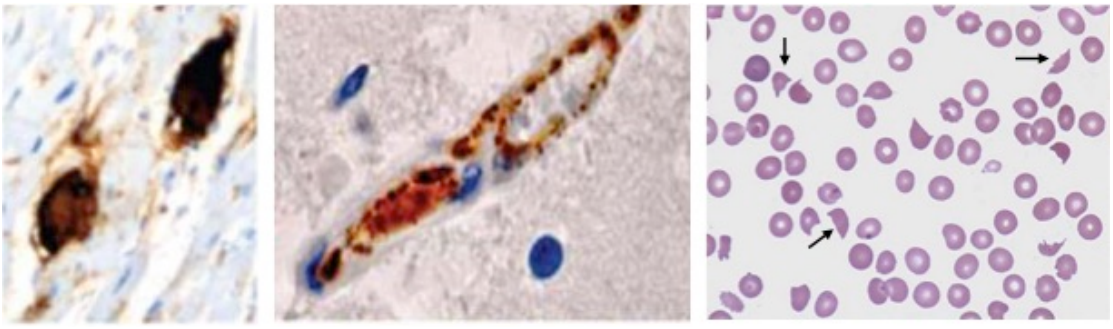

Figure 14: VWF-rich microthrombi and hemolytic anemia in acute TTP. (Left and middle panel) Immunohistopathology of TTP. Severe ADAMTS13 deficiency may lead to spontaneous recruitment of platelets by UL-VWF multimers resulting in the dissemination of VWF-rich (brown) microthrombi in arterioles and capillaries of multiple organs such as the heart (left) and brain (middle). (Right panel) Peripheral blood smear from a TTP patient showing numerous fragmented red blood cells, also known as schistocytes, which suggest the occurrence of haemolytic anemia. A few schistocytes are indicated with an arrow. Adapted from Tsai *et al*.[163] (left and middle panel) and www.ezio.com.br (right panel)

A definitive diagnosis based on the initial clinical assessment, however, is difficult as not all TTP patients present with these clinical features and clinical presentation may overlap with other thrombotic microangiopathies (TMA), such as hemolytic uremic syndrome and malignancy-associated TMA.[165] Therefore, measuring the plasma ADAMTS13 activity is helpful to confirm clinical diagnosis.[166,167] Although multiple methodologies exist, a fluorescent resonance energy transfer technique using a short 73 amino acid VWF peptide containing the ADAMTS13-cleavage site to detect cleavage is frequently performed in clinical laboratories.[168,169] Whereas other TMAs are associated with normal or mildly reduced plasma ADAMTS13 activity, TTP is most often characterised by a severe ADAMTS13 deficiency. Once low activities have been demonstrated, detection of anti-ADAMTS13 autoantibodies is required to confirm the diagnosis of acquired TTP. If no autoantibodies are found, sequencing of the ADAMTS13 gene may confirm the suspicion of congenital TTP. Additional, routine testing includes blood films, liver function tests, and pregnancy testing.[149]

1.4.4. Treatment

1.4.4.1. Current treatment options

Acute TTP episodes require prompt treatment in specialized centers. For more than 20 years, the use of plasma exchange (PEX) or plasma infusion has been crucial in the management of TTP episodes, reducing mortality rates from 90% to 10-20%.[170,171] PEX not only replaces the deficient or inhibited ADAMTS13 by active ADAMTS13 from donor plasma, but also removes potential disease-causing factors such as autoantibodies or bacterial toxins from the circulation. In contrast, plasma infusion only replenishes ADAMTS13 activity in acquired TTP patient's plasma. PEX is superior to plasma infusion for acquired TTP and should be initiated once a presumptive diagnosis is made.[170] When the initiation of plasma exchange is delayed, plasma infusion can provide temporary benefit.[172,173] The number of PEX required to achieve remission (i.e. normalization of platelet count) depends on the severity of initial disease or progression of the symptoms during admission. In general, patients with acquired TTP require a higher number of PEX and longer treatment to normalize platelet counts compared to congenital TTP patients.

In patients with acquired TTP, immunosuppressive drugs are used as adjuvant therapy to PEX. Immunosuppressive agents tone down the immune response and suppress the production of new autoantibodies. Consistent use of corticosteroids in addition to PEX seems to further increase survival and to reduce the frequency of relapses, especially in patients with severe acquired ADAMTS13 deficiency.[174] Recently, rituximab, a humanized anti-CD20 monoclonal antibody, has been shown to be a safe and effective adjunct to PEX, especially in patients with refractory or relapsing TTP.[174,175] Standard intravenous rituximab treatment (375 mg/m^2 weekly for 4 weeks) results in B-cell depletion, reduced anti-ADAMTS13 antibody titers and increased plasma ADAMTS13 activity in most patients.[174] Early administration, preferably within the first 3 days, is associated with faster attainment of remission, fewer number of PEX, shorter hospitalization, and a reduced relapsing risk.[176] These benefits have stimulated the use of rituximab as prophylactic therapy in patients with a history of TTP and deficient ADAMTS13 activity in remission. Although preventive rituximab infusions maintained a sustained remission in these patients, concerns regarding overtreatment and increased susceptibility for infections are raised.[177] Therefore, a risk/benefit ratio on an individual patient level has yet to be made.

Patients with known congenital TTP usually respond well to plasma infusion when admitted to the hospital. Once in remission, prophylactic plasma infusions alone are generally

sufficient to prevent TTP relapses for many years.[178] The frequency of prophylactic treatment is empirically determined, although residual plasma ADAMTS13 activity has been identified as a useful biomarker.[153] Patients having low residual activity and/or suffering from frequent recurrences require intermittent plasma infusions every 3-4 weeks in order to prevent symptomatic TTP episodes, while patients with higher residual activity only require prophylaxis in context of eliciting triggers (e.g. pregnancy or infection).[153]

1.4.4.2. Animal models for TTP

Since the introduction of PEX in clinical practice, survival rates did not further increase during the last 20 years. In addition, safer and more accessible alternatives for PEX are also highly warranted. The use of animal models is indispensable to validate novel treatment strategies. During the last ten years, several animal models for both congenital and acquired TTP have been established.[179]

Animal models for congenital TTP

In 2005, two independent research groups generated ADAMTS13 deficient (*Adamts13*$^{-/-}$) mice on a 129/Sv genetic background[180] and a mixed C57BL/6J x 129X1/SvJ genetic background[181] by disrupting the *Adamts13* gene through the insertion of a neomycin resistance cassette. Despite the complete lack of ADAMTS13 activity and the accumulation of UL-VWF multimers in plasma, *Adamts13*$^{-/-}$ mice did not spontaneously develop TTP.[180,181] Elevation of the plasma VWF antigen levels by backcrossing to the CASA/Rk genetic background (which is associated with 5-10 fold higher VWF levels[182]) into mixed C57BL/6J x 129X1/SvJ *Adamts13*$^{-/-}$ mice increased the frequency of TTP symptoms.[181] These observations indicated that the etiology of TTP cannot be explained by a defect in the *Adamts13* gene alone and secondary triggers may promote pathological thrombus formation, which is in accordance with clinical observations in humans.[183]

Given the need for a second hit, external triggers have been evaluated in *Adamts13*$^{-/-}$ mice. So far, administration of large amounts of exogenous rVWF (either human or murine VWF)[184,185] or *Escherichia coli*-derived shigatoxin[181], have been shown to successfully elicit TTP symptoms that resemble human TTP. With respect to the shigatoxin-induced TTP model, it has been demonstrated that EC activation and subsequent release of EC-derived VWF upon infusion of shigatoxin, are an absolute requirement to trigger TTP symptoms in this model.[186,187] Although these models suggest that external triggers associated with

increased levels of circulating VWF are sufficient to induce TTP symptoms in *Adamts13*$^{-/-}$ mice, also other factors (e.g. genetic factors) appear to determine the TTP phenotype.[181,186]

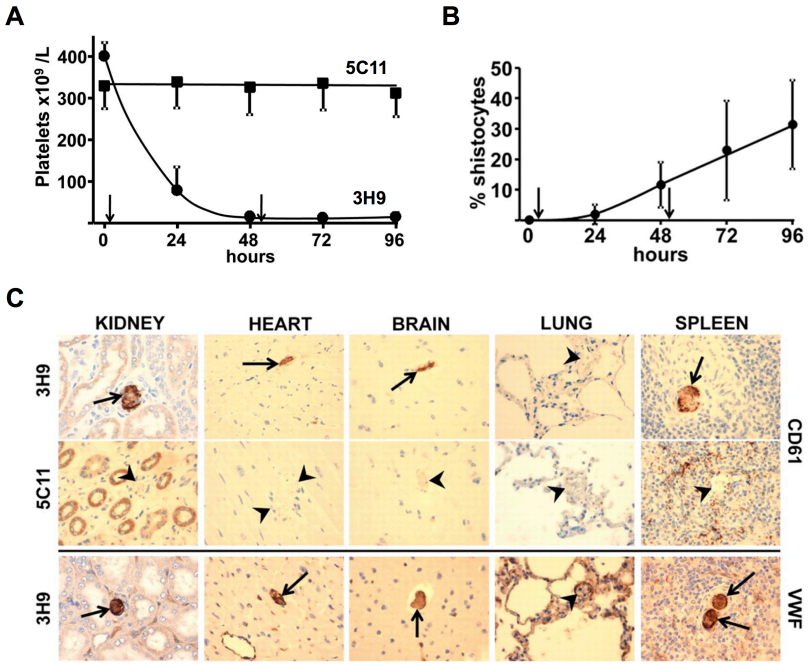

Figure 15: Clinical signs of acquired TTP in baboons (*Papio Ursinus*). Systemic inhibition of ADAMTS13 activity in subject animals was achieved following intravenous administration of 2 boluses of the inhibitory anti-ADAMTS13 antibody, 3H9 (600 µg/kg), over the course of 2 days. Control animals were treated with a non-inhibitory anti-ADAMTS13 antibody, 5C11. (A) Severe thrombocytopenia was observed within 24 hours in subject animals whereas normal platelet counts were observed in control animals. (B) Microangiopathic hemolytic anemia was evidenced by the continuous increase in the number of schistocytes in peripheral blood smears of subject animals. (C) Widespread microvascular thrombosis was confirmed by histopathologic analysis demonstrating deposition of VWF- and platelet (CD61)-rich aggregates in various organs of subject animals. Figures adapted from Feys *et al.*[188]

Animal models for acquired TTP

To date, acquired TTP models have been established in mice[185,189], rats[190], and baboons[188]. In mice, two research groups achieved acquired ADAMTS13 deficiency following administration of cross-reacting human monoclonal anti-ADAMTS13 antibody fragments derived from acquired TTP patients.[185,189] In rats and baboons, our group employed polyclonal goat anti-ADAMTS13 antibodies[190] or murine monoclonal antibodies[188], respectively, to inhibit ADAMTS13 activity. Whereas full inhibition of ADAMTS13 in non-

human primates resulted in symptoms that were representative for the early stages of acquired TTP[188] (Figure 15), no TTP symptoms were observed when an acquired deficiency was induced in rodents as observed for *Adamts13*$^{-/-}$ mice[185,189,190]. In rats and mice, the administration of an additional trigger such as rVWF or shigatoxin was needed to elicit TTP symptoms in a dose-dependent manner.

1.4.4.3. Future treatment options

In patients that still die, the formation of VWF-rich thrombi is probably disrupted not fast enough. Therefore, new agents that interfere with the binding of VWF to platelets or that process the highly adhesive UL-VWF multimers (thereby restoring the normal VWF multimer distribution) are being explored:

Blocking the VWF-GPIb interaction

One novel strategy encompasses the blockade of the VWF-GPIb interaction, thereby preventing the formation of VWF-rich platelet thrombi. By using agents that target the VWF A1 domain, our group and others provided proof of principle for this approach in the non-human primate model for acquired TTP.[191-193] Recently, a single-variable domain immunoglobulin (nanobody), called Caplacizumab, was tested in a multicentre phase II randomized, placebo-controlled trial, in which acquired TTP patients were given Caplacizumab as an adjunct to daily PEX.[194,195] Caplacizumab-treated patients achieved faster platelet normalization and developed less recurrent thrombocytopenia that required initiation of PEX <30 days after the last PEX therapy.[195] Interestingly, only minor bleeding episodes and manageable side effects were observed in patients in the active drug treatment arm. These data, together with data obtained from a less comprehensive clinical trial[196], suggest that by preventing the interaction between VWF and platelets, the standard of care of TTP patients might improve.

Recombinant ADAMTS13

Another promising future therapy is the use of recombinant ADAMTS13 (rADAMTS13) as a safer and simpler substitute for human plasma. Preclinical animal studies have demonstrated that administration of rADAMTS13 before or after induction of TTP in *Adamts13*$^{-/-}$ mice reduced the incidence of severe thrombocytopenia and organ damage.[184] A phase I clinical trial was recently initiated to assess rADAMTS13 in the treatment and prophylaxis of

congenital TTP. Although the approach seems more applicable to congenital TTP patients, our group and others have shown that rADAMTS13 is able to restore ADAMTS13 activity in the context of acquired TTP.[190,197] An elegant way to circumvent autoantibody inhibition of rADAMTS13 may be the administration of autoantibody-resistant ADAMTS13 variants[159] or platelet-delivered rADAMTS13[185].

Reduction of the VWF multimer size

Chen and colleagues demonstrated that VWF multimer size can be pharmacologically decreased with N-acetylcysteine (NAC), a drug that has long been used to treat acetaminophen toxicity and chronic obstructive lung disease.[198] Since administration of NAC in *Adamts13*$^{-/-}$ mice reduced the size of circulating UL-VWF multimers by reducing intrachain disulfide bonds, it is believed that NAC can reduce the size of UL-VWF multimers in TTP patients.[198] Human case reports on TTP treatment with NAC however demonstrated varying outcomes and a clinical trial is currently ongoing to test its efficacy under controlled conditions.[199-202] Another new treatment strategy that recently gained interest is the activation of plasminogen using thrombolytic agents. Plasmin indeed was shown to cleave VWF resulting in a reduction of TTP symptoms in a mouse model of congenital TTP.[203]

1.4.5. Gene replacement therapy

Survivors of an acute TTP episode suffer from various comorbidities, such as cognitive impairment and depression, and experience a decreased quality of life, suggesting that TTP may be more of a chronic disorder.[204,205] These long-term observations emphasize the need for prophylactic treatment. Taking the welfare of the patients into account, safer, more simple, and efficient alternatives to prophylactic plasma infusions are of great importance.

In case of congenital TTP, the therapeutic delivery of a functional copy of the *ADAMTS13* gene would ideally cure the underlying genetic defect and offer lifelong protection from TTP. Congenital ADAMTS13 deficiency is a good candidate for gene therapy as it is a monogenetic disease. Moreover, ADAMTS13 is secreted in the circulation; hence, cell- or tissue-specific targeting is not required. However, a prerequisite for successful gene therapy is the safe and effective delivery of the therapeutic gene. Current gene delivery vehicles, called vectors, are divided in 2 classes: viral and non-viral vectors.

1.4.5.1. Viral vector-mediated gene therapy

Viruses have evolved to efficiently deliver their genomes to mammalian cells. By replacing the viral genes that are responsible for replication and retaining signal sequences that are essential for packaging, viruses were transformed into non-replicative gene delivery vehicles. To date, these modified viruses have been used in approximately 70% of the gene therapy clinical trials so far. Gammaretroviral, lentiviral, adenoviral, and adeno-associated viral (AAV) vectors are the most widely used viral vectors in current gene therapy studies.

In case of congenital TTP, different viral vector-based gene therapeutic approaches have already been tested in *Adamts13*$^{-/-}$ mice. Lentiviral vectors encoding full-length ADAMTS13 have been used in 2 different gene transfer strategies. Laje *et al.* explored an *ex vivo* gene therapy in the setting of autologous hematopoietic progenitor cell transplantation[206], while Niiya *et al.* investigated the feasibility of *in utero* gene transfer[207]. Both strategies resulted in the expression and secretion of transgene enzyme into the murine plasma of *Adamts13*$^{-/-}$ mice for several months. Interestingly, the secreted ADAMTS13 was able to normalize the abnormal VWF multimer distribution indicating that newly released UL-VWF was adequately processed *in vivo*.[206,207] An adenoviral gene transfer strategy has also been tested in *Adamts13*$^{-/-}$ mice.[208] Systemic administration of an adenoviral vector encoding full-length ADAMTS13 efficiently transduced liver, kidney, lung, heart, and spleen, resulting in the secretion of ADAMTS13 into plasma. Transgene ADAMTS13 that was released into the blood stream was biologically active as it was able to reduce the formation of platelet thrombi on immobilized collagen under flow.[208] The occurrence of hepatotoxicity in response to adenoviral injection and the formation of anti-adenoviral and inhibitory anti-ADAMTS13 antibodies were a major drawback in this study.[208] Since the use of lentiviral and adenoviral vectors is associated with several safety concerns, Jin and colleagues tested the efficacy of an AAV8-mediated gene therapeutic approach.[209] Because of the low packaging capacity of AAV vectors (<4.3kb), the authors were forced to express the truncated murine ADAMTS13 variant MDTCS (truncated at the spacer domain). Intravenous infusion of $\geq 2.6 \times 10^{11}$ vector genomes per kilogram resulted in therapeutic activity levels that were sufficient to reduce circulating UL-VWF in *Adamts13*$^{-/-}$ mice.[209] Moreover, stable transgene expression of this ADAMTS13 variant prevented the development of severe thrombocytopenia and reduced mortality when treated mice were challenged with shigatoxin 2 weeks after gene transfer.[209] Whereas no data about the protective role in TTP were available in both lentiviral and adenoviral vector-mediated gene therapy studies, the findings of Jin *et al.* provide proof-of-

concept to support the development of a gene-therapeutic approach for the treatment of hereditary TTP.

Since the beginning of gene therapy clinical trials in 1990, viral vectors have substantially contributed to this emerging field. Moreover, viral vector-mediated therapies are progressing from investigational agents to approved products. In 2012, a muscle-directed AAV1-based gene therapy for the treatment of a rare form of familial dyslipidaemia (also known as Glybera®) was the first gene therapy to be commercially approved in Europe.[210] Despite vigorous efforts to improve the production and safety of viral vectors, high costs[211] and safety concerns, such as insertional mutagenesis[212] and immunotoxicity[213,214] remain major limitations. However, many of these limitations may be addressed by using non-viral gene therapy.

1.4.5.2. Non-viral vector-mediated gene therapy

Non-viral, plasmid-based gene therapy relies upon the use of a physical source or synthetic chemical compounds in order to force the cell to take up plasmid DNA (pDNA) carrying the therapeutic expression cassette. In contrast with viral vectors, non-viral delivery systems generally have an enhanced safety profile, are less immunogenic and easier to synthesize, and have the potential to carry a larger genetic cargo. Although the application of non-viral vectors in gene therapy clinical trials has increased during the last ten years, non-viral vectors were neglected for a long time due to their low delivery efficiency relative to viral vectors.

A variety of physical and chemical methods have been developed to successfully deliver therapeutic genes *in vivo*. Physical methods are based on making transient pores in the cell membrane by applying mechanical, electrical[215], hydrodynamic[216,217], or ultrasonic energy[218] to facilitate the entrance of nucleic acids. Unfortunately, these techniques are less applicable in humans. Chemical (synthetic) delivery methods are more common and are based on the compaction of negatively charged nucleic acids by cationic liposomes or cationic polymers (such as polyethylenimine (PEI)).[219] These nanoparticle carriers provide protection against degradation by endonucleases (improving its half-life) and improve cellular uptake and endosomal escape of pDNA. An important feature of both physical and chemical methods is the localisation of the delivered therapeutic gene in the nucleus of the target cell to allow access to the transcriptional machinery. Plasmids that are routinely used are non-integrating

and episomal which dramatically reduces the risk of insertional mutagenesis, making non-viral, plasmid-based gene therapy a safer alternative to viral vectors.

Transgene expression and production of the therapeutic protein are crucial for its function. In many cases, high level of transgene product is achieved within the first days after non-viral, plasmid-based gene transfer. Within a few weeks, however, expression falls to low levels even when vector DNA is still present within the target cell.[220] The short duration of expression, due to the lack of integration and epigenetic responses (i.e. transcriptional silencing), is a major obstacle in terms of developing plasmid-based gene therapy for the treatment of human diseases. Interestingly, this problem can be overcome by the use of transposable elements, a technology that combines the advantages of integrating viral vectors (i.e. prolonged expression) with those of non-viral delivery systems (i.e. lower immunogenicity, enhanced safety profile, and reduced costs).

1.4.5.3. The *'Sleeping Beauty'* transposon system

Transposable elements or transposons are discrete DNA sequences with the ability to jump from one location within the genome to another (also known as 'jumping genes'). Although it is estimated that transposons make up approximately 45% of the human genome[221,222], these were originally dismissed as 'junk' or useless DNA. However, it is now generally believed that transposons might carry out some biological function, most likely a regulatory function, and contribute to genetic diversity.[223]

DNA transposons are a particular class of transposable elements that constitutes 2-3% of the human genome. DNA transposons can move on their own in a process called transposition; these autonomous transposable elements can excise themselves from the genome, move as DNA, and insert themselves into new genomic sites by means of a so-called 'cut-and-paste' mechanism. DNA transposons exist as single units containing the transposase gene flanked by terminal inverted repeats (TIRs) carrying the transposase binding sites (Figure 16A). Although these elements were active during primate evolution, they are currently no longer active in the human genome due to the accumulation of several mutations.[222]

Researchers have found that DNA transposons can been converted into a bi-component gene delivery system: by placing a gene of interest between the TIRs and supplying a source of active transposase *in trans*, virtually any DNA sequence could be transferred (Figure 16B). Unfortunately, many transposons are non-functional outside their hosts, making the use of invertebrate transposons systems in vertebrates not efficient.[224] Interestingly, in 1997, Ivics

and co-workers awakened an active transposase gene from a long evolutionary 'sleep', hence the name *'Sleeping Beauty'* (SB).[225] By reverse engineering defective copies of an ancient *Tc1/mariner*-like transposon found in salmonid fish, they engineered the first DNA-based transposon sequence that allowed transposition-mediated gene transfer in higher vertebrate species via a 'cut-and-paste' mechanism (Figure 16C).[225] Indeed, this resurrected transposable element was shown to successfully integrate foreign genes into the chromosomes of cultured vertebrate cell lines, including murine and human cells.[225] The first *in vivo* proof-of-principle for the use of SB in human gene therapy was provided by Yant *et al.* who reported somatic integration of naked DNA into mouse chromosomes and long-term expression of therapeutic serum levels of human FIX after hydrodynamic delivery of the SB system in FIX deficient mice.[226]

Additional engineering of the transposase gene increased its activity, resulting in integration efficiencies 100-fold greater than that achieved by random integration[227,228], and making *SB* an interesting non-viral gene transfer strategy in various animal models of monogenetic[229-232] and acquired human diseases[233,234]. In addition to *SB*, other transposon-based vectors, such as *Frog Prince*[235] and *piggyBac*[236], have been developed to deliver therapeutic genes in vertebrate cells. Although these systems transpose genes via a similar 'cut-and-paste' mechanism as *SB*, they differ in their efficiency of gene insertion, cargo capacity, integration site preference, and effects on chromosomal stability.[237]

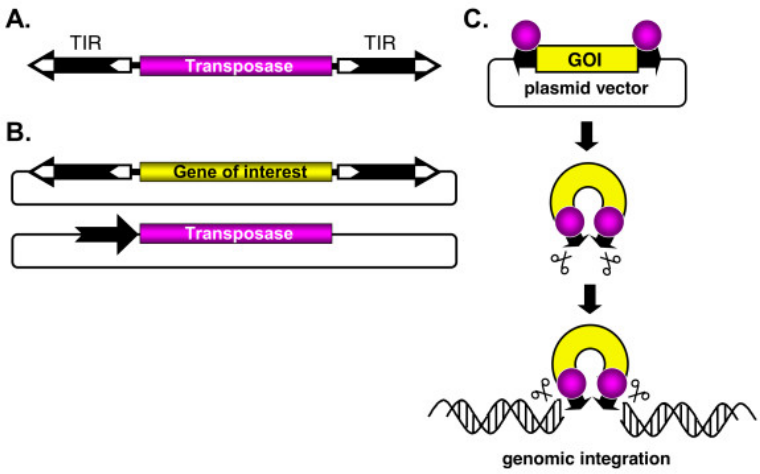

Figure 16: The *'Sleeping Beauty'* transposon toolbox. (A) In nature, DNA transposons (e.g. Tc-1/mariner-like transposable elements) consists of a single open reading frame encoding a transposase enzyme that is flanked by terminal inverted repeats (TIR; black arrow), which contain the transposase

binding sites. (B) Under laboratory conditions, DNA transposons can be used as a bi-component system to perform gene transfer. While one plasmid vector carries the gene of interest between the TIRs, the other component is a transposase expression plasmid, in which the black arrow represents the promoter driving its expression. (C) Co-delivery of both components results in genomic integration via a 'cut-and-paste' mechanism. Binding of the transposase results in the excision of the gene of interest from the donor plasmid and the subsequent integration in the genome of the host cell. Adapted from Ivics *et al.*[238]

During the process of transposition, the gene of interest is excised from the delivered pDNA and integrated into a genomic location (Figure 16C). At the primary DNA sequence level, SB transposons display specificity in target site selection in that they exclusively target their integration into TA dinucleotides that are duplicated upon transposition.[225] At genomic scale, insertion site analysis revealed that integration is fairly random. Whereas integration by retroviral vectors strongly favours active genes[239,240], SB transposons have no or little preference for transcriptionally active genes[240-242]. Insertion that occurs in genes is predominantly located in introns.[243] Moreover, the TIRs flanking the gene of interest do not have enhancer elements and therefore should be less likely to cause insertional activation of proto-oncogenes.

Despite its favourable insertion site preference, however, some safety concerns with respect to clinical application need to be addressed. First, integration and continued expression of a gene encoding SB transposase could lead to remobilization of the inserted transposon (a process called 'rehopping'), with risk of genotoxicity. A safer alternative would be the use of *in vitro*-transcribed mRNA as a transient source of transposase.[244] Second, with any vector that integrates into chromosomes comes the potential risk of insertional mutagenesis. Strategies that target integration into genomic safe 'harbours' could prevent these hazardous effects. Such strategies include the fusion of *SB* transposase with a heterologous DNA-binding domain that will tether the transposase to selected sites in the genome.[241,245]

Delivery of the SB transposon system is of crucial importance since transposition is dependent on the efficiency of uptake of the introduced plasmids into the cell nuclei. The SB transposon system can be administered either *ex vivo* or *in vivo*.

In *ex vivo* gene delivery, a selected cell population is derived from the host, treated, and then infused back into the same patient. SB vectors are frequently introduced into isolated cell populations by means of nucleofection, an electroporation-based technique that transfers

nucleic acids directly to the nucleus. In this way, SB-mediated transposition has already been demonstrated in human $CD34^+$ hematopoietic progenitor cells[228,246], primary T-cells[247], and embryonic stem cells[248]. The feasibility and robustness of this procedure in terms of human application holds much promise.[249]

Using *in vivo* gene delivery, the SB vectors are directly introduced into the organ or tissue where expression is desired. The most effective method for *in vivo* SB-mediated gene transfer is hydrodynamic injection (Figure 17).[250] This gene transfer technique is well established in mice and involves the injection of a large volume of DNA/saline solution (equivalent to 10% of the body weight) through the tail vein within 5-8 seconds.[216,217] The resulting hydrodynamic pressure expands the liver, enlarges the fenestrae of the endothelium, and forces invagination of the cellular membranes of hepatocytes allowing the uptake of DNA into about 10-40% of the hepatocytes.[251,252] Although hydrodynamic gene delivery is very efficient in small animal models, systemic application in larger animal models such as dogs and pigs is impractical and unsafe.

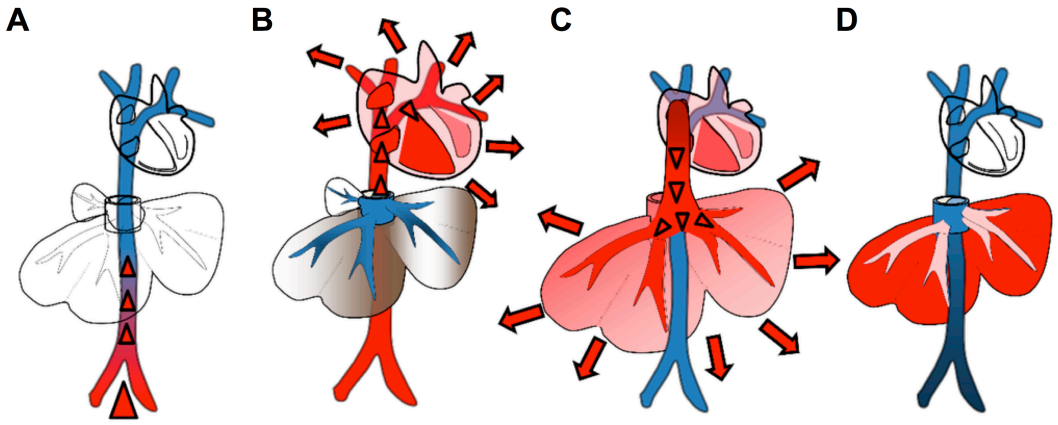

Figure 17: Schematic representation of the mechanisms leading to liver-directed transgene expression following hydrodynamic tail vein injection in mice. (A) A large volume of DNA solution goes directly to the heart and increases the intravascular pressure in the inferior vena cava upon rapid tail vein injection. (B) The DNA solution stretches myocardial fibres beyond their optimal length for contraction thereby inducing cardiac congestion. (C) Cardiac congestion generates a backflow to the organs that are connected to the inferior vena cava, in which the liver absorbs most of the solution and expands. (D) The intra-hepatic pressure increases the permeability of cellular membranes of hepatocytes and forces the DNA solution out of the endothelium into these cells. Adapted from Kamimura *et al.*[253]

In large animal models direct infusion of pDNA in the liver or other specific organs is the preferred route. By combining image-guided catheter insertion with the newly developed computer-controlled injection devices, site-specific gene delivery has been performed in liver[254,255] and skeletal muscle[256] of pigs (Figure 18). While this procedure is considered a safe, reproducible, and viable approach for clinical gene therapy[253,257], obtaining high levels of gene transfer and persistent gene expression remains challenging.[258] In addition to hydrodynamic injection, alternative strategies for the delivery of *SB* vectors have been investigated. These strategies include the cell or tissue type-specific gene delivery of *SB* vectors using PEI-DNA conjugates[259-261], nanocapsules[262], and adenoviral hybrid-vector systems[263]. Up-scaling and further improving these systems may pave the way towards clinical applications.

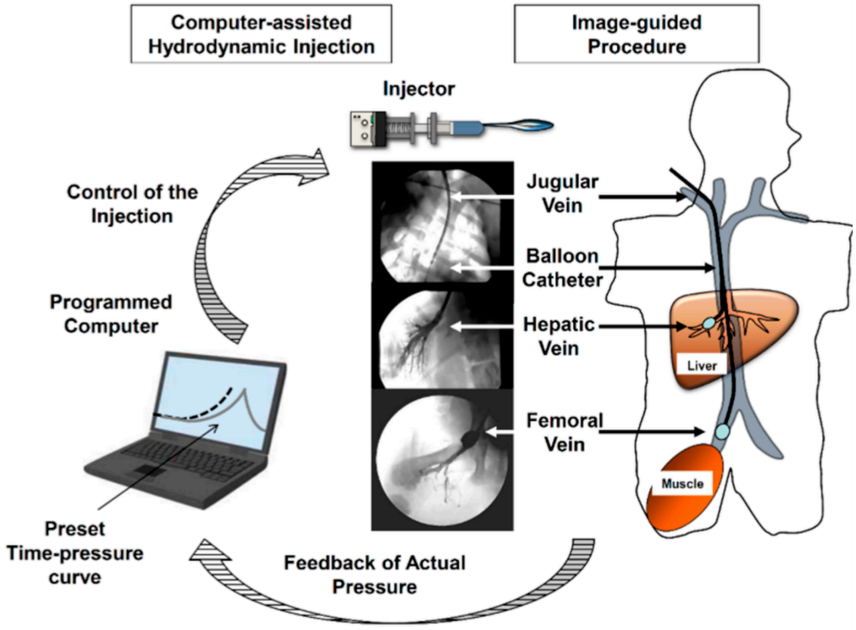

Figure 18: Schematic representation of regional gene delivery using image-guided, computer-assisted hydrodynamic injection. A balloon catheter (with injector) is inserted into the jugular vein, passed through the inferior vena cava, and placed at one of the lobular hepatic veins (for liver-directed gene transfer) or femoral veins (for muscle-directed gene transfer). A small amount of phase contrast medium is injected to confirm site-specific insertion after which the balloon is inflated to block backflow of the injected DNA solution. The vascular pressure that is measured at the distal tip of the catheter is transmitted to a computer and serves as the start/stop signal for hydrodynamic injection. Depending on the desired level of intravascular pressure that one wants to achieve, the computer starts an electric motor-driven injector that self-adjusts the injection power and reproduces preloaded pressure-time curves that are installed into the computer prior to injection. Figure adapted from Kamimura *et al.*[253]

Due to its reduced immunogenicity, its close-to-random integration profile, its ability to mobilize DNA up to 10kb in length, and its large-scale, affordable manufacture compared with viral vectors, the SB transposon technology holds much promise. Indeed, the first human clinical application of the SB system was launched in 2008 in the United States.[249] In these phase I trials, SB was used to incorporate a CD19-specific chimeric antigen receptor transcript into the genome of patient- or donor-derived T cells, rendering T-cells cytotoxic toward CD19+ B-lineage tumours.[264] These genetically modified CD19-specific T cells were administered to patients with advanced-stage CD19+ B-cell malignancies in an adjuvant setting following autologous or allogeneic hematopoietic stem cell transplantation. The procedure was considered safe and feasible, as clinicians did not observe acute toxicity (cytokine storm) or increased rates of infection or graft-versus-host disease. Interestingly, both overall and progression free survival rates appeared improved indicating that the procedure is an effective approach to augment disease control and to maintain remission in patients at a high risk of relapse.[264] More clinical trials involving CAR-T cells (e.g. NCT01492036, NCT02529813, and NCT01653717) to treat B-lymphoid malignancies are currently ongoing in the United States. In Europe, a SB transposon-based, targeted ex vivo gene therapy to treat age-related macular degeneration (TargetAMD; http://www.targetamd.eu/) is also moving toward clinical trials. The results obtained from these clinical trials are important to bring visibility to the clinical use of the SB transposon technology.

1.5. DISTURBED BALANCE BETWEEN VWF and ADAMTS13

The accumulation of UL-VWF multimers due to absent or low ADAMTS activity is associated with enhanced VWF-GPIbα binding and an increased risk of developing widespread microvascular thrombosis, as described earlier (section 1.4.). However, it has become clear that a dysregulated balance between VWF and ADAMTS13 is not exclusively restricted to TMAs but may also contribute to the pathogenesis of other diseases. Indeed, an imbalance between an overwhelming VWF release and a reduced VWF-cleaving capacity is thought to play a causal role in a variety of other disorders, of which most are known to be associated with an increased thrombotic tendency.[265,266] In this chapter we will focus on the clinical relevance of changes in the VWF/ADAMTS13 axis in ischemic stroke and malaria.

1.5.1. Ischemic stroke

Stroke is the fourth-leading cause of death and the leading cause of long-term rehabilitation in the Western world.[267] Approximately 87% of all strokes are caused by a blood clot occluding a cerebral blood vessel, often the middle cerebral artery (MCA) or one of its side branches. Such occlusions impair blood flow in particular areas of the brain (i.e. ischemic stroke). The remaining 13% of strokes are the result of hemorrhagic events due to vessel rupture (i.e. hemorrhagic stroke).[267] In ischemic stroke, urgent recanalization of the occluded blood vessel and restoration of the blood flow are considered important therapeutic steps in order to reduce morbidity and mortality. Rapid reperfusion can be achieved either via pharmacological thrombolysis using t-PA, or via endovascular thrombectomy (mechanical removal of the clot). Surprisingly, despite restoration of blood flow and reoxygenation, progressive stroke still develops in many patients, which has led to the concept of reperfusion injury. This phenomenon is a complex process that involves both thrombotic and inflammatory pathways, aggravating tissue injury that was produced by ischemia alone.[268,269] In recent years, clinical and preclinical evidence has emerged that support the crucial involvement of the VWF/ADAMTS13 axis in stroke-associated ischemia/reperfusion injury.

1.5.1.1. VWF and ADAMTS13 in clinical stroke studies

Several clinical cohort studies demonstrated that high VWF levels[270-273] and/or low ADAMTS13 levels[271,274,275] are associated with an increased risk of ischemic stroke. Although meta-analyses confirmed significant association[276], it remained debatable whether

high VWF and/or low ADAMTS13 levels were a cause or consequence of stroke since levels can be biased by poststroke changes. Fortunately, more definite conclusions were drawn from prospective, longitudinal cohort studies among subjects free from cerebrovascular disease. These large population-based studies have identified high levels of VWF[277-279] and low levels of ADAMTS13 activity[280] as strong predictors of the risk of ischemic stroke. The association between high VWF levels and/or low ADAMTS13 activity and ischemic stroke is likely to be explained by less cleavage of an excess amount of HMW VWF multimers, i.e. the most thrombogenic forms, leading to a procoagulant state.

1.5.1.2. VWF and ADAMTS13 in experimental stroke studies

In parallel with clinical studies, the pathophysiologic involvement of the VWF/ADAMTS13 axis has been extensively studied in murine ischemic stroke models mimicking transient occlusion of the MCA. The most frequently used mouse model is the so-called filament or suture model in which a silicon-coated nylon suture is advanced from the internal carotid artery to the origin of the MCA in order to occlude the blood vessel and induce tissue ischemia (Figure 19). The intra-luminal model is used to study permanent or transient ischemia by leaving the suture in place, or by withdrawing the filament at a fixed time point, respectively. In case of transient MCA occlusion (tMCAO), removal of the filament allows reperfusion to occur which initiates secondary infarct growth comprising the ipsilateral parietal neocortex as well as the basal ganglia within the first 24 hours.

Our group and others have demonstrated the crucial role of VWF and ADAMTS13 in stroke in *Vwf*$^{-/-}$ and *Adamts13*$^{-/-}$ mice, respectively (Figure 20). Whereas absence of VWF protected mice from ischemic stroke[281,282], lack of ADAMTS13 aggravated ischemic brain damage[283]. Indeed, one day after tMCAO, deficiency of VWF resulted in a functionally relevant reduction of the cerebral infarct size compared to WT controls (Figure 20A).[281,282] In contrast, ADAMTS13 deficiency caused a progressive decline in post-ischemic cerebral blood flow that resulted in larger cerebral lesions and a worse clinical outcome (Figure 20B).[283]

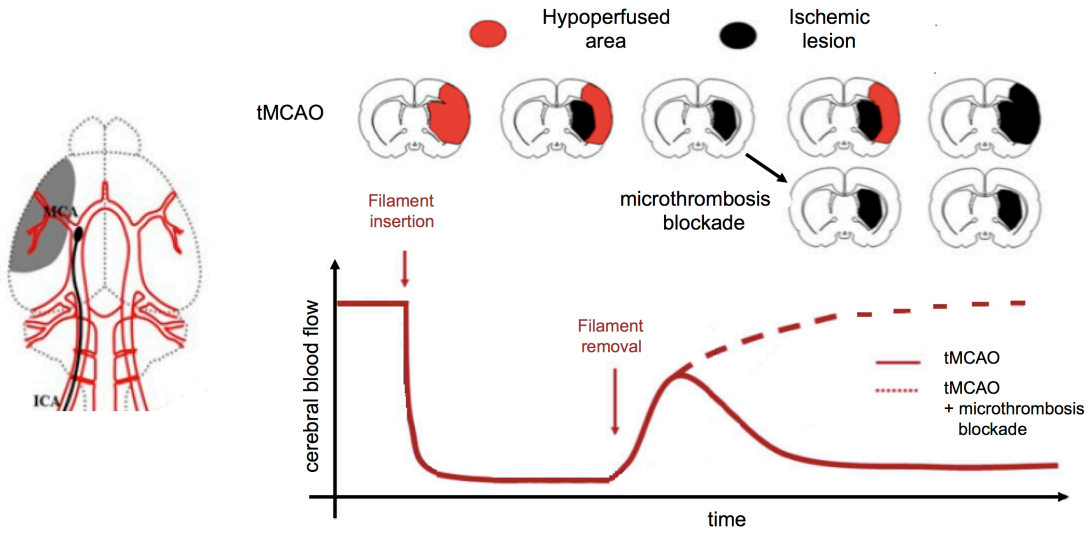

Figure 19: Transient middle cerebral artery occlusion. A silicon-coated filament is advanced from the internal carotid artery (ICA) to the origin of the middle cerebral artery (MCA) in mice. Occlusion of the MCA origin causes severe reduction of blood flow in the basal ganglia, and gradual reduction in blood flow in the cerebral cortex. Prolonged obstruction of the cerebral blood flow in the MCA territory causes irreversible damage (ischemic lesion, black) in the basal ganglia, i.e. the core, and reversible damage in the cortical area at risk, i.e. the area surrounding the core. Removal of the filament after a certain interval restores cerebral blood flow in previously hypoperfused regions resulting in the occurrence of thrombo-inflammatory processes, including secondary microthrombosis. This causes a reduction in blood flow, secondary ischemia, and infarct growth, a phenomenon also known as 'reperfusion' injury (solid line). Inhibition of secondary microthrombosis (dashed line), e.g. by blocking VWF-GPIbα interactions or by administration of recombinant ADAMTS13, reduces ischemic lesion size following transient MCA occlusion (tMCAO). Figures adapted from Lee *et al.*[284] and Gauberti *et al.*[285]

Additionally, indirect evidence for the involvement of the VWF/ADAMTS13 axis in transient ischemic stroke is provided by studies showing that blocking the interaction between VWF and its main ligand, platelet GPIbα[286-288], or administration of recombinant ADAMTS13[282,289] protected the brain from severe ischemia-reperfusion injury. Data from our and other groups have demonstrated that similar strategies may also promote lysis of already existing thrombi.[290,291] Altogether, these experimental studies have led to the concept that initial VWF-mediated platelet attachment and activation plays an important role in stroke pathogenesis and that ADAMTS13 has a neuroprotective effect, probably by cleaving UL-VWF multimers that are secreted from the endothelium by ischemia, and by cleaving VWF multimers on the surface of thrombi formed on ischemic ECs.

Although it is evident that pathological thrombus formation plays an important role in stroke, there is evidence indicating that also VWF-mediated inflammatory responses may contribute to ischemic brain damage. Following tMCAO, Khan *et al.* showed that the aggravated brain injury observed in *Adamts13*$^{-/-}$ mice was associated with an increased inflammatory cell infiltration in the damaged tissue compared with WT controls.[292] Further experiments revealed that the enhanced inflammation was VWF-dependent since mice deficient in VWF or both VWF and ADAMTS13 exhibited an identical reduction in inflammatory cell infiltration compared to WT controls.[292] These observations are in line with studies showing that VWF and GPIbα are involved in various inflammatory processes, such as leukocyte adhesion, rolling, and extravasation.[293-295]

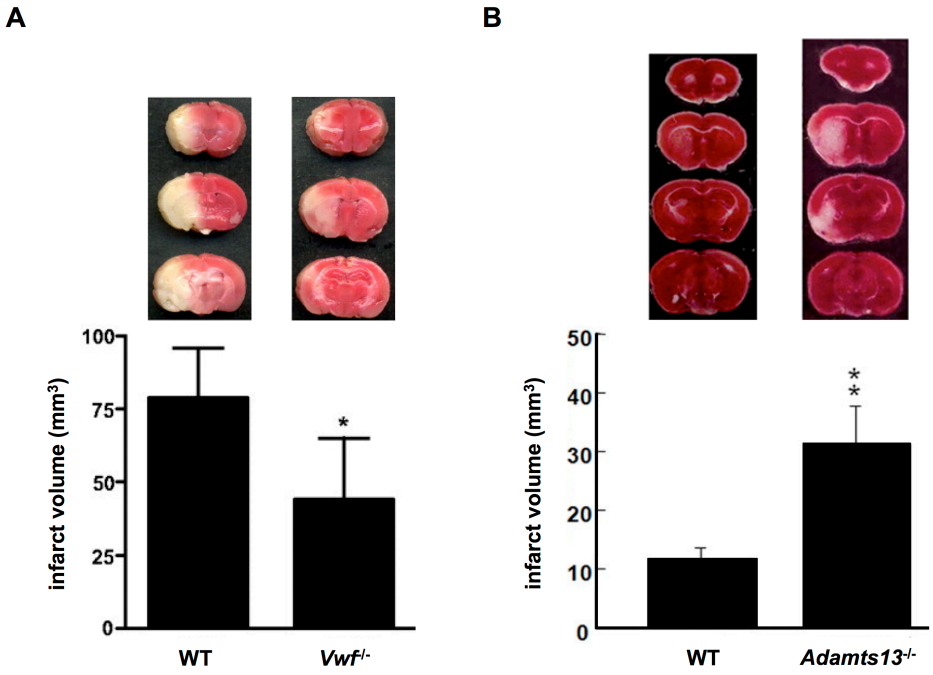

Figure 20: The pathophysiological relevance of the VWF/ADAMTS13 axis in ischemic stroke in mice. Effects of *Vwf* and *Adamts13* gene deletion on infarct size following tMCAO in mice are shown. Transient cerebral ischemia was induced by (A) 60 or (B) 30 minutes occlusion of the right middle cerebral artery, followed by 23 or 23.5 hours of reperfusion, respectively. Infarct sizes were assessed by sectioning the brain in consecutive sections and staining these with 2,3,5-triphenyltetrazolium chloride, an indicator that is used to differentiate between metabolically active and inactive tissue. Red areas represent vital brain tissue, whereas white areas represent infarcted brain tissue. (A) Deficiency of VWF protected mice from ischemic stroke, underlining the important pathophysiological role of VWF during ischemic stroke. (B) Lack of ADAMTS13 aggravated ischemic brain damage, demonstrating the neuroprotective effect of the VWF-cleaving protease in ischemic stroke. Figures adapted from (A) Kleinschnitz *et al.*[281] and (B) Fujioka *et al.*[283]

In summary, accumulating evidence from both clinical and preclinical studies indicate that a disturbed balance between VWF and ADAMTS13 (i.e. elevated VWF levels/activity and reduced ADAMTS13 levels/activity) predisposes individuals to a higher risk of stroke and contributes to both the acute phase of cerebral blood vessel obstruction and the subsequent reperfusion phase after re-opening of the artery. Therefore, interfering with the VWF/ADAMTS13 axis could become a promising novel approach in the treatment of ischemic stroke.

1.5.2. Malaria

Malaria is the most important parasitic disease in humans. According to the annual World Malaria Report of the World Health Organization, an estimated 214 million people were clinically affected in 2015, and approximately 438 000 people died of the disease, most of whom are children in sub-Saharan Africa (World Malaria Report 2016, Geneva, World Health Organization 2016). Malaria is a protozoan disease caused by species of the genus *Plasmodium* and transmitted by female *Anopheles* mosquitoes (Figure 21). Five species are known to infect humans: *P. falciparum*, *P. vivax*, *P. ovale*, *P. malariae*, and *P. knowlesi*, of which *P. falciparum* is the most deadly one. Most infections usually result in a mild, uncomplicated febrile disease, characterized by intermittent episodes of fever and peaks of parasitemia, reflecting the ability of adaptive immunity to prevent disease. In non-immune individuals, however, complications may arise suddenly and cause severe, life-threatening malaria syndromes. In infants and young children life-threatening disease typically encompasses metabolic acidosis (leading to respiratory distress), cerebral malaria (CM) associated with coma, and severe malarial anemia. Primary infection in adults frequently involves other disturbances such as pulmonary edema, renal failure, and shock. Current antimalarial treatments, e.g. chloroquine and artemisinin derivatives, target the asexual blood stage of the infection thereby reducing parasite loads, disease symptoms and the risk of disease progression. Besides frontline artemisinin therapy, severe malaria necessitates intensive nursing and supportive care management.

Although the global mortality rate due to malaria has decreased by 60% between 2000 and 2015, it still remains high (10-20% in children). Moreover, increased mortality and morbidity due to the development of parasite resistance to chloroquine and artemisinin therapy has been

observed. Therefore, efforts are made to develop new fast acting antimalarial drugs and to investigate new adjuvant therapies to better manage the clinical manifestations of severe malarial disease. To achieve this, a better understanding of the pathogenesis of malaria-associated manifestations is of great importance.

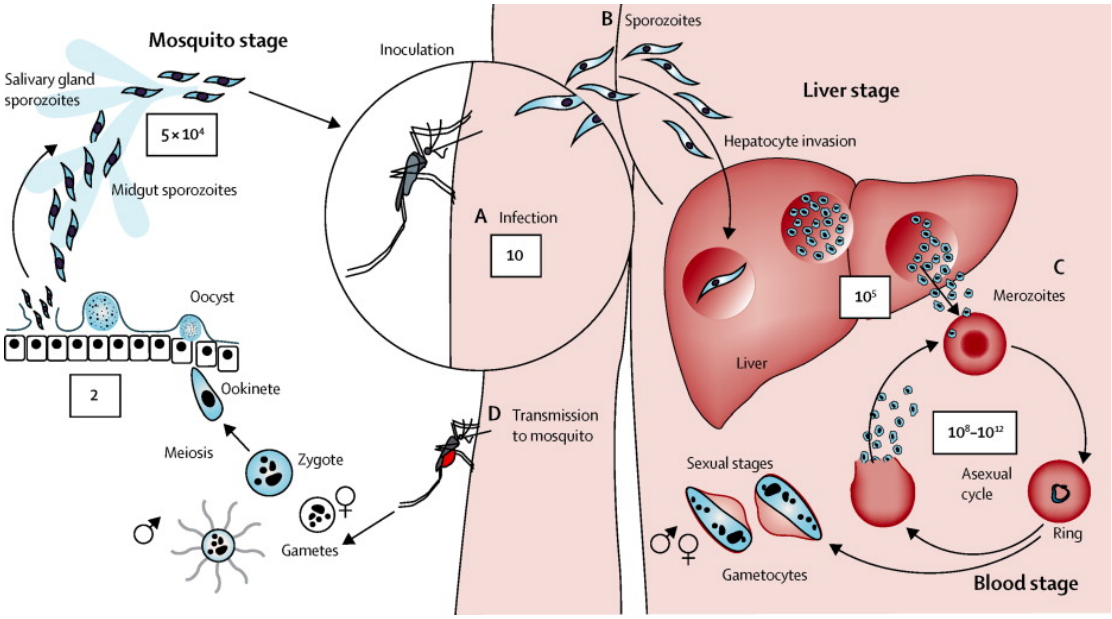

Figure 21: Life cycle of the malaria parasite. The life cycle of the malaria parasite involves 2 hosts. Human infection starts with a blood meal of an infected female *Anopheles* mosquito inoculating sporozoites into the human host. Sporozoites infect liver cells and mature in schizonts which in turn rupture and release merozoites into the circulation. Merozoites invade RBCs and begin an asexual life cycle: merozoites develop into ring-stage throphozoites that mature in schizonts releasing new merozoites upon rupture. This cycle of invasion and rupture is repeated every 1-3 days (depending on the *Plasmodium* species) resulting in thousands of parasitized RBCs and leading to illness and malaria-associated complications. Some parasites differentiate into male and female gametocytes that are ingested by a feeding mosquito. In the mosquito, the parasite reproduces sexually resulting in the formation of new sporozoites. Picture adapted from White.[296]

1.5.2.1. Pathogenesis

It is generally believed that *P. falciparum* malaria-related syndromes arise from the intersection of 2 different processes, i.e. (I) the sequestration of infected red blood cells (iRBCs) among target organs followed by (II) a dysregulated inflammatory anti-parasitic immune response.[297]

(I) Site-specific sequestration of *P. falciparum*-iRBCs is caused by the interaction between a family of cell-surface proteins, known as *P. falciparum* erythrocyte membrane protein-1, and multiple receptors expressed on ECs, such as intercellular adhesion molecule-1, vascular cell-adhesion molecule-1, thrombospondin, and CD36. While cytoadhesion of iRBCs is an important mechanism to evade clearance by the spleen, massive sequestration in different microvascular beds results in mechanical obstruction of the capillary blood flow, reduced perfusion, and decreased removal of waste products.[298] Intense sequestration of iRBCs has been observed in capillaries and post-capillary venules of lungs and brains in patients who died from malaria-associated acute respiratory distress syndrome (MA-ARDS)[299] or CM[300-302], respectively. In patients with severe *falciparum* malaria, the proportion of blocked capillaries is associated with disease severity.[298] However, parasite sequestration occurs in every *P. falciparum* infection, even in patients with uncomplicated malaria, indicating that the mere presence of parasites in peripheral blood and tissues is not enough to attribute a specific syndrome or death solely to mechanical obstruction.

(II) Besides mechanical obstruction of the capillary blood flow, a disproportional activation of pro-inflammatory immune mechanisms may contribute to clinical outcome as well.[297,303] Upon infection, both innate and adaptive immune mechanisms are required to clear the infection from the circulation. When this immune response is mounted early during infection and timely down-regulated, disease is absent or mild. An inefficient anti-parasitic response, however, favours excessive parasite replication, sequestration, and the release of parasite virulence factors (e.g hemozoin and glycophosphatidylinositol) into the blood, which may result in excessive endothelial activation and inflammation causing severe pathology (Figure 22). Indeed, late-stage *P. falciparum*-iRBCs are known to activate inflammatory pathways in ECs *in vitro*[304], while the released parasite virulence factors are known to bind receptors of the innate immune system and activate monocytes to secrete pro-inflammatory cytokines, such as tumor necrosis factor.[305-307] Moreover, widespread endothelial activation and sequestration of immune cells in brain microvasculature are evident in patients with CM.

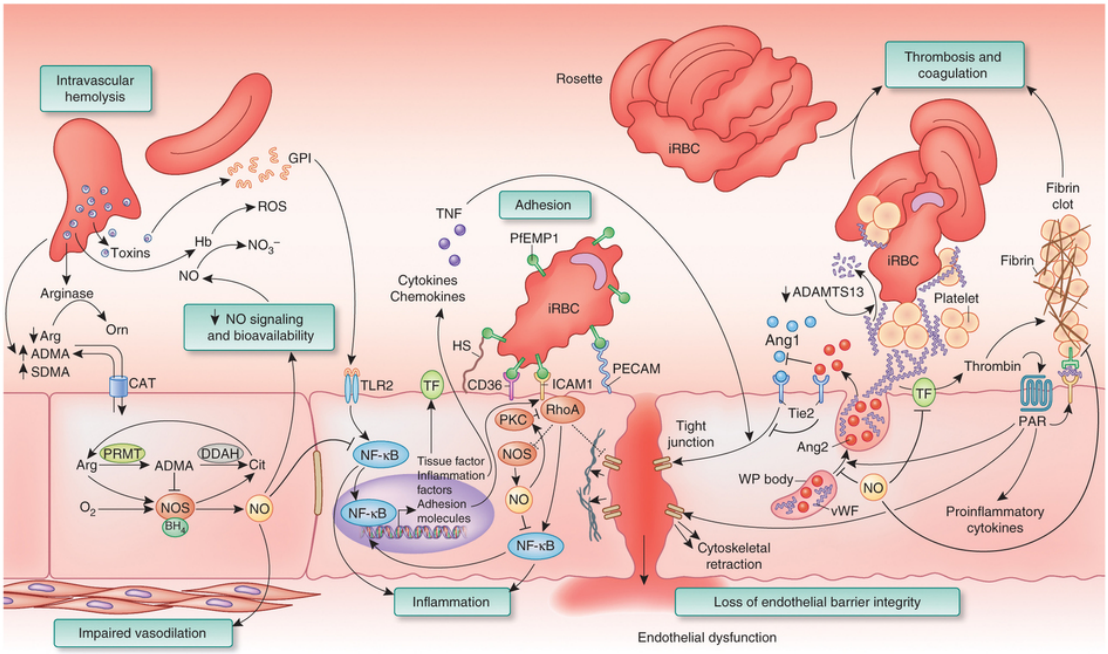

Figure 22: Pleiotropic effects on endothelium following *P. falciparum* infection. Malaria pathophysiology is complex and involves multiple balances that determine clinical outcome. Beyond mechanically obstructing microvessels, cytoadherence of infected RBCs initiates endothelial cell signalling pathways that promote adhesion, thrombosis, inflammation, and endothelial dysfunction, and impair vasoregulation. Figure adapted from Miller *et al.*[308]

1.5.2.2. VWF and ADAMTS13 levels in clinical and experimental studies

Recent findings have suggested that hematological abnormalities in terms of VWF and ADAMTS13 may play a role in malaria-associated pathology as well [309]. A series of clinical studies have demonstrated that either severe *falciparum* or *vivax* malaria is associated with elevated levels of both VWF and VWFpp (a useful marker for acute EC activation) in children[310-312] and adults[313,314]. For example, Phiri and co-workers showed that both plasma VWF and VWFpp levels upon admission were significantly higher in children with both cerebral and mild malaria when compared with the non-malarial control groups.[312] Increased levels of VWF and VWFpp are already observed early after onset of the blood-stage infection.[315] In addition, by using a nanobody that detects 'active' VWF (i.e. VWF that exposes the GPIbα platelet-binding domain)[37], De Mast *et al.* found that increased levels of activated VWF were present in plasma of *P. falciparum* patients[315], which corroborates the accumulation of UL-VWF multimers during malaria[311,316]. In line with these studies, a severe decrease in both ADAMTS13 antigen and activity levels has been identified in malaria-infected patients.[311,313,314,316] Whether these abnormalities constitute epiphenomena, or

whether they play direct roles in mediating the pathophysiology of the condition remains unclear.

Independent observations suggest that elevated levels of VWF with enhanced GPIbα-binding activity, whether or not in combination with low ADAMTS13 activity, may play a direct role in malaria pathogenesis. First, plasma VWFpp and VWF levels were correlated with disease severity[312], and both VWF and activated VWF levels were inversely correlated with platelet count[315]. These correlations support the idea that elevated levels of activated VWF may cause intravascular platelet adhesion and clumping resulting in thrombocytopenia (a common finding in malaria infection) and mechanical obstruction of blood flow in microvessels. Second, Bridges *et al.* demonstrated that mature *P. falciparum*-iRBCs were able to bind to platelet-decorated VWF strings on cultured ECs stimulated with histamine (Figure 23).[317] Further characterization of the binding revealed that pretreatment of the activated endothelium with rADAMTS13 or antibodies selectively blocking the VWF A1 domain dose-dependently decreased the number of iRBCs-bound VWF strings. These *in vitro* data support the hypothesis that the VWF/ADAMTS13 axis plays a role in the cytoadherence of iRBCs to vascular endothelium suggesting that VWF is not just a marker of malaria disease severity but instead actively contributes to malaria pathogenesis. Further investigation regarding its pathogenic involvement is highly warranted, preferably *in vivo*.

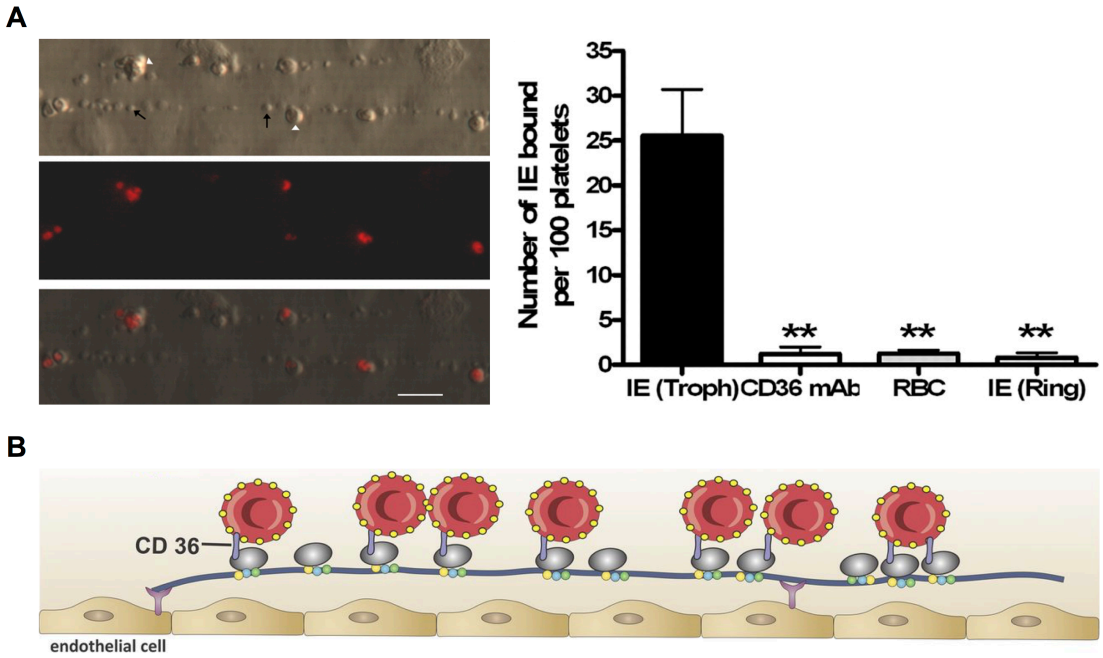

Figure 23: Binding of *P. falciparum*-infected RBCs to platelet-decorated VWF strings. (A) Human umbilical vein endothelial cells were stimulated with histamine before successive additions of platelets and RBCs infected with fluorescently labelled *P. falciparum* throphozoites (indicated with

white triangle). RBCs containing the mature, adhesive form of the parasite were able to interact with platelet-decorated VWF strings (indicated with black arrow; IE (troph)) in a CD36-dependent matter. No binding was observed in the presence of uninfected RBCs (RBC) or RBCs infected with immature, non-adhesive throphozoites (IE (ring)). (B) Schematic representation of VWF-mediated sequestration of infected RBCs. Endothelial cell-derived VWF, bound to the surface of ECs, elongates in the direction of the flow and recruits platelets in a GPIbα-dependent manner. Specific erythrocyte membrane proteins that are expressed on the surface of *P. falciparum*-infected RBCs may bind the platelet surface receptor CD36 thereby establishing the sequestration of infected RBCs in vascular beds. Figures adapted from (A) Bridges *et al.*[317] and (B) De Ceunynck *et al.*[318]

The most common animal model to study the pathobiology of malaria is the mouse model. Various models have been developed to study lethal and non-lethal malaria, which usually involves the infection of inbred mouse strains with rodent-specific *Plasmodium* species: *P. berghei*, *P. vinckei*, *P. chabaudi*, and *P. yoelii*. The characteristics of both infection and disease differ in the four species, and for each of the species in various mouse strains.[319] Unfortunately, no single mouse model mimics all the various clinical manifestations of severe malaria in humans. Therefore, by combining each of the species for rodent malaria with different mouse strains, different malaria syndromes can be mimicked. For example, C57BL/6J mice infected with *P. berghei* ANKA exhibit neurological symptoms such as ataxia, convulsions, and/or paralysis, and typically die between days 6 to 8 post-infection, making it the most widely used model to study CM.[320] On the other hand, infection of the same mouse strain with *P. berghei* NK65 is used to study lethal MA-ARDS, without occurrence of cerebral complications.[321] To date, only one study has investigated the direct role of VWF in a mouse model of experimental CM.[322] In this recent study, infection of C57BL/6J WT mice with *P. berghei ANKA* activated ECs resulting in increased plasma VWF levels, including the pathological UL-VWF multimers. To investigate whether VWF was directly involved in experimental CM pathogenesis, *P. berghei ANKA* infection was investigated in *Vwf*$^{-/-}$ mice. Interestingly, a prolonged survival of *Vwf*$^{-/-}$ mice was observed while parasitemia and platelet count were identical to controls, suggesting that VWF is an important regulator of malaria disease. The underlying mechanisms defining its role in disease pathology are not yet unravelled.

In summary, clinical and preclinical studies indicate that malaria infection is associated with acute EC activation, the accumulation of highly adhesive UL-VWF multimers, and a

significant reduction in ADAMTS13. Although the question whether these alterations are the ‘effect’ or ‘cause’ of decreased malaria resistance still requires further investigation, preclinical findings point towards a direct role of the VWF/ADAMTS13 axis in malaria pathogenesis. If true indeed, it will be of great importance to clarify the mechanisms linking these alterations and disease progression, and to explore new therapeutic strategies. Therefore, future studies using different mouse models for malaria are needed to provide more insight into these topics.

The unifying pathophysiological mechanism linking the above-mentioned disorders (ischemic stroke and malaria) is a dysfunctional activation of ECs resulting in the release of substantial amounts of highly adhesive UL-VWF multimers that may compromise the microcirculation, especially in context of reduced ADAMTS13 activity. Whether VWF-directed therapy can be translated into therapeutic practice and improve clinical outcome remains unclear and requires further investigation.

1.6. REFERENCES

1. Versteeg HH, Heemskerk JWM, Levi M, Reitsma PH. New fundamentals in hemostasis. *Physiol Rev*. 2013;93(1):327–358.
2. Ruggeri ZM. Platelet adhesion under flow. *Microcirculation*. 2009;16(1):58–83.
3. Varga-Szabo D, Pleines I, Nieswandt B. Cell adhesion mechanisms in platelets. *Arterioscler Thromb Vasc Biol*. 2008;28(3):403–412.
4. Moroi M, Jung SM, Shinmyozu K, et al. Analysis of platelet adhesion to a collagen-coated surface under flow conditions: the involvement of glycoprotein VI in the platelet adhesion. *Blood*. 1996;88(6):2081–2092.
5. Savage B, Almus-Jacobs F, Ruggeri ZM. Specific synergy of multiple substrate-receptor interactions in platelet thrombus formation under flow. *Cell*. 1998;94(5):657–666.
6. Yago T, Lou J, Wu T, et al. Platelet glycoprotein Ibalpha forms catch bonds with human WT vWF but not with type 2B von Willebrand disease vWF. *J Clin Invest*. 2008;118(9):3195–3207.
7. Pugh N, Simpson AMC, Smethurst PA, et al. Synergism between platelet collagen receptors defined using receptor-specific collagen-mimetic peptide substrata in flowing blood. *Blood*. 2010;115(24):5069–5079.
8. Li Z, Delaney MK, O'Brien KA, Du X. Signaling during platelet adhesion and activation. *Arterioscler Thromb Vasc Biol*. 2010;30(12):2341–2349.
9. Broos K, Feys HB, De Meyer SF, Vanhoorelbeke K, Deckmyn H. Platelets at work in primary hemostasis. *Blood Rev*. 2011;25(4):155–167.
10. Bennett JS. Regulation of integrins in platelets. *Biopolymers*. 2015;104(4):323–333.
11. Rao LVM, Pendurthi UR. Regulation of tissue factor coagulant activity on cell surfaces. *J Thromb Haemost*. 2012;10(11):2242–2253.
12. Furie B, Furie BC. Mechanisms of thrombus formation. *N Engl J Med*. 2008;359(9):938–949.
13. Mutch NJ. Polyphosphate as a haemostatic modulator. *Biochem Soc Trans*. 2016;44(1):18–24.
14. Rijken DC, Lijnen HR. New insights into the molecular mechanisms of the fibrinolytic system. *J Thromb Haemost*. 2009;7(1):4–13.
15. Chapin JC, Hajjar KA. Fibrinolysis and the control of blood coagulation. *Blood Rev*.

2015;29(1):17–24.

16. Wyseure T, Declerck PJ. Novel or expanding current targets in fibrinolysis. *Drug Discov Today*. 2014;19(9):1476–1482.
17. Sadler JE. von Willebrand factor: two sides of a coin. *J Thromb Haemost*. 2005;3(8):1702–1709.
18. Denis CV, Lenting PJ. von Willebrand factor: at the crossroads of bleeding and thrombosis. *Int J Hematol*. 2012;95(4):353–361.
19. Lenting PJ, Christophe OD, Denis CV. von Willebrand factor biosynthesis, secretion, and clearance: connecting the far ends. *Blood*. 2015;125(13):2019–2028.
20. Weibel ER, Palade GE. New cytoplasmic components in arterial endothelia. *J Cell Biol*. 1964;23:101–112.
21. Weibel ER. Fifty years of Weibel-Palade bodies: the discovery and early history of an enigmatic organelle of endothelial cells. *J Thromb Haemost*. 2012;10(6):979–984.
22. Nightingale T, Cutler D. The secretion of von Willebrand factor from endothelial cells; an increasingly complicated story. *J Thromb Haemost*. 2013;11 Suppl 1:192–201.
23. Metcalf DJ, Nightingale TD, Zenner HL, Lui-Roberts WW, Cutler DF. Formation and function of Weibel-Palade bodies. *J Cell Sci*. 2008;121(Pt 1):19–27.
24. Springer TA. von Willebrand factor, Jedi knight of the bloodstream. *Blood*. 2014;124(9):1412–1425.
25. Haberichter SL. von Willebrand factor propeptide: biology and clinical utility. *Blood*. 2015;126(15):1753–1761.
26. Cramer EM, Caen JP, Drouet L, Breton-Gorius J. Absence of tubular structures and immunolabeling for von Willebrand factor in the platelet alpha-granules from porcine von Willebrand disease. *Blood*. 1986;68(3):774–778.
27. Valentijn KM, Sadler JE, Valentijn JA, Voorberg J, Eikenboom J. Functional architecture of Weibel-Palade bodies. *Blood*. 2011;117(19):5033–5043.
28. Zhou Y-F, Eng ET, Zhu J, et al. Sequence and structure relationships within von Willebrand factor. *Blood*. 2012;120(2):449–458.
29. Wagner DD, Saffaripour S, Bonfanti R, et al. Induction of specific storage organelles by von Willebrand factor propolypeptide. *Cell*. 1991;64(2):403–413.
30. Mayadas TN, Wagner DD. Vicinal cysteines in the prosequence play a role in von Willebrand factor multimer assembly. *Proc Natl Acad Sci U S A*. 1992;89(8):3531–3535.

31. Furlan M. Von Willebrand factor: molecular size and functional activity. *Ann Hematol*. 1996;72(6):341–348.
32. Reininger AJ. Function of von Willebrand factor in haemostasis and thrombosis. *Haemophilia*. 2008;14 Suppl 5:11–26.
33. Federici AB, Bader R, Pagani S, et al. Binding of von Willebrand factor to glycoproteins Ib and IIb/IIIa complex: affinity is related to multimeric size. *Br J Haematol*. 1989;73(1):93–99.
34. Fischer BE, Kramer G, Mitterer A, et al. Effect of multimerization of human and recombinant von Willebrand factor on platelet aggregation, binding to collagen and binding of coagulation factor VIII. *Thromb Res*. 1996;84(1):55–66.
35. Gralnick HR, Williams SB, Morisato DK. Effect of multimeric structure of the factor VIII/von Willebrand factor protein on binding to platelets. *Blood*. 1981;58(2):387–397.
36. Stockschlaeder M, Schneppenheim R, Budde U. Update on von Willebrand factor multimers: focus on high-molecular-weight multimers and their role in hemostasis. *Blood Coagul Fibrinolysis*. 2014;25(3):206–216.
37. Hulstein JJJ, de Groot PG, Silence K, et al. A novel nanobody that detects the gain-of-function phenotype of von Willebrand factor in ADAMTS13 deficiency and von Willebrand disease type 2B. *Blood*. 2005;106(9):3035–3042.
38. Siedlecki CA, Lestini BJ, Kottke-Marchant KK, et al. Shear-dependent changes in the three-dimensional structure of human von Willebrand factor. *Blood*. 1996;88(8):2939–2950.
39. Vlot AJ, Koppelman SJ, van den Berg MH, Bouma BN, Sixma JJ. The affinity and stoichiometry of binding of human factor VIII to von Willebrand factor. *Blood*. 1995;85(11):3150–3157.
40. Vlot AJ, Koppelman SJ, Bouma BN, Sixma JJ. Factor VIII and von Willebrand factor. *Thromb Haemost*. 1998;79(3):456–465.
41. Federici AB. Current and emerging approaches for assessing von Willebrand disease in 2016. *Int J Lab Hematol*. 2016;38 Suppl 1:41–49.
42. Pipe SW, Montgomery RR, Pratt KP, Lenting PJ, Lillicrap D. Life in the shadow of a dominant partner: the FVIII-VWF association and its clinical implications for hemophilia A. *Blood*. 2016.
43. Casari C, Lenting PJ, Wohner N, Christophe OD, Denis CV. Clearance of von Willebrand factor. *J Thromb Haemost*. 2013;11 Suppl 1:202–211.

44. Gallinaro L, Cattini MG, Sztukowska M, et al. A shorter von Willebrand factor survival in O blood group subjects explains how ABO determinants influence plasma von Willebrand factor. *Blood*. 2008;111(7):3540–3545.

45. Castaman G, Tosetto A, Eikenboom JC, Rodeghiero F. Blood group significantly influences von Willebrand factor increase and half-life after desmopressin in von Willebrand disease Vicenza. *J Thromb Haemost*. 2010;8(9):2078–2080.

46. Casonato A, Pontara E, Sartorello F, et al. Reduced von Willebrand factor survival in type Vicenza von Willebrand disease. *Blood*. 2002;99(1):180–184.

47. Gezsi A, Budde U, Deak I, et al. Accelerated clearance alone explains ultra-large multimers in von Willebrand disease Vicenza. *J Thromb Haemost*. 2010;8(6):1273–1280.

48. Lenting PJ, Westein E, Terraube V, et al. An experimental model to study the in vivo survival of von Willebrand factor. Basic aspects and application to the R1205H mutation. *J Biol Chem*. 2004;279(13):12102–12109.

49. van Schooten CJ, Shahbazi S, Groot E, et al. Macrophages contribute to the cellular uptake of von Willebrand factor and factor VIII in vivo. *Blood*. 2008;112(5):1704–1712.

50. Rastegarlari G, Pegon JN, Casari C, et al. Macrophage LRP1 contributes to the clearance of von Willebrand factor. *Blood*. 2012;119(9):2126–2134.

51. Grewal PK, Uchiyama S, Ditto D, et al. The Ashwell receptor mitigates the lethal coagulopathy of sepsis. *Nat Med*. 2008;14(6):648–655.

52. Pegon JN, Kurdi M, Casari C, et al. Factor VIII and von Willebrand factor are ligands for the carbohydrate-receptor Siglec-5. *Haematologica*. 2012;97(12):1855–1863.

53. Rydz N, Swystun LL, Notley C, et al. The C-type lectin receptor CLEC4M binds, internalizes, and clears von Willebrand factor and contributes to the variation in plasma von Willebrand factor levels. *Blood*. 2013;121(26):5228–5237.

54. Bowen DJ. Genome-wide linkage analysis of von Willebrand factor plasma levels implicates the ABO locus as a principal determinant: should we overlook ADAMTS13? *Thromb Haemost*. 2003;90(5):961.

55. Stoddart JHJ, Andersen J, Lynch DC. Clearance of normal and type 2A von Willebrand factor in the rat. *Blood*. 1996;88(5):1692–1699.

56. Millar CM, Riddell AF, Brown SA, et al. Survival of von Willebrand factor released following DDAVP in a type 1 von Willebrand disease cohort: influence of

glycosylation, proteolysis and gene mutations. *Thromb Haemost*. 2008;99(5):916–924.

57. Badirou I, Kurdi M, Rayes J, et al. von Willebrand factor clearance does not involve proteolysis by ADAMTS-13. *J Thromb Haemost*. 2010;8(10):2338–2340.
58. Borchiellini A, Fijnvandraat K, Cate ten JW, et al. Quantitative analysis of von Willebrand factor propeptide release in vivo: effect of experimental endotoxemia and administration of 1-deamino-8-D-arginine vasopressin in humans. *Blood*. 1996;88(8):2951–2958.
59. Gill JC, Endres-Brooks J, Bauer PJ, Marks WJJ, Montgomery RR. The effect of ABO blood group on the diagnosis of von Willebrand disease. *Blood*. 1987;69(6):1691–1695.
60. Rodeghiero F, Castaman G, Dini E. Epidemiological investigation of the prevalence of von Willebrand's disease. *Blood*. 1987;69(2):454–459.
61. Werner EJ, Broxson EH, Tucker EL, et al. Prevalence of von Willebrand disease in children: a multiethnic study. *J. Pediatr.* 1993;123(6):893–898.
62. Bloom AL. von Willebrand factor: clinical features of inherited and acquired disorders. *Mayo Clin Proc*. 1991;66(7):743–751.
63. Sadler JE, Mannucci PM, Berntorp E, et al. Impact, diagnosis and treatment of von Willebrand disease. *Thromb Haemost*. 2000;84(2):160–174.
64. Bowman M, Hopman WM, Rapson D, Lillicrap D, James P. The prevalence of symptomatic von Willebrand disease in primary care practice. *J Thromb Haemost*. 2010;8(1):213–216.
65. Castaman G, Federici AB, Rodeghiero F, Mannucci PM. Von Willebrand's disease in the year 2003: towards the complete identification of gene defects for correct diagnosis and treatment. *Haematologica*. 2003;88(1):94–108.
66. Sadler JE, Budde U, Eikenboom JCJ, et al. Update on the pathophysiology and classification of von Willebrand disease: a report of the Subcommittee on von Willebrand Factor. *J Thromb Haemost*. 2006;4(10):2103–2114.
67. Lillicrap D. von Willebrand disease: advances in pathogenetic understanding, diagnosis, and therapy. *Blood*. 2013;122(23):3735–3740.
68. Robertson JD, Yenson PR, Rand ML, et al. Expanded phenotype-genotype correlations in a pediatric population with type 1 von Willebrand disease. *J Thromb Haemost*. 2011;9(9):1752–1760.
69. Flood VH. New insights into genotype and phenotype of VWD. *Hematology Am Soc*

Hematol Educ Program. 2014;2014(1):531–535.

70. Jacobi PM, Gill JC, Flood VH, et al. Intersection of mechanisms of type 2A VWD through defects in VWF multimerization, secretion, ADAMTS-13 susceptibility, and regulated storage. *Blood*. 2012;119(19):4543–4553.
71. Nishio K, Anderson PJ, Zheng XL, Sadler JE. Binding of platelet glycoprotein Ibalpha to von Willebrand factor domain A1 stimulates the cleavage of the adjacent domain A2 by ADAMTS13. *Proc Natl Acad Sci U S A*. 2004;101(29):10578–10583.
72. Ma Z, Su J, Zhang J, et al. The co-influence of VWD type 2B/2M mutations in the A1 domain and platelet GPIbalpha on the rate of cleavage to VWF by ADAMTS13. *Thromb Res*. 2015;136(5):987–995.
73. Casari C, Du V, Wu Y-P, et al. Accelerated uptake of VWF/platelet complexes in macrophages contributes to VWD type 2B-associated thrombocytopenia. *Blood*. 2013;122(16):2893–2902.
74. Mazurier C, Goudemand J, Hilbert L, et al. Type 2N von Willebrand disease: clinical manifestations, pathophysiology, laboratory diagnosis and molecular biology. *Best Pract Res Clin Haematol*. 2001;14(2):337–347.
75. van Meegeren MER, Mancini TL, Schoormans SCM, et al. Clinical phenotype in genetically confirmed von Willebrand disease type 2N patients reflects a haemophilia A phenotype. *Haemophilia*. 2015;21(5):e375–83.
76. Franchini M, Lippi G. Acquired von Willebrand syndrome: an update. *Am J Hematol*. 2007;82(5):368–375.
77. van Genderen PJ, Vink T, Michiels JJ, et al. Acquired von Willebrand disease caused by an autoantibody selectively inhibiting the binding of von Willebrand factor to collagen. *Blood*. 1994;84(10):3378–3384.
78. Richard C, Cuadrado MA, Prieto M, et al. Acquired von Willebrand disease in multiple myeloma secondary to absorption of von Willebrand factor by plasma cells. *Am J Hematol*. 1990;35(2):114–117.
79. Budde U, van Genderen PJ. Acquired von Willebrand disease in patients with high platelet counts. *Semin Thromb Hemost*. 1997;23(5):425–431.
80. Baghai M, Heilmann C, Beyersdorf F, et al. Platelet dysfunction and acquired von Willebrand syndrome in patients with left ventricular assist devices. *Eur J Cardiothorac Surg*. 2015;48(3):421–427.
81. Nascimbene A, Neelamegham S, Frazier OH, Moake JL, Dong J-F. Acquired von Willebrand syndrome associated with left ventricular assist device. *Blood*.

2016;127(25):3133–3141.

82. Curnow J, Pasalic L, Favaloro EJ. Treatment of von Willebrand Disease. *Semin Thromb Hemost*. 2016;42(2):133–146.

83. Kaufmann JE, Oksche A, Wollheim CB, et al. Vasopressin-induced von Willebrand factor secretion from endothelial cells involves V2 receptors and cAMP. *J Clin Invest*. 2000;106(1):107–116.

84. Kaufmann JE, Vischer UM. Cellular mechanisms of the hemostatic effects of desmopressin (DDAVP). *J Thromb Haemost*. 2003;1(4):682–689.

85. Halimeh S, Krumpel A, Rott H, et al. Long-term secondary prophylaxis in children, adolescents and young adults with von Willebrand disease. Results of a cohort study. *Thromb Haemost*. 2011;105(4):597–604.

86. Abshire T, Cox-Gill J, Kempton CL, et al. Prophylaxis escalation in severe von Willebrand disease: a prospective study from the von Willebrand Disease Prophylaxis Network. *J Thromb Haemost*. 2015;13(9):1585–1589.

87. Federici AB, Sacco R, Stabile F, et al. Optimising local therapy during oral surgery in patients with von Willebrand disease: effective results from a retrospective analysis of 63 cases. *Haemophilia*. 2000;6(2):71–77.

88. Turecek PL, Mitterer A, Matthiessen HP, et al. Development of a plasma- and albumin-free recombinant von Willebrand factor. *Hamostaseologie*. 2009;29 Suppl 1:S32–8.

89. Turecek PL, Schrenk G, Rottensteiner H, et al. Structure and function of a recombinant von Willebrand factor drug candidate. *Semin Thromb Hemost*. 2010;36(5):510–521.

90. Gill JC, Castaman G, Windyga J, et al. Hemostatic efficacy, safety, and pharmacokinetics of a recombinant von Willebrand factor in severe von Willebrand disease. *Blood*. 2015;126(17):2038–2046.

91. De Meyer SF, Vanhoorelbeke K, Chuah MK, et al. Phenotypic correction of von Willebrand disease type 3 blood-derived endothelial cells with lentiviral vectors expressing von Willebrand factor. *Blood*. 2006;107(12):4728–4736.

92. De Meyer SF, Deckmyn H, Vanhoorelbeke K. von Willebrand factor to the rescue. *Blood*. 2009;113(21):5049–5057.

93. Wang L, Rosenberg JB, De BP, et al. In vivo gene transfer strategies to achieve partial correction of von Willebrand disease. *Hum Gene Ther*. 2012;23(6):576–588.

94. Pergolizzi RG, Jin G, Chan D, et al. Correction of a murine model of von Willebrand

disease by gene transfer. *Blood*. 2006;108(3):862–869.

95. Lenting PJ, de Groot PG, De Meyer SF, et al. Correction of the bleeding time in von Willebrand factor (VWF)-deficient mice using murine VWF. *Blood*. 2007;109(5):2267–2268.
96. De Meyer SF, Vandeputte N, Pareyn I, et al. Restoration of plasma von Willebrand factor deficiency is sufficient to correct thrombus formation after gene therapy for severe von Willebrand disease. *Arterioscler Thromb Vasc Biol*. 2008;28(9):1621–1626.
97. McGrath RT, McRae E, Smith OP, O'Donnell JS. Platelet von Willebrand factor--structure, function and biological importance. *Br J Haematol*. 2010;148(6):834–843.
98. Williams SB, McKeown LP, Krutzsch H, Hansmann K, Gralnick HR. Purification and characterization of human platelet von Willebrand factor. *Br J Haematol*. 1994;88(3):582–591.
99. Matsui T, Shimoyama T, Matsumoto M, et al. ABO blood group antigens on human plasma von Willebrand factor after ABO-mismatched bone marrow transplantation. *Blood*. 1999;94(8):2895–2900.
100. McGrath RT, van den Biggelaar M, Byrne B, et al. Altered glycosylation of platelet-derived von Willebrand factor confers resistance to ADAMTS13 proteolysis. *Blood*. 2013;122(25):4107–4110.
101. Lenting PJ, Denis CV. Platelet von Willebrand factor: sweet resistance. *Blood*. 2013;122(25):4006–4007.
102. Ruggeri ZM, Zimmerman TS. Variant von Willebrand's disease: characterization of two subtypes by analysis of multimeric composition of factor VIII/von Willebrand factor in plasma and platelets. *J Clin Invest*. 1980;65(6):1318–1325.
103. Ruggeri ZM, Mannucci PM, Lombardi R, Federici AB, Zimmerman TS. Multimeric composition of factor VIII/von Willebrand factor following administration of DDAVP: implications for pathophysiology and therapy of von Willebrand's disease subtypes. *Blood*. 1982;59(6):1272–1278.
104. Gralnick HR, Williams SB, McKeown LP, et al. Platelet von Willebrand factor: comparison with plasma von Willebrand factor. *Thromb Res*. 1985;38(6):623–633.
105. Brinkhous KM. Animal models: importance in research on hemorrhage and thrombosis. *Adv Exp Med Biol*. 1978;102:123–133.
106. Johnson GS, Turrentine MA, Kraus KH. Canine von Willebrand's disease. A heterogeneous group of bleeding disorders. *Vet Clin North Am Small Anim Pract*.

1988;18(1):195–229.

107. Denis C, Methia N, Frenette PS, et al. A mouse model of severe von Willebrand disease: defects in hemostasis and thrombosis. *Proc Natl Acad Sci U S A*. 1998;95(16):9524–9529.

108. Nichols TC, Samama CM, Bellinger DA, et al. Function of von Willebrand factor after crossed bone marrow transplantation between normal and von Willebrand disease pigs: effect on arterial thrombosis in chimeras. *Proc Natl Acad Sci U S A*. 1995;92(7):2455–2459.

109. Nichols TC, Bellinger DA, Reddick RL, et al. The roles of von Willebrand factor and factor VIII in arterial thrombosis: studies in canine von Willebrand disease and hemophilia A. *Blood*. 1993;81(10):2644–2651.

110. Andre P, Brouland JP, Roussi J, et al. Role of plasma and platelet von Willebrand factor in arterial thrombogenesis and hemostasis in the pig. *Exp Hematol*. 1998;26(7):620–626.

111. Kanaji S, Fahs SA, Shi Q, Haberichter SL, Montgomery RR. Contribution of platelet vs. endothelial VWF to platelet adhesion and hemostasis. *J Thromb Haemost*. 2012;10(8):1646–1652.

112. Fressinaud E, Baruch D, Rothschild C, Baumgartner HR, Meyer D. Platelet von Willebrand factor: evidence for its involvement in platelet adhesion to collagen. *Blood*. 1987;70(4):1214–1217.

113. Bowie EJ, Solberg LAJ, Fass DN, et al. Transplantation of normal bone marrow into a pig with severe von Willebrand's disease. *J Clin Invest*. 1986;78(1):26–30.

114. Gralnick HR, Rick ME, McKeown LP, et al. Platelet von Willebrand factor: an important determinant of the bleeding time in type I von Willebrand's disease. *Blood*. 1986;68(1):58–61.

115. Levy GG, Nichols WC, Lian EC, et al. Mutations in a member of the ADAMTS gene family cause thrombotic thrombocytopenic purpura. *Nature*. 2001;413(6855):488–494.

116. Uemura M, Tatsumi K, Matsumoto M, et al. Localization of ADAMTS13 to the stellate cells of human liver. *Blood*. 2005;106(3):922–924.

117. Zhou W, Inada M, Lee T-P, et al. ADAMTS13 is expressed in hepatic stellate cells. *Lab Invest*. 2005;85(6):780–788.

118. Turner N, Nolasco L, Tao Z, Dong J-F, Moake J. Human endothelial cells synthesize and release ADAMTS-13. *J Thromb Haemost*. 2006;4(6):1396–1404.

119. Turner NA, Nolasco L, Ruggeri ZM, Moake JL. Endothelial cell ADAMTS-13 and VWF: production, release, and VWF string cleavage. *Blood*. 2009;114(24):5102–5111.

120. Suzuki M, Murata M, Matsubara Y, et al. Detection of von Willebrand factor-cleaving protease (ADAMTS-13) in human platelets. *Biochem Biophys Res Commun*. 2004;313(1):212–216.

121. Liu L, Choi H, Bernardo A, et al. Platelet-derived VWF-cleaving metalloprotease ADAMTS-13. *J Thromb Haemost*. 2005;3(11):2536–2544.

122. Manea M, Kristoffersson A, Schneppenheim R, et al. Podocytes express ADAMTS13 in normal renal cortex and in patients with thrombotic thrombocytopenic purpura. *Br J Haematol*. 2007;138(5):651–662.

123. Tauchi R, Imagama S, Ohgomori T, et al. ADAMTS-13 is produced by glial cells and upregulated after spinal cord injury. *Neurosci Lett*. 2012;517(1):1–6.

124. Zheng X, Chung D, Takayama TK, et al. Structure of von Willebrand factor-cleaving protease (ADAMTS13), a metalloprotease involved in thrombotic thrombocytopenic purpura. *J Biol Chem*. 2001;276(44):41059–41063.

125. Anderson PJ, Kokame K, Sadler JE. Zinc and calcium ions cooperatively modulate ADAMTS13 activity. *J Biol Chem*. 2006;281(2):850–857.

126. Ai J, Smith P, Wang S, Zhang P, Zheng XL. The proximal carboxyl-terminal domains of ADAMTS13 determine substrate specificity and are all required for cleavage of von Willebrand factor. *J Biol Chem*. 2005;280(33):29428–29434.

127. Gao W, Anderson PJ, Sadler JE. Extensive contacts between ADAMTS13 exosites and von Willebrand factor domain A2 contribute to substrate specificity. *Blood*. 2008;112(5):1713–1719.

128. Zheng XL. Structure-function and regulation of ADAMTS-13 protease. *J Thromb Haemost*. 2013;11 Suppl 1:11–23.

129. Akiyama M, Takeda S, Kokame K, Takagi J, Miyata T. Crystal structures of the noncatalytic domains of ADAMTS13 reveal multiple discontinuous exosites for von Willebrand factor. *Proc Natl Acad Sci U S A*. 2009;106(46):19274–19279.

130. Jin S-Y, Skipwith CG, Zheng XL. Amino acid residues Arg(659), Arg(660), and Tyr(661) in the spacer domain of ADAMTS13 are critical for cleavage of von Willebrand factor. *Blood*. 2010;115(11):2300–2310.

131. Pos W, Crawley JTB, Fijnheer R, et al. An autoantibody epitope comprising residues R660, Y661, and Y665 in the ADAMTS13 spacer domain identifies a binding site

for the A2 domain of VWF. *Blood*. 2010;115(8):1640–1649.

132. Xiang Y, de Groot R, Crawley JTB, Lane DA. Mechanism of von Willebrand factor scissile bond cleavage by a disintegrin and metalloproteinase with a thrombospondin type 1 motif, member 13 (ADAMTS13). *Proc Natl Acad Sci U S A*. 2011;108(28):11602–11607.
133. Tao Z, Wang Y, Choi H, et al. Cleavage of ultralarge multimers of von Willebrand factor by C-terminal-truncated mutants of ADAMTS-13 under flow. *Blood*. 2005;106(1):141–143.
134. Zanardelli S, Chion ACK, Groot E, et al. A novel binding site for ADAMTS13 constitutively exposed on the surface of globular VWF. *Blood*. 2009;114(13):2819–2828.
135. Feys HB, Anderson PJ, Vanhoorelbeke K, Majerus EM, Sadler JE. Multi-step binding of ADAMTS-13 to von Willebrand factor. *J Thromb Haemost*. 2009;7(12):2088–2095.
136. Zhang P, Pan W, Rux AH, Sachais BS, Zheng XL. The cooperative activity between the carboxyl-terminal TSP1 repeats and the CUB domains of ADAMTS13 is crucial for recognition of von Willebrand factor under flow. *Blood*. 2007;110(6):1887–1894.
137. Banno F, Chauhan AK, Kokame K, et al. The distal carboxyl-terminal domains of ADAMTS13 are required for regulation of in vivo thrombus formation. *Blood*. 2009;113(21):5323–5329.
138. De Maeyer B, De Meyer SF, Feys HB, et al. The distal carboxyterminal domains of murine ADAMTS13 influence proteolysis of platelet-decorated VWF strings in vivo. *J Thromb Haemost*. 2010;8(10):2305–2312.
139. Muia J, Zhu J, Gupta G, et al. Allosteric activation of ADAMTS13 by von Willebrand factor. *Proc Natl Acad Sci U S A*. 2014;111(52):18584–18589.
140. South K, Luken BM, Crawley JTB, et al. Conformational activation of ADAMTS13. *Proc Natl Acad Sci U S A*. 2014;111(52):18578–18583.
141. Deforche L, Roose E, Vandenbulcke A, et al. Linker regions and flexibility around the metalloprotease domain account for conformational activation of ADAMTS-13. *J Thromb Haemost*. 2015;13(11):2063–2075.
142. Crawley JTB, de Groot R, Xiang Y, Luken BM, Lane DA. Unraveling the scissile bond: how ADAMTS13 recognizes and cleaves von Willebrand factor. *Blood*. 2011;118(12):3212–3221.
143. Dong J-F, Moake JL, Nolasco L, et al. ADAMTS-13 rapidly cleaves newly secreted

ultralarge von Willebrand factor multimers on the endothelial surface under flowing conditions. *Blood*. 2002;100(12):4033–4039.

144. Tsai HM, Sussman II, Nagel RL. Shear stress enhances the proteolysis of von Willebrand factor in normal plasma. *Blood*. 1994;83(8):2171–2179.

145. Moake JL, Rudy CK, Troll JH, et al. Unusually large plasma factor VIII:von Willebrand factor multimers in chronic relapsing thrombotic thrombocytopenic purpura. *N Engl J Med*. 1982;307(23):1432–1435.

146. Veyradier A, Obert B, Houllier A, Meyer D, Girma JP. Specific von Willebrand factor-cleaving protease in thrombotic microangiopathies: a study of 111 cases. *Blood*. 2001;98(6):1765–1772.

147. Scully M, Yarranton H, Liesner R, et al. Regional UK TTP registry: correlation with laboratory ADAMTS 13 analysis and clinical features. *Br J Haematol*. 2008;142(5):819–826.

148. Lotta LA, Garagiola I, Palla R, Cairo A, Peyvandi F. ADAMTS13 mutations and polymorphisms in congenital thrombotic thrombocytopenic purpura. *Hum Mutat*. 2010;31(1):11–19.

149. Blombery P, Scully M. Management of thrombotic thrombocytopenic purpura: current perspectives. *J Blood Med*. 2014;5:15–23.

150. Lancellotti S, Basso M, De Cristofaro R. Proteolytic processing of von Willebrand factor by adamts13 and leukocyte proteases. *Mediterr J Hematol Infect Dis*. 2013;5(1):e2013058.

151. Uchida T, Wada H, Mizutani M, et al. Identification of novel mutations in ADAMTS13 in an adult patient with congenital thrombotic thrombocytopenic purpura. *Blood*. 2004;104(7):2081–2083.

152. Camilleri RS, Scully M, Thomas M, et al. A phenotype-genotype correlation of ADAMTS13 mutations in congenital thrombotic thrombocytopenic purpura patients treated in the United Kingdom. *J Thromb Haemost*. 2012;10(9):1792–1801.

153. Lotta LA, Wu HM, Mackie IJ, et al. Residual plasmatic activity of ADAMTS13 is correlated with phenotype severity in congenital thrombotic thrombocytopenic purpura. *Blood*. 2012;120(2):440–448.

154. Noris M, Bucchioni S, Galbusera M, et al. Complement factor H mutation in familial thrombotic thrombocytopenic purpura with ADAMTS13 deficiency and renal involvement. *J Am Soc Nephrol*. 2005;16(5):1177–1183.

155. Fujimura Y, Matsumoto M, Kokame K, et al. Pregnancy-induced thrombocytopenia

and TTP, and the risk of fetal death, in Upshaw-Schulman syndrome: a series of 15 pregnancies in 9 genotyped patients. *Br J Haematol*. 2009;144(5):742–754.

156. Falter T, Kremer Hovinga JA, Lackner K, et al. Late onset and pregnancy-induced congenital thrombotic thrombocytopenic purpura. *Hamostaseologie*. 2014;34(3):244–248.
157. Douglas KW, Pollock KGJ, Young D, Catlow J, Green R. Infection frequently triggers thrombotic microangiopathy in patients with preexisting risk factors: a single-institution experience. *J Clin Apher*. 2010;25(2):47–53.
158. Zheng XL, Wu HM, Shang D, et al. Multiple domains of ADAMTS13 are targeted by autoantibodies against ADAMTS13 in patients with acquired idiopathic thrombotic thrombocytopenic purpura. *Haematologica*. 2010;95(9):1555–1562.
159. Jian C, Xiao J, Gong L, et al. Gain-of-function ADAMTS13 variants that are resistant to autoantibodies against ADAMTS13 in patients with acquired thrombotic thrombocytopenic purpura. *Blood*. 2012;119(16):3836–3843.
160. Thomas MR, de Groot R, Scully MA, Crawley JTB. Pathogenicity of Anti-ADAMTS13 Autoantibodies in Acquired Thrombotic Thrombocytopenic Purpura. *EBioMedicine*. 2015;2(8):940–950.
161. Scheiflinger F, Knobl P, Trattner B, et al. Nonneutralizing IgM and IgG antibodies to von Willebrand factor-cleaving protease (ADAMTS-13) in a patient with thrombotic thrombocytopenic purpura. *Blood*. 2003;102(9):3241–3243.
162. Asada Y, Sumiyoshi A, Hayashi T, Suzumiya J, Kaketani K. Immunohistochemistry of vascular lesion in thrombotic thrombocytopenic purpura, with special reference to factor VIII related antigen. *Thromb Res*. 1985;38(5):469–479.
163. Tsai H-M. Pathophysiology of thrombotic thrombocytopenic purpura. *Int J Hematol*. 2010;91(1):1–19.
164. Tsai H-M. ADAMTS13 and microvascular thrombosis. *Expert Rev Cardiovasc Ther*. 2006;4(6):813–825.
165. George JN, Nester CM. Syndromes of thrombotic microangiopathy. *N Engl J Med*. 2014;371(19):1847–1848.
166. Kremer Hovinga JA, Vesely SK, Terrell DR, Lammle B, George JN. Survival and relapse in patients with thrombotic thrombocytopenic purpura. *Blood*. 2010;115(8):1500–1511.
167. Hassan S, Westwood J-P, Ellis D, et al. The utility of ADAMTS13 in differentiating TTP from other acute thrombotic microangiopathies: results from the UK TTP

Registry. *Br J Haematol*. 2015;171(5):830–835.

168. Kokame K, Nobe Y, Kokubo Y, Okayama A, Miyata T. FRETS-VWF73, a first fluorogenic substrate for ADAMTS13 assay. *Br J Haematol*. 2005;129(1):93–100.
169. Kremer Hovinga JA, Mottini M, Lammle B. Measurement of ADAMTS-13 activity in plasma by the FRETS-VWF73 assay: comparison with other assay methods. *J Thromb Haemost*. 2006;4(5):1146–1148.
170. Rock GA, Shumak KH, Buskard NA, et al. Comparison of plasma exchange with plasma infusion in the treatment of thrombotic thrombocytopenic purpura. Canadian Apheresis Study Group. *N Engl J Med*. 1991;325(6):393–397.
171. Bell WR, Braine HG, Ness PM, Kickler TS. Improved survival in thrombotic thrombocytopenic purpura-hemolytic uremic syndrome. Clinical experience in 108 patients. *N Engl J Med*. 1991;325(6):398–403.
172. George JN. How I treat patients with thrombotic thrombocytopenic purpura: 2010. *Blood*. 2010;116(20):4060–4069.
173. Scully M, Hunt BJ, Benjamin S, et al. Guidelines on the diagnosis and management of thrombotic thrombocytopenic purpura and other thrombotic microangiopathies. *Br J Haematol*. 2012;158(3):323–335.
174. Scully M, McDonald V, Cavenagh J, et al. A phase 2 study of the safety and efficacy of rituximab with plasma exchange in acute acquired thrombotic thrombocytopenic purpura. *Blood*. 2011;118(7):1746–1753.
175. Scully M, Goodship T. How I treat thrombotic thrombocytopenic purpura and atypical haemolytic uraemic syndrome. *Br J Haematol*. 2014;164(6):759–766.
176. Westwood J-P, Webster H, McGuckin S, et al. Rituximab for thrombotic thrombocytopenic purpura: benefit of early administration during acute episodes and use of prophylaxis to prevent relapse. *J Thromb Haemost*. 2013;11(3):481–490.
177. Bresin E, Gastoldi S, Daina E, et al. Rituximab as pre-emptive treatment in patients with thrombotic thrombocytopenic purpura and evidence of anti-ADAMTS13 autoantibodies. *Thromb Haemost*. 2009;1–6.
178. Barbot J, Costa E, Guerra M, et al. Ten years of prophylactic treatment with fresh-frozen plasma in a child with chronic relapsing thrombotic thrombocytopenic purpura as a result of a congenital deficiency of von Willebrand factor-cleaving protease. *Br J Haematol*. 2001;113(3):649–651.
179. Vanhoorelbeke K, De Meyer SF. Animal models for thrombotic thrombocytopenic purpura. *J Thromb Haemost*. 2013;11 Suppl 1:2–10.

180. Banno F, Kokame K, Okuda T, et al. Complete deficiency in ADAMTS13 is prothrombotic, but it alone is not sufficient to cause thrombotic thrombocytopenic purpura. *Blood*. 2006;107(8):3161–3166.

181. Motto DG, Chauhan AK, Zhu G, et al. Shigatoxin triggers thrombotic thrombocytopenic purpura in genetically susceptible ADAMTS13-deficient mice. *J Clin Invest*. 2005;115(10):2752–2761.

182. Mohlke KL, Purkayastha AA, Westrick RJ, et al. Mvwf, a dominant modifier of murine von Willebrand factor, results from altered lineage-specific expression of a glycosyltransferase. *Cell*. 1999;96(1):111–120.

183. Veyradier A, Lavergne J-M, Ribba A-S, et al. Ten candidate ADAMTS13 mutations in six French families with congenital thrombotic thrombocytopenic purpura (Upshaw-Schulman syndrome). *J Thromb Haemost*. 2004;2(3):424–429.

184. Schiviz A, Wuersch K, Piskernik C, et al. A new mouse model mimicking thrombotic thrombocytopenic purpura: correction of symptoms by recombinant human ADAMTS13. *Blood*. 2012;119(25):6128–6135.

185. Pickens B, Mao Y, Li D, et al. Platelet-delivered ADAMTS13 inhibits arterial thrombosis and prevents thrombotic thrombocytopenic purpura in murine models. *Blood*. 2015;125(21):3326–3334.

186. Chauhan AK, Walsh MT, Zhu G, et al. The combined roles of ADAMTS13 and VWF in murine models of TTP, endotoxemia, and thrombosis. *Blood*. 2008;111(7):3452–3457.

187. Huang J, Motto DG, Bundle DR, Sadler JE. Shiga toxin B subunits induce VWF secretion by human endothelial cells and thrombotic microangiopathy in ADAMTS13-deficient mice. *Blood*. 2010;116(18):3653–3659.

188. Feys HB, Roodt J, Vandeputte N, et al. Thrombotic thrombocytopenic purpura directly linked with ADAMTS13 inhibition in the baboon (Papio ursinus). *Blood*. 2010;116(12):2005–2010.

189. Ostertag EM, Bdeir K, Kacir S, et al. ADAMTS13 autoantibodies cloned from patients with acquired thrombotic thrombocytopenic purpura: 2. Pathogenicity in an animal model. *Transfusion*. 2016;56(7):1775–1785.

190. Tersteeg C, Schiviz A, De Meyer SF, et al. Potential for Recombinant ADAMTS13 as an Effective Therapy for Acquired Thrombotic Thrombocytopenic Purpura. *Arterioscler Thromb Vasc Biol*. 2015;35(11):2336–2342.

191. Diener JL, Daniel Lagassé HA, Duerschmied D, et al. Inhibition of von Willebrand

factor-mediated platelet activation and thrombosis by the anti-von Willebrand factor A1-domain aptamer ARC1779. *J Thromb Haemost*. 2009;7(7):1155–1162.

192. Feys HB, Roodt J, Vandeputte N, et al. Inhibition of von Willebrand factor-platelet glycoprotein Ib interaction prevents and reverses symptoms of acute acquired thrombotic thrombocytopenic purpura in baboons. *Blood*. 2012;120(17):3611–3614.
193. Callewaert F, Roodt J, Ulrichts H, et al. Evaluation of efficacy and safety of the anti-VWF Nanobody ALX-0681 in a preclinical baboon model of acquired thrombotic thrombocytopenic purpura. *Blood*. 2012;120(17):3603–3610.
194. Holz J-B. The TITAN trial--assessing the efficacy and safety of an anti-von Willebrand factor Nanobody in patients with acquired thrombotic thrombocytopenic purpura. *Transfus Apher Sci*. 2012;46(3):343–346.
195. Peyvandi F, Scully M, Kremer Hovinga JA, et al. Caplacizumab for Acquired Thrombotic Thrombocytopenic Purpura. *N Engl J Med*. 2016;374(6):511–522.
196. Cataland SR, Peyvandi FM, Mannucci PM, et al. Initial experience from a double-blind, placebo-controlled, clinical outcome study of ARC1779 in patients with thrombotic thrombocytopenic purpura. *Am J Hematol*. 2012;87(4):430–432.
197. Plaimauer B, Kremer Hovinga JA, Juno C, et al. Recombinant ADAMTS13 normalizes von Willebrand factor-cleaving activity in plasma of acquired TTP patients by overriding inhibitory antibodies. *J Thromb Haemost*. 2011;9(5):936–944.
198. Chen J, Reheman A, Gushiken FC, et al. N-acetylcysteine reduces the size and activity of von Willebrand factor in human plasma and mice. *J Clin Invest*. 2011;121(2):593–603.
199. Shortt J, Oh DH, Opat SS. ADAMTS13 antibody depletion by bortezomib in thrombotic thrombocytopenic purpura. *N Engl J Med*. 2013;368(1):90–92.
200. Shortt J, Opat SS, Wood EM. N-Acetylcysteine for thrombotic thrombocytopenic purpura: is a von Willebrand factor-inhibitory dose feasible in vivo? *Transfusion*. 2014;54(9):2362–2363.
201. Li GW, Rambally S, Kamboj J, et al. Treatment of refractory thrombotic thrombocytopenic purpura with N-acetylcysteine: a case report. *Transfusion*. 2014;54(5):1221–1224.
202. Rottenstreich A, Hochberg-Klein S, Rund D, Kalish Y. The role of N-acetylcysteine in the treatment of thrombotic thrombocytopenic purpura. *J Thromb Thrombolysis*. 2016;41(4):678–683.
203. Tersteeg C, de Maat S, De Meyer SF, et al. Plasmin cleavage of von Willebrand

factor as an emergency bypass for ADAMTS13 deficiency in thrombotic microangiopathy. *Circulation*. 2014;129(12):1320–1331.

204. George JN. The thrombotic thrombocytopenic purpura and hemolytic uremic syndromes: evaluation, management, and long-term outcomes experience of the Oklahoma TTP-HUS Registry, 1989-2007. *Kidney Int Suppl*. 2009;(112):S52–4.
205. Vesely SK. Life after acquired thrombotic thrombocytopenic purpura: morbidity, mortality, and risks during pregnancy. *J Thromb Haemost*. 2015;13 Suppl 1:S216–22.
206. Laje P, Shang D, Cao W, et al. Correction of murine ADAMTS13 deficiency by hematopoietic progenitor cell-mediated gene therapy. *Blood*. 2009;113(10):2172–2180.
207. Niiya M, Endo M, Shang D, et al. Correction of ADAMTS13 deficiency by in utero gene transfer of lentiviral vector encoding ADAMTS13 genes. *Mol Ther*. 2008;17(1):34–41.
208. Trionfini P, Tomasoni S, Galbusera M, et al. Adenoviral-mediated gene transfer restores plasma ADAMTS13 antigen and activity in ADAMTS13 knockout mice. *Gene Ther*. 2009;16(11):1373–1379.
209. Jin S-Y, Xiao J, Zhou S, Wright JF, Zheng XL. AAV-mediated expression of an ADAMTS13 variant prevents shigatoxin-induced thrombotic thrombocytopenic purpura. *Blood*. 2013;121(19):3825–3829.
210. Flotte TR. Birth of a new therapeutic platform: 47 years of adeno-associated virus biology from virus discovery to licensed gene therapy. *Mol Ther*. 2013;21(11):1976–1981.
211. Naldini L. Gene therapy returns to centre stage. *Nature*. 2015;526(7573):351–360.
212. Hacein-Bey-Abina S, Hauer J, Lim A, et al. Efficacy of gene therapy for X-linked severe combined immunodeficiency. *N Engl J Med*. 2010;363(4):355–364.
213. Sakurai H, Kawabata K, Sakurai F, Nakagawa S, Mizuguchi H. Innate immune response induced by gene delivery vectors. *Int J Pharm*. 2008;354(1-2):9–15.
214. Mingozzi F, High KA. Immune responses to AAV vectors: overcoming barriers to successful gene therapy. *Blood*. 2013;122(1):23–36.
215. Wells DJ. Gene therapy progress and prospects: electroporation and other physical methods. *Gene Ther*. 2004;11(18):1363–1369.
216. Liu F, Song Y, Liu D. Hydrodynamics-based transfection in animals by systemic administration of plasmid DNA. *Gene Ther*. 1999;6(7):1258–1266.

217. Zhang G, Budker V, Wolff JA. High levels of foreign gene expression in hepatocytes after tail vein injections of naked plasmid DNA. *Hum Gene Ther*. 1999;10(10):1735–1737.

218. Newman CMH, Bettinger T. Gene therapy progress and prospects: ultrasound for gene transfer. *Gene Ther*. 2007;14(6):465–475.

219. Yin H, Kanasty RL, Eltoukhy AA, et al. Non-viral vectors for gene-based therapy. *Nat Rev Genet*. 2014;15(8):541–555.

220. Herweijer H, Zhang G, Subbotin VM, et al. Time course of gene expression after plasmid DNA gene transfer to the liver. *J Gene Med*. 2001;3(3):280–291.

221. Smit AF. Interspersed repeats and other mementos of transposable elements in mammalian genomes. *Curr Opin Genet Dev*. 1999;9(6):657–663.

222. Lander ES, Linton LM, Birren B, et al. Initial sequencing and analysis of the human genome. *Nature*. 2001;409(6822):860–921.

223. Cordaux R, Batzer MA. The impact of retrotransposons on human genome evolution. *Nat Rev Genet*. 2009;10(10):691–703.

224. Handler AM, Gomez SP, O'Brochta DA. A functional analysis of the P-element gene-transfer vector in insects. *Arch Insect Biochem Physiol*. 1993;22(3-4):373–384.

225. Ivics Z, Hackett PB, Plasterk RH, Izsvak Z. Molecular reconstruction of Sleeping Beauty, a Tc1-like transposon from fish, and its transposition in human cells. *Cell*. 1997;91(4):501–510.

226. Yant SR, Meuse L, Chiu W, et al. Somatic integration and long-term transgene expression in normal and haemophilic mice using a DNA transposon system. *Nat Genet*. 2000;25(1):35–41.

227. Zayed H, Izsvak Z, Walisko O, Ivics Z. Development of hyperactive sleeping beauty transposon vectors by mutational analysis. *Mol Ther*. 2004;9(2):292–304.

228. Mates L, Chuah MKL, Belay E, et al. Molecular evolution of a novel hyperactive Sleeping Beauty transposase enables robust stable gene transfer in vertebrates. *Nat Genet*. 2009;41(6):753–761.

229. Montini E, Held PK, Noll M, et al. In vivo correction of murine tyrosinemia type I by DNA-mediated transposition. *Mol Ther*. 2002;6(6):759–769.

230. He C-X, Shi D, Wu W-J, et al. Insulin expression in livers of diabetic mice mediated by hydrodynamics-based administration. *World J Gastroenterol*. 2004;10(4):567–572.

231. Ohlfest JR, Frandsen JL, Fritz S, et al. Phenotypic correction and long-term

expression of factor VIII in hemophilic mice by immunotolerization and nonviral gene transfer using the Sleeping Beauty transposon system. *Blood*. 2005;105(7):2691–2698.

232. Aronovich EL, Bell JB, Belur LR, et al. Prolonged expression of a lysosomal enzyme in mouse liver after Sleeping Beauty transposon-mediated gene delivery: implications for non-viral gene therapy of mucopolysaccharidoses. *J Gene Med*. 2007;9(5):403–415.
233. Kumaresan PR, Manuri PR, Albert ND, et al. Bioengineering T cells to target carbohydrate to treat opportunistic fungal infection. *Proc Natl Acad Sci U S A*. 2014;111(29):10660–10665.
234. Krishnamurthy J, Rabinovich BA, Mi T, et al. Genetic Engineering of T Cells to Target HERV-K, an Ancient Retrovirus on Melanoma. *Clin Cancer Res*. 2015;21(14):3241–3251.
235. Miskey C, Izsvak Z, Plasterk RH, Ivics Z. The Frog Prince: a reconstructed transposon from Rana pipiens with high transpositional activity in vertebrate cells. *Nucleic Acids Res*. 2003;31(23):6873–6881.
236. Ding S, Wu X, Li G, et al. Efficient transposition of the piggyBac (PB) transposon in mammalian cells and mice. *Cell*. 2005;122(3):473–483.
237. Skipper KA, Andersen PR, Sharma N, Mikkelsen JG. DNA transposon-based gene vehicles - scenes from an evolutionary drive. *J Biomed Sci*. 2013;20:92.
238. Ivics Z, Izsvak Z. The expanding universe of transposon technologies for gene and cell engineering. *Mob DNA*. 2010;1(1):25.
239. Mitchell RS, Beitzel BF, Schroder ARW, et al. Retroviral DNA integration: ASLV, HIV, and MLV show distinct target site preferences. *PLoS Biol*. 2004;2(8):E234.
240. Gogol-Doring A, Ammar I, Gupta S, et al. Genome-wide profiling reveals remarkable parallels between insertion site selection properties of the MLV retrovirus and the piggyBac transposon in primary human CD4(+) T cells. *Mol Ther*. 2016;24(3):592–606.
241. Voigt K, Gogol-Doring A, Miskey C, et al. Retargeting sleeping beauty transposon insertions by engineered zinc finger DNA-binding domains. *Mol Ther*. 2012;20(10):1852–1862.
242. Yant SR, Wu X, Huang Y, et al. High-resolution genome-wide mapping of transposon integration in mammals. *Mol Cell Biol*. 2005;25(6):2085–2094.
243. Vigdal TJ, Kaufman CD, Izsvak Z, Voytas DF, Ivics Z. Common physical properties

of DNA affecting target site selection of sleeping beauty and other Tc1/mariner transposable elements. *J Mol Biol*. 2002;323(3):441–452.

244. Wilber A, Frandsen JL, Geurts JL, et al. RNA as a source of transposase for Sleeping Beauty-mediated gene insertion and expression in somatic cells and tissues. *Mol Ther*. 2006;13(3):625–630.
245. Izsvak Z, Hackett PB, Cooper LJN, Ivics Z. Translating Sleeping Beauty transposition into cellular therapies: victories and challenges. *Bioessays*. 2010;32(9):756–767.
246. Xue X, Huang X, Nodland SE, et al. Stable gene transfer and expression in cord blood-derived CD34+ hematopoietic stem and progenitor cells by a hyperactive Sleeping Beauty transposon system. *Blood*. 2009;114(7):1319–1330.
247. Singh H, Manuri PR, Olivares S, et al. Redirecting specificity of T-cell populations for CD19 using the Sleeping Beauty system. *Cancer Res*. 2008;68(8):2961–2971.
248. Wilber A, Linehan JL, Tian X, et al. Efficient and stable transgene expression in human embryonic stem cells using transposon-mediated gene transfer. *Stem Cells*. 2007;25(11):2919–2927.
249. Williams DA. Sleeping beauty vector system moves toward human trials in the United States. *Mol Ther*. 2008;16(9):1515–1516.
250. Bell JB, Podetz-Pedersen KM, Aronovich EL, et al. Preferential delivery of the Sleeping Beauty transposon system to livers of mice by hydrodynamic injection. *Nat Protoc*. 2007;2(12):3153–3165.
251. Suda T, Liu D. Hydrodynamic gene delivery: its principles and applications. *Mol Ther*. 2007;15(12):2063–2069.
252. Casari C, Lenting PJ, Christophe OD, Denis CECV. Von Willebrand factor abnormalities studied in the mouse model: What we learned about VWF functions. *Mediterr J Hematol Infect Dis*. 2013;5(1):e2013047.
253. Kamimura K, Yokoo T, Abe H, et al. Image-guided hydrodynamic gene delivery: Current status and future directions. *Pharmaceutics*. 2015;7(3):213–223.
254. Fabre JW, Grehan A, Whitehorne M, et al. Hydrodynamic gene delivery to the pig liver via an isolated segment of the inferior vena cava. *Gene Ther*. 2008;15(6):452–462.
255. Kamimura K, Suda T, Xu W, Zhang G, Liu D. Image-guided, lobe-specific hydrodynamic gene delivery to swine liver. *Mol Ther*. 2009;17(3):491–499.
256. Kamimura K, Zhang G, Liu D. Image-guided, intravascular hydrodynamic gene

delivery to skeletal muscle in pigs. *Mol Ther*. 2010;18(1):93–100.

257. Kamimura K, Kanefuji T, Yokoo T, et al. Safety assessment of liver-targeted hydrodynamic gene delivery in dogs. *PLoS ONE*. 2014;9(9):e107203.
258. Khorsandi SE, Bachellier P, Weber JC, et al. Minimally invasive and selective hydrodynamic gene therapy of liver segments in the pig and human. *Cancer Gene Ther*. 2008;15(4):225–230.
259. Liu L, Sanz S, Heggestad AD, et al. Endothelial targeting of the Sleeping Beauty transposon within lung. *Mol Ther*. 2004;10(1):97–105.
260. Belur LR, Podetz-Pedersen K, Frandsen J, McIvor RS. Lung-directed gene therapy in mice using the nonviral Sleeping Beauty transposon system. *Nat Protoc*. 2007;2(12):3146–3152.
261. Podetz-Pedersen KM, Bell JB, Steele TWJ, et al. Gene expression in lung and liver after intravenous infusion of polyethylenimine complexes of Sleeping Beauty transposons. *Hum Gene Ther*. 2010;21(2):210–220.
262. Kren BT, Unger GM, Sjeklocha L, et al. Nanocapsule-delivered Sleeping Beauty mediates therapeutic Factor VIII expression in liver sinusoidal endothelial cells of hemophilia A mice. *J Clin Invest*. 2009;119(7):2086–2099.
263. Hausl MA, Zhang W, Muther N, et al. Hyperactive sleeping beauty transposase enables persistent phenotypic correction in mice and a canine model for hemophilia B. *Mol Ther*. 2010;18(11):1896–1906.
264. Kebriaei P, Singh H, Huls MH, et al. Phase I trials using Sleeping Beauty to generate CD19-specific CAR T cells. *J Clin Invest*. 2016;126(9):3363–3376.
265. Rangarajan S, Kessler C, Aledort L. The clinical implications of ADAMTS13 function: the perspectives of haemostaseologists. *Thromb Res*. 2013;132(4):403–407.
266. Schwameis M, Schorgenhofer C, Assinger A, Steiner MM, Jilma B. VWF excess and ADAMTS13 deficiency: a unifying pathomechanism linking inflammation to thrombosis in DIC, malaria, and TTP. *Thromb Haemost*. 2015;113(4):708–718.
267. Mozaffarian D, Benjamin EJ, Go AS, et al. Heart disease and stroke statistics--2015 update: a report from the American Heart Association. *Circulation*. 2015;131(4):e29–322.
268. Nieswandt B, Kleinschnitz C, Stoll G. Ischaemic stroke: a thrombo-inflammatory disease? *J Physiol*. 2011;589(Pt 17):4115–4123.
269. Denorme F, De Meyer SF. The VWF-GPIb axis in ischaemic stroke: lessons from animal models. *Thromb Haemost*. 2016;116(1):.

270. Catto AJ, Carter AM, Barrett JH, et al. von Willebrand factor and factor VIII: C in acute cerebrovascular disease. Relationship to stroke subtype and mortality. *Thromb Haemost*. 1997;77(6):1104–1108.

271. Bongers TN, de Maat MPM, van Goor M-LPJ, et al. High von Willebrand factor levels increase the risk of first ischemic stroke: influence of ADAMTS13, inflammation, and genetic variability. *Stroke*. 2006;37(11):2672–2677.

272. van Schie MC, de Maat MPM, de Groot PG, et al. Active von Willebrand factor and the risk of stroke. *Atherosclerosis*. 2010;208(2):322–323.

273. Andersson HM, Siegerink B, Luken BM, et al. High VWF, low ADAMTS13, and oral contraceptives increase the risk of ischemic stroke and myocardial infarction in young women. *Blood*. 2012;119(6):1555–1560.

274. Bongers TN, de Bruijne ELE, Dippel DWJ, et al. Lower levels of ADAMTS13 are associated with cardiovascular disease in young patients. *Atherosclerosis*. 2009;207(1):250–254.

275. Lambers M, Goldenberg NA, Kenet G, et al. Role of reduced ADAMTS13 in arterial ischemic stroke: a pediatric cohort study. *Ann Neurol*. 2013;73(1):58–64.

276. Sonneveld MAH, de Maat MPM, Leebeek FWG. Von Willebrand factor and ADAMTS13 in arterial thrombosis: a systematic review and meta-analysis. *Blood Rev*. 2014;28(4):167–178.

277. Folsom AR, Rosamond WD, Shahar E, et al. Prospective study of markers of hemostatic function with risk of ischemic stroke. The Atherosclerosis Risk in Communities (ARIC) Study Investigators. *Circulation*. 1999;100(7):736–742.

278. Wieberdink RG, van Schie MC, Koudstaal PJ, et al. High von Willebrand factor levels increase the risk of stroke: the Rotterdam study. *Stroke*. 2010;41(10):2151–2156.

279. Samai A, Monlezun D, Shaban A, et al. Von Willebrand factor drives the association between elevated factor VIII and poor outcomes in patients with ischemic stroke. *Stroke*. 2014;45(9):2789–2791.

280. Sonneveld MAH, de Maat MPM, Portegies MLP, et al. Low ADAMTS13 activity is associated with an increased risk of ischemic stroke. *Blood*. 2015;126(25):2739–2746.

281. Kleinschnitz C, De Meyer SF, Schwarz T, et al. Deficiency of von Willebrand factor protects mice from ischemic stroke. *Blood*. 2009;113(15):3600–3603.

282. Zhao B-Q, Chauhan AK, Canault M, et al. von Willebrand factor – cleaving protease

ADAMTS13 reduces ischemic brain injury in experimental stroke. *Blood*. 2009;114(15):1–3.

283. Fujioka M, Hayakawa K, Mishima K, et al. Brief report ADAMTS13 gene deletion aggravates ischemic brain damage: a possible neuroprotective role of ADAMTS13 by ameliorating postischemic hypoperfusion. *Blood*. 2010;115(8):1–3.
284. Lee S, Lee M, Hong Y, et al. Middle cerebral artery occlusion methods in rat versus mouse models of transient focal cerebral ischemic stroke. *Neural Regen Res*. 2014;9(7):757–758.
285. Gauberti M, Martinez de Lizarrondo S, Orset C, Vivien D. Lack of secondary microthrombosis after thrombin-induced stroke in mice and non-human primates. *J Thromb Haemost*. 2014;12(3):409–414.
286. Kleinschnitz C, Pozgajova M, Pham M, et al. Targeting platelets in acute experimental stroke: impact of glycoprotein Ib, VI, and IIb/IIIa blockade on infarct size, functional outcome, and intracranial bleeding. *Circulation*. 2007;115(17):2323–2330.
287. De Meyer SF, Schwarz T, Schatzberg D, Wagner DD. Platelet glycoprotein Ibα is an important mediator of ischemic stroke in mice. *Exp Transl Stroke Med*. 2011;3(1):9.
288. De Meyer SF, Schwarz T, Deckmyn H, et al. Binding of von Willebrand factor to collagen and glycoprotein Ibalpha, but not to glycoprotein IIb/IIIa, contributes to ischemic stroke in mice--brief report. *Arterioscler Thromb Vasc Biol*. 2010;30(10):1949–1951.
289. Nakano T, Irie K, Hayakawa K, et al. Delayed treatment with ADAMTS13 ameliorates cerebral ischemic injury without hemorrhagic complication. *Brain Res*. 2015;1624:330–335.
290. Le Behot A, Gauberti M, Martinez De Lizarrondo S, et al. GpIbalpha-VWF blockade restores vessel patency by dissolving platelet aggregates formed under very high shear rate in mice. *Blood*. 2014;123(21):3354–3363.
291. Denorme F, Langhauser F, Desender L, et al. ADAMTS13-mediated thrombolysis of t-PA-resistant occlusions in ischemic stroke in mice. *Blood*. 2016;127(19):2337–2345.
292. Khan MM, Motto DG, Lentz SR, Chauhan AK. ADAMTS13 reduces VWF-mediated acute inflammation following focal cerebral ischemia in mice. *J Thromb Haemost*. 2012;10(8):1665–1671.
293. Bernardo A, Ball C, Nolasco L, et al. Platelets adhered to endothelial cell-bound

ultra-large von Willebrand factor strings support leukocyte tethering and rolling under high shear stress. *J Thromb Haemost*. 2005;3(3):562–570.

294. Pendu R, Terraube V, Christophe OD, et al. P-selectin glycoprotein ligand 1 and beta2-integrins cooperate in the adhesion of leukocytes to von Willebrand factor. *Blood*. 2006;108(12):3746–3752.
295. Petri BOR, Broermann A, Li H, et al. von Willebrand factor promotes leukocyte extravasation. *Blood*. 2010;116(22):4712–4719.
296. White NJ, Pukrittayakamee S, Hien TT, et al. Malaria. *Lancet*. 2014;383(9918):723–735.
297. Deroost K, Pham T-T, Opdenakker G, Van Den Steen PE. The immunological balance between host and parasite in malaria. *FEMS Microbiol Rev*. 2016;40(2):208–257.
298. Dondorp AM, Ince C, Charunwatthana P, et al. Direct in vivo assessment of microcirculatory dysfunction in severe falciparum malaria. *J Infect Dis*. 2008;197(1):79–84.
299. Corbett CE, Duarte MI, Lancellotti CL, Silva MA, Andrade Junior HF. Cytoadherence in human falciparum malaria as a cause of respiratory distress. *J Trop Med Hyg*. 1989;92(2):112–120.
300. Pongponratn E, Turner GDH, Day NPJ, et al. An ultrastructural study of the brain in fatal Plasmodium falciparum malaria. *Am J Trop Med Hyg*. 2003;69(4):345–359.
301. Taylor TE, Fu WJ, Carr RA, et al. Differentiating the pathologies of cerebral malaria by postmortem parasite counts. *Nat Med*. 2004;10(2):143–145.
302. Ponsford MJ, Medana IM, Prapansilp P, et al. Sequestration and microvascular congestion are associated with coma in human cerebral malaria. *J Infect Dis*. 2012;205(4):663–671.
303. Schofield L. Intravascular infiltrates and organ-specific inflammation in malaria pathogenesis. *Immunol Cell Biol*. 2007;85(2):130–137.
304. Tripathi AK, Sha W, Shulaev V, Stins MF, Sullivan DJJ. Plasmodium falciparum-infected erythrocytes induce NF-kappaB regulated inflammatory pathways in human cerebral endothelium. *Blood*. 2009;114(19):4243–4252.
305. Krishnegowda G, Hajjar AM, Zhu J, et al. Induction of proinflammatory responses in macrophages by the glycosylphosphatidylinositols of Plasmodium falciparum: cell signaling receptors, glycosylphosphatidylinositol (GPI) structural requirement, and regulation of GPI activity. *J Biol Chem*. 2005;280(9):8606–8616.

306. Nebl T, De Veer MJ, Schofield L. Stimulation of innate immune responses by malarial glycosylphosphatidylinositol via pattern recognition receptors. *Parasitology*. 2005;130 Suppl:S45–62.

307. Tyberghein A, Deroost K, Schwarzer E, Arese P, Van Den Steen PE. Immunopathological effects of malaria pigment or hemozoin and other crystals. *Biofactors*. 2014;40(1):59–78.

308. Miller LH, Ackerman HC, Su X-Z, Wellems TE. Malaria biology and disease pathogenesis: insights for new treatments. *Nat Med*. 2013;19(2):156–167.

309. O'Sullivan JM, Preston RJS, O'Regan N, O'Donnell JS. Emerging roles for hemostatic dysfunction in malaria pathogenesis. *Blood*. 2016;127(19):2281–2288.

310. Hollestelle MJ, Donkor C, Mantey EA, et al. von Willebrand factor propeptide in malaria: evidence of acute endothelial cell activation. *Br J Haematol*. 2006;133(5):562–569.

311. Larkin D, de Laat B, Jenkins PV, et al. Severe Plasmodium falciparum malaria is associated with circulating ultra-large von Willebrand multimers and ADAMTS13 inhibition. *PLoS Pathog*. 2009;5(3):e1000349.

312. Phiri HT, Bridges DJ, Glover SJ, et al. Elevated plasma von Willebrand factor and propeptide levels in Malawian children with malaria. *PLoS ONE*. 2011;6(11):e25626.

313. Lowenberg EC, Charunwatthana P, Cohen S, et al. Severe malaria is associated with a deficiency of von Willebrand factor cleaving protease, ADAMTS13. *Thromb Haemost*. 2010;103(1):181–187.

314. Barber BE, William T, Grigg MJ, et al. Parasite biomass-related inflammation, endothelial activation, microvascular dysfunction and disease severity in vivax malaria. *PLoS Pathog*. 2015;11(1):e1004558.

315. de Mast Q, Groot E, Lenting PJ, et al. Thrombocytopenia and release of activated von Willebrand Factor during early Plasmodium falciparum malaria. *J Infect Dis*. 2007;196(4):622–628.

316. de Mast Q, Groot E, Asih PB, et al. ADAMTS13 deficiency with elevated levels of ultra-large and active von Willebrand factor in P. falciparum and P. vivax malaria. *Am J Trop Med Hyg*. 2009;80(3):492–498.

317. Bridges DJ, Bunn J, Van Mourik JA, et al. Rapid activation of endothelial cells enables Plasmodium falciparum adhesion to platelet-decorated von Willebrand factor strings. *Blood*. 2010;115(7):1472–1474.

318. De Ceunynck K, De Meyer SF, Vanhoorelbeke K. Unwinding the von Willebrand factor strings puzzle. *Blood*. 2013;121(2):270–277.

319. Langhorne J, Quin SJ, Sanni LA. Mouse models of blood-stage malaria infections: immune responses and cytokines involved in protection and pathology. *Chem Immunol*. 2002;80:204–228.

320. de Oca MM, Engwerda C, Haque A. Plasmodium berghei ANKA (PbA) infection of C57BL/6J mice: a model of severe malaria. *Methods Mol Biol*. 2013;1031:203–213.

321. Van Den Steen PE, Geurts N, Deroost K, et al. Immunopathology and dexamethasone therapy in a new model for malaria-associated acute respiratory distress syndrome. *Am J Resp Crit Care Med*. 2010;9(Suppl 2):I13.

322. O'Regan N, Gegenbauer K, O'Sullivan JM, et al. A novel role for von Willebrand factor in the pathogenesis of experimental cerebral malaria. *Blood*. 2016;127(9):1192–1201.

AIMS of the STUDY

The general aim of this PhD thesis was to study different aspects of VWF and ADAMTS13 in stroke, thrombotic thrombocytopenic purpura, and malaria. More specifically, we wanted (I) to gain more insight in the relative importance of plasma VWF and platelet-derived VWF in hemostatic and thrombotic processes, (II) to develop a non-viral gene therapy for congenital TTP, and (III) to unravel the contribution of the VWF/ADAMTS13 axis in malaria disease using a murine model of malaria-associated acute respiratory distress syndrome.

AIM I: To gain more insight in the relative importance of plasma VWF and platelet-derived VWF in hemostasis and thrombosis.

VWF is a multimeric plasma glycoprotein that plays a crucial role in hemostasis. At sites of vascular injury, VWF acts as a bridge between the exposed subendothelium and the circulating platelets, thereby promoting the formation of a platelet plug that prevents excessive blood loss. VWF circulates in the blood either in plasma or in platelets. Even though plasma VWF and platelet-derived VWF are products of the same gene with a similar protein backbone, experimental studies have described a number of biochemical and *in vitro* functional differences. While it is generally assumed that plasma VWF is the major contributor in maintaining normal hemostasis, a limited number of preclinical and clinical studies have demonstrated a significant contribution of platelet VWF as well. Given the distinctive features of platelet VWF, and variable platelet VWF antigen and activity levels between VWD patients, it is important to elucidate and understand the biological activity of this specific pool of VWF.

To reach this aim we will perform crossed bone marrow transplantations between *Vwf*$^{-/-}$ and WT mice, generating chimeric mice specifically lacking platelet VWF or with VWF only in platelets. Three to four weeks after transplantation, full chimerism will be evaluated by measuring the relative amount of VWF-positive platelets in blood using flow cytometry. To assess whether platelets constitutively secrete VWF in circulation, plasma VWF levels and FVIII activity levels will be determined using ELISA. To evaluate the role of platelet VWF in hemostasis, we will use the chimeric mice in a tail clip bleeding time assay. To address the question whether platelet VWF contributes to thrombotic processes, we will first perform a $FeCl_3$-induced carotid artery thrombosis model and assess the time that is needed to form an occlusive thrombus. Second, we will explore the specific contribution of platelet VWF in a

murine model of ischemic stroke. Twenty-four hours after induction of transient cerebral ischemia, we will evaluate brain infarct sizes and measure fibrin(ogen) deposition in brain lysates using Western Blot followed by densitometric analysis. The results obtained from this study will further clarify the specific role of platelet VWF in hemostasis and shed new light on the specific activity of platelet VWF in different thrombotic processes, such as ischemic stroke.

AIM II: To develop a non-viral gene therapeutic approach that offers long-term protection against TTP in mice.

The platelet-binding capacity of VWF is determined by its multimeric size, ranging from low reactive dimers to hyper-reactive UL-VWF multimers. In normal circulation, the multimer size is regulated by the VWF-cleaving protease, ADAMTS13, which processes unusually large multimers into smaller, less reactive fragments. In case of a congenital deficiency in ADAMTS13, however, these highly adhesive UL-VWF multimers persist in circulation and may cause the life-threatening thrombotic disorder TTP (congenital TTP).

Despite appropriate treatment, 10-20% of all patients still die following an acute TTP episode, while survivors may relapse. In congenital TTP patients, prophylactic plasma infusions are generally sufficient to prevent disease relapse. Lifelong plasma therapy, however, is stressful and has a negative impact on the patient's quality of life. In addition, adverse events following the administration of plasma products have been observed. Novel therapeutic strategies that improve clinical outcome are highly warranted. Correction of the underlying genetic defect using gene therapy has been considered an appealing alternative that may offer long-term protection against TTP.

To accomplish this aim we will use the *'Sleeping Beauty'* transposon system (SB100X) to deliver and express a functional copy of the *Adamts13* gene in ADAMTS13 knockout (*Adamts13*$^{-/-}$) mice. In this study the SB100X transposon system will consist of a transposon plasmid containing a murine ADAMTS13 expression cassette (i.e. the murine *Adamts13* gene under transcriptional control of a liver-specific promotor) and a transposase plasmid encoding a hyperactive version of the transposase. To obtain stable murine ADAMTS13 expression, both SB100X plasmids will be delivered by hydrodynamic injection. Injection of the single transposon plasmid will be used as a control. Transgene expression of murine ADAMTS13 in plasma will be measured using ELISA. Its proteolytic activity will be assessed by analysis of the plasma VWF multimer distribution using SDS agarose gel electrophoresis. Different groups of *Adamts13*$^{-/-}$ mice treated with SB100X will be challenged with human rVWF at

different time points to induce TTP symptoms. The TTP phenotype will be evaluated by measuring platelet counts, plasma lactate dehydrogenase levels, hemoglobin levels, and weight loss. *Adamts13*$^{-/-}$ mice hydrodynamically injected with saline solution and triggered with rVWF will be used as a control group for each different time point.

The results obtained from this study will provide proof-of-concept supporting the development of an SB100X-mediated gene therapeutic approach as an alternative treatment option for congenital TTP in humans.

AIM III: To unravel the role of the VWF/ADAMTS13 axis in a murine model of malaria-associated acute respiratory distress syndrome.

An excess of (UL-) VWF along with a reduction in ADAMTS13 activity has been observed in various life-threatening conditions. Recent clinical findings have demonstrated that human malaria infection is associated with increased levels of hyper-reactive VWF multimers and marked ADAMTS13 inhibition. Although it has been proposed to use VWF solely as a marker for disease severity, it is reasonable to assume that a dysregulated balance between VWF and ADAMTS13 may contribute to malarial microangiopathic organ damage. To date, only a few preclinical studies that tried to dissect the direct role of VWF in malaria disease have supported this hypothesis. However, future studies using different animal models for experimental malaria are required to unravel the mechanisms linking alterations in the VWF/ADAMTS13 axis and malaria disease, and to explore novel therapeutic avenues.

To reach this aim, we will induce malaria-associated acute respiratory distress syndrome (MA-ARDS) in WT mice on a C57BL/6J background via intraperitoneal injection of *Plasmodium berghei* NK65-infected red blood cells. To evaluate hemostatic alterations in terms of VWF and ADAMTS13, we will take blood samples at regular time points following infection. We will assess plasma VWF and ADAMTS13 levels by using ELISA. The distribution of plasma VWF multimers will be assessed using SDS agarose gel electrophoresis, while the activity of ADAMTS13 will be measured using the FRETS-VWF73 assay. Daily Giemsa-stained blood smears will be prepared to measure peripheral blood parasitemia levels. To investigate the direct role of VWF, we will infect *Vwf*$^{-/-}$ mice and compare survival rates, peripheral parasitemia levels, platelet counts, and lung pathology with infected WT mice. Lung pathology will be assessed by measuring protein levels in the broncho-alveolar lavage fluid.

The results obtained from this study will demonstrate whether changes in plasma VWF levels and ADAMTS13 activity in a murine model of MA-ARDS are in accordance with human

malaria infection or other murine malaria models. These results will also shed more light on the potential role of VWF as primary player in malaria pathogenesis and whether VWF-directed therapy may offer novel therapeutic opportunities.

CHAPTER 2

WHILE NOT ESSENTIAL FOR NORMAL HEMOSTASIS, PLATELET-DERIVED VWF FOSTERS ISCHEMIC STROKE INJURY IN MICE

Sebastien Verhenne[1], Frederik Denorme[1], Sarah Libbrecht[1], Aline Vandenbulcke[1], Inge Pareyn[1], Hans Deckmyn[1], Antoon Lambrecht[2], Bernhard Nieswandt[3], Christoph Kleinschnitz[4], Karen Vanhoorelbeke[1], Simon F. De Meyer[1]

[1]Laboratory for Thrombosis Research, KU Leuven, Campus Kulak Kortrijk, Kortrijk, Belgium; [2]Department of Radiotherapy, AZ Groeninge Campus Loofstraat, Kortrijk, Belgium; [3]Rudolf Virchow Center, Wuerzburg, Germany; [4]Department of Neurology, University Clinic of Wuerzburg, Wuerzburg, Germany

This manuscript was published in *Blood*. 2015 Oct 1;126(14):1715-22

2.1. ABSTRACT

Von Willebrand factor (VWF) is a key hemostatic protein synthesized in both endothelial cells and megakaryocytes. Megakaryocyte-derived VWF is stored in α-granules of platelets and is enriched in hyperactive 'ultra-large' VWF multimers. To elucidate the specific contribution of platelet VWF in hemostasis and thrombosis we performed crossed bone marrow transplantations between C57BL/6J and *Vwf*$^{-/-}$ mice to generate chimeric mice. Chimeric mice specifically lacking platelet VWF showed normal tail bleeding and carotid artery thrombosis, similar to wild type mice. Chimeric mice with VWF present only in platelets were not able to support normal thrombosis and hemostasis. However, using a mouse model of transient middle cerebral artery occlusion, we observed that cerebral infarct sizes and fibrin(ogen) deposition in chimeric mice with only platelet VWF were significantly increased compared with *Vwf*$^{-/-}$ mice ($p < 0.01$). Blocking of the platelet VWF-GPIb interaction abrogated this platelet VWF-mediated injury. These data suggest that whereas platelet-derived VWF does not play a crucial role in hemostasis and arterial thrombosis, it aggravates thrombo-inflammatory diseases such as stroke via a GPIb-dependent mechanism.

2.2. INTRODUCTION

Von Willebrand factor (VWF) is an adhesive multimeric glycoprotein that is crucial for normal hemostasis. The best-known functions of VWF are facilitating platelet adhesion at sites of vascular injury and protecting clotting factor VIII against early degradation in the circulation. Consequently, absence or dysfunction of VWF results in bleeding symptoms as observed in patients with von Willebrand disease (VWD).[1] Intriguingly, it has become clear that VWF is also implicated in various non-hemostatic processes, such as tumor metastasis, inflammation and angiogenesis.[2] In particular, the pathophysiological role of VWF in ischemic stroke has recently gained increased attention.[3-7]

Biosynthesis of VWF is restricted to endothelial cells (ECs) and megakaryocytes. Endothelial VWF is constitutively secreted into plasma and subendothelium or stored as 'ultra-large' VWF (UL-VWF) multimers in Weibel-Palade bodies. VWF produced in megakaryocytes ends up as UL-VWF in the α-granules of platelets. VWF present in endothelial and platelet storage organelles is secreted in a regulated process in response to stimulation by secretagogues. Platelets contain a significant amount of VWF, accounting for 15-20% of the total amount of circulating VWF. Interestingly, an increasing body of evidence shows that platelet VWF differs in various biochemical aspects from endothelial VWF.[8] Williams *et al*. showed that, in comparison with plasma VWF, platelet VWF binds more efficiently to glycoprotein (GP)IIb/IIIa and heparin whereas it is less capable of binding to GPIb.[9] Divergent glycosylation profiles could explain these differences. Indeed, platelet VWF exists as a distinct glycoform, characterized by a significantly reduced degree of N-linked sialylation and by the absence of expression of AB blood group determinants.[8,10] This differential glycosylation also renders platelet VWF more resistant to ADAMTS13 proteolysis.[10] With platelet VWF being enriched in UL-VWF, this resistance to ADAMTS13 cleavage could become particularly relevant in settings where local accumulation of UL-VWF is detrimental, like cerebral or myocardial ischemia/reperfusion injury.[6,11,12] Given variable platelet VWF antigen and activity levels between individuals, it is important to understand the biological activity of this specific pool of VWF. Only a few studies have tried to dissect the different (patho)physiological roles of platelet and plasma VWF. Although experimental evidence shows that platelet VWF indeed contributes to initial platelet adhesion to collagen at sites of vascular injury[13-15] *in vivo* data on the role of platelet VWF in thrombosis is limited. The role of VWF from platelets in ischemic stroke has never been

investigated. In the present study, we found that plasma VWF but not platelet VWF is needed for normal hemostasis and carotid artery thrombus formation whereas platelet VWF by itself is able to mediate ischemic brain injury via a GPIb-dependent mechanism, shedding new light on the role of platelet VWF in thrombo-inflammatory disease.

2.3. METHODS

2.3.1. Mice

Male and female *Vwf*$^{-/-}$ (VWF KO)[16] and littermate wild-type (WT) C57BL/6J mice were used. All animal experiments were performed in accordance with protocols approved by the Institutional Animal Care and Use Committee of the KU Leuven (Belgium).

2.3.2. Bone marrow transplantation

Bone marrow cells were collected from the femur and tibia of six to ten week old donor mice. The mononuclear cell population (MNC) was isolated using ficoll gradient centrifugation (Ficoll-Paque™ Premium 1.084; GE Healthcare, Waukesha, IL). Six to eight week old recipient VWF KO and WT mice were conditioned for cellular transplantation with a single lethal dose of 1100 cGy total body irradiation using a dual linear energy accelerator (Clinac DHX, 6MV; Varian Medical Systems, CA). Twenty-four hours after irradiation, 10 x 10^6 MNC dissolved in 250µl sterile phosphate buffered saline (PBS) were infused by intravenous injection in irradiated recipient mice. Three to four weeks after transplantation full chimerism was confirmed via flow cytometry.

2.3.3. Blood collection

Animals were anesthetized using 5% isoflurane (Nicholas Piramal Limited, London, UK) in 100% O_2. Blood was collected by retro-orbital puncture on 0.5M EDTA (1 volume to 40 volumes of blood) or 3.8% trisodium citrate (1 volume to 6 volumes of blood). EDTA-treated blood was used to determine platelet counts using the Hemavet 950FS Multi-species Hematology system (Drew Scientific, Oxford, CT). Platelet-rich plasma (PRP) was prepared from citrated blood by centrifugation at 325g for 5 minutes at room temperature (RT) and immediately used for flow cytometric analysis. Platelet-poor plasma (PPP) was prepared from citrated blood by centrifugation at 4300g for 6 minutes at 4°C and stored at -20°C for further analysis.

2.3.4. Flow cytometry

Three to four weeks after transplantation, citrated PRP was prepared from chimeric and control mice. After fixation with 2% formaldehyde in Hepes Tyrode (HT) buffer for 20

minutes, 10 x 10^6 platelets were washed with HT buffer containing 0.35% bovine serum albumin (BSA) (HT + 0.35% BSA). Resuspended platelets were permeabilized with 2.5% Triton X-100 in HT + 0.35% BSA for 5 minutes, rinsed with HT + 0.35% BSA and subsequently incubated for 15 minutes at RT with polyclonal anti-human VWF antibody (1:100; Dako, Glostrup, Denmark). Following a washing step, FITC-conjugated swine anti-rabbit antibody (1:40; Dako) was added for 15 minutes at RT. After washing, platelets were fixated and stored at 4°C for further analysis. To quantify the relative amount of VWF-positive platelets, a standard curve (0%, 25%, 50%, 75%, and 100% VWF-positive platelets) was made by combining PRP from WT and VWF KO mice. Results were expressed as percentage of WT values. To identify the platelet population, platelets were stained with rat anti-mouse CD41 antibody conjugated with PE (1:50; eBioscience, San Diego, CA). Expression of CD41 and intracellular platelet VWF was determined using a Beckman Coulter EPICS XL-MCL flow cytometer and analysed with the WinMDI 2.9 free FACS analysis software.

2.3.5. VWF and FVIII analysis

VWF antigen levels in plasma were determined using an in-house developed enzyme-linked immunosorbent assay (ELISA). VWF was captured by polyclonal anti-human VWF antibodies (1/1000; Dako) coated on a microtiter plate. After blocking the wells with 3% milk powder solution, test PPP, as well as plasma pool samples (in duplicate), were applied at 1:10 to 1:640 dilutions. The captured VWF from plasma was detected using a mixture of in-house generated biotinylated anti-murine VWF monoclonal antibodies (15H2 and 2C12; 1 μg/ml) followed by incubation with horseradish peroxidase-labeled streptavidin (Roche, Mannheim, Germany). After addition of ortho-phenylenediamine (Sigma-Aldrich, St Louis, MO) the coloring reaction was stopped with 4 M H_2SO_4. The absorbance was determined at 490 nm. FVIII activity (FVIII:C) in mouse plasma was determined using the COATEST® SP_4 FVIII (Chromogenix, Molndal, Sweden) according to the manufacturer's protocol. Pooled plasma from 10 to 20 WT mice was used as a reference (100%) and results were expressed as percentage of WT values.

2.3.6. Tail clip bleeding time assay

Tail clip bleeding times were assessed as described.[17] Five to six weeks after transplantation, mice were anesthetized with intraperitoneal injection of pentobarbital (60 mg/ml; Nembutal,

Ceva Santé Animale, Brussels, Belgium). Immediately after removing 5 mm of the tail tip using a surgical scalpel, the tail was immersed in 0.9% NaCl pre-warmed at 37°C. The time until blood loss ceased was monitored. The experiment was stopped when bleeding did not stop within 600 seconds.

2.3.7. $FeCl_3$-induced carotid artery thrombosis model

Eight to ten weeks after transplantation, mice were anesthetized using 2.5% isoflurane in 100% O_2. The right carotid artery was subsequently exposed and a doppler flow probe (Transonic TS420 perivascular flow meter module; AD Instruments, Oxford, UK) was positioned around the artery to monitor blood flow via a laser doppler perfusion monitor (PeriFlux System 5000; Perimed AB, Järfälla-Stockholm, Sweden) coupled to a PowerLab 8/35 data acquisition unit (AD Instruments) using LabChart v8.0.5 software (AD Instruments). Arterial thrombosis was induced by applying a piece of Whatman™ filter paper (1 x 1 mm; GE Healthcare) saturated in 12% $FeCl_3$ solution, for 3 minutes downstream of the flow probe. The time to occlusion was recorded. If the time to occlusion exceeded 50 minutes, the experiment was ended.

2.3.8. Transient middle cerebral artery occlusion

Focal cerebral ischemia was induced 8 to 10 weeks after transplantation by 60 minutes transient middle cerebral artery occlusion (tMCAO) as described.[5] Mice were anesthetized with 2.5% isoflurane in 100% O_2. Following a midline skin incision in the neck, the proximal right common carotid artery and the external carotid artery were ligated, and a standardized silicon rubber-coated 6.0 nylon monofilament (6021; Doccol Corp., Redlands, CA) was advanced through the right internal carotid artery to occlude the origin of the right MCA. The intraluminal suture was left *in situ* for 60 minutes, after which the animals were re-anesthetized and the occluding monofilament was withdrawn to allow reperfusion. This model typically results in a reduction of blood flow in the MCA territory by 90% during occlusion. Upon removal of the filament, blood flow is restored to approximately 80% of baseline.[3,18] To block the VWF-GPIb interaction, 100 µg rat anti-mouse GPIbα (p0p/B) Fab[19] or rat IgG Fab control was injected intravenously 5 minutes after inducing reperfusion of the right middle cerebral artery. All stroke experiments were conducted according to the recommendations for research in experimental stroke studies and the current ARRIVE guidelines (http://www.nc3rs.org/ARRIVE). Animals were randomly assigned to the

operators by independent persons not involved in data acquisition and analysis. Surgeries and evaluation of all readout parameters were performed while being blinded to the experimental groups.

2.3.9. Determination of infarct size

Assessment of infarct size was performed 24 hours after induction of cerebral ischemia as described.[5] After sacrificing the animal, the brain was removed and sectioned in three consecutive 2 mm thick sections. Sections were stained with 2% 2,3,5-triphenyltetrazolium chloride (TTC; Sigma-Aldrich) in PBS and fixated. Pictures were taken and the infarct volume was calculated via planimetry (ImageJ Software, National Institutes of Health, USA).

2.3.10. Western blot analysis

Western blot for fibrin/fibrinogen was performed as previously described.[5] Three TTC-stained coronal brain sections of 1 mouse were separated in ipsi- and contralateral parts, pooled, and homogenized in RIPA buffer (25 mM Tris pH 7.4, 150 mM NaCl, 1% NP-40) containing 0.1% sodium dodecylsulfate (SDS) and a proteinase inhibitor cocktail (cOmplete, EDTA-free; Roche Applied Science, Penzberg, Germany). After sonication of the samples for 10 seconds, tissue lysates were centrifuged at 15,000 g for 30 minutes at 4°C and supernatants were used for Bradford protein assay and subsequent Western blot analysis.

For Western blot analysis, equal amounts (determined via Bradford protein assay) of the supernatant of ipsi- and contralateral homogenates were run on SDS-PAGE (10% running and 4% stacking gel) under reducing conditions and blotted to Amersham™ Hybond™ C extra membranes (Amersham Bioscience, Piscataway, NJ). After blocking for 30 minutes with blocking buffer (5% non-fat dry milk, 50 mM Tris–HCl pH 7.5, 0.05% Tween-20) membranes were incubated with primary rat anti-fibrin(ogen) (1:500; Acris Antibodies GmbH, Herford, Germany) and murine anti-actin (1:500; Merck Millipore, Darmstadt, Germany) antibodies overnight at 4°C. After washing with tris buffered saline (50 mM Tris–HCl pH 7.5, 0.05% Tween-20), membranes were incubated for 1 hour with horse radish peroxidase-conjugated goat anti-rabbit IgG (for fibrin(ogen); at a dilution of 1:5000) or goat anti-mouse IgG (for actin; at a dilution of 1:50 000) and were finally developed using Supersignal® West Pico Chemiluminescent Substrate (Thermo Scientific, Rockford, IL). The amount of fibrin(ogen) was quantified by densitometry from scanned (LAS-4000 Imager, Fujifilm, Tokyo, Japan) Western blots normalized to the actin signal, using ImageJ software.

The ratio of the normalized ipsilateral fibrin(ogen) band density relative to the normalized band density of contralateral fibrin(ogen) served as a measurement for relative fibrin deposition.

2.3.11. Statistics

Data are expressed as mean ± SEM. For statistical analysis, the Prism Version 6.0 software (GraphPad Software; La Jolla, CA) was used. Statistical analysis was conducted using one-way ANOVA followed by the Tukey's multiple comparison post hoc test to assess variance between FVIII:C levels, cerebral infarct sizes and fibrinogen deposition in different experimental groups. The Kruskal-Wallis test followed by Dunn's multiple comparison post hoc test was used to compare plasma VWF antigen levels, tail clip bleeding times and arterial occlusion times. *P* values less than .05 were considered statistically significant.

2.4. RESULTS

2.4.1. Generation of chimeric mice expressing VWF only in megakaryocytes or endothelial cells

To determine the contribution of platelet VWF in hemostasis and thrombosis, we generated chimeric mice that produce VWF only in megakaryocytes or endothelial cells, respectively. MNCs were isolated from WT donor mice and transplanted into lethally irradiated VWF KO acceptor mice, resulting in chimeric mice with only platelet VWF (VWF PLT, Figure 1A). By transplanting VWF KO MNCs into WT acceptor mice, chimeric mice that specifically lack VWF in platelets were obtained (VWF EC, figure 1B). No difference in platelet count between chimeric mice and VWF KO and WT mice was observed (data not shown). To confirm successful transplantation, the relative amount of VWF-containing platelets was determined via flow cytometry (Figure 1C). As in VWF KO mice, no VWF-positive platelets were detected in VWF EC chimeric mice. On the other hand, the relative amount of VWF-positive platelets in VWF PLT chimeric mice (98.44 ± 1.87%, n = 18) was similar to WT mice (99.94 ± 1.31%, n = 12) (Figure 1C).

Absence of VWF-positive platelets in VWF EC chimeric mice confirms previous findings that endocytosis of VWF from plasma to platelet α-granules does not occur.[15,19] As expected, platelets do not seem to release significant amounts of VWF into the circulation under normal conditions (Figure 1D). Indeed, normal plasma levels of VWF antigen were found in WT mice (99.9 ± 7.1%, n = 16) and VWF EC chimeric mice (106.3 ± 9.3%, n = 8) whereas no detectable levels of VWF were observed in plasma of VWF KO mice (n = 14) and most VWF PLT chimeric mice (n = 21). However, in some (7 out 21) VWF PLT chimeric mice trace amounts of VWF were observed, which could account for the slightly (but non-significantly) increased FVIII activity (14.3 ± 1%, n = 16) compared to VWF KO mice (6.3 ± 0.4%, n = 12) (Figure 1E). FVIII activity levels in the VWF EC chimeric mice (83.6 ± 3.1%, n = 10) were slightly decreased when compared to WT mice (100 ± 4.6%, n = 12) but remained in the normal range (Figure 1E). These data further confirm the notion that plasma VWF mainly originates from endothelial cells and that no platelet VWF is constitutively secreted into the circulation under normal circumstances.

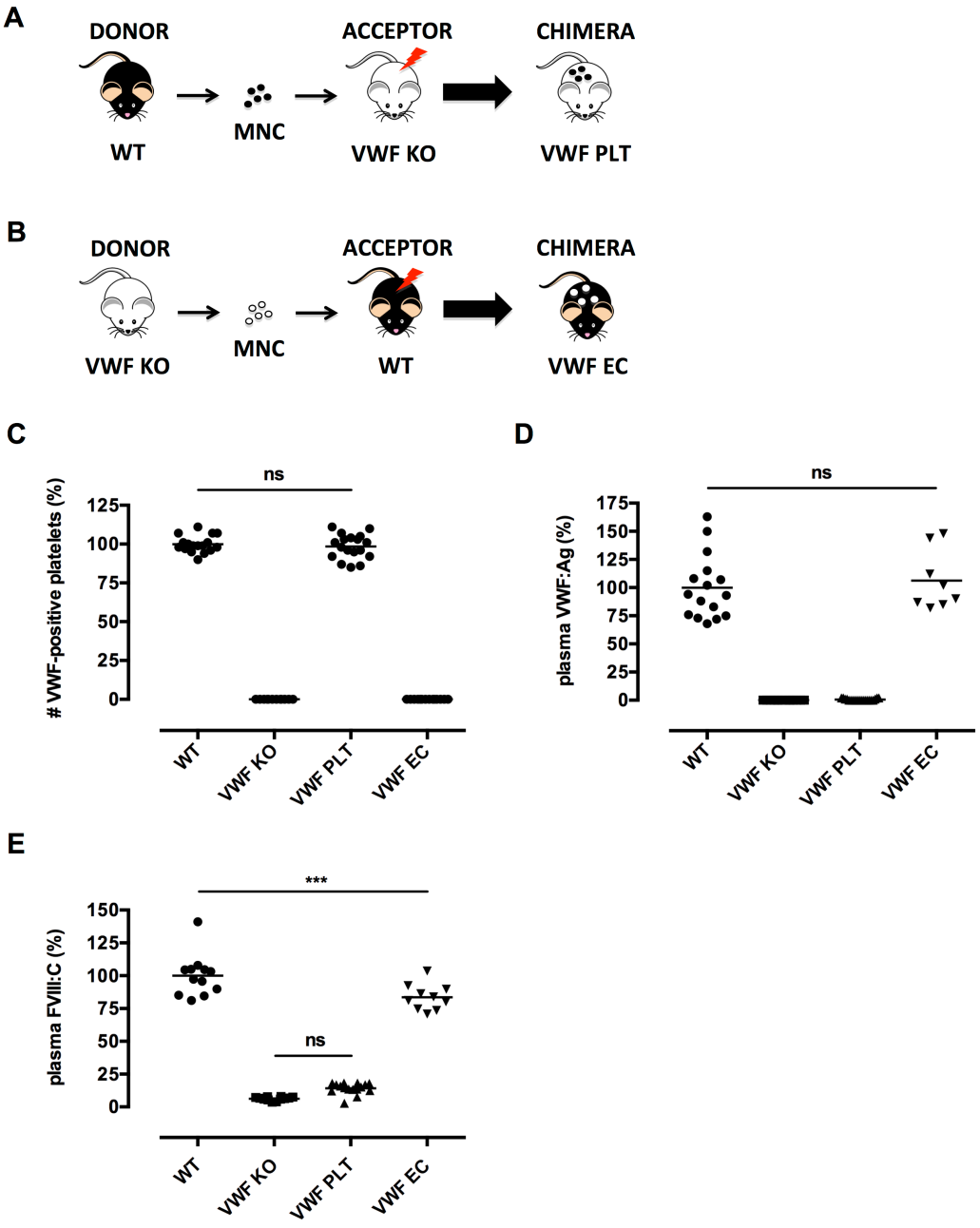

Figure 1: Generation and characterization of chimeric mice that lack VWF in either megakaryocytes or endothelial cells. Mononuclear cells (MNC), isolated from donor WT (black) or VWF KO mice (white), were transplanted into lethally irradiated VWF KO or WT acceptor mice to generate (A) chimeric mice that have VWF only in platelets (VWF PLT) or (B) chimeric mice that specifically lack VWF in their platelets (VWF EC), respectively. (C) Relative amount of VWF-positive platelets detected in WT (n = 17), VWF KO (n = 12), VWF PLT chimeric (n = 18) and VWF EC chimeric (n = 14) mice. (D) VWF antigen levels (VWF:Ag) were determined in plasma samples from WT (n = 16), VWF KO (n =14), VWF PLT chimeric (n = 21), and VWF EC chimeric (n = 8) mice. (E) FVIII activity (FVIII:C) was determined in plasma samples from WT (n = 12), VWF KO (n =12), VWF PLT chimeric (n = 16), and VWF EC chimeric (n = 10) mice. Results are expressed as percentage of WT values. ***, $P < 0.001$; ns, not statistically significant.

2.4.2. Plasma but not platelet VWF is the major determinant for normal hemostasis

To unravel the specific role of platelet VWF in hemostasis, we used our chimeric mice in a tail clip bleeding assay. After removing 5 mm of the tip of the tail, the time needed to stop bleeding was recorded (Figure 2). As expected, most WT animals stopped bleeding within 3 min (100.9 ± 18.7 s, n = 15) while VWF KO mice were not able to control the bleeding within 10 min (> 600 s, n = 14). Interestingly, most of the VWF PLT chimeric mice also bled longer than 10 min (528.2 ± 38.9 s, n = 16). Bleeding stopped spontaneously in 3 out of 16 mice (19%). In chimeric mice that only produce endothelial VWF (VWF EC), bleeding times were comparable to those of WT mice (101.1 ± 17.3 s, n = 9). These data suggest that platelet VWF alone is not able to support normal hemostasis and that lack of platelet VWF does not affect bleeding in this model.

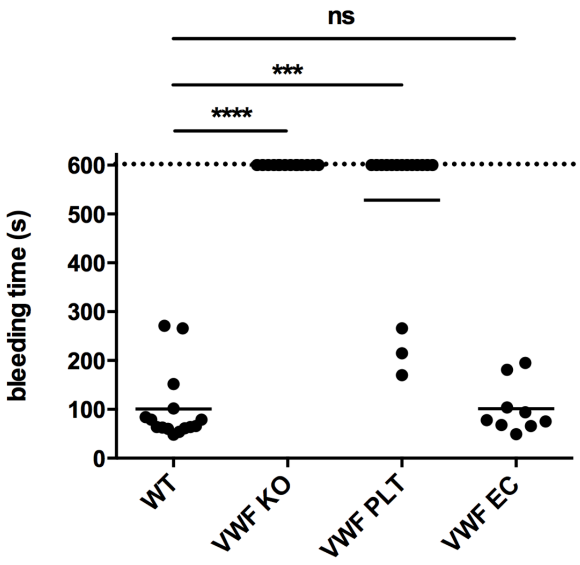

Figure 2: Plasma VWF is the major determinant to control bleeding in a tail clip bleeding assay. Five mm of the tail of WT (n = 15), VWF KO (n = 14), VWF PLT chimeric (n = 16), and VWF EC chimeric (n = 9) mice was removed. Subsequent tail bleeding in pre-warmed saline was monitored and the time needed to stop the bleeding was recorded. If bleeding did not end within the first 10 min, the experiment was ended with a recorded bleeding time of 600 s. ***, $P < 0.001$; ****, $P < 0.0001$; ns, not statistically significant.

2.4.3. Plasma but not platelet VWF regulates arterial thrombus formation

Ex vivo flow chamber studies have previously shown that platelet-derived VWF plays a role in platelet adhesion to collagen.[13-15] However, the exact role of platelet VWF in *in vivo* thrombus formation in mice has never been studied. To address this question, we performed a $FeCl_3$-induced carotid artery thrombosis model (Figure 3). In WT mice, an occlusive thrombus was consistently formed within 10 min (9.2 ± 0.5 min, n = 8). In contrast, no occlusive thrombus was formed within the first 50 min in VWF KO mice (n = 5). Interestingly, arterial occlusion times in VWF EC chimeric mice (10.6 ± 0.4 min, n = 6) were similar to WT mice while no occlusive thrombi were formed in VWF PLT chimeric mice (n = 8). These results indicate that on the one hand platelet-derived VWF alone is not able to support normal thrombus formation in this model, and that on the other hand lack of VWF in platelets does not affect normal arterial thrombosis.

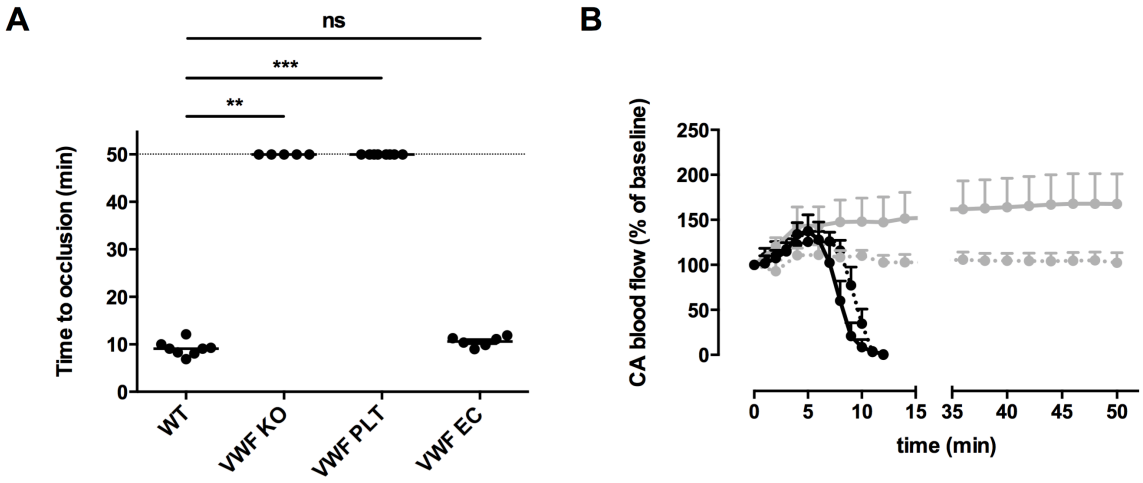

Figure 3: (A) The carotid artery of WT (n = 8), VWF KO (n = 5), VWF PLT chimeric (n = 8), and VWF EC chimeric (n = 6) mice was exposed and a local injury was generated by topical application of a filter paper saturated with 12% $FeCl_3$. Carotid artery blood flow was monitored and the time needed to form an occlusive thrombus was recorded. If no occlusion occurred within 50 min, the experiment was ended (time to occlusion of 50 min). (B) Carotid artery (CA) blood flow profiles of WT (black; n = 8), VWF KO (grey; n = 5), VWF PLT chimeric (dashed grey; n = 8), and VWF EC chimeric (dashed black; n = 6) mice were recorded using a laser doppler flow monitor. **, $P < 0.01$; ***, $P < 0.001$; ns, not statistically significant.

2.4.4. Both endothelial cell- and platelet-derived VWF alone are able to mediate ischemic brain injury

We and others showed that VWF plays a crucial role in ischemic stroke most probably by recruiting platelets and leukocytes in the reperfused tissue.[3-5] Interestingly, absence of ADAMTS13 further aggravates ischemic brain damage, suggesting a specific contribution of UL-VWF multimers in the pathophysiology of stroke.[4,12,20] Given the abundance of UL-VWF multimers in α-granules of platelets, we explored the specific contribution of platelet VWF in ischemic brain injury. After 60 minutes of focal cerebral ischemia, blood flow in the middle cerebral artery was restored to allow reperfusion of the ischemic territory. Twenty-four hours after induction of ischemia, cerebral infarction sizes were determined (Figure 4). In accordance with our previous studies,[3,5] cerebral infarct sizes observed in VWF KO mice (34.4 ± 5.2 mm^3, n = 12) were significantly reduced compared to WT mice (78.9 ± 10.2 mm^3, n = 10). As expected, VWF EC chimeric mice developed infarcts that were similar in size to WT animals (76.7 ± 8.4 mm^3, n = 9). Surprisingly however, VWF PLT chimeric mice expressing VWF only in platelets also showed infarct sizes that were similar to WT mice (79.6 ± 8.1 mm^3, n = 16). Because cranial irradiation may induce persistent neuroinflammation in C57BL/6J mouse brain[21,22] we tested lethally irradiated VWF KO mice transplanted with VWF KO MNCs to exclude any potential effect of irradiation on cerebral injury in our model (Figure 4C). In this separate set of experiments, infarct sizes were still small (18.71 ± 4.31 mm^3, n = 7) and comparable with those observed in VWF KO mice (19.43 ± 5.49 mm^3, n = 7). Hence, the irradiation procedure had no effect on infarct size in VWF KO animals. Together, these data show that the presence of either platelet VWF or plasma VWF alone is sufficient to cause VWF-mediated ischemic stroke injury.

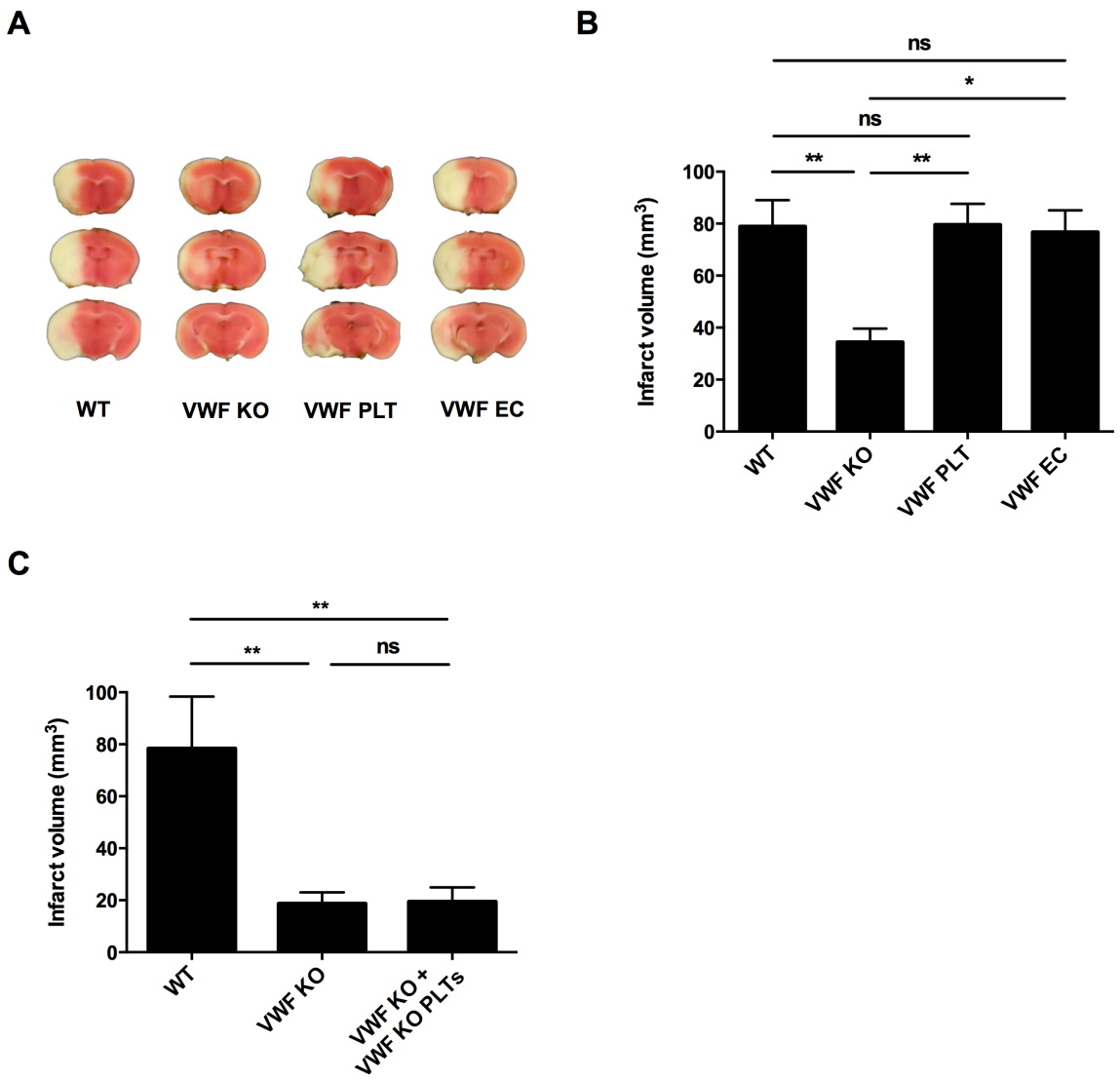

Figure 4: Platelet-derived VWF alone mediates ischemic stroke injury. Transient focal cerebral ischemia was induced by 60 min occlusion of the right middle cerebral artery, followed by 23 hours of reperfusion in WT (n = 12), VWF KO (n = 10), VWF PLT chimeric (n = 16), and VWF EC chimeric (n = 9) mice. (A) Representative TTC staining of 3 consecutive coronal brain sections 24 hours after induction of transient middle cerebral artery occlusion (tMCAO) are shown. White color indicates infarcted area, whereas a pink color shows unaffected brain tissue. (B) Brain infarct volumes as quantified by planimetric analysis 24 hours after tMCAO. (C) To exclude potential irradiation-mediated effects on cerebral injury, transient focal cerebral ischemia was induced in irradiated VWF KO mice transplanted with MNCs derived from VWF KO mice (VWF KO + VWF KO PLTs). Planimetric analysis of brain infarct volumes 24 hours after tMCAO in WT (n = 5), VWF KO (n = 7), and VWF KO + VWF KO PLTs chimeric mice (n = 7). *, $P < 0.05$; **, $P < 0.01$; ns, not statistically significant.

2.4.5. Platelet VWF-mediated ischemic brain injury is GPIbα-dependent.

We next wanted to further elucidate the mechanism by which platelet VWF exacerbates ischemic stroke. The main interactions of VWF in platelet adhesion and thrombus formation are binding to platelet GPIb, collagen and platelet GPIIb/IIIa. Interestingly however, Williams and colleagues have shown that platelet-derived VWF binds GPIbα with lower affinity than plasma VWF.[9] To test whether binding of platelet VWF to GPIb is important in ischemic stroke, we blocked the VWF-GPIbα axis using an anti-GPIbα (p0p/B) Fab fragment (Figure 5).[23] Interestingly, administration of p0p/B significantly reduced cerebral infarct development in VWF PLT chimeric mice (44.8 ± 10.19 mm^3, n = 8) to levels as observed in VWF KO mice (43.38 ± 10.02 mm^3, n = 5). These were half the size of those observed in non-treated WT mice (92.19 ± 11.52 mm^3, n = 6) or VWF PLT chimeric mice that received IgG control Fab (83.07 ± 3.7 mm^3, n = 12). These data suggest that the detrimental effect of platelet VWF in ischemic stroke is mediated by a platelet GPIbα-dependent mechanism. It is interesting to note that no cerebral hemorrhagic events were observed in all experimental groups after macroscopic analysis of whole brains and of 2-mm brain sections (data not shown), which is in line with our previous studies.[3,5,23]

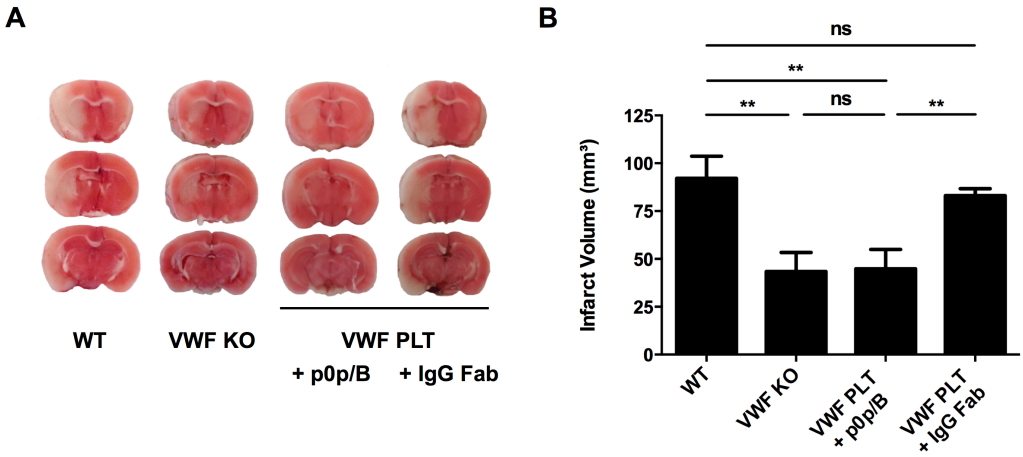

Figure 5: Blockade of platelet GPIbα reduces platelet VWF-mediated ischemic stroke injury. Transient focal cerebral ischemia was induced by 60 min occlusion of the right middle cerebral artery, followed by 23 hours of reperfusion in non-treated WT (n = 6) and VWF KO (n = 5) mice, and VWF PLT chimeric mice treated with 100 µg anti-GPIbα Fab (+ p0p/B; n = 8) or rat IgG Fab control (+ IgG Fab; n = 12). (A) Representative TTC stainings of 3 consecutive coronal brain sections 24 hours after tMCAO. White color indicates infarcted area, whereas a pink color shows unaffected brain tissue. (B) Brain infarct volumes as quantified by planimetric analysis 24 hours after tMCAO. **, $P < 0.01$; ns, not statistically significant.

2.4.6. Platelet-derived VWF exacerbates ischemic brain injury by promoting intracerebral thrombosis

To gain further insight on how platelet VWF promotes cerebral injury, we measured fibrin(ogen) deposition in the brain after stroke (Figure 6). In WT mice, the ischemic hemisphere contained almost four times more fibrin(ogen) than the contralateral hemisphere (ratio ipsilateral/contralateral of 3.69 ± 0.37, n = 9) 24 hours after stroke, suggesting thrombotic events occurring during the ischemia/reperfusion phase. In VWF KO mice, significantly less fibrin(ogen) was found in the ipsilateral hemisphere (only a 1.44 ± 0.17-fold increase of contralateral, n = 8). Reconstitution of the platelet VWF compartment in VWF KO mice (VWF PLT) again significantly increased cerebral fibrin(ogen) deposition in the affected hemisphere (ratio ipsilateral/contralateral of 2.99 ± 0.56, n = 7). Interestingly, when VWF PLT chimeric mice were treated with anti-GPIbα Fab, fibrin(ogen) in the ipsilateral hemispheres was reduced (ratio ipsilateral/contralateral of 1.28 ± 0.10, n = 5). Administration of control IgG Fab to VWF PLT chimeric mice did not alter fibrin(ogen) deposition in the brain (ratio ipsilateral/contralateral of 3.75 ± 0.34, n = 6). These data suggest a significant contribution of platelet-derived VWF in intracerebral fibrin(ogen) deposition during ischemic stroke that depends on VWF binding to GPIbα.

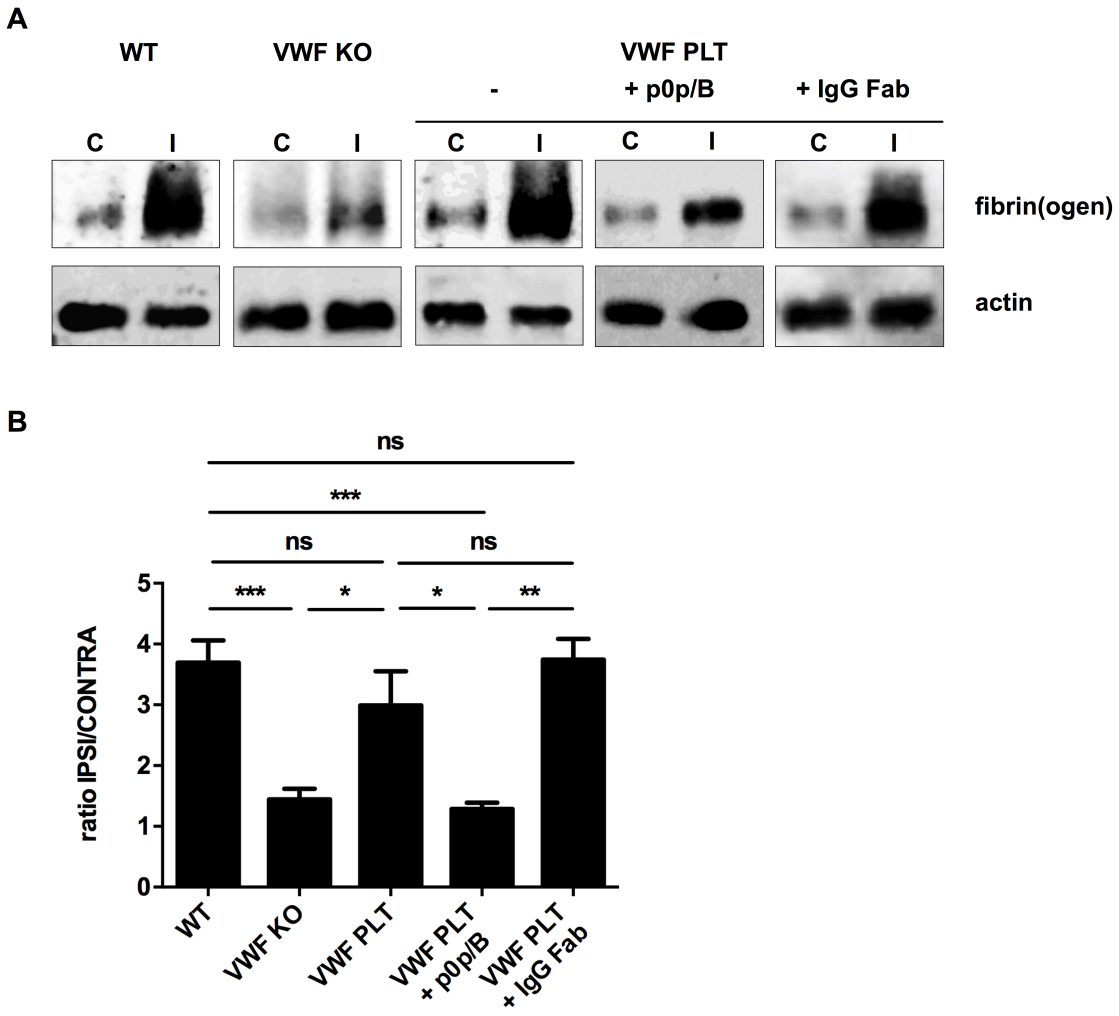

Figure 6: Platelet-derived VWF contributes to ischemic brain injury by promoting intracerebral thrombosis. Transient focal cerebral ischemia was induced by 60 min occlusion of the right middle cerebral artery, followed by 23 hours of reperfusion in WT (n = 9), VWF KO (n = 8), non-treated VWF PLT chimeric (n = 7), anti-GPIbα Fab-treated VWF PLT chimeric (p0p/B, n = 5), and control IgG Fab-treated VWF PLT chimeric (IgG Fab; n = 6) mice. Twenty-four hours after induction of ischemia, the amount of fibrin(ogen) in both the contralateral and ipsilateral hemisphere was determined by semi-quantitative Western blot. (A) Representative immunoblot showing accumulation of fibrin(ogen) in ipsi- (I) and contralateral (C) hemispheres. (B) Band intensities from A were quantified by densitometry. Each fibrin(ogen) density signal was first normalized to the corresponding actin density signal. The ratio of the normalized ipsilateral fibrin(ogen) density relative to the normalized contralateral fibrin band served as a measurement for relative fibrin(ogen) deposition (ratio ipsilateral/contralateral). *, $P < 0.05$; **, $P < 0.01$; ***, $P < 0.001$; ns, not statistically significant.

2.5. DISCUSSION

As a main finding of this study, we showed that platelet VWF is not essential for normal hemostasis and arterial thrombus formation but that this specific pool of VWF can contribute to ischemic brain injury via a GPIbα-dependent mechanism.

Although normal plasma VWF levels were observed in VWF EC chimeric mice, no VWF was detected in their platelets. This observation confirms earlier transplantation studies performed in both mice[15] and pigs[19] and corroborates the absence of VWF in platelets of VWD type 3 patients after replacement therapy.[24] Hence, our data further support the hypothesis that platelet VWF originates solely from megakaryocytes and is not taken up from plasma, in contrast to e.g. fibrinogen. Chimeric mice with VWF only in platelets did not show any significant amounts of VWF in plasma. In addition, no significant increase in circulating FVIII was observed. Similar observations were obtained in chimeric pigs.[19] Interestingly, Kanaji *et al*.[15] showed trace amounts of circulating VWF in chimeric mice that only have VWF in platelets. One possible explanation of this discrepancy could be a difference in VWF ELISA detection sensitivities. Alternatively, slight platelet activation can result in the release of VWF in the plasma.

The contribution of platelet-derived VWF in normal hemostasis is still not totally clear. Case studies in humans suggested that platelet-derived VWF is beneficial for normalization of bleeding.[25-28] Our tail clip bleeding experiments show that endothelial cell-derived VWF is the major determinant in the process of normal hemostasis. This concept is further supported by earlier observations of defective hemostasis in mice[15] and pigs[29,30] with VWF only in platelets. Furthermore, hydrodynamic gene transfer experiments that target the liver for VWF expression also show that VWF present only in plasma can correct the bleeding diathesis of VWF KO mice[17,31]. Nevertheless, we observed that a small subset (19%) of mice expressing VWF only in platelets had partially corrected bleeding times, suggesting that in some cases platelet-derived VWF is more or less able to support hemostasis. Similar results were obtained by Kanaji and colleagues who showed that 38% of their VWF PLT mice also had a partially corrected bleeding time.[15] Why bleeding stopped in some of our VWF PLT mice remains unclear. These mice did not show higher platelet counts nor did they have higher levels of plasma VWF or FVIII. Although less likely, differences in size and quantity of VWF in the platelet granules might contribute to these observations. More studies, preferably

using bleeding models that more closely mimic clinically relevant human hemorrhage, are needed to further clarify the specific function of platelet VWF in bleeding.

Platelet VWF is important for initial *in vitro* platelet adhesion on collagen-coated surfaces.[15,30] To test whether this is relevant for *in vivo* thrombus formation, we used a $FeCl_3$-induced carotid artery thrombosis model. Interestingly, mice having VWF only in platelets (VWF PLT) could not form occlusive thrombi, whereas chimeric mice with only endothelial cell-derived VWF (VWF EC) did so within 10 minutes. Thus, overall arterial thrombus formation does not seem to be largely dependent on VWF in platelets, which is in line with earlier thrombosis studies in chimeric pigs.[29] In our model, we were not able to assess initial platelet adhesion rates after carotid artery injury but lack of VWF in platelets seemed to slow down the rate of blood flow reduction compared with WT mice, an effect that was however lost in the total kinetics of occlusive thrombus formation in the large carotid artery. Studies using other thrombosis models would be helpful to further explore the specific role of platelet VWF in thrombus formation.

Increased platelet adhesion at sites of vascular injury could be important in thrombotic pathologies affecting the microcirculation such as ischemic stroke. We and others have shown that VWF KO mice are protected from stroke.[3-5] Chimeric mice that lack VWF in platelets (VWF EC) developed the same cerebral infarctions as observed in WT animals, suggesting that plasma VWF alone can mediate the VWF-dependent ischemic brain injury. These findings are in agreement with the same large infarctions observed in VWF KO mice reconstituted with plasma VWF via hydrodynamic VWF gene transfer.[5] Surprisingly, stroke lesions in VWF PLT chimeric mice were also similar to those seen in WT mice. Indeed, whereas VWF PLT chimeric mice display a phenotype similar to VWF KO animals in the tail-clipping bleeding and carotid artery thrombosis model, this is not the case in the stroke model. Hence, the contribution of VWF in platelets seems to be specifically relevant in the setting of cerebral ischemia. In addition, we observed an increased intracerebral deposition of fibrin(ogen) in VWF PLT chimeric mice compared with VWF KO mice indicating that local release of platelet VWF can promote intracerebral thrombosis. It is tempting to speculate that platelets adhere to activated endothelium (or subendothelium) in the area of ischemia/reperfusion and upon activation, secrete their granular contents, including large amounts of UL-VWF. This may result in the formation of platelet-derived VWF strings that may even be more resistant to ADAMTS13 proteolysis.[10,32] Similar to endothelial-derived

VWF strings, VWF strings from platelets could recruit new platelets and inflammatory cells resulting in platelet/leukocyte plugs that block the microvasculature and contribute to the no-reflow phenomenon. Interestingly, such platelet derived-VWF strings have been shown *in vitro*.[33] Future studies specifically addressing the inflammatory nature of platelet-derived VWF will definitely shed more light on its role in this thrombo-inflammatory process.

Despite *in vitro* data showing that purified platelet VWF has a lower affinity for GPIbα than plasma VWF,[9] we found that platelet VWF mediates ischemic brain injury via a GPIb-dependent mechanism. This finding further supports the crucial importance of the VWF-GPIb axis in stroke.[5-7,23,34] Although p0p/B is not cytotoxic to platelets,[23] we observed a small decrease in platelet count in p0p/B-treated mice compared with the control group (657.4 ± 115.6 versus 895.7 ± 107.1, respectively; $p < 0.01$). This difference in platelet count can however not account for the observed difference in infarct size as 10% of normal platelet counts is already sufficient to induce full brain infarction following transient ischemic stroke.[35]

In conclusion, our data shed an unexpected new light on the activity of platelet VWF and expand our insights on VWF-mediated mechanisms underlying ischemic stroke. This study further supports the idea that blocking the GPIb-VWF axis would be an interesting novel treatment strategy in stroke.

2.6. ACKNOWLEDGEMENTS

The authors thank E. Verhenne, N. Hertsens, and J.-P. Coutant (Department of Radiotherapy, AZ Groeninge Campus Loofstraat, Kortrijk, Belgium) for their help with the irradiation of mice. This work was supported by the Fonds voor Wetenschappelijk Onderzoek Vlaanderen (FWO G.0298.12) and the Deutsche Forchsungsgemeinschaft (SFB 688).

2.7. AUTHORSHIP

Contribution: S.V. and S.F.D.M. designed research and wrote the manuscript; S.V., F.D., S.L., A.V., I.P., and S.F.D.M. performed experiments; S.V., F.D., S.L., and S.F.D.M analyzed data and interpreted results. A.L., C.K., and B.N. provided essential materials and equipment; F.D., C.K., B.N., H.D., and K.V. helped editing the manuscript.

Conflict-of-interest disclosure: The authors declare no competing financial interests.

2.8. REFERENCES

1. De Meyer SF, Deckmyn H, Vanhoorelbeke K. von Willebrand factor to the rescue. *Blood*. 2009;113(21):5049–5057.
2. Rauch A, Wohner N, Christophe OD, et al. On the versatility of von Willebrand factor. *Mediterr J Hematol Infect Dis*. 2013;5(1):e2013046.
3. Kleinschnitz C, De Meyer SF, Schwarz T, et al. Deficiency of von Willebrand factor protects mice from ischemic stroke. *Blood*. 2009;113(15):3600–3603.
4. Zhao B-Q, Chauhan AK, Canault M, et al. von Willebrand factor – cleaving protease ADAMTS13 reduces ischemic brain injury in experimental stroke. *Blood*. 2009;114(15):1–3.
5. De Meyer SF, Schwarz T, Deckmyn H, et al. Binding of von Willebrand factor to collagen and glycoprotein Ibalpha, but not to glycoprotein IIb/IIIa, contributes to ischemic stroke in mice--brief report. *Arterioscler Thromb Vasc Biol*. 2010;30(10):1949–1951.
6. De Meyer SF, Stoll G, Wagner DD, Kleinschnitz C. von Willebrand factor: an emerging target in stroke therapy. *Stroke*. 2012;43(2):599–606.
7. Mannucci PM. Platelet/von Willebrand Factor Inhibitors to the Rescue of Ischemic Stroke. *Arterioscler Thromb Vasc Biol*. 2010;30(10):1882–1884.
8. McGrath RT, McRae E, Smith OP, O'Donnell JS. Platelet von Willebrand factor--structure, function and biological importance. *Br J Haematol.* 2010;148(6):834–843.
9. Williams SB, McKeown LP, Krutzsch H, Hansmann K, Gralnick HR. Purification and characterization of human platelet von Willebrand factor. *Br J Haematol.* 1994;88(3):582–591.
10. McGrath RT, van den Biggelaar M, Byrne B, et al. Altered glycosylation of platelet-derived von Willebrand factor confers resistance to ADAMTS13 proteolysis. *Blood*. 2013;4107–4110.
11. De Meyer SF, Savchenko AS, Haas MS, et al. Protective anti-inflammatory effect of ADAMTS13 on myocardial ischemia/reperfusion injury in mice. *Blood*. 2012;120(26):5217–5223.
12. Khan MM, Motto DG, Lentz SR, Chauhan AK. ADAMTS13 reduces VWF-mediated acute inflammation following focal cerebral ischemia in mice. *J Thromb Haemost.* 2012;10(8):1665–1671.

13. Fressinaud E, Baruch D, Rothschild C, Baumgartner HR, Meyer D. Platelet von Willebrand factor: evidence for its involvement in platelet adhesion to collagen. *Blood*. 1987;70(4):1214–1217.
14. Fressinaud E, Federici AB, Castaman G, et al. The role of platelet von Willebrand factor in platelet adhesion and thrombus formation: a study of 34 patients with various subtypes of type I von Willebrand disease. *Br J Haematol.* 1994;86(2):327–332.
15. Kanaji S, Fahs SA, Shi Q, Haberichter SL, Montgomery RR. Contribution of platelet vs. endothelial VWF to platelet adhesion and hemostasis. *J Thromb Haemost.* 2012;10(8):1646–1652.
16. Denis C, Methia N, Frenette PS, et al. A mouse model of severe von Willebrand disease: defects in hemostasis and thrombosis. *Proc Natl Acad Sci USA*. 1998;95(16):9524–9529.
17. De Meyer SF, Vandeputte N, Pareyn I, et al. Restoration of plasma von Willebrand factor deficiency is sufficient to correct thrombus formation after gene therapy for severe von Willebrand disease. *Arterioscler Thromb Vasc Biol*. 2008;28(9):1621–1626.
18. Massberg S, Gawaz M, Gruner S, et al. A crucial role of glycoprotein VI for platelet recruitment to the injured arterial wall in vivo. *J Exp Med.* 2003;197(1):41–49.
19. Roussi J, Drouet L, Sigman J, et al. Absence of incorporation of plasma von Willebrand factor into porcine platelet alpha-granules. *Br J Haematol.* 1995;90(3):661–668.
20. Fujioka M, Hayakawa K, Mishima K, et al. Brief report ADAMTS13 gene deletion aggravates ischemic brain damage : a possible neuroprotective role of ADAMTS13 by ameliorating postischemic hypoperfusion. *Blood*. 2010;115(8):1–3.
21. Morganti JM, Jopson TD, Liu S, Gupta N, Rosi S. Cranial irradiation alters the brain's microenvironment and permits CCR2+ macrophage infiltration. *PLoS ONE*. 2014;9(4):e93650.
22. Moravan MJ, Olschowka JA, Williams JP, O'Banion MK. Cranial irradiation leads to acute and persistent neuroinflammation with delayed increases in T-cell infiltration and CD11c expression in C57BL/6 mouse brain. *Radiat Res*. 2011;176(4):459–473.
23. Kleinschnitz C, Pozgajova M, Pham M, et al. Targeting platelets in acute experimental stroke: impact of glycoprotein Ib, VI, and IIb/IIIa blockade on infarct size, functional outcome, and intracranial bleeding. *Circulation*. 2007;115(17):2323–2330.
24. Sultan Y, Jeanneau C, Lamaziere J, Maisonneuve P, Caen JP. Platelet factor VIII-

related antigen: studies in vivo after transfusion in patients with von Willebrand disease. *Blood*. 1978;51(4):751–761.

25. Castillo R, Escolar G, Monteagudo J, et al. Role for platelet von Willebrand factor in supporting platelet-vessel wall interactions in von Willebrand disease. *Am J Hematol*. 1989;31(3):153–158.
26. Castillo R, Monteagudo J, Escolar G, et al. Hemostatic effect of normal platelet transfusion in severe von Willebrand disease patients. *Blood*. 1991;77(9):1901–1905.
27. Ware RE, Parker RI, McKeown LP, Graham ML. A human chimera for von Willebrand disease following bone marrow transplantation. *Am J Pediatr Hematol Oncol*. 1993;15(3):338–342.
28. Castillo R, Escolar G, Monteagudo J, et al. Hemostasis in patients with severe von Willebrand disease improves after normal platelet transfusion and normalizes with further correction of the plasma defect. *Transfusion*. 1997;37(8):785–790.
29. Nichols TC, Samama CM, Bellinger DA, et al. Function of von Willebrand factor after crossed bone marrow transplantation between normal and von Willebrand disease pigs: effect on arterial thrombosis in chimeras. *Proc Natl Acad Sci USA*. 1995;92(7):2455–2459.
30. Andre P, Brouland JP, Roussi J, et al. Role of plasma and platelet von Willebrand factor in arterial thrombogenesis and hemostasis in the pig. *Exp Hematol*. 1998;26(7):620–626.
31. Denis CV, Marx I, Badirou I, Pendu R, Christophe O. Mouse models to study von Willebrand factor structure-function relationships in vivo. *Hamostaseologie*. 2009;29(1):17–8– 20.
32. Lenting PJ, Denis CV. Platelet von Willebrand factor: sweet resistance. *Blood*. 2013;122(25):4006–4007.
33. Tersteeg C, Seinen C, Heijnen HF. Platelet granules patterns under flow. *J Thromb Haemost.* 2013;11(supplement s2).
34. De Meyer SF, Schwarz T, Schatzberg D, Wagner DD. Platelet glycoprotein Ibα is an important mediator of ischemic stroke in mice. *Exp Transl Stroke Med.* 2011;3(1):9.
35. Morowski M, Vogtle T, Kraft P, et al. Only severe thrombocytopenia results in bleeding and defective thrombus formation in mice. *Blood*. 2013;121(24):4938–4947.

CHAPTER 3

LONG-TERM PROTECTION OF THROMBOTIC THROMBOCYTOPENIC PURPURA IN ADAMTS13 KNOCKOUT MICE BY *'SLEEPING BEAUTY'* TRANSPOSON-MEDIATED GENE THERAPY

Sebastien Verhenne[1], Nele Vandeputte[1], Inge Pareyn[1], Zsuzsanna Izsvák[2], Hanspeter Rottensteiner[3], Hans Deckmyn[1], Simon F. De Meyer[1], and Karen Vanhoorelbeke[1]

[1]Laboratory for Thrombosis Research, KU Leuven Campus Kulak Kortrijk, Kortrijk, Belgium; [2]Mobile DNA, Max Delbrück Center for Molecular Medicine in the Helmholtz Association, Berlin, Germany; [3]Shire, Gene therapy, Vienna, Austria

Manuscript was submitted to *Arteriosclerosis, Thrombosis, and Vascular Biology* (minor revisions)

3.1. ABSTRACT

Severe deficiency in the von Willebrand factor (VWF)-cleaving protease ADAMTS13 (A Disintegrin And Metalloproteinase with ThromboSpondin type-1 motif, member 13), due to mutations in the *ADAMTS13* gene, can lead to acute episodes of congenital thrombotic thrombocytopenic purpura (TTP), requiring prompt treatment. In order to replenish plasma ADAMTS13 activity, current treatment consists of therapeutic or prophylactic infusions of fresh frozen plasma. However, lifelong treatment with plasma products is a stressful therapy for TTP patients. Here, we describe a gene therapeutic approach of using the *'Sleeping Beauty'* (SB100X) transposon system to realize lifelong expression of ADAMTS13 that protects against congenital TTP. We demonstrate that hydrodynamic tail vein injection of the SB100X system expressing murine ADAMTS13 in *Adamts13*$^{-/-}$ mice resulted in long-term expression of supraphysiological levels of transgene ADAMTS13 over a period of 25 weeks. The stable expression of ADAMTS13 efficiently removed the prothrombotic ultra large VWF multimers present in the circulation of *Adamts13*$^{-/-}$ mice. Moreover, mice stably expressing ADAMTS13 were protected against TTP. The treated mice did not develop severe thrombocytopenia nor did organ damage occur when triggered with recombinant VWF, and this up to 20 weeks after gene transfer. These data demonstrate the feasibility of using SB100X-mediated gene therapy to achieve sustained expression of transgene ADAMTS13 and long-term prophylaxis against TTP in *Adamts13*$^{-/-}$ mice.

3.2. INTRODUCTION

Thrombotic thrombocytopenic purpura (TTP) is a rare thrombotic disorder caused by deficiency in the von Willebrand factor (VWF)-cleaving protease ADAMTS13 (A Disintegrin And Metalloproteinase with ThromboSpondin type 1 motif, member 13). In normal circulation, ADAMTS13 cleaves highly reactive ultra large VWF (UL-VWF) multimers into smaller, less prothrombotic multimers preventing spontaneous platelet aggregation. Severe ADAMTS13 deficiency, caused by mutations of the *ADAMTS13* gene (congenital TTP) or autoantibodies against ADAMTS13 (acquired TTP), can result in the accumulation of UL-VWF multimers and intravascular deposition of VWF- and platelet-rich thrombi in the microcirculation.[1-3] During an acute episode, TTP patients typically present with thrombocytopenia, hemolytic anemia and organ injury including cerebral, renal, and cardiac manifestations.[4,5]

Acute TTP is a medical emergency with a mortality rate as high as 90% if left untreated. In patients with congenital TTP, infusion of fresh frozen plasma (FFP; 10-15mL/kg) replenishes the missing ADAMTS13 and ameliorates disease outcome.[6,7] However, congenital TTP patients with low residual plasma ADAMTS13 activity have frequent disease recurrences necessitating prophylactic FFP infusions.[8,9] Indeed, regular plasma infusions (every 2-3 weeks) may prevent acute TTP episodes.[8,10,11] Although the number of prophylactic infusions needed depends on the patient's phenotype, lifelong plasma therapy is stressful and has a significant negative impact on the lifestyle and quality of life of TTP patients.[12,13] In addition, administration of plasma products may result in fluid overload or elicit allergic reactions to plasma proteins. The risk of viral/prion transmission also remains a major concern.

Given the severity of the disease and the limitations of FFP prophylaxis, gene therapy for congenital TTP would offer an attractive alternative, as correction of the underlying genetic defect would result in lifelong expression of ADAMTS13 avoiding the need for plasma infusions. Gene therapeutic approaches have been viewed as highly promising for both rare genetic diseases and more common complex disorders. The therapeutic potential of this strategy has recently been demonstrated in clinical trials for haemophilia B[14], Leber's congenital amaurosis[15], X-linked severe combined immunodeficiency disorder[16], and metachromatic leukodystrophy[17]. In the TTP model, an initial preclinical study demonstrated that viral vector-mediated expression of a truncated form of ADAMTS13 protected *Adamts13*$^{-/-}$ mice from developing TTP symptoms elicited by bacterial shigatoxin.[18] Although protection from TTP was only assessed 2 weeks after gene transfer, this study

provided evidence that supports the validity of a gene therapeutic approach. However, to successfully translate gene therapy into a clinical setting, a long-term expression of ADAMTS13 is required that guarantees lifelong protection of congenital TTP patients from acute TTP episodes.

To achieve long-term prevention of congenital TTP, we use the non-viral '*Sleeping Beauty'* (SB100X) transposon system to deliver and express a functional copy of the *Adamts13* gene to *Adamts13*$^{-/-}$ mice in order to achieve stable, robust gene expression. This plasmid-based transposon system consists of a transposon DNA sequence and a transposase protein that excises the transposon from the donor plasmid and integrates it into the target genome (Figure 1).[19,20] The SB100X system utilizes a hyperactive version of the transposase.[20] The SB transposon system has already been used to successfully integrate therapeutic genes into the host cell genome resulting in long-term transgene expression and phenotypic correction of monogenetic diseases such as haemophilia[20-22] and lysosomal storage disorders[23,24] in preclinical animal studies. In this study, we report that delivery of the SB transposon, encoding the murine *Adamts13* gene, along with a SB100X transposase to the liver of *Adamts13*$^{-/-}$ mice can mediate long-term expression of supraphysiological levels of plasma ADAMTS13 and long-term prevention of the onset of TTP symptoms in *Adamts13*$^{-/-}$ mice.

3.3. METHODS

3.3.1. Plasmids

The plasmid expressing the transposase (Figure 1), pCMV(CAT)T7-SB100 (referred as pCMV-SB100x in the text), contains the hyperactive transposase (SB100x) cDNA of which expression is driven from a cytomegalovirus (CMV) enhancer/promoter.[20] The transposon plasmid, pT2/HCRHPi-ADAMTS13, was constructed using the In-Fusion® HD Cloning Kit (Clontech Laboratories, Mountain View, CA). The expression cassette containing a liver-specific promoter (HCRHPi: apolipoprotein hepatic control locus region (ApoE-HCR) linked to a human α1-anti-trypsin promoter and a truncated 1.4 kb human factor IX) coupled to the murine *Adamts13* cDNA was amplified from pBS-II-SK-HCHRPi-muADAMTS13[25] using Phusion® High Fidelity DNA polymerase (New England Laboratories, Ipswich, MA) and primers flanking the desired region. In parallel, pT2/CAGGS-GFP[20] was digested with *Cla*I/*Not*I-HF (New England Laboratories) thereby excising the CAGGS-GFP expression cassette. Subsequently, the HCRHPi-ADAMTS13 polymerase chain reaction product was ligated into the linearized pT2-vector backbone according to the In-Fusion cloning procedure for spin-column purified PCR fragments. The HCRHPi-ADAMTS13 cassette was sequenced to confirm the sequence (GATC Biotech AG, Konstanz, Germany). Plasmid DNA used for hydrodynamic tail vein injection was prepared using the Endofree® Plasmid Mega Kit (Qiagen, Venlo, The Netherlands).

3.3.2. Mice

Male and female ADAMTS13 knockout (*Adamts13*$^{-/-}$) and wild-type (*Adamts13*$^{+/+}$) mice were bred from heterozygous *Adamts13*$^{+/-}$ (with a mixed C57BL/6J-129X1/SvJ-CASA/Rk background).[26] All animal experiments were performed in accordance with protocols approved by the Institutional Animal Care and Use Committee of the KU Leuven (License LA1300114, project number P163/2015, KU Leuven, Belgium).

3.3.3. Hydrodynamic gene transfer

Five to 7-week old *Adamts13*$^{-/-}$ mice (weighing 16-21 g) were injected with 5 μg transposon plasmid DNA and 0.2 μg transposase plasmid DNA via hydrodynamic tail vein injection.[27-29] Plasmid DNA was diluted in a saline solution (0.9% NaCl) equivalent to 10% of the body weight and administered via the lateral tail vein in 5-7 seconds. *Adamts13*$^{-/-}$ mice that were

hydrodynamically injected with only transposon plasmid DNA (no transposase) or with saline solution were used as controls.

3.3.4. Blood collection

Animals were anesthetized using 5% isoflurane (Nicholas Piramal Limited, London, UK) in 100% O_2. Whole blood was drawn from the retro-orbital plexus and collected on 0.5M EDTA (1 volume to 40 volumes of blood) or 3.8% sodium citrate (1 volume to 7 volumes of blood). Platelet-poor plasma was prepared from citrated blood by centrifugation at 4300 g for 6 minutes at room temperature and stored at -80°C for further analysis.

3.3.5. Induction of TTP

To induce TTP symptoms, saline- or SB-treated *Adamts13*$^{-/-}$ mice were challenged with a single intravenous bolus injection of recombinant human VWF (rVWF; 2000 VWF:RCoU/kg body weight) in the lateral tail vein as described.[30] Twenty-four hours after challenge, blood was collected to monitor TTP symptoms. Platelet count and hemoglobin levels were determined in EDTA-anticoagulated blood using the Hemavet 950FS Multi-species Hematology system (Drew Scientific Inc., Dallas, TX). Lactate dehydrogenase (LDH) activity was measured in citrated plasma using an LDH activity colorimetric assay kit (Biovision, Milpitas, CA) according to the manufacturer's instructions. Body weight loss was determined by calculating the difference in body weight assessed before and 24h after challenge with rVWF.

3.3.6. ADAMTS13 antigen analysis

Transgene ADAMTS13 antigen levels in plasma were determined via an in-house developed enzyme-linked immunosorbent assay (ELISA) as described, with some minor modifications.[25] A 96-well microtiter plate was coated overnight at 4°C with our anti-mouse ADAMTS13 monoclonal antibody 14H7B8 (5 μg/mL in phosphate buffered saline (PBS)). After blocking with a 3% skimmed milk solution, plasma samples (diluted in PBS containing 0.3% (m/v) skimmed milk) were added and incubated for 90 minutes at 37°C. Captured ADAMTS13 was detected via our in-house developed polyclonal rabbit anti-mouse ADAMTS13 antibodies (5 μg/ml in PBS containing 0.3% skimmed milk) and polyclonal goat anti-rabbit antibodies labeled with horseradish peroxidase (HRP; Jackson ImmunoResearch Laboratories Inc., West Grove, PA) (1/10,000 in PBS containing 0.3%

skimmed milk). The colouring reaction was initiated after addition of ortho-phenylenediamine (Sigma-Aldrich, St Louis, MO) and H_2O_2, and stopped with 4 M H_2SO_4. The ADAMTS13 antigen level in pooled plasma of more than 20 *Adamts13*$^{+/+}$ mice was used as a reference (100%, normal murine plasma, NMP).

3.3.7. Immunohistochemistry

After sacrificing the animal, the left liver lobe was removed, embedded in Tissue-Tek® O.C.T.™ Compound (Sakura Finetek Europe B.V., Alphen aan den Rijn, The Netherlands), snap-frozen in liquid nitrogen and stored at -80°C. Liver lobes were cut in 10 µm thick cryosections using a Leica CM1950 Cryostat (Leica Biosystems, Richmond, IL) and stored at -20°C. Before use, sections were air-dried and fixed in 4% paraformaldehyde. Sections were then blocked and permeabilized with 5% normal goat serum in PBS containing 0.1% Triton X-100, 1% bovine serum albumin (BSA), and 0.1% Tween20 for 1 hour at room temperature followed by overnight incubation with our polyclonal rabbit anti-mouse ADAMTS13 antibodies[31] (10 µg/ml in PBS containing 1% BSA and 0.1% Tween20) at 4°C. After washing in PBS, endogenous peroxidase activity was blocked using 0.3% H_2O_2 in PBS for 15 min at room temperature. Subsequently, sections were washed and incubated with HRP-labeled goat anti-rabbit antibodies (1/500 in PBS containing 1% BSA and 0.1% Tween20; Jackson ImmunoResearch Laboratories Inc.) for 45 minutes at room temperature. After another washing step, ADAMTS13-positive liver cells were visualized with 3,3'-diaminobenzidine (DAB; Dako, Glostrup, Denmark) followed by counterstaining with hematoxylin (Sigma-Aldrich) for 2 minutes. Sections were dehydrated and mounted in DPX (Fluka, Bornem, Belgium). Pictures were taken at 10x magnification using a Zeiss Primo Star microscope (Carl Zeiss Microscopy GmbH, Jena, Germany).

3.3.8. Analysis of murine plasma VWF multimers

Citrated plasma samples were 1/5 diluted in sample buffer (8 M urea, 5% (m/v) sodium dodecyl sulphate (SDS), 10 mM Tris, 1 mM EDTA, and 0.3% bromophenol blue; pH 8.0) and incubated at 60°C for 30 minutes. VWF multimers were separated on a low-resolution (1.2%) SDS isoelectric focusing agarose gel (GE Healthcare Europe GmbH, Diegem, Belgium), fixed on a GelBond® film (Lonza, San Diego, CA), by electrophoresis at 10-15 mA in a multiphor II apparatus (GE Healthcare). Following electrophoresis, the gel was rinsed in distilled water, dried under cooled air and blocked in 5% skimmed milk in TBS

containing 0.05% Tween20. After overnight incubation with polyclonal anti-human VWF antibodies (1/750 diluted in TBS; Dako), in-house conjugated with alkaline phosphatase, and subsequent rinsing with TBS containing 0.05% Tween20, VWF multimers were visualized using an Alkaline Phosphate conjugate substrate kit (BioRad, Hercules, CA).[29] Densitometric analysis was performed using Image J software (version 1.47, National Institute of Health, Bethesda, MD). The density-profile of each VWF multimer pattern was graphed. Distinguishable bands were divided into 3 subclasses: (1) 1-5 dimers were designated as low molecular weight VWF multimers (LMW), (2) 6-10 dimers as medium molecular weight VWF multimers (MMW), and (3) >10-dimers as high molecular weight VWF multimers (HMW; including UL-VWF multimers). UL-VWF multimers did not resolve in single bands but appeared as a smear that was included in the HMW subclass. The total density of each subclass was divided by the density of all multimer bands to calculate the relative abundance of all subclasses.[29]

3.3.9. Statistical analysis

Data are represented as mean ± SEM. For statistical analysis, Prism Version 6.0 software (GraphPad Software, La Jolla, CA) was used. One-way analysis of variance followed by Dunnett's multiple comparisons post hoc test was conducted to assess the variance of the relative amounts of HMW multimers between *Adamts13*$^{-/-}$ mice and the different experimental groups. Unpaired t testing was used to compare saline- and SB-treated *Adamts13*$^{-/-}$ mice challenged with rVWF at different time points. A probability value < 0.05 was considered as statistically significant.

3.4. RESULTS

3.4.1. Long-term expression of supraphysiological levels of transgene murine ADAMTS13 in *Adamts13*$^{-/-}$ mice

We aimed at obtaining long-term expression of transgene murine ADAMTS13 in *Adamts13*$^{-/-}$ mice by using the SB100X transposon system (Figure 1). We cloned an expression cassette consisting of murine *Adamts13* cDNA under control of the liver-specific α_1-antitrypsin promoter (HCRHPi)[32] into the SB transposon vector to obtain pT2/HCRHPi-ADAMTS13. To integrate the *Adamts13* transgene into the mouse genome, the plasmid containing the hyperactive variant of the original transposase under control of the ubiquitous CMV promoter was used (pCMV-SB100X).[20] Plasmids were hydrodynamically injected in *Adamts13*$^{-/-}$ mice resulting in *in vivo* transfection of murine hepatocytes.[27-29]

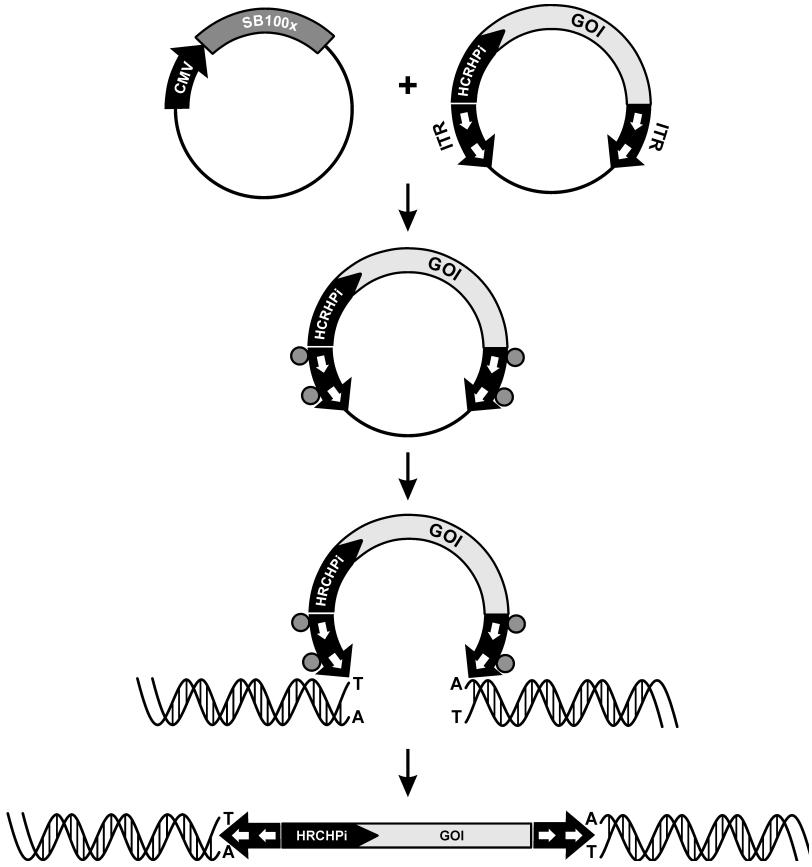

Figure 1: Schematic representation of '*Sleeping Beauty*'-transposon mediated gene transfer. The '*Sleeping Beauty*' (SB100X) transposon system is a two-component system consisting of a transposon plasmid comprised of inverted terminal repeats (ITR, white arrow) flanking the gene of interest

(GOI), and a transposase plasmid pCMV(CAT)T7-SB100X (pCMV-SB100X) encoding the hyperactive SB transposase (SB100X). Upon SB transposon-mediated gene transfer, the SB100X transposase (grey circles) will bind the inverted terminal repeats (ITR, white arrows), excise the engineered therapeutic gene (gene of interest, GOI) from the plasmid DNA, and integrate it into genomic TA dinucleotides of chromosomal DNA.

In the first group of *Adamts13*$^{-/-}$ mice (n=7), both transposon (pT2/HCRHPi-ADAMTS13) and transposase (pCMV-SB100X) plasmids were hydrodynamically injected. In this group, the integration of the murine *Adamts13* cDNA into the mouse genome was promoted by the transposase (gene therapy group). In the second group, *Adamts13*$^{-/-}$ mice (n = 7) were injected with a solution containing only the transposon (pT2/HCRHPi-ADAMTS13), but no transposase (control group). At 3 days post injection, levels of transgene ADAMTS13 were remarkably high in both groups of mice (368 ± 52% and 392 ± 91% in the gene therapy group and in the control group, respectively; Figure 2A). Notably, long-term follow up of transgene ADAMTS13 expression levels indicated that transgene expression was only transient in the control group, as ADAMTS13 antigen levels rapidly decreased over time (Figure 2A). On the contrary, transgene ADAMTS13 levels remained high in the gene therapy group up to 25 weeks after gene transfer, the time point at which the experiment was ended (184 ± 17% and 10 ± 2% in the gene therapy group and the control group, respectively; Figure 2A).

Immunohistochemical analysis of liver sections confirmed the above results. Mice with long-term and high-level expression of transgene ADAMTS13 (gene therapy group) had a high number of ADAMTS13-expressing hepatocytes at 25 weeks post injection (Figure 2B, right panel). In contrast, in mice with transient ADAMTS13 transgene expression (control group) only a few ADAMTS13-positive hepatocytes were found in liver sections at 25 weeks post injection (Figure 2B, middle panel). Finally, we addressed whether the treatment induced immune response. We observed no profound anti-ADAMTS13 antibody response in either group (data not shown).

In conclusion, these data indicate that SB100X transposon-mediated gene delivery is a powerful technique to obtain long-term expression of supraphysiological levels of transgene ADAMTS13 in *Adamts13*$^{-/-}$ mice.

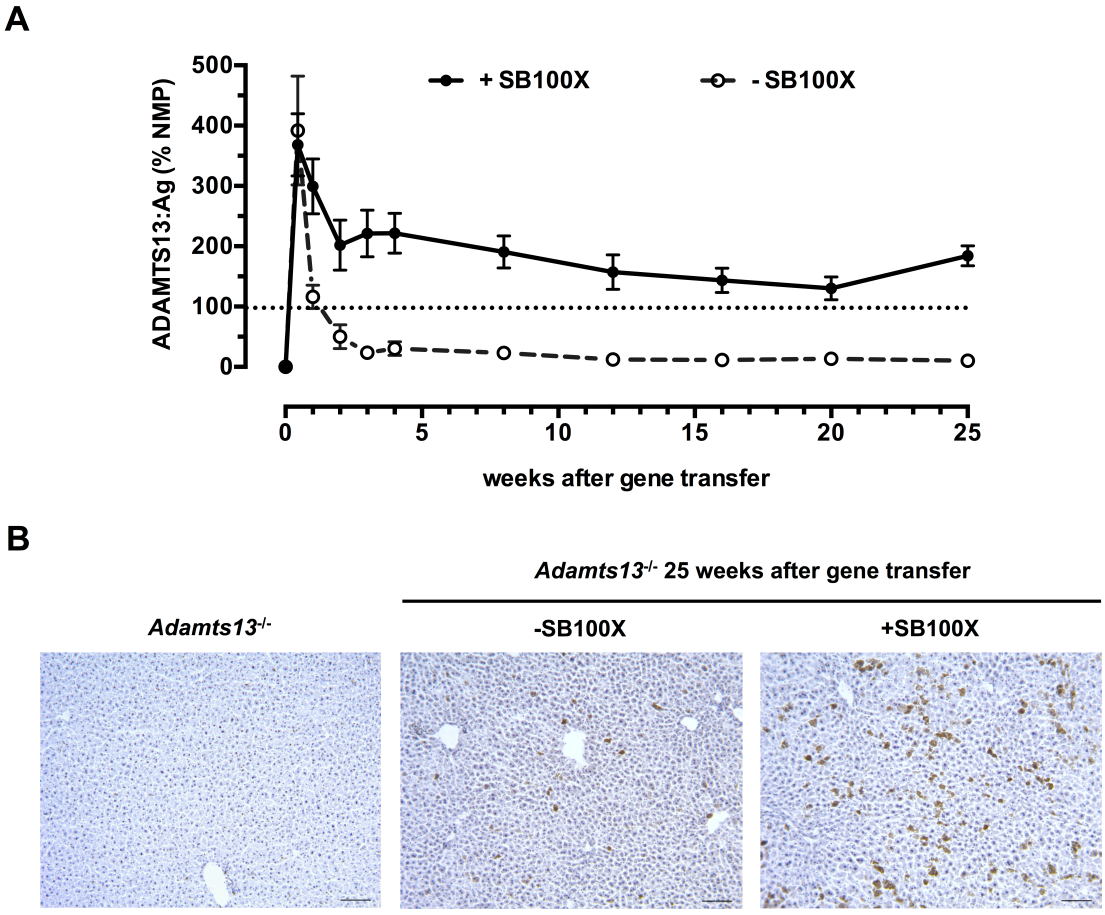

Figure 2: Long-term and stable expression of transgene ADAMTS13 in plasma and liver after *'Sleeping Beauty'* transposon-mediated gene transfer. *Adamts13*$^{-/-}$ mice were hydrodynamically injected with 5 µg pT2-HCRHPi-ADAMTS13 with (+SB100X, gene therapy group; n = 7) or without (-SB100X, control group; n = 7) 0.2 µg pCMV-SB100X. (A) Therapeutic ADAMTS13 antigen levels in plasma. Blood was collected at the indicated time points. Plasma ADAMTS13 antigen levels were determined by an in-house developed ELISA. Mean values ± SEM are expressed as percentage of normal murine plasma pool (% NMP). Dashed line indicates ADAMTS13 antigen level in NMP. (B) Transgene expression of ADAMTS13 in liver. A representative mouse of each group was sacrificed and liver sections were subjected to immunohistochemistry. ADAMTS13-positive liver cells were detected with polyclonal rabbit anti-ADAMTS13 antibodies and secondary HRP-labeled goat anti-rabbit antibodies, and visualized using DAB (dark brown color). Sections were counterstained with hematoxylin. Representative images of stained liver sections of a non-treated *Adamts13*$^{-/-}$ mouse (plasma ADAMTS13 antigen level: 0% of NMP), an *Adamts13*$^{-/-}$ mouse expressing low levels of ADAMTS13 antigen (-SB100x; plasma ADAMTS13 antigen level: 9% of NMP), and an *Adamts13*$^{-/-}$ mouse expressing high levels of ADAMTS13 antigen (+SB100x; plasma ADAMTS13 antigen level: 125% of NMP) at 25 weeks post injection are shown. ADAMTS13 antigen levels (%) are indicated below each image. Original magnifications, 10x; scale bar represents 50 µm.

3.4.2. Long-term expression of transgene ADAMTS13 prevents the accumulation of prothrombotic UL-VWF multimers in *Adamts13*$^{-/-}$ mice

Previous studies have demonstrated that *Adamts13*$^{-/-}$ mice exhibit a prothrombotic phenotype. Due to the absence of ADAMTS13 activity, prothrombotic UL-VWF multimers accumulate in *Adamts13*$^{-/-}$ mice compared to wild-type littermates.[26,33] Since these UL-VWF multimers are the major cause of TTP in humans, we assessed whether transgene ADAMTS13 was able to proteolyze UL-VWF multimers in *Adamts13*$^{-/-}$ mice. At day 3 post injection, when transgene ADAMTS13 levels were high in both groups (Figure 2A), UL-VWF multimers were absent (Figure 3). The percentage of HMW VWF multimers (including the UL-VWF multimers) in both the gene therapy group (29.9 ± 0.9%; n = 4) and the control group (30.7 ± 2.2%; n = 5) was comparable to the percentage observed in *Adamts13*$^{+/+}$ mice (36.0 ± 1.6%; n =7) showing that UL-VWF multimers were efficiently proteolyzed by transgene ADAMTS13 (Figure 3). At 25 weeks post injection however, the percentage of HMW VWF multimers (39.9 ± 1.2%; n = 5) in the control group increased again to values observed in *Adamts13*$^{-/-}$ mice (41.3 ± 1.4%; n = 8), indicating that the low levels of transgene ADAMTS13 were not sufficient to digest the UL-VWF multimers (Figure 3). In contrast, the relative amount of HMW VWF multimers was still normalized in the gene therapy group at 25 weeks post injection (31.7 ± 1.3%; n = 4), which is in line with the high levels of transgene ADAMTS13 present in these mice (Figure 2A).

In conclusion, SB transposon-mediated expression of the therapeutic ADAMTS13 gene leads to long-term normalization of the VWF multimer distribution in circulation and prevents accumulation of prothrombotic UL-VWF multimers in *Adamts13*$^{-/-}$ mice.

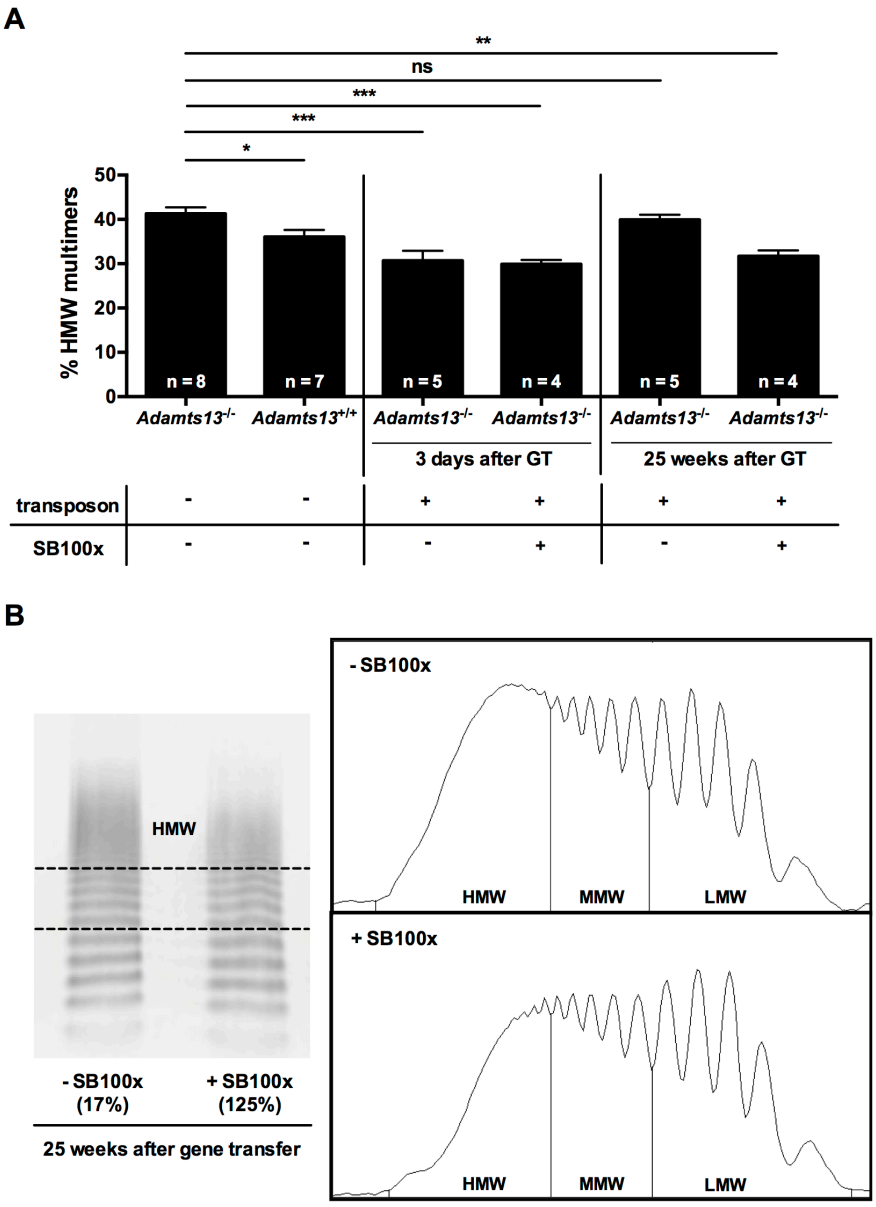

Figure 3: Long-term *'Sleeping Beauty'* transposon-mediated expression of high levels of transgene ADAMTS13 reduces VWF multimer size in *Adamts13*$^{-/-}$ mice. *Adamts13*$^{-/-}$ mice were hydrodynamically injected with 5 µg pT2-HCRHPi-ADAMTS13 with (+SB100X, gene therapy group) or without (-SB100X, control group) 0.2 µg pCMV-SB100x. Plasma samples of non-treated *Adamts13*$^{-/-}$ and *Adamts13*$^{+/+}$ mice were used as controls. (A) VWF multimer gel analysis was performed on plasma samples collected at 3 days and 25 weeks after gene transfer (GT). The relative abundance of high molecular weight (HMW) multimers, including the ultra-large VWF multimers, was determined by densitometric analysis. (B) Representative image of VWF multimer patterns and corresponding densitometric profiles of mice expressing low (-SB100X: 17% of NMP) or high (+SB100X: 125% of NMP) ADAMTS13 antigen levels at 25 weeks after gene transfer. Distinguishable bands were divided into 3 subclasses: 1-5 dimers were designated as low molecular weight (LMW) VWF multimers, 6-10 dimers as medium molecular weight (MMW) VWF multimers,

and >10-dimers as high molecular weight (HMW) and ultra-large VWF multimers. Ns, not significant; *, P < 0.05; **, P < 0.01; ***, P < 0.001 compared to *Adamts13*$^{-/-}$ mice.

3.4.3. *'Sleeping Beauty'* transposon-mediated gene therapy prevents the onset of TTP symptoms in *Adamts13*$^{-/-}$ mice up to 20 weeks following gene transfer

It was previously shown that *Adamts13*$^{-/-}$ mice develop TTP symptoms when they are triggered with recombinant VWF (rVWF).[30] We next investigated whether our SB100X-mediated gene therapeutic strategy could be an effective prophylactic approach to prevent acute TTP in *Adamts13*$^{-/-}$ mice.

We therefore hydrodynamically injected 3 groups of *Adamts13*$^{-/-}$ mice with the SB100X transposon system (gene therapy groups) to obtain long-term and high levels of transgene ADAMTS13 expression (as described in Figure 2A). To induce TTP symptoms, each group was challenged with a single dose of human rVWF (2000 VWF:RCoU/kg) at different time points (1, 4, or 10 weeks after gene transfer). In parallel, we hydrodynamically injected 3 groups of *Adamts13*$^{-/-}$ mice with a saline solution to serve as non-expressing controls and also challenged these mice with rVWF at different time points (control groups). A single group of *Adamts13*$^{-/-}$ mice that was hydrodynamically injected with PBS and treated with PBS instead of challenged with rVWF was used as a healthy control group. Twenty-four hours following the challenge, platelet count, plasma LDH levels (marker for tissue damage), hemoglobin levels (marker for hemolytic anemia) and weight loss were determined in all groups to assess TTP-like symptoms (Figure 4). As expected, all mice in the control groups (no gene transfer) developed TTP at all time points of rVWF challenge: platelet counts were dramatically decreased (>80%) (Figure 4A), plasma LDH levels were substantially elevated (Figure 4B), hemoglobin levels were decreased (Figure 4C), and a dramatic weight loss was observed (Figure 4D) when compared to values observed in healthy *Adamts13*$^{-/-}$ mice. Importantly and in stark contrast, regardless of the time point of the challenge, mice of the gene therapy groups did not develop TTP-like symptoms: they did not suffer from severe thrombocytopenia, (Figure 4A), their plasma LDH and hemoglobin levels remained within the normal range (Figure 4B and C) and they did not lose weight upon induction of TTP, reflecting a healthy state (Figure 4D). To further emphasize the long-term prophylactic efficacy of our gene therapeutic approach, an additional gene therapy group was challenged with rVWF at 20 weeks after gene transfer (Figure 4). Again, mice did not develop TTP as platelet counts, plasma LDH and hemoglobin levels remained within the normal range, nor

did these mice lose weight. Taken together, these results demonstrate that long-term SB transposon-mediated expression of ADAMTS13 results in long-lasting prophylaxis against TTP in this animal model.

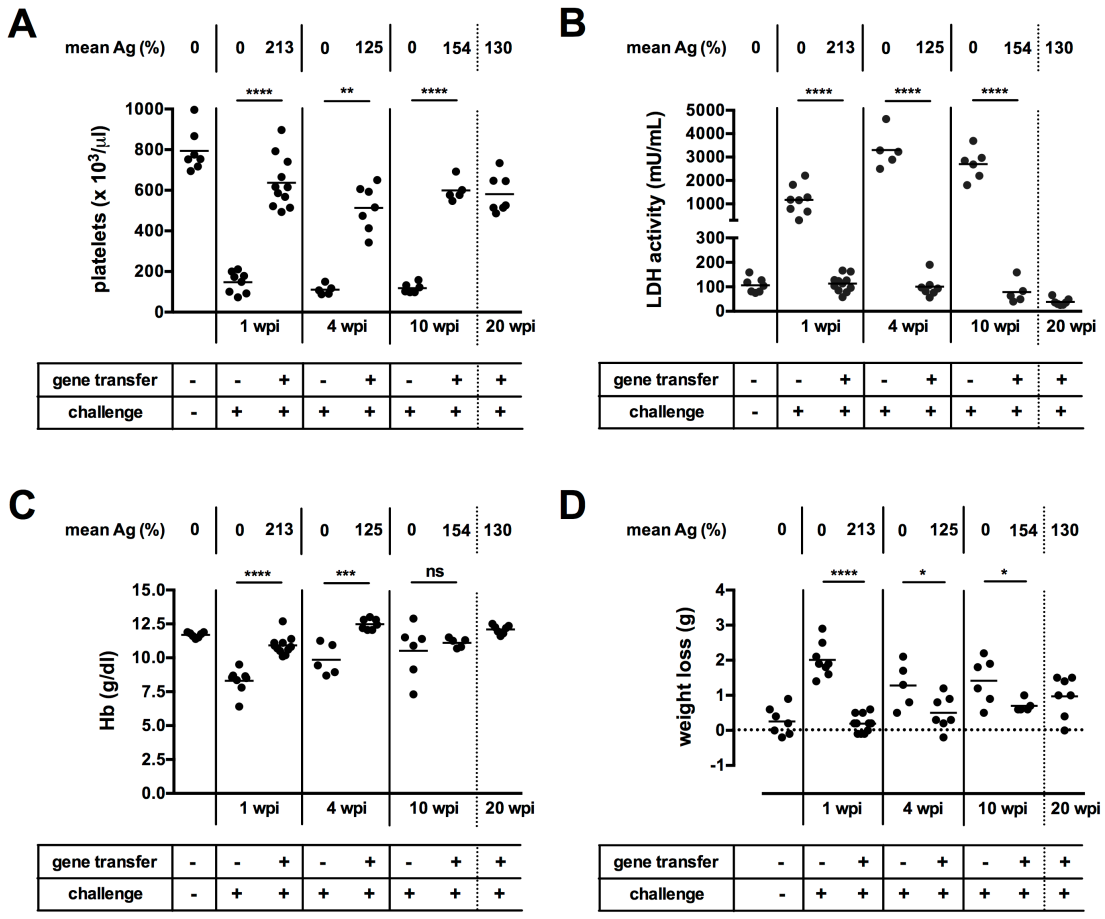

Figure 4: Long-term *'Sleeping Beauty'* transposon-mediated expression of high levels of transgene ADAMTS13 prevents the onset of TTP symptoms in *Adamts13*$^{-/-}$ mice challenged with rVWF. *Adamts13*$^{-/-}$ mice were injected with saline solution (control group, no gene transfer) or with the plasmids coding for the SB100X system (gene therapy group) via hydrodynamic injection. Mice were subsequently challenged with a single dose of recombinant human VWF (rVWF; 2000 VWF:RCoU/kg) at different weeks post hydrodynamic injection (wpi) (control group and gene therapy group). Another control group (no gene transfer) was hydrodynamically injected with saline and subsequently injected with PBS instead of challenged with rVWF (healthy control group). Twenty-four hours after challenge with rVWF, blood was collected and analysed. (A) Thrombocytopenia was assessed by measuring platelet counts in EDTA-treated blood using an automated cell counter. (B) Tissue damage was determined by measuring lactate dehydrogenase (LDH) activity in citrated plasma using a colorimetric assay kit. (C) Hemoglobin (Hb) levels were measured in EDTA-treated blood using an automated cell counter. (D) Weight loss was determined

by calculating the difference in weight before and 24 hours after challenge with rVWF. Mean ADAMTS13 antigen levels at the indicated time points are shown. Ns, not significant; *, $P < 0.05$; **, $P < 0.01$; ****, $P < 0.0001$.

3.5. DISCUSSION

In this study, we developed a novel integrating, non-viral gene therapy strategy to prevent congenital TTP in a mouse model. We demonstrated that SB100X-mediated gene transfer of murine *Adamts13* cDNA in *Adamts13*$^{-/-}$ mice results in long-term and high-level expression of the therapeutic protein, ADAMTS13. Importantly, this gene therapeutic strategy was able to prevent onset of acute TTP disease up to 20 weeks following gene transfer.

The SB transposon-mediated technology allowed sustained expression of high levels of transgene ADAMTS13 (184 ± 17%) in *Adamts13*$^{-/-}$ mice for 25 weeks post injection (almost six months; the end of the study). Stable expression of high plasma ADAMTS13 antigen levels was associated with the presence of a high number of ADAMTS13-expressing hepatocytes. When the SB100X transposase was absent, transgene expression rapidly dropped below WT levels within 3 weeks post injection, resulting in a low number of ADAMTS13-expressing hepatocytes. Still, low-level transgene expression, associated with a low number of ADAMTS13-expressing hepatocytes persisted for 25 weeks post injection (10 ± 2%), indicating that not all non-integrated prokaryotic DNA was degraded or epigenetically silenced.[32,34,35]

Notably, expressed ADAMTS13 was biologically active *in vivo*, as demonstrated by the normalization of the VWF multimer pattern in *Adamts13*$^{-/-}$ mice. Only mice expressing sustained high therapeutic ADAMTS13 levels were able to normalize the VWF multimer pattern for the whole 25-week period. These results indicate that the corresponding plasma ADAMTS13 activity was high enough to process newly secreted UL-VWF multimers. Furlan *et al.* showed that 5% plasma ADAMTS13 activity might be already sufficient to degrade the most adhesive VWF multimers into smaller forms that do not spontaneously recruit platelets in congenital TTP patients.[36] In line with this observation, data obtained by Lotta *et al.* indicate that a small increase in residual plasma ADAMTS13 activity is sufficient to lower the risk of disease recurrence and the need for FFP prophylaxis in congenital TTP patients.[9] In contrast, in the present study we observed that the plasma ADAMTS13 activity associated with a mean antigen value of 10% (range 2-17%) was not yet sufficient to alter the VWF multimer distribution. Whether this can be explained by species-specific differences in threshold ADAMTS13 levels required to normalize the VWF multimer pattern or due to synthesis of the therapeutic enzyme in heterologous cells (hepatocytes), requires further

investigation. Nevertheless, our study shows that the SB100X transposon system results in expression levels of ADAMTS13 of 184 ± 17% in *Adamts13*$^{-/-}$ mice for up to six months after gene transfer. Thus, it might be reasonable to assume that the SB100X system could be a proper vector able to provide stable therapeutic ADAMTS13 levels of more than 10% in congenital TTP patients.

In addition to studying expression levels, we next investigated whether SB transposon-mediated gene therapy would be a potent strategy to protect *Adamts13*$^{-/-}$ mice from developing TTP. TTP was triggered with rVWF as previously described.[30] As expected, severe thrombocytopenia, increased plasma LDH levels, decreased haemoglobin levels, and increased weight loss were observed in all *Adamts13*$^{-/-}$ mice that did not receive therapeutic gene transfer and hence did not express ADAMTS13. Intriguingly, treatment with the SB transposon system was a very effective prophylactic strategy. When *Adamts13*$^{-/-}$ mice expressing the therapeutic gene ADAMTS13, were triggered with rVWF at 1, 4 or 10 weeks after gene transfer, TTP symptoms did not appear. Even 20 weeks after gene transfer, expression levels of ADAMTS13 were still high enough to protect mice from developing TTP, as no profound thrombocytopenia, elevated LDH levels, decreased hemoglobin levels or increased weight loss were observed. These data demonstrate that the expression level of ADAMTS13 and its corresponding VWF-cleaving activity were high enough to process the large amounts of exogenous VWF, and prevent extensive organ damage and hemolysis. To our knowledge this is the first gene therapy-based preclinical study demonstrating long-term prophylaxis for congenital TTP using a non-viral gene therapeutic approach.

The use of the SB transposon technology holds high promise as it combines low cost and simplicity of naked DNA with the efficiency of gene transfer associated with retroviral vectors. SB has proven successful as a therapeutic vector in various preclinical studies demonstrating long-term gene expression in a wide range of tissues and primary cells.[37] Moreover, SB technology reached clinical level as the first phase I clinical trials using SB transposons have recently been conducted for adjuvant treatment of patients with advanced B-cell malignancies.[38] The results obtained from these trials are encouraging in terms of safety and patient's outcome, and support further clinical development of this non-viral gene therapeutic approach. To transfer the SB transposon-mediated approach described in this preclinical study from bench to clinical setting, the issue of hydrodynamics-based delivery and safety must be addressed. First, while hydrodynamic tail vein injection may be an

efficient delivery system in rodent animal models, the procedure is not readily applicable to a human clinical setting. However, efforts are made to apply this method to clinical gene therapy. Image-guided, computer-assisted hydrodynamic gene delivery restricted to the liver has been shown to be safe and effective in dogs, pigs, and non-human primates.[39] A second issue regarding to the clinical use of the SB transposon system is the safety of SB-mediated integration. It has been shown that SB-mediated transposition mediates integration into target dinucleotides without preference for transcriptionally active sites.[19,40] In fact, the *SB* transposon system has the most random integration profile of all vectors used in gene therapeutic approaches.[41,42] Although occurrence of insertional mutagenesis after SB-mediated gene therapy cannot be excluded, attempts are made to minimize the risk of accidental transactivation of genes. Studies have shown that engineered fusion proteins comprised of zinc finger proteins and the SB transposase can be used to effectively redirect transposon insertion into specific sequences in the genome.[43,44]

In conclusion, we successfully achieved long-term therapeutic expression of full-length ADAMTS13 in *Adamts13*$^{-/-}$ mice using the SB transposon system. This study is the first report demonstrating that a single administration of naked plasmid DNA can result in long-term correction of ADAMTS13 deficiency and prophylaxis of TTP in *Adamts13*$^{-/-}$ mice. We believe that the present study may pave the way to a SB transposon-mediated gene therapy that will cure congenital TTP in humans.

3.6. ACKNOWLEDGEMENTS

Adamts13$^{+/-}$ mice on a mixed C57BL/6J-129X1/SvJ-CASA/Rk background were a kind gift from Dr. D. Ginsburg (University of Michigan, MI). The authors thank L. Deforche for help with preparing the figures. This work was supported by Fonds voor Wetenschappelijk Onderzoek Vlaanderen (FWO) G.0584.11, G.0D13.15N, KU Leuven grant OT/14/071 and Answering TTP foundation grant RXO-D0264.

3.7. AUTHORSHIP

Contribution: S.V. and K.V. designed research and wrote the manuscript; S.V., N.V., I.P., and K.V. performed experiments; S.V., S.F.D.M., and K.V. analyzed data and interpreted results; Z.I. and H.R. provided essential materials; Z.I., H.R., H.D., and S.F.D.M critically reviewed the manuscript.

Conflict-of-interest disclosure: H. Rottensteiner is an employee of Baxalta Innovations GmbH, Vienna, Austria. All other authors declare that they have no competing financial interests.

3.8. REFERENCES

1. Moake JL, Rudy CK, Troll JH, et al. Unusually large plasma factor VIII:von Willebrand factor multimers in chronic relapsing thrombotic thrombocytopenic purpura. *N Engl J Med*. 1982;307(23):1432–1435.
2. Asada Y, Sumiyoshi A, Hayashi T, Suzumiya J, Kaketani K. Immunohistochemistry of vascular lesion in thrombotic thrombocytopenic purpura, with special reference to factor VIII related antigen. *Thromb Res*. 1985;38(5):469–479.
3. Tsai H-M. Pathophysiology of thrombotic thrombocytopenic purpura. *Int J Hematol*. 2010;91(1):1–19.
4. Coppo P, Veyradier A. Current management and therapeutical perspectives in thrombotic thrombocytopenic purpura. *Presse Med*. 2012;41(3 Pt 2):e163–76.
5. Blombery P, Scully M. Management of thrombotic thrombocytopenic purpura: current perspectives. *J Blood Med*. 2014;5:15–23.
6. Rock GA, Shumak KH, Buskard NA, et al. Comparison of plasma exchange with plasma infusion in the treatment of thrombotic thrombocytopenic purpura. Canadian Apheresis Study Group. *N Engl J Med*. 1991;325(6):393–397.
7. Loirat C, Coppo P, Veyradier A. Thrombotic thrombocytopenic purpura in children. *Curr Opin Pediatr*. 2013;25(2):216–224.
8. Furlan M, Robles R, Morselli B, Sandoz P, Lammle B. Recovery and half-life of von Willebrand factor-cleaving protease after plasma therapy in patients with thrombotic thrombocytopenic purpura. *Thromb Haemost*. 1999;81(1):8–13.
9. Lotta LA, Wu HM, Mackie IJ, et al. Residual plasmatic activity of ADAMTS13 is correlated with phenotype severity in congenital thrombotic thrombocytopenic purpura. *Blood*. 2012;120(2):440–448.
10. Barbot J, Costa E, Guerra M, et al. Ten years of prophylactic treatment with fresh-frozen plasma in a child with chronic relapsing thrombotic thrombocytopenic purpura as a result of a congenital deficiency of von Willebrand factor-cleaving protease. *Br J Haematol*. 2001;113(3):649–651.
11. Mansouri Taleghani M, Krogh von A-S, Fujimura Y, et al. Hereditary thrombotic thrombocytopenic purpura and the hereditary TTP registry. *Hamostaseologie*. 2013;33(2):138–143.
12. Deford CC, Reese JA, Schwartz LH, et al. Multiple major morbidities and increased mortality during long-term follow-up after recovery from thrombotic

thrombocytopenic purpura. *Blood*. 2013;122(12):2023–2029.

13. Han B, Page EE, Stewart LM, et al. Depression and cognitive impairment following recovery from thrombotic thrombocytopenic purpura. *Am J Hematol*. 2015;90(8):709–714.
14. Nathwani AC, Reiss UM, Tuddenham EGD, et al. Long-term safety and efficacy of factor IX gene therapy in hemophilia B. *N Engl J Med*. 2014;371(21):1994–2004.
15. Bainbridge JWB, Mehat MS, Sundaram V, et al. Long-term effect of gene therapy on Leber's congenital amaurosis. *N Engl J Med*. 2015;372(20):1887–1897.
16. Hacein-Bey-Abina S, Pai S-Y, Gaspar HB, et al. A modified gamma-retrovirus vector for X-linked severe combined immunodeficiency. *N Engl J Med*. 2014;371(15):1407–1417.
17. Biffi A, Montini E, Lorioli L, et al. Lentiviral hematopoietic stem cell gene therapy benefits metachromatic leukodystrophy. *Science*. 2013;341(6148):1233158.
18. Jin S-Y, Xiao J, Zhou S, Wright JF, Zheng XL. AAV-mediated expression of an ADAMTS13 variant prevents shigatoxin-induced thrombotic thrombocytopenic purpura. *Blood*. 2013;121(19):3825–3829.
19. Ivics Z, Hackett PB, Plasterk RH, Izsvak Z. Molecular reconstruction of Sleeping Beauty, a Tc1-like transposon from fish, and its transposition in human cells. *Cell*. 1997;91(4):501–510.
20. Mates L, Chuah MKL, Belay E, et al. Molecular evolution of a novel hyperactive Sleeping Beauty transposase enables robust stable gene transfer in vertebrates. *Nat Genet*. 2009;41(6):753–761.
21. Yant SR, Meuse L, Chiu W, et al. Somatic integration and long-term transgene expression in normal and haemophilic mice using a DNA transposon system. *Nat Genet*. 2000;25(1):35–41.
22. Ohlfest JR, Frandsen JL, Fritz S, et al. Phenotypic correction and long-term expression of factor VIII in hemophilic mice by immunotolerization and nonviral gene transfer using the Sleeping Beauty transposon system. *Blood*. 2005;105(7):2691–2698.
23. Aronovich EL, Bell JB, Belur LR, et al. Prolonged expression of a lysosomal enzyme in mouse liver after Sleeping Beauty transposon-mediated gene delivery: implications for non-viral gene therapy of mucopolysaccharidoses. *J Gene Med*. 2007;9(5):403–415.
24. Aronovich EL, Bell JB, Khan SA, et al. Systemic correction of storage disease in MPS I NOD/SCID mice using the sleeping beauty transposon system. *Mol Ther*.

2009;17(7):1136–1144.

25. De Cock E, Hermans C, De Raeymaecker J, et al. The novel ADAMTS13-p.D187H mutation impairs ADAMTS13 activity and secretion and contributes to thrombotic thrombocytopenic purpura in mice. *J Thromb Haemost*. 2015;13(2):283–292.
26. Motto DG, Chauhan AK, Zhu G, et al. Shigatoxin triggers thrombotic thrombocytopenic purpura in genetically susceptible ADAMTS13-deficient mice. *J Clin Invest*. 2005;115(10):2752–2761.
27. Liu F, Song Y, Liu D. Hydrodynamics-based transfection in animals by systemic administration of plasmid DNA. *Gene Ther*. 1999;6(7):1258–1266.
28. Zhang G, Budker V, Wolff JA. High levels of foreign gene expression in hepatocytes after tail vein injections of naked plasmid DNA. *Hum Gene Ther*. 1999;10(10):1735–1737.
29. De Meyer SF, Vandeputte N, Pareyn I, et al. Restoration of plasma von Willebrand factor deficiency is sufficient to correct thrombus formation after gene therapy for severe von Willebrand disease. *Arterioscler Thromb Vasc Biol*. 2008;28(9):1621–1626.
30. Schiviz A, Wuersch K, Piskernik C, et al. A new mouse model mimicking thrombotic thrombocytopenic purpura: correction of symptoms by recombinant human ADAMTS13. *Blood*. 2012;119(25):6128–6135.
31. Haberichter SL. von Willebrand factor propeptide: biology and clinical utility. *Blood*. 2015;126(15):1753–1761.
32. Miao CH, Ye X, Thompson AR. High-level factor VIII gene expression in vivo achieved by nonviral liver-specific gene therapy vectors. *Hum Gene Ther*. 2003;14(14):1297–1305.
33. Banno F, Kokame K, Okuda T, et al. Complete deficiency in ADAMTS13 is prothrombotic, but it alone is not sufficient to cause thrombotic thrombocytopenic purpura. *Blood*. 2006;107(8):3161–3166.
34. Peng B, Ye P, Rawlings DJ, Ochs HD, Miao CH. Anti-CD3 antibodies modulate anti-factor VIII immune responses in hemophilia A mice after factor VIII plasmid-mediated gene therapy. *Blood*. 2009;114(20):4373–4382.
35. Aronovich EL, Hall BC, Bell JB, McIvor RS, Hackett PB. Quantitative analysis of alpha-L-iduronidase expression in immunocompetent mice treated with the Sleeping Beauty transposon system. *PLoS ONE*. 2013;8(10):e78161.
36. Furlan M, Lammle B. Aetiology and pathogenesis of thrombotic thrombocytopenic

purpura and haemolytic uraemic syndrome: the role of von Willebrand factor-cleaving protease. *Best Pract Res Clin Haematol*. 2001;14(2):437–454.

37. Narayanavari SA, Chilkunda SS, Ivics Z, Izsvak Z. Sleeping Beauty transposition: from biology to applications. *Crit Rev Biochem Mol Biol*. 2016;1–27.
38. Kebriaei P, Singh H, Huls MH, et al. Phase I trials using Sleeping Beauty to generate CD19-specific CAR T cells. *J Clin Invest*. 2016;126(9):3363–3376.
39. Kamimura K, Yokoo T, Abe H, et al. Image-guided hydrodynamic gene delivery: Current status and future directions. *Pharmaceutics*. 2015;7(3):213–223.
40. Yant SR, Wu X, Huang Y, et al. High-resolution genome-wide mapping of transposon integration in mammals. *Mol Cell Biol*. 2005;25(6):2085–2094.
41. Hackett CS, Geurts AM, Hackett PB. Predicting preferential DNA vector insertion sites: implications for functional genomics and gene therapy. *Genome Biol*. 2007;8 Suppl 1:S12.
42. Gogol-Doring A, Ammar I, Gupta S, et al. Genome-wide profiling reveals remarkable parallels between insertion site selection properties of the MLV retrovirus and the piggyBac transposon in primary human CD4(+) T cells. *Mol Ther*. 2016;24(3):592–606.
43. Yant SR, Huang Y, Akache B, Kay MA. Site-directed transposon integration in human cells. *Nucleic Acids Res*. 2007;35(7):e50.
44. Voigt K, Gogol-Doring A, Miskey C, et al. Retargeting sleeping beauty transposon insertions by engineered zinc finger DNA-binding domains. *Mol Ther*. 2012;20(10):1852–1862.

CHAPTER 4

THE ROLE OF THE VON WILLEBRAND FACTOR/ADAMTS13 AXIS IN A MURINE MALARIA-ASSOCIATED LUNG PATHOLOGY MODEL

Sebastien Verhenne[1], Sirima Kraisin[1], Thy Pham[2], Nele Vandeputte[1], Inge Pareyn[1], Philippe Van den Steen[2], Hans Deckmyn[1], Karen Vanhoorelbeke[1], and Simon F. De Meyer[1]

[1]Laboratory for Thrombosis Research, IRF Life Sciences, KU Leuven Campus Kulak Kortrijk, Kortrijk, Belgium; [2]Laboratory of Immunobiology, Rega Institute for Medical Research, KU Leuven, Leuven, Belgium

4.1. ABSTRACT

Malaria is a major cause of cause of morbidity and mortality in the developing world. Malaria-associated acute respiratory distress syndrome (MA-ARDS) is a common complication of malaria, with a mortality rate of up to 80%. Recent clinical studies have demonstrated that severe malaria infection is associated with high von Willebrand factor (VWF) and low ADAMTS13 activity levels. Whether this prothrombotic state constitutes an epiphenomenon, or whether this plays an active role in the pathophysiology of MA-ARDS is currently unknown. To address this issue, we used an established murine model of MA-ARDS, in which C57BL/6J mice are infected with *Plasmodium (P.) berghei* NK65 parasites. Plasma VWF levels in infected wild-type (WT) mice significantly increased early after infection, but normalized afterwards. During the course of infection, VWF multimer patterns remained normal until end stage disease at which a marked decrease in high molecular weight VWF multimers was observed. This was accompanied by a significant reduction of the ADAMTS13 activity/antigen ratio and severe thrombocytopenia. To determine the direct role of VWF in MA-ARDS pathogenesis, we investigated *P. berghei* NK65 infection in VWF knockout ($Vwf^{-/-}$) mice. Similar to WT mice, thrombocytopenia was also observed in the absence of VWF indicating that VWF does not contribute to malaria-associated thrombocytopenia. Overall mouse survival times were slightly but significantly shortened in $Vwf^{-/-}$ mice. $Vwf^{-/-}$ mice showed an increased number of infected red blood cells but reduced lung pathology compared to WT mice. Further studies are needed to unravel the biological mechanisms by which VWF might influence peripheral blood parasitemia levels and the development of lung pathology in MA-ARDS.

4.2. INTRODUCTION

Malaria remains a major global health burden with an estimated number of 214 million clinical cases and 438 000 deaths in 2015, of which most are caused by *Plasmodium falciparum* (World Malaria Report 2015, World Health Organization). The pathophysiological mechanisms of life-threatening *P. falciparum*-associated complications are multifactorial involving mechanical obstruction of organ microvasculature by sequestered *P. falciparum*-infected erythrocytes[1,2] and the initiation of atypical inflammatory cascades in target organs[3,4]. Despite the availability of anti-malarial drugs, the lethality rate associated with severe complications remains high. Besides malarial anemia and cerebral malaria, malaria-associated acute respiratory distress syndrome (MA-ARDS) is a common complication with a mortality rate of up to 80%.[5] All five malaria species able to infect humans have been reported to cause MA-ARDS, although clear differences exist between different species.[6] MA-ARDS is often observed in association with other complications but also occurs as a single manifestation of otherwise uncomplicated malaria. No treatment is currently available and very little is known about its pathogenesis. Hence, better understanding of the mechanisms that mediate MA-ARDS will be crucial to develop novel treatment strategies for this often-lethal complication. Both thrombotic and inflammatory processes are known to be involved in malaria pathology and in recent years, the thrombo-inflammatory molecule von Willebrand factor (VWF) has gained increased attention.[7]

VWF is an adhesive multimeric glycoprotein that is synthesized by endothelial cells (ECs) and megakaryocytes. VWF is best known for its crucial role in primary hemostasis, where it participates in the adhesion of platelets to sites of vascular injury and the protection of clotting factor VIII against premature degradation in circulation. The hemostatic efficacy of VWF is determined by its multimeric composition, with ultra large (UL-) VWF multimers being the most active forms, capable of spontaneously binding, activating, and aggregating platelets.[8] In ECs, these highly adhesive VWF multimers are stored within specific endothelial storage sites, called Weibel-Palade bodies (WPBs), from where they are released into the circulation upon EC activation. A number of case-control studies carried out in children and adults with naturally acquired *P. falciparum* infection have demonstrated that human malaria infection is associated with acute EC activation and WPB exocytosis resulting in elevated concentrations of plasma VWF[9-13] and pathological accumulation of UL-VWF multimers[11,14,15]. In normal conditions, the VWF multimer size, and therefore VWF platelet-binding potential, is regulated by the VWF-cleaving protease, ADAMTS13, which degrades

UL-VWF multimers in smaller, less thrombogenic forms before entering circulation.[16] In malaria, however, ADAMTS13 activity is markedly reduced.[11,14,17,18] Furthermore, in vitro studies have shown that released UL-VWF multimers can form platelet-decorated VWF strings that are able to bind multiple *P. falciparum*-infected red blood cells.[19] All together, these data suggest that a dysregulated VWF balance, i.e. high VWF and low ADAMTS13 activity, may play a direct role in the underlying pathophysiology of malaria-associated syndromes.

So far, nothing is known on the potential involvement of the VWF/ADAMTS13 axis in MA-ARDS. The goal of this study therefore was to elucidate the role of VWF and ADAMTS13 in severe malaria pathogenesis using a murine model of malaria-associated lung pathology.[20]

4.3. METHODS

4.3.1. Mice

Five to 8-week old male and female wild-type (WT) and VWF knockout (*Vwf*$^{-/-}$)[21] mice on a C57BL/6J background were bred and maintained in a conventional animal facility with water and food *ad libitum*. To ensure optimal parasite growth, drinking water was supplemented with 0.375 mg/ml 4-amino-benzoic acid (Sigma-Aldrich, Bornem, Belgium). Experimental groups were weight- and age-matched for each experiment. All animal experiments were performed in accordance with protocols approved by the Institutional Animal Care and Use Committee of the KU Leuven (License LA1300114, project number P173/2015, KU Leuven Belgium).

4.3.2. Parasites

Mice were inoculated with 10^4 *P. berghei* NK65 parasites via intraperitoneal injection.[20] Infected mice were monitored daily for the progression of malaria-associated lung pathology. Clinical parameters comprised loss in body weight, piloerection, spontaneous activity, body tone, limb grasping, and abnormal breathing. Mice suffering from severe disease were defined as 'end-stage' and sacrificed by cervical dislocation according to the ethical guidelines.

4.3.3. Determination of parasitemia

Peripheral blood parasitemia levels were monitored by examination of blood smears. A droplet of blood was collected from the tail tip and smeared on glass slides. After fixation in methanol, blood smears were stained with 10% Giemsa solution (Giemsa's stain R66 solution Gurr®; VWR International, Lutterworth, UK) for 15-20 minutes. After washing and air-drying, parasitemia was estimated by calculating the percentage of infected red blood cells after counting a minimum of 800 red blood cells.

4.3.4. Blood collection

Animals were anesthetized using 5% isoflurane (Nicholas Piramal Limited, London, UK) in 100% O_2. Blood was collected by retro-orbital puncture on 0.5M EDTA (1 volume to 40 volumes of blood) or 3.8% trisodium citrate (1 volume to 6 volumes of blood). EDTA-treated blood was used to determine whole blood counts using the Hemavet 950FS Multi-species

Hematology system (Drew Scientific, Oxford, CT). Platelet-poor plasma (PPP) was prepared from citrated blood by centrifugation at 4300 g for 6 minutes at room temperature (RT), aliquoted, and stored at -80°C for further analysis.

4.3.5. Determination of plasma VWF and ADAMTS13 levels

VWF and ADAMTS13 antigen levels in plasma were determined using in-house developed enzyme-linked immunosorbent assays (ELISAs). Plasma VWF or ADAMTS13 was captured by either polyclonal anti-human VWF antibodies (1/1000 in phosphate buffered saline (PBS); Dako, Glostrup, Denmark) or the anti-mouse ADAMTS13 monoclonal antibody 14H7B8 (5 μg/ml in PBS) immobilized on a 96-well microtiter plate, respectively. After blocking the wells with 3% skimmed milk in PBS, plasma samples were applied at 1:20 to 1:1480 dilutions. Captured VWF from plasma was detected using a mixture of in-house generated biotinylated anti-murine VWF monoclonal antibodies (15H2 and 2C12; 1 μg/ml in PBS containing 0.3% skimmed milk) followed by incubation with horseradish peroxidase (HRP)-labeled streptavidin (Roche, Mannheim, Germany). In the ADAMTS13 assay, bound ADAMTS13 was detected after addition of in-house generated polyclonal rabbit anti-mouse ADAMTS13 antibodies (5 μg/ml in PBS containing 0.3% skimmed milk) followed by incubation with polyclonal goat anti-rabbit antibodies labeled with HRP (1/10,000 in PBS containing 0.3% skimmed milk; Jackson ImmunoResearch Laboratories Inc., West Grove, PA). Washing steps with PBS + 0.1% Tween20 were performed between each step. The coloring reaction was initiated by addition of ortho-phenylenediamine (Sigma-Aldrich, St Louis, MO) and H_2O_2, and stopped with 4 M H_2SO_4. The absorbance was determined at 490 nm using a FLUOstar OPTIMA ELISA reader (BMG Labtech GmbH, Offenburg, Germany). Plasma VWF and ADAMTS13 levels in infected mice were expressed as percentages of baseline levels that were determined in plasma collected 2 weeks before infection.

4.3.6. Determination of plasma ADAMTS13 activity

The proteolytic activity of ADAMTS13 was determined by fluorescent resonance energy transfer using a short fluorogenic 73 amino acid VWF peptide (FRETS-VWF73; Peptides International, Louisville, KY), as decribed previously.[22] Briefly, plasma was incubated at 37°C with 2 μM FRETS-VWF73 substrate in a HEPES-buffered saline solution (50 mM HEPES, 5 mM $CaCl_2$, 1 mM $ZnCl_2$, 150 mM NaCl; pH 7.4) containing 1 mg/ml bovine serum albumin (Sigma). Digestion of the FRETS-VWF73 substrate generated a fluorescent

signal that was measured using the FLUOstar OPTIMA ELISA reader during 40 cycli of 300 seconds using excitation at 355 nm and emission at 460 nm. Fluorescence intensities were depicted in function of time and the slope of the resulting curve was used as a measure for activity. Plasma ADAMTS13 activity levels in infected mice were expressed as percentages of baseline levels observed in plasma from 2 weeks before infection.

4.3.7. In vivo inhibition of ADAMTS13

ADAMTS13 activity in WT mice was inhibited by retro-orbital injection of a mixture of in-house developed inhibitory monoclonal anti-mouse ADAMTS13 inhibitory antibodies, 13B4 and 14H7 (1.25 mg/kg of each).[23] Injection of a non-functional anti-mouse ADAMTS13 monoclonal antibody, 20A10 (2.5 mg/kg), was used as a negative control.

4.3.8. Plasma VWF multimer analysis

Plasma samples were diluted in sample buffer (8 M urea, 5% (m/v) sodium dodecyl sulphate (SDS), 10 mM Tris, 1 mM EDTA, and 0.3% bromophenol blue; pH 8.0) and denatured at 60°C for 30 minutes. The denatured VWF was fractionated on a low-resolution (1.2%) SDS isoelectric focusing agarose gel (GE Healthcare Europe GmbH, Diegem, Belgium), fixed on a GelBond® film (Lonza, San Diego, CA), by electrophoresis at 10-15mA in a multiphor II apparatus (GE Healthcare). Following electrophoresis, the gel was rinsed in distilled water, air-dried, and blocked in 5% skimmed milk in tris buffered saline (TBS) solution containing 0.05% Tween20 (TBST). After overnight incubation with alkaline phosphatase-conjugated polyclonal anti-human VWF antibodies (1/750 diluted in TBS; Dako) and subsequent rinsing with TBST, VWF multimers were visualized using an Alkaline Phosphate conjugate substrate kit (BioRad, Hercules, CA). To quantify differences in the VWF multimer composition, densitometric analysis of each VWF multimer pattern was performed using Image J software (version 1.47, National Institute of Health, Bethesda, MD). Distinguishable bands were divided into 3 subclasses: (1) 1-5 dimers were designated as low molecular weight VWF multimers (LMW), (2) 6-10 dimers as medium molecular weight VWF multimers (MMW), and (3) >10-dimers as high molecular weight VWF multimers (HMW; including UL-VWF multimers). The total density of each subclass was divided by the total density of all multimer bands to calculate the relative abundance of each subclass. The relative amount of LMW, MMW, and HMW VWF multimers in infected mice were expressed as percentages of baseline levels observed in plasma 2 weeks before infection.

4.3.9. Broncho-alveolar lavage

To obtain broncho-alveolar lavage (BAL) fluid, mice were anesthetized by intraperitoneal injection of pentobarbital (60 mg/ml; Nembutal®, Ceva Santé Animale, Brussels, Belgium). Broncho-alveolar lavages were performed by intratracheal instillation of 0.75 mL PBS in both lungs for 30 seconds after which the PBS was slowly withdrawn. This procedure was performed twice and both lavages were combined. BAL fluid samples were centrifuged at 335 g for 10 minutes at 4°C. Protein concentrations in supernatants were determined using a Bradford assay (BioRad, Hercules, CA) according to the manufacturer's protocol.

4.3.10. Statistical analysis

Data are represented as mean ± SEM. For statistical analysis, the Prism Version 6.0 software (GraphPad Software, La Jolla, CA) was used. One-way analysis of variance followed by Dunnett's multiple comparisons post hoc test was conducted to assess the variance of VWF levels, ADAMTS13 activity levels, and the relative amounts of HMW multimers between plasma samples before (pre) and at different time points during infection. Paired t testing was used to assess differences in ADAMTS13 levels and the ratio of ADAMTS13 activity to antigen between plasma samples before infection (pre) and at end-stage disease (end). Unpaired t testing was used to compare protein levels in BAL fluid of infected or non-infected WT and *Vwf*$^{-/-}$ mice. A log-rank test was used to determine differences between Kaplan-Meier survival curves. Values of $P < 0.05$ were considered as statistically significant.

4.4. RESULTS

4.4.1. Effect of *P. berghei* NK65 infection on circulating VWF and ADAMTS13 levels

Observational studies in malaria patients showed increased levels of VWF and decreased ADAMTS13 activities.[11,14,17,18] How and when exactly parasite infection influences these parameters is however not well understood. We therefore used an established murine model of MA-ARDS, in which C57BL/6J mice are infected with *P. berghei* NK65.[20,24] VWF antigen levels in plasma of *P. berghei* NK65-infected C57BL/6J mice doubled 3 days after infection (pre: 100 ± 4.1% versus day 3: 200.2 ± 7.1%; $P < 0.0001$) and remained increased during the development of malaria pathology (Figure 1A). At the end stage of the disease (day 8 or 9 after infection), however, VWF levels were again normalized. Remarkably, the early increase of VWF antigen occurred before a noticeable rise in peripheral blood parasitemia levels (Figure 1B), suggesting that *P. berghei* NK65 infection is associated with early EC activation. In non-infected control mice, VWF antigen levels remained within normal range (Figure 1A). Mean plasma ADAMTS13 activity levels stayed within the normal range during the initial course of infection, but markedly decreased from day 7 after infection (pre: 100 ± 7% versus day 7: 57.2 ± 6.3%; $P < 0.01$) (Figure 1C). No significant changes were observed in plasma of non-infected mice (Figure 1C). Interestingly, the decrease in ADAMTS13 activity in *P. berghei* NK65-infected mice near end-stage disease could not be attributed to reduced antigen levels, as ADAMTS13 antigen remained normal (Figure 1D) resulting in a significant reduction of the ADAMTS13 activity over antigen ratio (Figure 1E). These data suggest that *P. berghei* NK65-mediated MA-ARDS is associated with a significant reduction of ADAMTS13 activity during the later stages of disease.

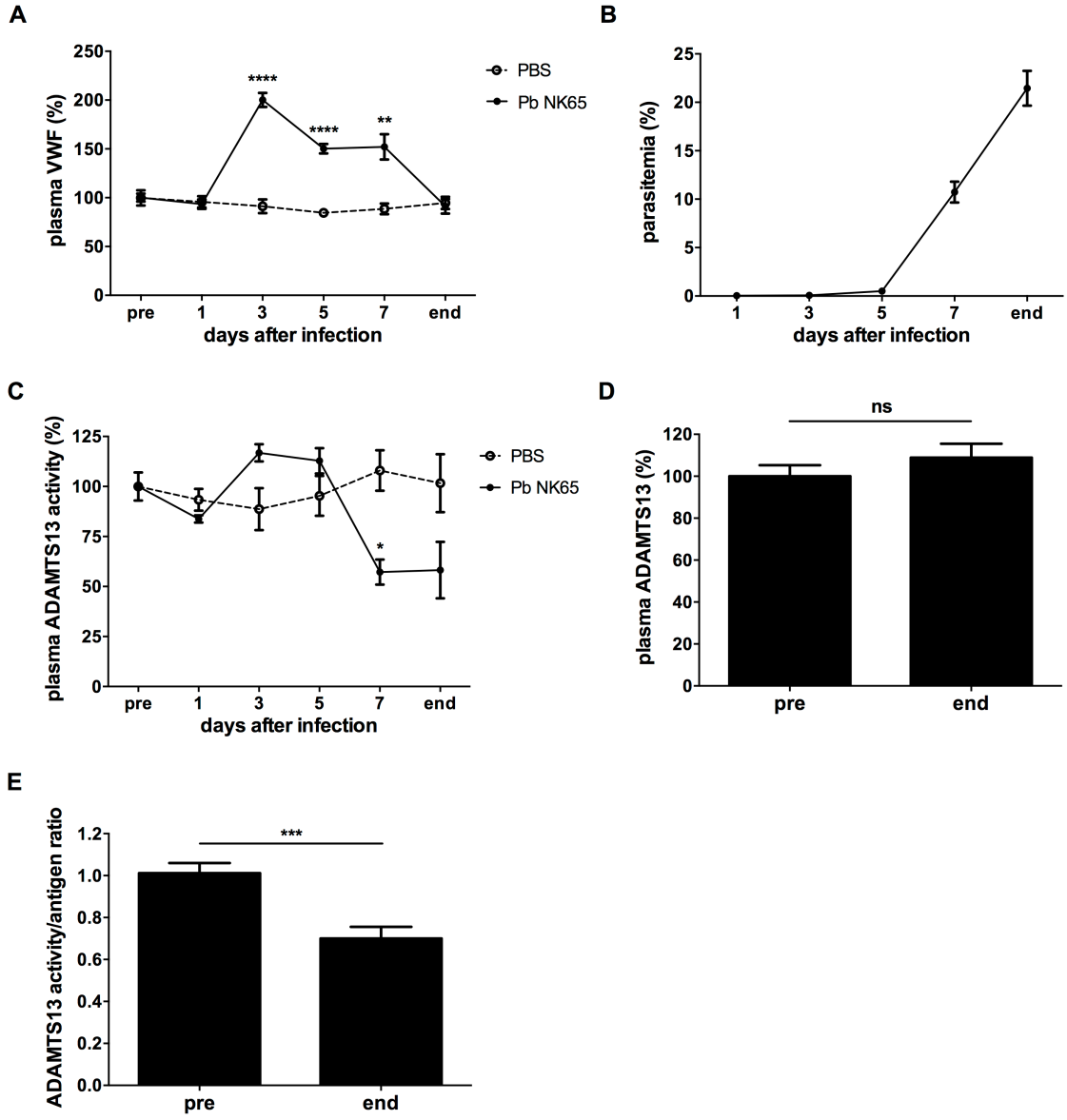

Figure 1: Early increase in plasma VWF levels and late stage reduction in ADAMTS13 activity in MA-ARDS. C57BL/6J mice were injected with 10^4 *P. berghei* NK65 parasites (infected mice; solid line) or PBS (non-infected mice; dashed line). Blood samples were collected 2 weeks before infection (pre) and at indicated time points after infection. The final blood sample was withdrawn at end-stage disease (end), i.e. when mice were considered moribund (day 8 or 9 after infection). (A) Plasma VWF levels in infected (n = 12) and non-infected (n = 7) mice were measured by ELISA (n = 12). (B) Peripheral blood parasitemia levels in infected mice (n = 12) were determined from Giemsa-stained blood smears. (C) Plasma ADAMTS13 activity levels in infected (n = 5) and non-infected (n = 3) mice were measured using a FRETS-VWF73 assay. (D) Plasma ADAMTS13 antigen levels in infected mice (n = 6) were determined via ELISA at indicated time points. (E) Ratio of ADAMTS13 activity to antigen in infected mice (n = 6) at indicated time points. Ns, not significant; *, $P < 0.05$; **, $P < 0.01$; ***, $P < 0.001$; ****, $P < 0.0001$.

4.4.2. Murine MA-ARDS is associated with loss of HMW VWF multimers

Patient studies have reported that severe *P. falciparum* infection is associated with accumulation of abnormally HMW VWF multimers.[11,14] We therefore analyzed the multimer distribution of plasma VWF at different time points after infection by *P. berghei* NK65 (Figure 2). Prior to end-stage disease, VWF multimer patterns were (near-) normal (Figure 2A-B). At end-stage disease, however, multimer distribution appeared abnormal, with a severe reduction in the relative amount of HMW VWF multimers (pre: 46.6 ± 1.7% vs end: 19.8 ± 2.3%; $P < 0.0001$; Figure 2A-B).

VWF multimer size is controlled through continuous proteolysis by ADAMTS13, and a decreased average size of plasma VWF multimers has been associated with an increased susceptibility of VWF for ADAMTS13-mediated cleavage.[25] To investigate whether increased ADAMTS13-mediated proteolysis caused the loss of HMW VWF multimers at end-stage disease, we blocked endogenous ADAMTS13 activity in *P. berghei* NK65-infected mice. Inhibitory anti-ADAMTS13 antibodies were administered at day 5 after infection, prior to the observed drop in HMW VWF multimers. Injection of these inhibitory antibodies results in complete inhibition of plasma ADAMTS13 activity for up to 7 days.[23] Administration of a non-inhibitory monoclonal anti-ADAMTS13 antibody was used as control. Full inhibition of the proteolytic activity of plasma ADAMTS13 was indeed observed at day 7 after infection and end-stage disease, whereas in the group receiving non-inhibitory monoclonal anti-ADAMTS13 antibodies, ADAMTS13 activity was not affected (data not shown). Interestingly, we still found a severe reduction in the number of HMW VWF multimers in plasma of moribund mice with inhibited ADAMTS13 activity (pre: 41.4 ± 2.0% versus end: 23.1 ± 2.8%; $P < 0.05$) (Figure 2C). This reduction was similar to the reduction observed in the control group (Figure 2C), indicating that loss of HMW VWF multimers was not attributable to an increased degradation by ADAMTS13. These data clearly demonstrate that infection of C57BL/6 mice with *P. berghei* NK65 parasites is not associated with a pathological accumulation of abnormal HMW VWF multimers, but instead is characterized by a pronounced loss of HMW VWF multimers at end-stage disease, which is in contrast with human findings.

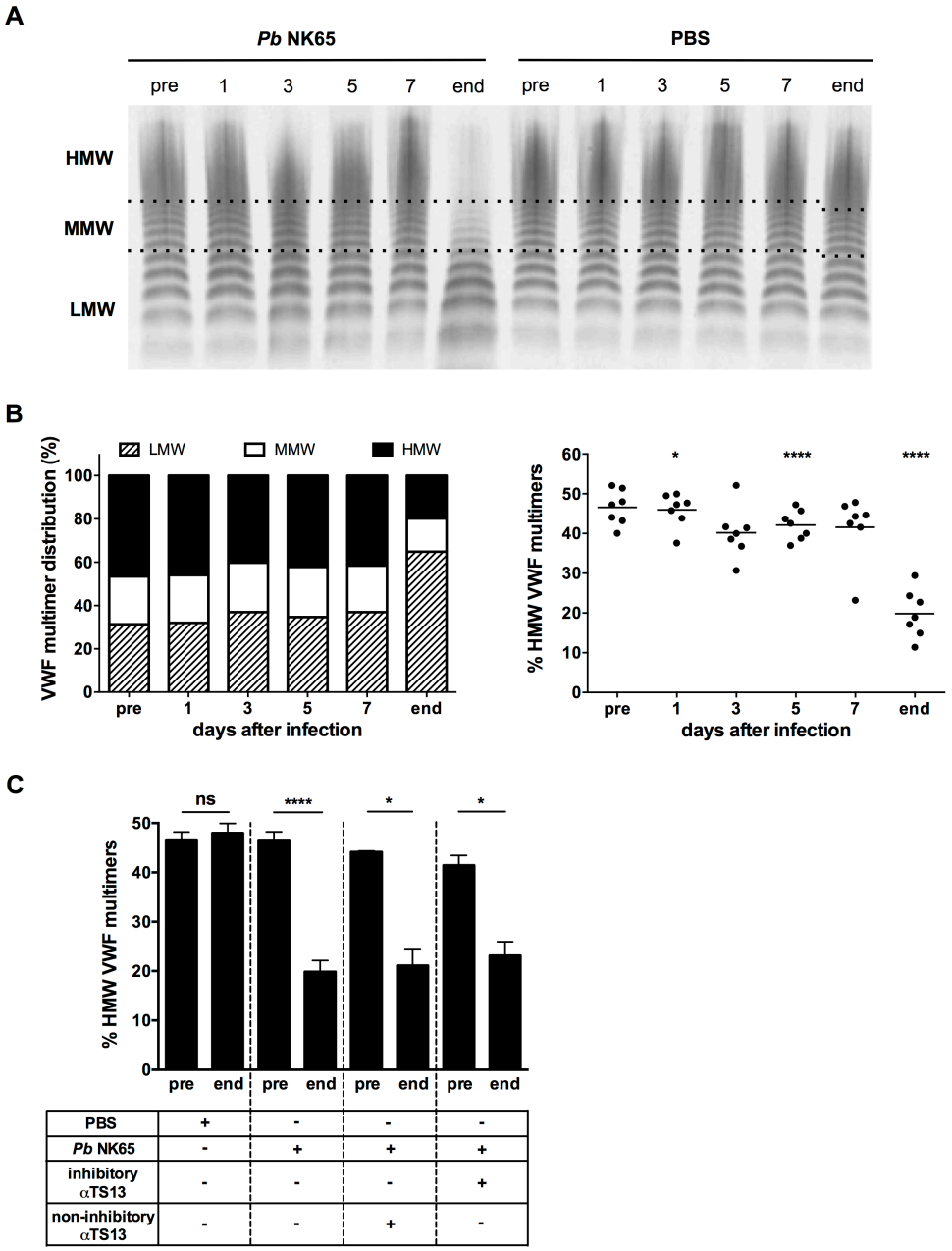

Figure 2: Loss of HMW VWF multimers during end-stage *P. berghei* NK65 infection. C57BL/6J mice were injected with 10^4 *P. berghei* NK65 parasites (infected mice; n = 7) or PBS (non-infected mice; n = 4). Blood samples were collected 2 weeks before infection (pre), at indicated time points during infection, and at end-stage disease (day 8 or 9 after infection; end). Multimer composition of circulating plasma VWF was analyzed via 1.2% agarose gel electrophoresis and densitometry. (A) Representative VWF multimer patterns from infected and non-infected mice. Distinguishable bands were divided into 3 subclasses: 1-5 dimers were designated as low molecular weight (LMW) VWF multimers, 6-10 dimers as medium molecular weight (MMW) VWF multimers, and >10-dimers as high molecular weight (HMW) VWF multimers, including the ultra large VWF portion. (B) VWF multimer distribution (left) and the relative abundance of HMW VWF multimers (right) during the course of infection. (C) Effect of ADAMTS13 inhibition on VWF multimer composition during end-

stage *P. berghei* NK65 infection. Activity of ADAMTS13 in infected mice was inhibited via intravenous administration of inhibitory anti-ADAMTS13 antibodies at day 5 after infection (n = 4). Infected mice treated with non-inhibitory anti-ADAMTS13 antibodies were used as a negative control (n = 3). Paired t-testing was used to assess differences the relative abundance of HMW VWF multimers between plasma samples before infection (pre) and plasma samples at end-stage disease (end). Ns, not significant *, P < 0.05; ****, P < 0.0001.

4.4.3. VWF deficiency influences the course of *P. berghei* NK65 infection

Several patient studies have suggested that elevated levels of VWF inversely correlate with clinical outcome, making VWF an informative biomarker of malarial disease severity.[12,15,26,27] Increasing evidence, however, points towards a direct role of VWF in malaria pathogenesis, where for example, VWF is thought to facilitate adhesion of *P. falciparum*-infected red blood cells to endothelial cells in microvascular beds of various organs.[19] To investigate whether VWF plays a direct role in MA-ARDS pathogenesis in mice, we studied *P. berghei* NK65 infection in *Vwf*$^{-/-}$ mice compared with WT mice. Median survival time in *Vwf*$^{-/-}$ mice (9 days) was slightly but significantly shorter than in WT mice (10 days, P < 0.05) (Figure 3A). Whereas 75% of *Vwf*$^{-/-}$ mice died within the first 9 days, only 30% of WT mice had died in the same period. Interestingly, we found that the overall course of peripheral blood parasitemia levels was significantly different between WT and *Vwf*$^{-/-}$ mice starting from day 6 after infection, with parasitemia levels being significantly higher in *Vwf*$^{-/-}$ mice (Figure 3B).

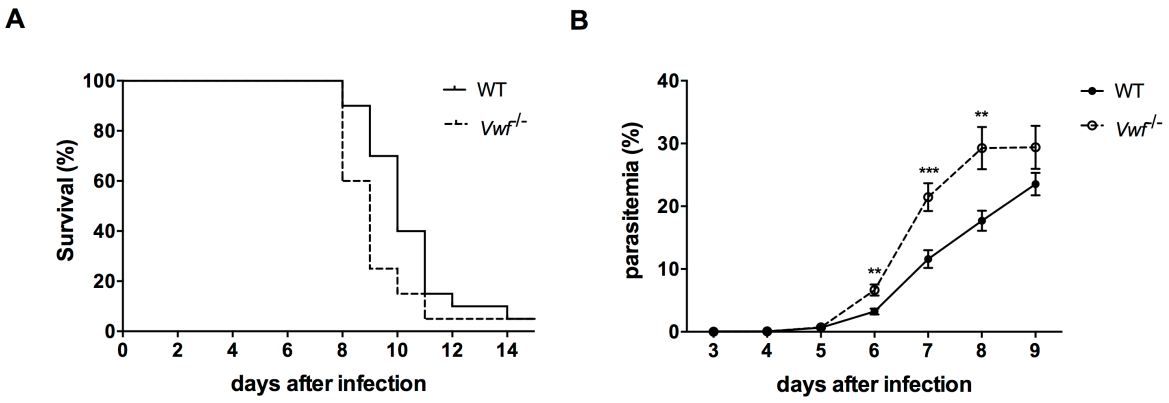

Figure 3: Lack of VWF alters the course of *P. berghei* NK65 infection. WT (n = 20; solid line) and *Vwf*$^{-/-}$ (n = 20; dashed line) mice on a C57BL/6J background were inoculated with 10^4 *P. berghei* NK65 parasites. (A) Survival and (B) peripheral blood parasitemia levels were monitored daily. **, P < 0.01; ***, P < 0.001.

Infection of WT C57BL/6J mice with *P. berghei* NK65 parasites causes pulmonary complications characterized by pulmonary edema, vascular permeabilization, and leukocyte infiltration.[20] To further elucidate the involvement of VWF in MA-ARDS in mice, we investigated pulmonary pathology in *Vwf*$^{-/-}$ mice compared with WT mice following *P. berghei* NK65 infection. We determined protein levels in BAL fluid, which is indicative for edema and alveolar leakage, to measure the extent of lung pathology. At day 8 after infection, protein levels in BAL fluid of WT and *Vwf*$^{-/-}$ mice were significantly elevated compared to non-infected controls (Figure 4A). However, protein concentrations were significantly lower in BAL fluid of *P. berghei* NK65-infected *Vwf*$^{-/-}$ mice compared to infected WT mice (*Vwf*$^{-/-}$: 1.79 ± 0.42 mg/ml versus WT: 3.58 ± 0.48 mg/ml; $P < 0.001$), indicating that edema and alveolar leakage were less pronounced in *Vwf*$^{-/-}$ mice. Altogether, these data demonstrate that lack of VWF in mice reduces pulmonary pathology following *P. berghei* NK65 infection but alters the course of infection by modulating peripheral blood parasitemia levels.

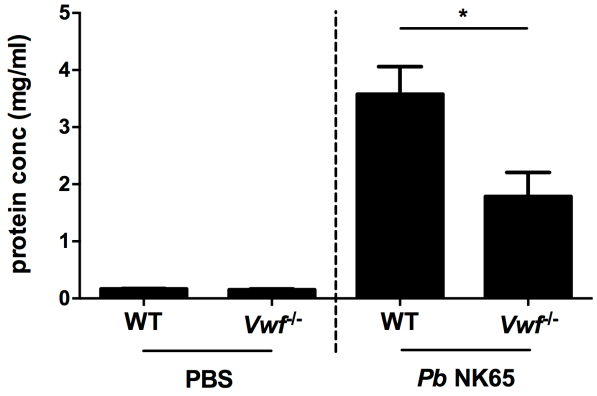

Figure 4: Reduced edema and alveolar leakage in *Vwf*$^{-/-}$ mice following *P. berghei* NK65 infection. WT and *Vwf*$^{-/-}$ mice on a C57BL/6J background were injected with 10^4 *P. berghei* NK65 parasites (infected mice) or PBS (non-infected mice). Broncho-alveolar lavage fluid samples were collected from non-infected WT (n = 5) and *Vwf*$^{-/-}$ (n = 7) mice, and infected WT (n = 13) and *Vwf*$^{-/-}$ (n = 7) mice at day 8 following injection. After centrifugation, protein content of the supernatants was determined using Bradford assay. *, $P < 0.05$

4.4.4. Malaria-related thrombocytopenia in MA-ARDS occurs independent of VWF

Severe thrombocytopenia is a risk factor of adverse clinical outcome in children and adults following *P. falciparum* infection.[28,29] The exact mechanism underlying this phenomenon

remains poorly understood although recent studies suggested that VWF might be implicated in malaria-related thrombocytopenia.[10,30] To test this hypothesis, we measured platelet numbers in WT and *Vwf*$^{-/-}$ mice following *P. berghei* NK65 infection (Figure 5). In WT mice, platelet numbers started to decrease after day 5 post infection, indicating that thrombocytopenia constituted a hallmark also in this murine model. Within the following 2-3 days, mean platelet counts had fallen by approximately 90%, resulting in a profound thrombocytopenia at end-stage disease (Figure 5). Interestingly, a similar reduction in platelet count was observed in *P berghei* NK65-infected *Vwf*$^{-/-}$ mice, demonstrating that VWF does not contribute to malaria-related thrombocytopenia in mice (Figure 5).

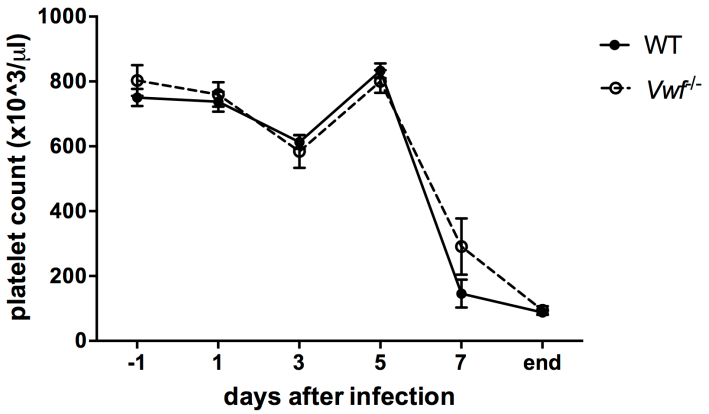

Figure 5: Thrombocytopenia following *P. berghei* NK65 infection is not VWF-mediated. WT (n = 10; solid line) and *Vwf*$^{-/-}$ (n = 7; dashed line) mice were infected with 10^4 *P. berghei* NK65 parasites. Blood was collected one day before injection (day -1) and at indicated time points during infection, until end-stage disease (day 8 or 9 after infection; end). Platelet counts were measured using an automated cell counter.

4.5. DISCUSSION

In this study we wanted to unravel the direct role of VWF in malaria pathogenesis using a murine model for MA-ARDS. C57BL/6 mice infected with *P. berghei NK65* develop severe pulmonary complications, of which the pathophysiological findings are in agreement with human MA-ARDS.[20] Here, we demonstrated that *P. berghei* NK65 infection is associated with elevated plasma VWF levels, which resembles the activated EC phenotype observed in both uncomplicated and complicated human malaria infection.[11,17,18,27] In parallel with human studies, VWF levels increased from a very early stage following infection, at the time that only a small percentage red blood cells were infected, indicating that early EC activation constitutes a hallmark of *P. berghei* NK65.[10] To date, the trigger for this early activation remains unclear. Further studies are needed to define how exposure to malaria parasites modulates EC activation.

VWF released following EC activation and subsequent exocytosis of WPBs consists of highly adhesive HMW VWF multimers that are rapidly cleaved by ADAMTS13 at the endothelial surface under normal conditions.[16] Throughout most of the course of *P. berghei* NK65 infection, ADAMTS13 activity levels were within normal range and capable of properly processing secreted VWF as indicated by the appearance of (near) normal VWF multimer patterns. Near end-stage disease, however, ADAMTS13 activity levels were severely decreased. Surprisingly, the decrease in ADAMTS13 activity was not accompanied by a concomitant accumulation of UL-VWF multimers. Instead, we observed a loss of HMW VWF multimers at end-stage disease. The clinical relevance of this phenomenon remains unclear since these findings differ from severe *P. falciparum* malaria, where reduced ADAMTS13 activity results in the presence of circulating UL-VWF multimers.[11,14] Whether loss of HMW VWF multimers could serve as a potential biomarker for end-stage disease remains to be studied. One potential explanation for the loss of HMW VWF multimers could be enhanced ADAMTS13-mediated cleavage of VWF in the hyperdynamic microcirculatory blood flow environment of *P. berghei* NK65-infected mice. Indeed, exposure of VWF to pathological shear stress can result in increased VWF proteolysis by ADAMTS13 and subsequent loss of HMW VWF multimers.[25] Full inhibition of ADAMTS13 activity prior to the observed drop, however, did not alter the degree of VWF proteolysis indicating that excess VWF cleavage is not caused by ADAMTS13. This, however, does not rule out the possible involvement of other proteolytic enzymes, such as leukocyte-derived proteases[31,32]

and plasmin[33]. In addition to increased VWF proteolysis, other mechanisms, such as increased clearance or consumption of the larger VWF multimers, may explain the abnormal VWF multimer distribution at end-stage disease. Future studies are warranted to shed more light on the mechanisms and clinical relevance of this intruiging phenotype.

Another interesting observation is the reduction of ADAMTS13 activity near end-stage disease, which is in line with the presence of reduced ADAMTS13 activity in patients with severe *P. falciparum* or *P. vivax* malaria.[11,14,17,18] Here, we demonstrated that the reduced ADAMTS13 activity, however, was not caused by a decrease in antigen levels indicating that specific factors may regulate ADAMTS13 function during MA-ARDS. Several factors such as free hemoglobin and inflammatory cytokine interleukin-6 are known to reduce ADAMTS13 activity *in vitro*[34,35]. Although their levels are increased during malaria infection, their absolute concentrations do not approach the concentrations that were reported necessary to inhibit ADAMTS13 activity *in vitro*.[14,17] Nevertheless, by performing mixing studies, Larkin and colleagues demonstrated the presence of an unidentified inhibitor that might explain the severe reduction in ADAMTS13 activity.[14] In the near future mixing studies will be performed to find out whether reduced ADAMTS13 activity in near end-stage *P. berghei* NK65 infection is caused by the presence of an inhibitor.

An increasing body of evidence suggests the direct involvement of high levels of VWF in the underlying pathophysiology of human malaria-associated disease syndromes. Thrombocytopenia is one of the most common hematological alterations in *P. falciparum* and *P. vivax* malaria and has occasionaly been associated with disease severity.[28,36] The mechanism underlying the decrease in platelet count remains to be elucidated, although it is believed to be a multifactorial phenomenon.[37] The pathogenic mechanisms include cell- and antibody-mediated immune mechanisms[38,39], splenic alterations[40], oxidative stress[41], and platelet apoptosis[42]. Recently, independent research groups have demonstrated an inverse correlation between platelet numbers and VWF levels, suggesting that increased VWF levels, and in particular UL-VWF multimers, may be an important inducer of thrombocytopenia in malaria.[10,11,17] In this study, we showed that thrombocytopenia constituted a hallmark of *P. berghei* NK65 infection in C57BL/6 mice, which allowed us to define whether VWF modulates malaria-associated thrombocytopenia. Absence of VWF, however, did not prevent thrombocytopenia as an equally profound decrease in platelet count was observed in *P. berghei* NK65-infected *Vwf*$^{-/-}$ mice. These data clearly suggest that VWF-mediated platelet

adhesion or aggregation is not involved in the multifactorial process underlying malaria-associated platelet clearance in mice.

In addition to clinical findings, *in vitro* experiments suggested that VWF may contribute to the sequestration of *P. falciparum*-infected red blood cells on activated endothelium, thereby promoting microvascular dysfunction in various organs.[19] Whereas one therefore should expect a beneficial effect of the absence of VWF, we demonstrated that median survival times were slightly, but significantly shortened in *P. berghei* NK65-infected *Vwf*$^{-/-}$ mice compared to WT mice. Although we have not yet unravelled the mechanism, we hypothesize that differences in parasite sequestration between both genotypes may explain the difference in survival. Indeed, protein levels in BAL fluid of *Vwf*$^{-/-}$ mice were significantly lower compared to WT mice, indicating less severe lung pathology in *Vwf*$^{-/-}$ mice. In addition, we observed that peripheral blood parasitemia levels were significantly higher in *Vwf*$^{-/-}$ mice. In the absence of VWF, perhaps fewer numbers of parasites sequester in the pulmonary circulation, which results in less severe lung pathology but increased blood parasitemia levels. Preliminary data demonstrating a higher number of schizont stages in peripheral blood of *Vwf*$^{-/-}$ mice compared to WT mice at day 7 after infection further support this concept (data not shown). Future studies that focus on the parasite sequestration in lungs of *P. berghei* NK65-infected WT and *Vwf*$^{-/-}$ mice will be performed to further investigate this hypothesis.

Recently, O'Regan and colleagues investigated the role of VWF in experimental cerebral malaria, in which C57BL/6 mice were infected with *P. berghei* ANKA.[13] Infection with *P. berghei* ANKA was associated with early EC activation, pathological accumulation of UL-VWF multimers, and thrombocytopenia. Interestingly, they demonstrated that clinical progression was delayed and overall survival was prolonged in *Vwf*$^{-/-}$ mice compared to WT mice.[13] Absence of VWF did not affect platelet counts or peripheral blood parasitemia levels in the *P. berghei* ANKA model.[13] Whereas some observations are in accordance with our findings, others clearly differ. Although the use of different parasite strains may explain the discordant results, these differences indicate that studies using different animal models are useful to better understand the involvement of the VWF/ADAMTS13 axis in malaria-associated syndromes. Such insights could become valuable for the design of potential novel treatment strategies that interfere with VWF activity in malarial disease.[43]

In conclusion, we used a relatively new mouse model of malaria to investigate for the first time the role of VWF and ADAMTS13 in MA-ARDS. Although we observed some

interesting findings, further research is required to elucidate the underlying biological mechanisms and their clinical relevance.

4.6. REFERENCES

1. Dondorp AM, Ince C, Charunwatthana P, et al. Direct in vivo assessment of microcirculatory dysfunction in severe falciparum malaria. *J Infect Dis*. 2008;197(1):79–84.
2. Ponsford MJ, Medana IM, Prapansilp P, et al. Sequestration and microvascular congestion are associated with coma in human cerebral malaria. *J Infect Dis*. 2012;205(4):663–671.
3. Schofield L, Grau GE. Immunological processes in malaria pathogenesis. *Nat Rev Immunol*. 2005;5(9):722–735.
4. Deroost K, Pham T-T, Opdenakker G, Van Den Steen PE. The immunological balance between host and parasite in malaria. *FEMS Microbiol Rev*. 2016;40(2):208–257.
5. Taylor WRJ, White NJ. Malaria and the lung. *Clin Chest Med*. 2002;23(2):457–468.
6. Van Den Steen PE, Deroost K, Deckers J, et al. Pathogenesis of malaria-associated acute respiratory distress syndrome. *Trends Parasitol*. 2013;29(7):346–358.
7. O'Sullivan JM, Preston RJS, O'Regan N, O'Donnell JS. Emerging roles for hemostatic dysfunction in malaria pathogenesis. *Blood*. 2016;127(19):2281–2288.
8. Federici AB, Bader R, Pagani S, et al. Binding of von Willebrand factor to glycoproteins Ib and IIb/IIIa complex: affinity is related to multimeric size. *Br J Haematol*. 1989;73(1):93–99.
9. Hollestelle MJ, Donkor C, Mantey EA, et al. von Willebrand factor propeptide in malaria: evidence of acute endothelial cell activation. *Br J Haematol*. 2006;133(5):562–569.
10. de Mast Q, Groot E, Lenting PJ, et al. Thrombocytopenia and release of activated von Willebrand Factor during early Plasmodium falciparum malaria. *J Infect Dis*. 2007;196(4):622–628.
11. de Mast Q, Groot E, Asih PB, et al. ADAMTS13 deficiency with elevated levels of ultra-large and active von Willebrand factor in P. falciparum and P. vivax malaria. *Am J Trop Med Hyg*. 2009;80(3):492–498.
12. Phiri HT, Bridges DJ, Glover SJ, et al. Elevated plasma von Willebrand factor and propeptide levels in Malawian children with malaria. *PLoS ONE*. 2011;6(11):e25626.
13. O'Regan N, Gegenbauer K, O'Sullivan JM, et al. A novel role for von Willebrand factor in the pathogenesis of experimental cerebral malaria. *Blood*. 2016;127(9):1192–

1201.

14. Larkin D, de Laat B, Jenkins PV, et al. Severe Plasmodium falciparum malaria is associated with circulating ultra-large von Willebrand multimers and ADAMTS13 inhibition. *PLoS Pathog*. 2009;5(3):e1000349.
15. Graham SM, Chen J, Chung DW, et al. Endothelial activation, haemostasis and thrombosis biomarkers in Ugandan children with severe malaria participating in a clinical trial. *Malar J*. 2016;15(1):56.
16. Dong J-F, Moake JL, Nolasco L, et al. ADAMTS-13 rapidly cleaves newly secreted ultralarge von Willebrand factor multimers on the endothelial surface under flowing conditions. *Blood*. 2002;100(12):4033–4039.
17. Lowenberg EC, Charunwatthana P, Cohen S, et al. Severe malaria is associated with a deficiency of von Willebrand factor cleaving protease, ADAMTS13. *Thromb Haemost*. 2010;103(1):181–187.
18. Barber BE, William T, Grigg MJ, et al. Parasite biomass-related inflammation, endothelial activation, microvascular dysfunction and disease severity in vivax malaria. *PLoS Pathog*. 2015;11(1):e1004558.
19. Bridges DJ, Bunn J, Van Mourik JA, et al. Rapid activation of endothelial cells enables Plasmodium falciparum adhesion to platelet-decorated von Willebrand factor strings. *Blood*. 2010;115(7):1472–1474.
20. Van Den Steen PE, Geurts N, Deroost K, et al. Immunopathology and dexamethasone therapy in a new model for malaria-associated acute respiratory distress syndrome. *Am J Resp Crit Care Med*. 2010;9(Suppl 2):I13.
21. Denis C, Methia N, Frenette PS, et al. A mouse model of severe von Willebrand disease: defects in hemostasis and thrombosis. *Proc Natl Acad Sci U S A*. 1998;95(16):9524–9529.
22. De Cock E, Hermans C, De Raeymaecker J, et al. The novel ADAMTS13-p.D187H mutation impairs ADAMTS13 activity and secretion and contributes to thrombotic thrombocytopenic purpura in mice. *J Thromb Haemost*. 2015;13(2):283–292.
23. Deforche L, Tersteeg C, Roose E, et al. Generation of Anti-Murine ADAMTS13 Antibodies and Their Application in a Mouse Model for Acquired Thrombotic Thrombocytopenic Purpura. *PLoS ONE*. 2016;11(8):e0160388.
24. Deroost K, Tyberghein A, Lays N, et al. Hemozoin induces lung inflammation and correlates with malaria-associated acute respiratory distress syndrome. *Am J Respir Cell Mol Biol*. 2013;48(5):589–600.

25. Tsai H-M. Shear stress and von Willebrand factor in health and disease. *Semin Thromb Hemost*. 2003;29(5):479–488.
26. Conroy AL, Phiri H, Hawkes M, et al. Endothelium-based biomarkers are associated with cerebral malaria in Malawian children: a retrospective case-control study. *PLoS ONE*. 2010;5(12):e15291.
27. Park GS, Ireland KF, Opoka RO, John CC. Evidence of Endothelial Activation in Asymptomatic Plasmodium falciparum Parasitemia and Effect of Blood Group on Levels of von Willebrand Factor in Malaria. *J Pediatric Infect Dis Soc*. 2012;1(1):16–25.
28. Gerardin P, Rogier C, Ka AS, et al. Prognostic value of thrombocytopenia in African children with falciparum malaria. *Am J Trop Med Hyg*. 2002;66(6):686–691.
29. Lampah DA, Yeo TW, Malloy M, et al. Severe malarial thrombocytopenia: a risk factor for mortality in Papua, Indonesia. *J Infect Dis*. 2015;211(4):623–634.
30. de Mast Q, de Groot PG, van Heerde WL, et al. Thrombocytopenia in early malaria is associated with GP1b shedding in absence of systemic platelet activation and consumptive coagulopathy. *Br J Haematol*. 2010;151(5):495–503.
31. Raife TJ, Cao W, Atkinson BS, et al. Leukocyte proteases cleave von Willebrand factor at or near the ADAMTS13 cleavage site. *Blood*. 2009;114(8):1666–1674.
32. Wohner N, Kovacs A, Machovich R, Kolev K. Modulation of the von Willebrand factor-dependent platelet adhesion through alternative proteolytic pathways. *Thromb Res*. 2012;129(4):e41–6.
33. Tersteeg C, de Maat S, De Meyer SF, et al. Plasmin cleavage of von Willebrand factor as an emergency bypass for ADAMTS13 deficiency in thrombotic microangiopathy. *Circulation*. 2014;129(12):1320–1331.
34. Studt J-D, Kremer Hovinga JA, Antoine G, et al. Fatal congenital thrombotic thrombocytopenic purpura with apparent ADAMTS13 inhibitor: in vitro inhibition of ADAMTS13 activity by hemoglobin. *Blood*. 2005;105(2):542–544.
35. Bernardo A, Ball C, Nolasco L, Moake JF, Dong J-F. Effects of inflammatory cytokines on the release and cleavage of the endothelial cell-derived ultralarge von Willebrand factor multimers under flow. *Blood*. 2004;104(1):100–106.
36. Rogier C, Gerardin P, Imbert P. Thrombocytopenia is predictive of lethality in severe childhood falciparum malaria. *Arch Dis Child*. 2004;89(8):795–796.
37. Cox D, McConkey S. The role of platelets in the pathogenesis of cerebral malaria. *Cell Mol Life Sci*. 2010;67(4):557–568.

38. Gramaglia I, Sahlin H, Nolan JP, et al. Cell- rather than antibody-mediated immunity leads to the development of profound thrombocytopenia during experimental Plasmodium berghei malaria. *J Immunol*. 2005;175(11):7699–7707.
39. Coelho HCC, Lopes SCP, Pimentel JPD, et al. Thrombocytopenia in Plasmodium vivax malaria is related to platelets phagocytosis. *PLoS ONE*. 2013;8(5):e63410.
40. Urban BC, Hien TT, Day NP, et al. Fatal Plasmodium falciparum malaria causes specific patterns of splenic architectural disorganization. *Infect Immun*. 2005;73(4):1986–1994.
41. Erel O, Vural H, Aksoy N, Aslan G, Ulukanligil M. Oxidative stress of platelets and thrombocytopenia in patients with vivax malaria. *Clin Biochem*. 2001;34(4):341–344.
42. Piguet PF, Kan CD, Vesin C. Thrombocytopenia in an animal model of malaria is associated with an increased caspase-mediated death of thrombocytes. *Apoptosis*. 2002;7(2):91–98.
43. Miller LH, Ackerman HC, Su X-Z, Wellems TE. Malaria biology and disease pathogenesis: insights for new treatments. *Nat Med*. 2013;19(2):156–167.

GENERAL DISCUSSION & FUTURE PERSPECTIVES

During my PhD thesis we focussed on VWF and/or ADAMTS13 in stroke, TTP and malaria. In this section, we will briefly summarize the results, discuss the implications of our research results and put forward future research lines.

Aim 1: To gain more insight in the relative importance of plasma VWF and platelet-derived VWF in hemostasis and thrombosis.

Endothelial cell- and platelet-derived VWF are products of the same gene but show remarkable biochemical differences which may point towards a significant difference in their role in hemostasis and thrombosis. Although their specific contribution to these processes has been addressed using chimeric pigs, their relative importance remained unclear. In this study, we successfully generated chimeric mice that expressed VWF only in ECs or platelets by performing crossed BMT between WT and *Vwf*$^{-/-}$ mice. Chimeric mice specifically lacking platelet VWF showed normal hemostasis in a tail clip bleeding model and normal carotid artery thrombosis. Chimeric mice with VWF only in platelets were not able to support normal hemostasis and thrombosis. Using a mouse model of transient middle cerebral artery occlusion, however, chimeric mice with only platelet VWF experienced significant cerebral infarction compared to *Vwf*$^{-/-}$ mice, suggesting a clear role for platelet-derived VWF that is specific to ischemic stroke injury.

However, mice are not humans. Therefore, it will be of great interest to study whether our findings can be translated to the human setting. In particular, the lack of necessity for platelet-derived VWF in hemostasis in murine studies remains intriguing. Indeed, measuring hemostasis in mice is challenging, and tail clip bleeding does not always mimic clinical relevant bleeding. Therefore, we believe that a large-scale clinical study involving type I VWD patients with equally low plasma VWF concentrations but variable platelet VWF concentrations (‘platelet normal’, ‘platelet low’, and ‘platelet discordant’) is of great interest to confirm a hemostatic role of platelet VWF in humans. By linking variable platelet VWF content and frequency of bleeding symptoms in this specific study population, more information on the importance of platelet-derived VWF in hemostasis in humans could be obtained. Moreover, such diverse study population would be interesting to link platelet VWF content and frequency of thrombotic events (such as ischemic stroke). This aim, however, is less feasible since the number of type 1 VWD patients with thrombotic events will be very low.

In addition, our data provide an intriguing base for further study of the role of platelet VWF besides hemostasis. Indeed, there is increasing evidence that VWF-platelet complexes, and in particular VWF-GPIb interactions, play an important role in leukocyte extravasation thereby linking VWF to leukocyte recruitment. Therefore, future studies addressing the inflammatory nature of platelet-derived VWF will be highly relevant, especially in inflammation and in thrombo-inflammatory conditions such as transient ischemic stroke and myocardial ischemia/reperfusion injury.

Aim 2: To develop a non-viral gene therapeutic approach that offers long-term protection against TTP in mice.

TTP is a rare life-threatening condition with a high mortality rate, if left untreated. In case of congenital TTP, prophylactic plasma therapy is considered in patients with a chronic relapsing disease course. Lifelong prophylaxis, however, is stressful and not without risk, and has a negative impact on the lifestyle and health-related quality of life. Here, we demonstrate that a single administration of the *Sleeping Beauty* (SB) transposon system, carrying a correct copy of the gene, can result in long-term correction of ADAMTS13 deficiency and prophylaxis of TTP in *Adamts13*$^{-/-}$ mice. Therefore, we believe that our non-viral integrating *Sleeping Beauty*-mediated gene therapeutic approach can ultimately cure congenital TTP patients, obviating the need for prophylactic plasma infusions.

Failed and fatal clinical trials in the late 1990s have threatened to doom gene therapy technology. However, recent successful viral-vector mediated gene therapy trials for hemophilia B and inherited immune deficiencies have led to a surprising revival in gene therapy research. Indeed, gene therapy continues to grow as a treatment strategy toward numerous diseases. This ‘renaissance’ has drawn attention from pharmaceutical and biotechnology companies, which has led to the marketing authorization of the first gene therapy-medicine, called Glybera® (an AAV-mediated gene therapy for treatment of lipoprotein lipase deficiency), in 2012.

Despite its progress, clinical success of viral vector-mediated gene therapy is often hindered by safety concerns and other limitations concerning high production costs, scale up, and size of delivered gene construct. These drawbacks have drawn attention to the field of non-viral gene therapy in which recent advances (in terms of gene transfer efficiency, duration of gene expression, and safety) have led to an increased number of non-viral gene products entering clinical trials.

With respect to the development of novel non-viral gene therapy platforms, the SB

transposon technology holds high promise as it combines low cost and simplicity of naked DNA with the efficiency of gene transfer associated with retroviral vectors. Interestingly, SB-mediated gene therapy has reached clinical level in the United States, where various trials involving CAR T-cells generated with the SB system to treat B-cell malignancies are ongoing. Recently published clinical data from these trials are encouraging and support further clinical development of this non-viral gene therapeutic approach.

The success of SB in early clinical trails encourages us to work out strategies that will turn our preclinical gene therapeutic approach for congenital TTP into a more clinical relevant approach. Efficient gene delivery is a crucial factor for clinically applicable gene therapy. Hydrodynamic gene delivery is very efficient in small animal models and significant progress in image-guided catheterization-based procedures has enabled researchers to deliver plasmid DNA in specific target organs of larger animals, such as pigs. However, the procedure is still not readily applicable to a human clinical setting. To circumvent this issue, the use of hybrid helper-dependent adenoviral vectors that incorporate the SB transposon system could be explored. Adenoviral vectors are widely used in gene therapy clinical trials and therefore well characterized in a human clinical setting. Moreover, the research group of A. Ehrhardt (University of Witten/Herdecke) has already successfully evaluated a similar hybrid-vector system in a canine model for hemophilia B. Collaboration with this group would allow us to develop a hybrid adenoviral/SB system carrying a correct copy of the *ADAMTS13* gene and test its efficacy in preclinical studies using *Adamts13*$^{-/-}$ mice.

Although the use of the SB transposon system in the field of gene therapy holds much promise, one should take into account that this transposon-based system is an integrating gene transfer technique, and therefore the risk of insertional mutagenesis is immanent. To overcome safety issues related to integration, the use of episomal minicircle vectors can offer an ideal alternative. Minicircles are circular DNA with only mammalian expression cassettes and devoid of bacterial backbone. Despite their non-integrating nature, minicircles lead to persistent expression of transgene proteins in various tissues. Recently, PharmAbs, the KU Leuven Antibody Center, launched the start of a spin-off company where the minicircle technology will be used to express human antibodies as therapeutic agents in patients. Preclinical animal studies showed that electrotransfer of minicircle DNA containing therapeutic antibody sequences to skeletal muscles of mice allowed efficient expression of the therapeutic antibody. Hence, it will be interesting to study if electrotransfer of minicircle DNA containing a correct copy of the *ADAMTS13* gene to skeletal muscles of mice will be another interesting gene therapeutic approach to treat TTP.

SB-mediated gene transfer hinges on the insertion of a correct copy of the gene to achieve a therapeutic effect, whereas more recent strategies focus on the precise manipulation of the human genome. With respect to these latter strategies, the advent of the type II bacterial clustered, regularly interspaced, palindromic repeats (CRISPR) and CRISPR-associated (Cas) gene transfer system has been phenomenal. Although originally described as an adaptive immune system used by microbes to defend themselves against specific infections, the CRISPR/Cas system (and in particular the CRISPR/Cas9) has been repurposed into a cheap and effective genome editing tool to correct disease-causing mutations in a broad range of mammalian cells, including human cells. Therefore, it would be interesting to look into the possibility of performing CRISPR/Cas9-mediated strategies that target pathogenic genes found in congenital TTP patients.

Aim 3: To unravel the role of the VWF/ADAMTS13 axis in a murine model of malaria-associated acute respiratory distress syndrome.

Severe malaria remains a major cause of death in tropical countries. Increasing clinical and preclinical evidence shows that alteration in the VWF/ADAMTS13 axis may play a key role in malaria-associated disease syndromes. However, in-depth mechanisms concerning the direct role of VWF and ADAMTS13 in malaria pathogenesis have not yet been elucidated. Many studies focus on cerebral malaria pathogenesis, while little is known about the pathogenesis of malaria-associated lung pathology. By infecting C57BL/6J mice with *P. berghei* NK65 parasites, we studied alterations in VWF and ADAMTS13 associated with murine MA-ARDS. We observed early elevated levels of VWF and late-stage reduction of ADAMTS13 activity without accumulation of highly reactive HMW VWF multimers. Our findings also showed that VWF does not contribute to malaria-associated thrombocytopenia. Furthermore, we believe that VWF may influence the development of parasitemia and lung pathology, potentially by interfering with the sequestration of infected red blood cells.

Many findings in this study are preliminary and therefore many questions remain to be resolved. Is the loss of HMW VWF multimers at end-stage MA-ARDS clinically relevant? If so, what causes this intriguing phenotype? Is the reduction in ADAMTS13 activity despite normal antigen levels due to the presence of (an) inhibitor(s)? Does VWF influences the course of malarial disease by affecting the parasite sequestration in specific organs? Consequently, definitive conclusions cannot yet be drawn from this study and further investigations are needed before one can discuss its added value to the field. Nevertheless, in

depth studies using experimental models are invaluable for elucidating pathogenesis of human diseases, particularly infectious diseases.

In murine malaria, no single mouse model mimics all the various clinical manifestations of severe malaria in humans. Therefore, it will be interesting to investigate the involvement of VWF and ADAMTS13 in different mouse models of malaria, ranging from lethal to non-lethal infections. For example, infection of C57BL/6 mice with *P. berghei ANKA* can be used to unravel the role of VWF and ADAMTS13 in experimental cerebral malaria, whereas infection with *P. chabaudi* AS can be used to study the cellular and molecular mechanisms of the VWF/ADAMTS13 axis in a non-lethal infection. Testing these parasite strains in different transgenic (knockout) mouse strains will hopefully lead to a better understanding in the involvement of the VWF/ADAMTS13 axis in various malaria-associated syndromes. In this way novel targets for therapeutic interventions that improve survival may be identified. However, regardless of the model that is used, extrapolating results from murine models of malaria to human malaria will be an interesting challenge.

CURRICULUM VITAE

LIST of PUBLICATIONS

1. Van den Steen PE, Geurts N, Deroost K, Van Aelst I, **Verhenne S**, Heremans H, Van Damme J, Opdenakker G: Immunopathology and dexamethasone therapy in a new model for malaria-associated acute respiratory distress syndrome. **American Journal of Respiratory and Critical Care Medicine**. 2010;181(9):957-968

2. Geurts N, Martens E, **Verhenne S**, Lays N, Thijs G, Magez S, Cauwe B, Li S, Heremans H, Opdenakker G, Van den Steen PE: Insufficiently defined genetic background confounds phenotypes in transgenic studies as exemplified by malaria infection in Tlr9 knockout mice. **PLoS One**. 2011;6(11):e27131

3. Vanhoorelbeke K, **Verhenne S**, De Meyer SF: Development of gene therapy for von Willebrand disease. **Proceedings of the Belgian Royal Academies of Medicine**. 2014;3:114-128

4. **Verhenne S**, Denorme F, Libbrecht S, Vandenbulcke A, Pareyn I, Deckmyn H, Lambrecht A, Nieswandt B, Kleinschnitz C, Vanhoorelbeke K, De Meyer SF: Platelet-derived VWF is not essential for normal thrombosis and hemostasis but fosters ischemic stroke injury in mice. **Blood**. 2015;126(14):1715-1722

   with editorial comment by Flood VH: Platelet-derived VWF in the stroke spotlight. Blood. 2015;126(14):1640-1641

5. Tersteeg C, **Verhenne S**, Roose E, Schelpe AS, Deckmyn H, De Meyer SF, Vanhoorelbeke K: ADAMTS13 and anti-ADAMTS13 antibodies in thrombotic thrombocytopenic purpura – current perspective and new treatment strategies. **Expert Review of Hematology**. 2016;9(2):209-221

6. **Verhenne S**, Vandeputte N, Pareyn I, Rottensteiner H, Izsvák Z, Deckmyn H, De Meyer SF, Vanhoorelbeke K. Long-term prophylaxis of thrombotic thrombocytopenic purpura in ADAMTS13 knockout mice by *'Sleeping Beauty'* transposon-mediated gene therapy. **Manuscript submitted to *Arteriosclerosis, Thrombosis, and Vascular Biology* (minor revisions).**

7. Vanhoorelbeke K, Portier I, **Verhenne S**, Pareyn I, Vandeputte N, Deckmyn H, Ivics Z, Izsvák Z, De Meyer SF. High and long-term expression of von Willebrand factor after Sleeping Beauty transposon-mediated gene therapy in a mouse model of severe von Willebrand disease. **Manuscript in preparation.**

LIST of ABSTRACTS

▪ ORAL communications

1. **Verhenne S**, Libbrecht S, Vandenbulcke A, Deckmyn H, Vanhoorelbeke K, and De Meyer SF. *The hemostatic role of platelet von Willebrand factor in mice.* **XXth annual meeting of the Belgian Society on Thrombosis and Haemostasis 2012 - Antwerp, Belgium** (November 22-23, 2012)

2. Vanhoorelbeke K, **Verhenne S**, Pareyn I, Deckmyn H, Isvak Z, and De Meyer SF. *Long-term correction of von Willebrand disease via Sleeping Beauty transposon-mediated gene therapy.* **XXth annual meeting of the Belgian Society on Thrombosis and Haemostasis 2012 - Antwerp, Belgium** (November 22-23, 2012)

3. **Verhenne S**, Libbrecht S, Vandenbulcke A, Deckmyn H, Vanhoorelbeke K, and De Meyer SF. *The role of platelet von Willebrand factor in mice.* **XXIVth Congress of the International Society on Thrombosis and Haemostasis 2013 - Amsterdam, The Netherlands** (June 29 – July 4, 2013)

4. Vanhoorelbeke K, **Verhenne S**, Pareyn I, Deckmyn H, Isvak Z, and De Meyer SF. *Long-term correction of von Willebrand disease via Sleeping Beauty transposon-mediated gene therapy.* **XXIVth Congress of the International Society on Thrombosis and Haemostasis 2013 - Amsterdam, The Netherlands** (June 29 – July 4, 2013)

5. **Verhenne S**, Libbrecht S, Vandenbulcke A, Denorme F, Deckmyn H, Vanhoorelbeke K, and De Meyer SF. *The role of platelet von Willebrand factor in mice.* **The joint British Society for Haemostasis and Thrombosis/Belgian Society on Thrombosis and Haemostasis meeting 2013 - Nottingham, United Kingdom** (October 10-11, 2013)

6. **Verhenne S**, Vandeputte N, Pareyn I, Izsvák Z, Rottensteiner H, Deckmyn H, De Meyer SF, and Vanhoorelbeke K: *Correction of murine ADAMTS13 deficiency and TTP-like symptoms using the 'Sleeping Beauty' transposon system.* **8th Bari International Conference (BIC) 2014 - Bari, Italy** (October 3-5, 2014)

7. **Verhenne S**, Vandeputte N, Pareyn I, Izsvák Z, Rottensteiner H, Deckmyn H, De Meyer SF, and Vanhoorelbeke K. *'Sleeping Beauty'-mediated gene transfer of ADAMTS13 prevents the onset of TTP-like symptoms in ADAMTS13-deficient mice.* **XXIIst annual meeting of the Belgian Society on Thrombosis and Haemostasis 2014 - Mechelen, Belgium** (November 27-28, 2014)

8. **Verhenne S**, Vandeputte N, Pareyn I, Izsvák Z, Rottensteiner H, Deckmyn H, De Meyer SF, and Vanhoorelbeke K. *Long-term gene therapy for thrombotic thrombocytopenic purpura using the 'Sleeping Beauty' transposon system.* **XXVth Congress of the International Society Thrombosis and Haemostasis 2015 – Toronto, Canada** (June 20-25, 2015)

9. Portier I, Vanhoorelbeke K, **Verhenne S**, Pareyn I, Deckmyn H, Izsvak Z, De Meyer SF. *Long-term expression of von willebrand factor via Sleeping Beauty sandwich transposon-mediated gene therapy.* **XXVth Congress of the International Society Thrombosis and Haemostasis 2015 – Toronto, Canada** (June 20-25, 2015)

10. **Verhenne S**, Vandeputte N, Pareyn I, Izsvák Z, Rottensteiner H, De Meyer SF, and Vanhoorelbeke K. *Long-term gene therapy for congenital thrombotic thrombocytopenic purpura using the 'Sleeping Beauty' transposon system.* **Annual Department Event of Cardiovascular Sciences 2015 – Leuven, Belgium** (October 16, 2015)

11. Kraisin S, **Verhenne S**, Pham T, Vandeputte N, Deckmyn H, Vanhoorelbeke K, Van den Steen PE, and De Meyer SF: *The role of von Willebrand factor in a malaria-associated lung pathology model.* **Ist Congress of the European Society on Thrombosis and Haemostasis 2016 – The Hague, The Netherlands** (September 28-30, 2016)

12. Portier I, Vanhoorelbeke K, **Verhenne S**, Pareyn I, Vandeputte N, Deckmyn H, Ivics Z, Izsvák Z, and De Meyer SF. *High and long-term expression of von Willebrand factor after Sleeping Beauty transposon-mediated gene therapy in mice.* **Ist Congress of the European Society on Thrombosis and Haemostasis 2016 – The Hague, The Netherlands** (September 28-30, 2016)

▪ POSTER presentations

13. **Verhenne S**, Libbrecht S, Vandenbulcke A, Deckmyn H, Vanhoorelbeke K, and De Meyer SF. *The hemostatic role of platelet von Willebrand factor in mice.* **The Hemostasis Gordon Research Conference - Waterville Valley, New Hampshire, USA** (July 22-27, 2012)

14. **Verhenne S**, Vandeputte N, Pareyn I, Izsvák Z, Rottensteiner H, De Meyer SF, and Vanhoorelbeke K. *Correction of murine ADAMTS13 deficiency using the 'Sleeping Beauty' transposon system.* **European Society of Cell and Gene Therapy congress - Madrid, Spain** (October 25-28, 2013)

15. **Verhenne S**, Kraisin S, Pham T, Vandeputte N, Deckmyn H, Vanhoorelbeke K, Van den Steen PE, and De Meyer SF: *The role of von Willebrand factor in a malaria-associated lung pathology model.* **The Hemostasis Gordon Research Conference - Stowe, Vermont, USA** (July 24-29, 2016)

AWARDS & GRANTS

▪ AWARDS

1. Paul Capel Prize 2014

Prize granted for the best oral presentation entitled *"'Sleeping Beauty'-mediated gene transfer of ADAMTS13 prevents the onset of TTP-like symptoms in ADAMTS13-deficient mice"* at the XXIInd Annual Meeting of the Belgian Society on Thrombosis and Haemostasis, Mechelen, Belgium, 2014. (EUR 750)

2. Young Investigator Award 2015

Prize granted for the abstract entitled *"Long-term gene therapy for thrombotic thrombocytopenic purpura using the 'Sleeping Beauty' transposon system"* accepted as oral communication at the XXVth meeting of the International Society on Thrombosis and Haemostasis in Toronto, Canada, 2015. (CAD 700)

3. PhD Poster Contest Winner 2015

Prize granted for the best oral presentation entitled *"Long-term gene therapy for congenital thrombotic thrombocytopenic purpura using the 'Sleeping Beauty' transposon system"* at the Annual Department Event of Cardiovascular Sciences, Leuven, 2015. (EUR 800)

▪ GRANTS

1. Travel grant 2012 – Belgian Society on Thrombosis and Haemostasis

Travel grant awarded for the poster presentation entitled *"The hemostatic role of platelet von Willebrand factor in mice"* at the Hemostasis Gordon Research Conference, New Hampshire, USA, 2012

2. Travel grant 2013 – Belgian Society on Thrombosis and Haemostasis

Travel grant awarded for the oral communication entitled *"The role of platelet von Willebrand factor in mice"* at the XXIVth meeting of the International Society on Thrombosis and Haemostasis in Amsterdam, The Netherlands, 2013.

3. **FWO travel grant 2013**

   Travel grant awarded for the oral communication entitled *"The hemostatic role of platelet von Willebrand factor in mice"* at the XXIVth meeting of the International Society on Thrombosis and Haemostasis in Amsterdam, The Netherlands, 2013.

4. **FWO travel grant 2016**

   Travel grant awarded for the poster presentation entitled *"The role of von Willebrand factor in a malaria-associated lung pathology model"* at the Hemostasis Gordon Research Conference, Vermont, USA, 2016.

5. **Travel grant 2016 – Belgian Society on Thrombosis and Haemostasis**

   Travel grant awarded for the poster presentation entitled *"The role of von Willebrand factor in a malaria-associated lung pathology model"* at the Hemostasis Gordon Research Conference, Vermont, USA, 2016.